

# **A Study of Some Factors in Mechanistic Railway Track Design**

**Kjell Arne Skoglund**

Thesis submitted to the Faculty of Engineering and Technology,  
Norwegian University of Science and Technology, in partial fulfilment of  
the requirements for the degree of Doctor of Engineering.



**Department of Road and Railway Engineering  
Norwegian University of Science and Technology  
NTNU**

March, 2002

*The committee for the appraisal of this thesis  
was comprised of the following members:*

Professor, Dr.Techn. **Pauli Juhani Kolisoja**,  
Department of Civil Engineering,  
Tampere University of Technology,  
Tampere, Finland.

Senior engineer, Dr.Ing. **Geir Berntsen**,  
Public Roads Administration,  
Tromsø, Norway.

Senior engineer **Hallstein Gåsemyr**,  
Norwegian National Rail Administration,  
Oslo, Norway.

Associate Professor, Dr.Ing. **Helge Mork**,  
Department of Road and Railway Engineering,  
Norwegian University of Science and Technology,  
Trondheim, Norway.

*The advisors during the study have been:*

Professor, Dr.Ing. **Ivar Horvli**,  
Department of Road and Railway Engineering,  
Norwegian University of Science and Technology,  
Trondheim, Norway.

Professor emeritus, M.S. **Rasmus S. Nordal**,  
Department of Road and Railway Engineering,  
Norwegian University of Science and Technology,  
Trondheim, Norway.

---

## Summary

This thesis is composed of three main parts: The first part that uses classic track models as a basis for further developments, the second part that deals with constitutive behaviour of granular materials and the third part that describes the development of a new triaxial cell apparatus and the testing of a ballast material using this apparatus.

The description of classic track models is focused on the beam-on-elastic-foundation model (abbr. BOEF model), which make use of the Winkler foundation, and a simple beam element model with linear discrete support. The shortcomings of the BOEF model is discussed: It assumes a continuous foundation, a continuously welded track, the weight of the track ladder is not incorporated, linear support which imply prediction of tension in the uplift regions, no shear deformation in the rails is taken into account, it cannot predict stresses and strains within the granular layers. While some of the shortcomings may easily be incorporated others are not: Especially to remove tension in the uplift zones, and to calculate stresses and strains in the granular layers. The latter actually requires a continuum approach. A track model that approximately eliminates the tension in the uplift regions has been developed for a single axle load. As expected, the model shows that the length of the uplift zone and the amount of uplift have higher values than predicted by the BOEF model. The model may be useful when considering contact problems in the track, for instance in a buckling-of-rails analysis.

For the BOEF model a tool that makes use of dimensionless sensitivity diagrams has been developed. The method will in an easy way provide the new maximum track reactions when one or more track parameters are changed. It is hoped that this tool will prove very helpful in a design process, at least as a first step. Dimensionless sensitivity diagrams have been worked out for rail deflection, rail moment, rail seat load, tensional rail base stress and vertical stress between sleeper and ballast. The parameters considered are the design wheel load, rail moment of inertia, position of neutral axis in the rail, sleeper spacing, sleeper width and the length of the sleeper that carries the vertical load. The dimensionless sensitivity diagrams for the BOEF model may be used both for a single axle load and for a double axle load. Also for a beam element model with linear discrete support the dimensionless sensitivity diagrams may be used, but only for a single axle load which is located directly above one of the supports, i.e. a sleeper. For the beam element model the diagrams for the rail deflection, rail seat load and vertical stress between sleeper and ballast are almost identical to the ones for the BOEF model, while the diagrams for the rail moment and tensile rail base stress are somewhat different.

A beam element model with Euler-Bernoulli beam elements resting on nonlinear discrete supports was developed for a single axle load. The discrete supports, which were located at the sleeper positions, were modelled by a two-parameter power function. The model takes advantage of a measured load-deflection relationship, which is also modelled by a two-parameter power function. These latter parameters are generally found by regression of the measured data, while the two parameters for the discrete supports are found as part of the overall solution to the problem. The present version of the model only takes into account a short track section and further development of the model is therefore needed. The track ladder weight and a no tension option in the uplift region are not incorporated in the present version. The model is useful when the BOEF model cannot be used because of nonlinear track response.

Regarding constitutive behaviour it is argued that the plastic strain per load cycle in a well functioning railway track must be very small and normally below 1/100 000 of the elastic strain per load cycle. If also the hysteresis of the material during a load cycle is small, then an elastic approximation could be justified when it comes to calculating the stresses. The plastic strains may

then be detached from the stress-strain calculation and modelled separately on the basis of laboratory or field measurements.

Several elastic constitutive models are described: The Hooke's law generalised to three dimensions, the cross anisotropic elastic model, two versions of the  $k$ - $\theta$  model, and two hyperelastic models. The general elasto-plastic framework with isotropic hardening is also described.

The basics of repeated loading of a frictional system is described by analogy to a simple model with springs and frictional sliders. This model can be viewed as the basis for the pure kinematic multisurface model by Mróz and Iwan. Through energy considerations in cyclic loading of the frictional system the concept of reclaimed plastic strain is rejected.

The concept of initial stresses and strains is discussed. It is argued that initial stresses cannot be large in the upper part of a road or railway embankment. The main reason for this is that granular materials cannot self equilibrate stresses through tension.

The development and construction of triaxial equipment for testing railway ballast in its original grading is described. The specimens are 300 mm by 600 mm (diameter by height). A new and direct way of applying the confining load was developed, which allowed faster variation of the confining stress. A new instrumentation concept was invented where instrumentation rings are fastened to material particles instead of being attached to the outer membrane or to plugs embedded in the material. This arrangement measures the horizontal deformation. The vertical deformation has to be measured over the whole specimen length as resilient particle rotations prevented on-sample instrumentation.

A test series on Vassfjell railway ballast was conducted to evaluate the feasibility of the new apparatus and to characterise the ballast material. The overall performance of the apparatus was found to be good with a reliable repeatability, but some modifications were suggested to improve the loading procedure in the beginning of the load steps.

The test series on Vassfjell ballast was rather limited and no advanced modelling of the results was found to be appropriate. Instead an isotropic linear elastic approach was followed. Moisture was added, to the natural retention capacity, to some of the specimens. It was found that the added moisture only slightly affected the mechanical behaviour of the material. A somewhat denser grading was also tested, but the observed effect on the material properties was limited.

# Contents

<b>Summary</b> .....	<b>iii</b>
<b>Contents</b> .....	<b>v</b>
<b>Preface</b> .....	<b>ix</b>
<b>List of symbols</b> .....	<b>xi</b>
<b>Chapter 1 Introduction and scope</b> .....	<b>1</b>
1.1 The importance of railway track design .....	1
1.2 Scope of the thesis .....	1
1.3 The contents of the thesis .....	2
<b>Chapter 2 The design of railway tracks based upon classic approaches</b> .....	<b>3</b>
2.1 Introduction .....	3
2.2 Finding the design wheel load .....	3
2.2.1 The German and Austrian procedure .....	4
2.2.2 The North American procedure .....	6
2.2.3 The British procedure .....	7
2.2.4 Concluding remarks .....	8
2.3 The beam on elastic foundation model (BOEF model) .....	8
2.3.1 Introduction .....	8
2.3.2 The basics - deflection and moment caused by a single axle load .....	9
2.3.3 Finding the rail seat load .....	12
2.3.4 Multiple axle loads .....	14
2.3.5 Fictitious longitudinal sleepers and foundation coefficient .....	15
2.3.6 Finding the track modulus .....	16
2.3.7 Some comments about predictability .....	19
2.3.8 Limitations of the BOEF model .....	20
2.4 The sleeper as a beam on elastic foundation .....	22
2.5 Tensionless BOEF models found in the literature .....	24
2.5.1 Model according to Tsai and Westmann .....	24
2.5.2 Model according to Adin et al. ....	26
2.6 A compensating load approach to the no tension problem .....	27
2.6.1 The basic idea and an interpretation of Tsai and Westmann's model .....	27
2.6.2 The main ingredients of the new model .....	29
2.6.3 The set of equations to be solved .....	30
2.6.4 Some results from the new model .....	31
2.6.5 Conclusions of the new model .....	32
2.7 Dimensionless sensitivity diagrams .....	33
2.7.1 BOEF model with a single axle load .....	33
2.7.2 BOEF model with multiple axle loads .....	34
2.8 Other types of continuous models .....	40
2.9 Classic beam element models for railway track .....	41
2.9.1 An Euler-Bernoulli beam element model .....	42
2.9.2 Comparison between beam element models and BOEF models .....	43
2.9.3 Dimensionless sensitivity diagrams for an Euler-Bernoulli beam element model .....	44
2.10 Outline of a new beam element model with nonlinear support .....	47
2.10.1 The relationship between wheel load and maximum deflection .....	47
2.10.2 Establishing and solving the model equations .....	49
2.10.3 Some results for the new beam element model .....	50
2.10.4 Concluding remarks .....	52
2.11 Dynamic models .....	53

2.11.1	Models with given loading . . . . .	54
2.11.2	Static versus dynamic analysis . . . . .	55
<b>Chapter 3</b>	<b>Elements of constitutive modelling of railway ballast . . . . .</b>	<b>57</b>
3.1	Introduction . . . . .	57
3.2	Some comments on modelling . . . . .	57
3.2.1	General requirements to a mathematical model . . . . .	57
3.2.2	Strain and stress measures . . . . .	59
3.2.3	Types of nonlinearities . . . . .	60
3.3	The finite element method . . . . .	60
3.3.1	Introduction . . . . .	60
3.3.2	The finite element method for structural mechanics . . . . .	61
3.4	Elastic models for transportation structures . . . . .	63
3.4.1	Linear, isotropic elasticity . . . . .	63
3.4.2	Cross anisotropic elasticity . . . . .	66
3.4.3	Nonlinear resilient models for pavement design . . . . .	67
3.4.4	Nonlinear hyperelastic models . . . . .	68
3.5	Features of elasto-plasticity . . . . .	71
3.5.1	Introduction . . . . .	71
3.5.2	Classic elasto-plastic continuum theory . . . . .	74
3.5.3	Other plasticity theories . . . . .	79
3.6	Simplifying approaches to elasto-plasticity in cyclic loading . . . . .	80
3.6.1	The use of classic and generalised plasticity in cyclic loading . . . . .	80
3.6.2	The elastic approximation . . . . .	81
3.6.3	Definitions of loading and unloading. The cause of the plastic strain. . . . .	83
3.6.4	Relations for plastic strains . . . . .	85
3.7	Cyclic loading of frictional systems . . . . .	86
3.7.1	Basics of cyclic loading of a frictional system . . . . .	86
3.7.2	Modelling cyclic behaviour by adapting the Iwan model . . . . .	90
3.7.3	Basic modelling of the conservative and dissipative stresses . . . . .	94
3.8	Initial stresses and initial strains . . . . .	95
3.9	Using constitutive models and FEM for a railway track . . . . .	97
<b>Chapter 4</b>	<b>Triaxial equipment and testing of railway ballast . . . . .</b>	<b>99</b>
4.1	Introduction . . . . .	99
4.2	Conventional triaxial testing units found in the literature . . . . .	99
4.3	The triaxial testing unit used in the present study . . . . .	102
4.3.1	The triaxial cell with loading actuators . . . . .	102
4.3.2	The load control unit . . . . .	105
4.3.3	The data capture unit . . . . .	105
4.4	Specifications for ballast material . . . . .	106
4.4.1	Norwegian specifications . . . . .	106
4.4.2	Ballast specifications of some other railway administrations . . . . .	108
4.5	Specimen preparation . . . . .	109
4.5.1	Fractioning and blending . . . . .	109
4.5.2	Compaction of specimens . . . . .	110
4.5.3	Instrumentation and mounting of specimens into the triaxial cell . . . . .	111
4.5.4	Discussion of the selected instrumentation concept . . . . .	113
4.5.5	Membranes and sealing . . . . .	115
4.5.6	Adding moisture to the specimens . . . . .	117
4.6	Materials tested in the present study . . . . .	117
4.6.1	Parent material . . . . .	117
4.6.2	Material meeting the requirements . . . . .	118

---

4.6.3	Material with increased amount of smaller grains	118
4.6.4	Moisture content	119
4.6.5	Summary of specimen data	120
4.7	Triaxial testing procedures found in the literature	120
4.7.1	Introduction	120
4.7.2	Procedures found in the literature	121
4.8	Triaxial testing procedure used in this study	122
4.8.1	The objectives and outlines of the testing	122
4.8.2	A discussion of stresses for variable confining stress tests	123
4.8.3	The stresses used in the test	124
<b>Chapter 5 Results and discussion of results from triaxial testing</b>		<b>127</b>
5.1	Introduction	127
5.2	Interpreting the test results	127
5.2.1	Introduction	127
5.2.2	Expressions for Young's modulus and Poisson's ratio	128
5.2.3	From sensor signals to elastic and plastic parameters	129
5.2.4	Uncertainties in results because of the testing procedure	130
5.3	Results from the variable confining stress tests	131
5.4	Results from the constant confining stress tests	144
5.5	Results from the static tests	146
5.6	Summary of test results	147
<b>Chapter 6 Conclusions and recommendations</b>		<b>149</b>
6.1	Conclusions	149
6.2	Suggestions for further work	150
<b>References</b>		<b>153</b>
<b>Appendix A</b>	<b>Dimensionless sensitivity diagrams</b>	
<b>Appendix B</b>	<b>Brief thermomechanical background</b>	
<b>Appendix C</b>	<b>Stresses applied to the specimens</b>	
<b>Appendix D</b>	<b>Measured stresses and strains from the tests</b>	

---

## Preface

The present thesis is a result of a project where the beginning is dating back to the summer of 1995. At that time a scholarship was granted to the author from The Research Council of Norway with the goal of looking into existing models of railway track design and to improve the current modelling practice. The years that have passed since the start of the project have been giving me a unique opportunity of getting insight into mechanistic design of railway tracks, constitutive modelling and triaxial testing of railway ballast materials.

The project has been financed by The Research Council of Norway, Norwegian National Rail Administration (JBV), and Norwegian University of Science and Technology (NTNU). NATO Science Fellowship granted me a scholarship that enabled me to spend the fall semester of 1996 at the University of Illinois at Urbana-Champaign.

Needless to say, in such a project numerous people have been involved both by doing practical work and also commenting and advising the work on the thesis.

Professor Rasmus S. Nordal was the one that encouraged me to apply for the aforementioned scholarship and to start the work with the intention of fulfilling a Doctor of Engineering degree. He was also my first advisor and has also in the period from his retirement to the present date been involved in the project as a co-advisor. After Nordal's retirement Professor Ivar Horvli took over as my advisor. The effort and dedication of both are highly appreciated.

The laboratory work has been very comprehensive and much more challenging than anticipated from the start. Without the help and dedication from laboratory staff it would not have been possible to carry out this project. Especially I would like to mention Laboratory Engineer Stein Høseth and Researcher Einar Værnes. Stein has been a constant source of ideas when mechanical, hydraulic and instrumentation problems were to be solved. He has also performed some of the triaxial testing of the ballast material. Einar has spent countless hours doing all the programming and adaptation of software for the triaxial testing unit. Both have had a genuine dedication to the project. Research Technician Tore Menne has been of great help both with mechanical topics and by assisting in ballast material processing. Researcher Randi Skoglund and Civil Engineer Kjell Enoksen have been assisting in ballast material processing. Laboratory Engineer Kjell O. Roksvåg has been helping with the instrumentation work.

Dr.ing. Inge Hoff has also performed some of the triaxial testing for me. In addition he has been a valuable source of knowledge into the more theoretical aspects of triaxial testing and of constitutive modelling of unbound aggregates. Some parts of the present work are undoubtedly founded on work done by Inge. Dr.ing.-student Rabbira Garba has advised me on topics in constitutive modelling, not only regarding models for viscous materials, which is his speciality, but also for a broader range of materials.

Senior Researcher Terje Lindland, the leader of the joint railway group at the Dept. of Road and Railway Engineering at NTNU and Dept. of Highway Engineering at SINTEF, allocated adequate financial resources to the project despite the problems of forecasting the time and resources needed. Professor Asbjørn Hovd, the head of the department, has also taken part in administrating and providing financial support.

A major part of the machining of the triaxial apparatus was done by the company Langland & Schei, Trondheim. But we were also greatly dependent on the in-house workshop Fellesverkstedet, as much of the smaller parts for instrumentation were machined here, often on short no-



tice. The major part of the technical drawings for the triaxial testing equipment was made by Kjell Moen, Fellesverkstedet.

I will like to thank my present employer the Norwegian National Rail Administration for allowing me to finalise my work with the dr.ing.-project. I am also indebted to my colleagues at the Rail Administration in Trondheim as I know they have had extra strain because I was occupied with my research project.

The members of the committee for the appraisal of the thesis are warmly acknowledged for their time and effort spent.

Last but not least I will thank Eli and our two children Øyvor and Einar for their patience and love during this work.

Trondheim, March 2002

Kjell Arne Skoglund

## List of symbols

### Latin letters:

$A$	a plastic resistance number
$A_{33}$	wheel-rail contact area of a wheel of diameter of 33 inches
$A, B, C, D, E$	regression coefficients
$A_w$	wheel-rail contact area of a wheel of diameter of $w$ inches
$a$	axle spacing
$a$	attraction
$a, b, c$	coefficients in a general foundation model
$B_1, B_2, B_3$	material parameters from triaxial testing
$b$	width of the fictitious longitudinal sleeper
$C$	foundation coefficient
$C_u$	uniformity coefficient for material gradations
$c$	sleeper spacing
$c$	track damping
$c_1, c_2$	parameters in the Reissner foundation model
<b>D</b>	constitutive matrix
<b>D</b> <sub>ep</sub>	elasto-plastic constitutive matrix
$D$	a dilatancy parameter
$d$	width of cross sleeper
$d$	measured permanent vertical strain after 10 000 load cycles
$d_0$	reference strain, equals 1‰
<b>E</b>	strain matrix
<b>E</b> '	deviatoric strain matrix
$E$	Young's modulus of elasticity
$E_{ext}$	external energy
$E_H$	Young's modulus for horizontal compression
$E_{int}$	internal energy
$E_n$	energy stored in rail support no. $n$
$E_{rail}$	energy stored in the rail
$E_f$	Young's modulus for the foundation material
$E_V$	Young's modulus for vertical compression
<b>e</b>	deviatoric strain vector
$e$	a deviatoric strain measure
$e_{ij}$	deviatoric strain components
$F$	yield surface
$F_f$	slip force for frictional element
$F_f^*$	slip force for frictional element in the St. Vénant model with parallel spring
$f$	frequency

---

$f$	degree of mobilisation
$f$	shape factor for the plastic strain development
$f_d$	multiple axle load factor for deflection and derived quantities
$f_{dcorr}$	correction factor used for double axle loads to calculate maximum deflection
$f_i$	the ratio of rail-wheel contact area of a wheel of 33 inches of diameter to a wheel of $w$ inches of diameter ( $= A_{33}/A_w$ )
$f_m$	multiple axle load factor for moment and tensile stress in rail base
$G$	shear modulus
$G_f$	shear modulus for the foundation material
$G_{VH}$	shear modulus for shear deformation in a vertical plane
$g$	assumed function describing the variation of vertical displacement with depth
$h_n$	distance from rail neutral axis
$H$	thickness of foundation layer
$H()$	Heaviside step function
$\mathbf{I}$	identity matrix
$I$	moment of inertia for a rail
$I_1^{\epsilon}$	first strain invariant ( $= \epsilon_v$ )
$J_2^{\epsilon}$	second deviatoric strain invariant
$K$	track stiffness
$K$	bulk modulus
$K$	principal stress ratio
$K_1, K_2$	regression coefficients
$K_1^*$	regression coefficient
$K_{nl}$	nonlinear track stiffness
$K_{pad}$	sleeper pad stiffness
$\mathbf{k}$	element stiffness matrix
$k$	track quality factor, used in design load calculations
$k$	track modulus
$k_f$	spring constant to spring coupled to a frictional element
$k_{nt}$	track modulus for a no tension track model
$k_p$	parameter used in the uplift function in a no tension track model
$k_{quasi}$	quasi-static load factor, accounts for additional load caused by cant deficiency
$k_s$	spring constant to a spring in a friction model
$k_{sleeper}$	foundation modulus for the sleeper
$k_{spring}$	foundation spring constant in a beam element model
$k_{spring,nt}$	no tension foundation spring constant in a beam element model
$k^*$	complex track modulus
$L$	characteristic length, a track parameter
$L_p$	parameter used in the uplift function in a no tension track model
$l$	length of cross sleeper
$l$	coefficient for long term strains

---

$M$	rail moment
$M_0$	end conditioning moment when analysing a sleeper as a BOEF
$M_r$	resilient modulus
$m$	length of an assumed unsupported area in the middle of the sleepers
$m$	track vibrating mass
$m_u$	unsprung mass of the vehicle
$N$	number of load repetitions
$N$	normal force
$\mathbf{n}$	direction vector
$P_1$	peak force for vibrations between 30 and 100 Hz
$P_2$	peak force for vibrations above 200 Hz
$p$	resisting line force beneath the rail foundation
$p$	mean stress, used in triaxial testing
$p_c$	preconsolidation pressure
$p_n$	resisting line force beneath the rail foundation for sleeper no. $n$
$Q$	plastic potential
$Q$	shearing force
$Q_0$	end conditioning force when analysing a sleeper as a BOEF
$Q_0$	wheel load amplitude
$Q_d$	design axle load
$Q_m$	measured or known wheel load
$Q_{nom}$	nominal (static) axle load
$Q_p$	parameter used in the uplift function in a no tension track model
$Q_{sleeper}$	weight of a sleeper
$q$	line load accounting for the weight of the track ladder
$q$	deviatoric stress in conventional triaxial testing
$q_p$	parameter used in the uplift function in a no tension track model
$q_{rail}$	longitudinal unit weight of rail
$r^d$	ratio of dissipative stress to total stress
$\mathbf{S}$	nodal force vector
$S_{BOEF}$	rail seat load for a beam on elastic foundation model
$Sm$	calculated degree of shear mobilization
$S_n$	rail seat load for sleeper no. $n$
$S_{NL}$	rail seat load for a nonlinear beam element model
$\mathbf{s}$	deviatoric stress vector
$s$	value of the standard deviation, used in design load calculations
$T$	tensional force
$t$	number of standard deviations, used in design load calculations
$t$	time
$U$	strain energy density
$V$	vehicle velocity when measured in units of km/h

---

$V_{mph}$	vehicle velocity when measured in miles per hour (m.p.h.)
$\mathbf{v}$	nodal displacement vector
$v$	vehicle velocity in units of m/s
$W$	work or energy
$W^{ext}$	external applied energy
$W_l^d$	dissipated energy during loading
$W_l^q$	stored elastic energy during loading that is released during unloading
$W_l^s$	stored energy during loading that is not released upon unloading
$W_u^d$	dissipated energy during unloading
$W_u^q$	energy given back during unloading
$W_u^s$	energy stored during unloading
$w$	rail deflection that varies with time
$x$	longitudinal coordinate
$x_i$	longitudinal coordinate for axle no. $i$
$x_{max}$	position coordinate where the maximum deflection occurs
$x_n$	longitudinal coordinate at sleeper no. $n$
$y$	deflection
$y_m$	measured deflection of the rail directly below the wheel load
$y_{max}$	maximum deflection
$y_n$	deflection of rail at sleeper no. $n$
$y_{nt}$	rail deflection in a no tension model
$y_p$	uplift function in a no tension track model
$y_q$	deflection of the rail when the track ladder weight is included
$y_{ref}$	a reference deflection, set equal to 1.0 mm
$y_{res}$	resulting deflection when several wheel loads contribute

### Greek letters:

$\alpha$	dip angle in rail joints; for design load purposes this is set to 20 milliradians
$\alpha, \beta$	regression constants
$\gamma$	velocity factor, used in design load calculations
$\Delta$	symbol denoting a change in the parameter that follows
$\delta_f$	stretch of spring before frictional element releases
$\delta(\cdot)$	Dirac delta function
$\boldsymbol{\varepsilon}$	strain vector
$\boldsymbol{\varepsilon}_m$	mean strain vector
$\varepsilon$	error of tolerance in track modulus calculations
$\varepsilon$	one-dimensional strain
$\varepsilon_d$	direct deviatoric strain ( $= \varepsilon_1 - \varepsilon_3$ )
$\varepsilon^e$	resilient (elastic) strain
$\varepsilon^i$	instantaneous strain

$\varepsilon^{ie}$	instantaneous elastic strain
$\varepsilon^{ip}$	instantaneous plastic strain
$\varepsilon_i$	principal strains, $i = 1, 2, 3$
$\varepsilon_{ij}$	component of strain
$\varepsilon^p$	plastic (permanent) strain
$\varepsilon_q$	work consistent deviatoric strain
$\varepsilon^t$	time dependent strain
$\varepsilon^{te}$	time dependent elastic strain
$\varepsilon^{tp}$	time dependent plastic strain
$\varepsilon_v$	volumetric strain
$\eta$	rail deflection influence coefficient
$\eta$	ratio of deviatoric stress to mean stress ( $= q/p$ )
$\theta$	mean stress ( $= \sigma_m$ )
$\kappa$	state variable
$\mu$	rail moment influence coefficient
$\nu$	Poisson's ratio
$\nu_f$	Poisson's ratio for the foundation material
$\nu_{HH}$	Poisson's ratio for expansion in one horizontal direction due to compression in the other horizontal direction
$\nu_{HV}$	Poisson's ratio for expansion in the vertical plane due to horizontal loading
$\nu_{VH}$	Poisson's ratio for expansion in the horizontal plane due to vertical loading
$\xi$	parameter in Green's function
$\xi$	longitudinal coordinate used in convolution integrals
$\xi_{01}, \xi_{02}$	zero deflection intercepts on the $x$ -axis in a no tension model
$\sigma$	stress vector
$\sigma$	stress
$\sigma_a$	a reference pressure, often set to 100 kPa
$\sigma^d$	part of the stress that dissipates energy
$\sigma_d$	deviatoric stress
$\sigma_i$	principal stresses, $i = 1, 2, 3$
$\sigma_m$	mean stress
$\sigma_n$	stress between sleeper and ballast for sleeper no. $n$
$\sigma^q$	part of the stress that stores and releases energy
$\varphi$	friction angle at failure in a static triaxial test

**Other symbols:**

$\mathcal{U}$	bulk strain energy
$\mathcal{V}$	deviatoric strain energy

**Abbreviations:**

AEA	United Kingdom Atomic Energy Authority, now part of the company AEA Technology
AREA	American Railway Engineering Association
AREMA	American Railway Engineering and Maintenance-of-Way Association
ASTM	American Society for Testing and Materials
BOEF	beam on elastic foundation
CCP	constant confining pressure
CEN	European Committee for Standardization
CRW	continuously welded rails
dof	degree(s) of freedom
ERRI	European Rail Research Institute
FEM	the finite element method
JBV	Norwegian National Railway Administration
LA	Los Angeles (e.g. LA test, LA value)
LVDT	Linear Variable Differential Transformer
NGI	Norwegian Geotechnical Institute
NTNU	Norwegian University of Science and Technology
SHRP	Strategic Highway Research Program
UIC	International Union of Railways
VCP	variable confining pressure

---

# CHAPTER 1 Introduction and scope

---

## 1.1 The importance of railway track design

Throughout the time since the invention of guided ground transport, of which conventional railway systems are the most prominent, an appropriate design of the various track elements has been of major importance. While the earliest years were affected by 'trial and error', the design procedures soon became an engineering discipline. In the later decades this field of engineering has grown to be a science where a lot of research is going on. This increasing tendency of 'scientification' has many causes, but two motivation factors seem very important: The everlasting demand of more cost-effective transports and the scientists' curiosity. These two factors are closely interconnected, as both are needed in a fruitful development of railway track design. Examples hereof are the development of high speed rail transport and heavy haul services.

As this thesis focuses on the track foundation, and especially on the ballast layer, a relevant question is how the ballast layer could contribute to an increased overall cost-effectiveness. To answer such a question one needs to understand what functions the ballast layer should have, and, consequently, how the ballast layer fulfils these functions. And here, at this junction, the science comes along.

In order to give an idea of the economics involved some figures from the 4178 km of Norwegian public railway network will be given. In 2002 about NOK 2.9 billion, equivalent of € 380 million, will be spent on operating and maintaining the railway network /24/. About two thirds of this amount is spent on operational tasks, while the rest is spent on maintenance. No figures for the costs of maintaining the ballast layer are available. As a rule of thumb, ballast cleaning have a cost of about NOK 1000 (€ 130) per metre of track. However, the costs of fouled ballast are not limited to the cost of ballast cleaning. It is well known that fouled ballast also causes track misalignment, poor drainage and increased dynamic loads, just to mention a few of the main related problems. These effects will generate needs for maintenance of other parts of the track - with increased costs as a result.

## 1.2 Scope of the thesis

The overall scope of the present work can be summarised in the following items:

- (1) Review classic mechanical design procedures of railway tracks.
- (2) Suggest improvements of current design practices.
- (3) Look into the constitutive behaviour of frictional granular materials.
- (4) To build a triaxial testing device for railway ballast material.
- (5) To use the triaxial device to test ballast materials.



The first two items of the list may be found in Chapter 2. The third item is considered in Chapter 3. Item no. 4 and 5 are dealt with in Chapters 4 and 5.

### 1.3 The contents of the thesis

A short chapter by chapter description will be given here. Reference is also made to the table of contents.

**Chapter 2** deals with the design of a railway track as based upon classic theory, and first of all, the model that treats the track superstructure as beams on a Winkler foundation. Some basic features of this model are discussed as for instance the rail moment and the seat load. Also the main shortcomings of this classic model are explored. Design charts called dimensionless sensitivity diagrams are presented by which it is possible to estimate in an easy way how a change in various track parameters will alter the maximum track reactions. A new track model has been developed where no tension is assumed between the sleepers and the ballast. A simple beam element model with linear discrete support is described and compared with the Winkler foundation model. The beam element model is modified by applying nonlinear discrete support. A short description of time dependent (dynamic) models is also given.

**Chapter 3** describes constitutive modelling of granular materials. The finite element method is briefly described. Also the fundamentals of classic elasto-plasticity are presented and some of its deficiencies when it comes to describing repeated response are commented. A phenomenological model of repeated loading of frictional materials is given. Anisotropy is briefly described. The topic of initial effects, i.e. initial stresses and initial strains, is discussed in a qualitative manner.

**Chapter 4** is mostly devoted to the development of the large-scale triaxial equipment, the testing materials and the procedures related to triaxial testing of railway ballast. Various ballast requirements are described, both Norwegian and those from some other countries. The purpose-built triaxial apparatus, with its instrumentation and data acquisition system, is presented. The materials tested are described along with the test procedures.

**Chapter 5** describes the results from the triaxial testing along with discussions.

**Chapter 6** states the conclusions drawn from the present work. In addition suggestions for further work are made.

---

## CHAPTER 2    **The design of railway tracks based upon classic approaches**

---

### **2.1 Introduction**

Before the invention of the Finite Element Method (which will be described briefly later, in Chapter 3) in the early sixties there were not many options when the problem of mechanical behaviour of a railway track structure was to be examined. In the literature the various options more or less boil down to the so-called ‘beam-on-elastic-foundation model’, or the BOEF model (an abbreviation also used by others, see /7/). This model is in European terms also known under the name ‘Zimmermanns method’, after the German H. Zimmermann who made substantial contributions to the BOEF model and its use in railway track design. In North America it is called either ‘beam-on-elastic-foundation model’ or ‘Winkler’s method’. During the years some modifications to this model have been implemented.

A common feature of most classic approaches is that they are specifically tailored to railway tracks and try to describe the track behaviour as a whole with very simplified material models. The results obtained by such methods are commonly quite selective in accuracy: While some reactions are accurately computed, others display poor accuracy or are even left unknown. As opposed to this, the finite element method (FEM) is a general-purpose method and can be applied to almost any structure with arbitrary geometrical shape and of compound materials. Dependent upon modelling aspects the reactions can be calculated within an acceptable accuracy. However, with complex material models, included behaviour at the material interfaces, and with involved geometry in 3D, the FEM is very expensive in terms of computational resources. As a result a general-purpose FEM code is not the preferred design tool for the practising railway engineer, although this might change within a few years because of ever increasing capacity of computers. But for the time being, the engineer is still apt to use a classic track model or simple FEM models tailored for railway track usage. Both types of models are described in the present chapter, but in terms of FEM models only simple 2D beam element models are included as these are based on much the same philosophy as the BOEF method.

### **2.2 Finding the design wheel load**

Throughout this chapter the emphasis will be on the *vertical* behaviour of the track, consequently the vertical load will be of major concern. Tacitly the loads in the longitudinal and transversal directions are assumed to be zero although this is almost never the case in reality due to factors like curve negotiation, hunting, track irregularities and thermal effects.

There exist several methods for calculating the vertical load for which the railway track is to be designed. The reason for this situation is that the design load is dependent upon a whole range

of complicating factors. A conspicuous example is the problem of dynamic interaction between the train and the track. However, a common approach is to divide the design load into three contributions: The static, the quasi-static and the dynamic components. These contributions represent the nominal wheel load<sup>1</sup>, the load due to load transfer in curves and side wind effects, and finally the load due to track and wheel irregularities. In this section three well known procedures for calculating the vertical design load will be briefly presented, namely the German and Austrian procedure, the North American procedure, and the British procedure.

### 2.2.1 The German and Austrian procedure

This method was originally developed by Eisenmann /18/, but the version described here is taken from Riessberger /69/. Also Brandl /6/ describes this approach, and he points out that this procedure is commonly used by German Railway Authorities. The basic formula for assessing the design axle load adopts a probabilistic approach assuming a Gaussian normal distribution of the axle loads:

$$Q_d = Q_{nom} \cdot k_{quasi} \cdot (1 + t \cdot s) \quad (2.1)$$

where

- $Q_d$  = design axle load [kN]
- $Q_{nom}$  = nominal (static) axle load [kN]
- $k_{quasi}$  = additional load due to cant deficiency (or cant *excess* when low or zero velocity), usually assigned a value of 1.1-1.2. Often denoted the *quasi-static* load increment.
- $t$  = number of standard deviations, assures the appropriate security for the various track components, see Table 2.1 below.
- $s$  = value of the standard deviation (to be explained below)

**Table 2.1:** Number of standard deviations and level of security for track components according to /69/.

Track components	Number of $t$	Probability for not exceeding <sup>a</sup>
Rails and fastening components	3	99.85 %
Sleepers	2	97.50 %
Ballast, subbase and subgrade	1	84.15 %

- a. Equals the probability that the value is *within* the range of the expected value  $\pm ts$ , added to the probability that the value is *below* this range.

This method of assessing the design wheel load is based on extensive measurements in the track and may as such be denoted an empirical method.

The value of the standard deviation,  $s$ , in Eqn. (2.1) is calculated according to  $s = k \cdot \gamma$ . Here,  $k$  is a track quality factor assumed to be related to the importance or traffic of the line in question

1. Throughout the thesis the term *wheel load* will be utilised assuming that the track is always loaded with two identical wheel loads that sums up to one axle load.

and  $\gamma$  is a velocity factor which is also dependent upon the type of train. Values of  $k$  are given in Table 2.2 and values of  $\gamma$  are given in Table 2.3.

**Table 2.2:** *The track quality factor  $k$  /69/.*

Type of track	k-value
High speed lines Heavily trafficked main lines Suburban lines (e.g., the German 'S-Bahn')	0.15
Less trafficked main lines	0.20
Other lines	0.25

**Table 2.3:** *The velocity factor  $\gamma$  /69/.*

Velocity and train type	Velocity factor $\gamma$
Both passenger and freight trains: $V \leq 60$ km/h	1
Passenger trains: $60 < V \leq 300$ km/h	$1 + 0.5 \cdot \frac{V - 60}{190}$
Freight trains: $60 < V \leq 140$ km/h	$1 + 0.5 \cdot \frac{V - 60}{80}$

By way of example, Table 2.4 gives the design loads for the various track components for typical Norwegian train characteristics. The table is made on the basis of Eqn. (2.1), Table 2.1, Table 2.2 and Table 2.3.

**Table 2.4:** *Design loads according to the German and Austrian method for typical Norwegian trains.  $k_{quasi}$  is assumed to be 1.15 and the line is a heavily trafficked main line (implies  $k = 0.15$ ).*

Track component	Design loads [kN]	
	Passenger train, $V = 100$ km/h, $Q_{nom} = 80$ kN	Freight train, $V = 80$ km/h, $Q_{nom} = 100$ kN
Rails and fastening components ( $t = 3$ )	138	173
Sleepers ( $t = 2$ )	123	154
Ballast, subbase and subgrade ( $t = 1$ )	108	134

### 2.2.2 The North American procedure

In /29/ Hay describes two more or less similar ways of assessing the design loads.

The first of these methods is due to professor Talbot and calculates the design load according to Eqn. (2.2):

$$Q_d = Q_{nom} \cdot \{1 + 0,01 \cdot f_i \cdot (V_{mph} - 5)\} \quad (2.2)$$

where

$$\begin{aligned} V_{mph} &= \text{velocity in miles per hour} \\ f_i &= A_{33}/A_w = \text{the ratio of rail-wheel contact area of a wheel of 33 inches of diameter to a wheel of } w \text{ inches of diameter} \end{aligned}$$

Table 2.5 gives the rail-wheel contact areas for different wheel diameters.

**Table 2.5:** American procedure: Rail-wheel contact areas for different wheel diameters.

Wheel diameter [in.]	28	33	36	38	40	42
Contact area [sq. in.]	0.160	0.190	0.210	0.230	0.240	0.250

Eqn. (2.2) increases the design load with increasing speed, and the relationship also takes into account that smaller wheels exert larger impact loads on the track than larger wheels (the  $f_i$ -factor).

The AREA<sup>1</sup> manual from 1980-81, cited by Hay /29/, uses the following equation:

$$Q_d = Q_{nom} \cdot \left\{ 1 + \frac{D_{33}}{D_w} \cdot \frac{V_{mph}}{100} \right\} \quad (2.3)$$

where

$$\begin{aligned} D_{33} &= 33 \text{ inches (diameter of the reference wheel)} \\ D_w &= \text{diameter of the wheel for which the load is to be calculated} \end{aligned}$$

The formula in Eqn. (2.3) is the same as in AREA Manual for 1996 /2/. The term to the right of the plus sign is often called *the AREA impact factor for track*.

The two formulas Eqn. (2.2) and Eqn. (2.3) are quite similar, while they both differ somewhat from the procedure described in Section 2.2.2.

1. American Railway Engineering Association; from October 1, 1997, reorganised as American Railway Engineering and Maintenance-of-Way Association (AREMA).

### 2.2.3 The British procedure

This procedure from British Rail Research<sup>1</sup>, as described by Hunt /38/, was originally designed to calculate the dynamic load contribution in a dipped rail joint. Based on measurement in the track the total wheel-rail force was modelled as in Figure 2.1 for a particular vehicle.

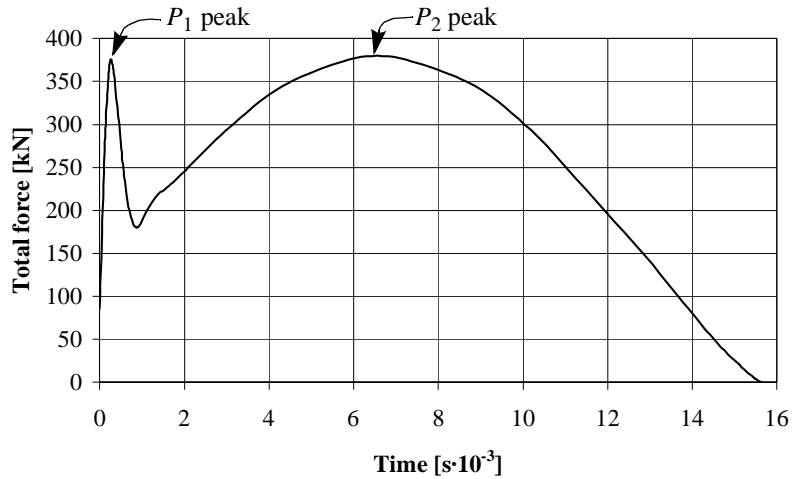


**Figure 2.1:** Predicted wheel rail forces at an idealised dipped joint. Redrawn from /38/.

In Figure 2.1 the  $P_1$  and  $P_2$  are dynamic load contributions associated with certain modes of vibration. In frequency terms  $P_1$  is associated with frequencies greater than 200 Hz, while  $P_2$  is associated with frequencies in the interval 30-100 Hz. The  $P_2$ -forces were found to be particularly damaging to the track, and these forces were adopted by British Rail as a design criterion for vehicles in order to minimise track damage. When damping and track mass terms are neglected the expression for the  $P_2$ -force, in Newtons, reads

$$P_2 = \alpha v \sqrt{K m_u} \quad (2.4)$$

where

- $\alpha$  = dip angle [rad]; for design load purposes this is set to 20 milliradians
- $v$  = vehicle velocity [m/s]
- $K$  = track stiffness [N/m]; this parameter is defined through Eqn. (2.22) and the value lies normally between  $30 \cdot 10^6$  N/m and  $100 \cdot 10^6$  N/m.
- $m_u$  = unsprung mass of the vehicle [kg], usually between 2000-3500 kg.

The total load exerted by the wheel is then

$$Q_d = Q_{nom} + P_2 \quad (2.5)$$

The more sophisticated versions of this procedure take into account more detailed characteristics of the railway vehicle as well as the track structure. For instance, rail profile irregularities can be prescribed in more detail such that idealised or measured track profiles can be studied. The computer code Vampire is a further development of these methods and integrates vehicle and track behaviour. More details on dynamic track models are found in Section 2.11.

1. Now a part of AEA Technology, and renamed AEA Technology Rail.

### 2.2.4 Concluding remarks

The German/Austrian method and the North American method are empirical methods, while the British method is more linked to mathematical solution of a mechanical vehicle-rail system. It is worth noting that all three procedures predict a strong dependence on the vehicle velocity.

For a routine calculation the German/Austrian method may give sufficient accuracy as it differs between passenger and freight trains and also takes into account the track quality to a certain extent. In addition it provides a sound probabilistic philosophy regarding the design process of the different elements in a railway track structure. The method is also easy to use, as the parameters that enter the equations are quite readily accessible. On the other hand, the method is not very specific when it comes to quantifiable train and track characteristics.

The AREA method only takes into account the wheel diameter in addition to the train velocity. Besides, the wheel diameter is not that easy to have reliable information about as the wheel diameter is reduced during its lifetime because of wear and workshop reprofiling.

The British method, in its simple version, requires knowledge about the track modulus and the unsprung mass of the vehicle. The former is not easy to assess without measurement in the track, but such measurements will be necessary if the track is to be modelled mathematically. The unsprung mass is given in the specifications from the rail vehicle manufacturer.

It should also be mentioned that the rail car industry uses sophisticated software packages to analyse track-train interaction where the wheel-rail loads are also calculated [40]. The loads are then a function of track and train characteristics and of the velocity of the train. This way of calculating the wheel-rail forces represents a shift in perspective as these forces are generated as part of the analysis. These forces are thus treated as any other internal forces of the total train-track system and are not explicitly defined prior to analysis.

For the rest of the thesis, when not explicitly mentioned otherwise, the German and Austrian method will be employed whenever a wheel design load is needed. This particular choice was made mainly because of the easy access to the parameters and the appealing differentiating of load levels for the various parts of the track.

## 2.3 The beam on elastic foundation model (BOEF model)

### 2.3.1 Introduction

Given the design wheel loads and some track parameters, the BOEF model may be used to calculate the rail deflection, the rail moment and the rail shear force together with their distribution along the rail. From the rail deflection the foundation pressure, as a line load, may be calculated and from the rail moment the rail bending stress is calculated. With the help of some auxiliary assumptions it is also possible to calculate the rail seat forces and the average vertical stress between the sleeper and the ballast. When it comes to the stress distribution below the interface between the sleeper and the ballast, the method is not suitable.

In a historic view, the BOEF model is by far *The Classic Method* and also forms the backbone of many of the subsequent improvements made to track design. The likely reason for its popu-

larity is that this model has a sound mathematical formulation with a quite clear and simple physical interpretation.

A good historic review on the development of the beam on elastic foundation track model is given by Kerr /48/. It seems that E. Winkler in 1867 was the first to formulate and solve the beam on elastic foundation differential equation (Eqn. (2.7)) for railway track purposes. Other contributors to the early stages of the beam on elastic foundation model are J. W. Schwedler (in 1882, found bending moments in the rail with one concentrated load) and H. Zimmermann (in 1888, solutions for many special cases including a double axle load). When the cross sleeper gradually substituted the longitudinal sleeper, a fundamental question arose whether the cross sleeper design could be analysed using the continuous support assumption of the BOEF differential equation. Investigators like A. Flamache (in 1904), S. Timoshenko (in 1915) and the ASCE-AREA Special Committee on Stresses in the Railroad Track (in 1918-1929, whose reports are often referred to as the 'Talbot reports') used the continuous approach also for the cross sleeper track design. The latter development was supported by the fact that the sleeper spacing decreased as the axle loads were increasing over the years. Other researchers compared analyses of discrete elastic support with the continuous support case. Also measurements in the track were carried out for comparison.

An overview of various techniques of foundation analysis can, among others, be found in Ronald Scott's book 'Foundation Analysis' /71/. This reference offers a broad range of foundation topics, including solutions for beams on elastic foundations.

### 2.3.2 The basics - deflection and moment caused by a single axle load

Since the basic features of the model are well known by most railway engineers only a brief presentation is given here. More elaborate presentations of the model are, among others, given by Hetényi /30/ and Timoshenko /78/, both from a mechanical and mathematical point of view. Eisenmann /18/ presents the model in a more railway-like setting.

The model assumes the rail modelled as an infinite Euler-Bernoulli beam with a continuous, longitudinal support from a Winkler foundation. The concept is illustrated in Figure 2.2.

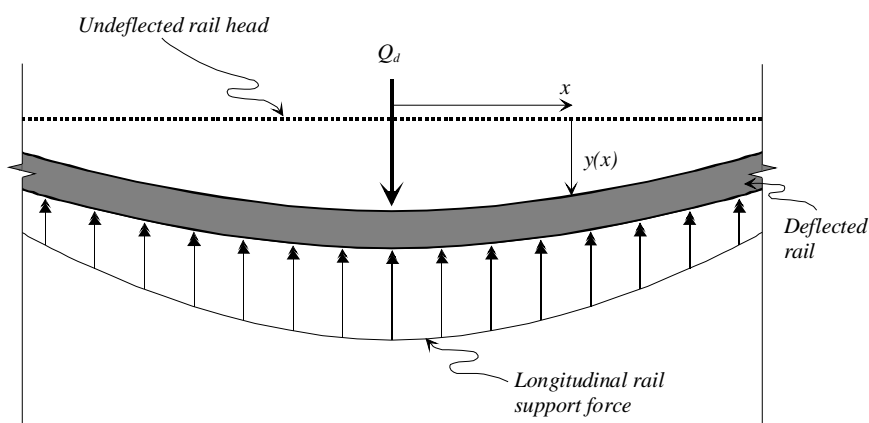


**Figure 2.2:** *Beam on elastic foundation model.*



The Winkler foundation may be regarded as equivalent to an infinite longitudinal line of vertical, uncoupled and elastic springs. This foundation is characterised by the following equation:

$$p(x) = -k \cdot y(x) \quad (2.6)$$

where

$$\begin{aligned} p(x) &= \text{compressive stress exerted on the rail at position } x \text{ [N/mm]} \\ x &= \text{longitudinal coordinate [mm]} \\ k &= \text{track modulus [N/mm}^2\text{]} \\ y(x) &= \text{vertical deflection at position } x \text{ [mm]} \end{aligned}$$

The track modulus can be interpreted as the foundation resisting force per mm when the rail is deflected 1 mm. Esvelde /22/ indicates that a track modulus<sup>1</sup> of 9 N/mm<sup>2</sup> is a poor one, while 90 N/mm<sup>2</sup> is a good track modulus.

It should be noted that in this context a positive  $p(x)$  is directed downward, hence the minus sign in Eqn. (2.6). This makes the sign of  $p(x)$  consistent with that of  $y(x)$ .

By taking the static equilibrium between the distributed force needed to bend the rail and the foundation resisting force according to Winkler one arrives at the following differential equation:

$$EI \frac{d^4 y}{dx^4} + ky = 0 \quad (2.7)$$

where

$$\begin{aligned} E &= \text{Young's modulus of elasticity for rail steel [N/mm}^2\text{] or [MPa], } E = 2.1 \cdot 10^5 \text{ MPa.} \\ I &= \text{moment of inertia of the rail with respect to vertical bending [mm}^4\text{]} \end{aligned}$$

The product  $EI$  is often denoted the *flexural rigidity*.

The boundary conditions may be listed as follows:

- (1)  $y$  approaches zero as  $x$  approaches  $\pm$  infinity
- (2)  $y''$  (the curvature) approaches zero as  $x$  approaches  $\pm$  infinity
- (3) at  $x=0$ ,  $y'=0$
- (4) at  $x=0$  the shear force equals  $0.5Q_d$  for one half of the beam

The solution of Eqn. (2.7) given the boundary conditions above is

$$y(x) = \frac{Q_d}{2kL} e^{-\frac{|x|}{L}} \left( \cos\left(\frac{x}{L}\right) + \sin\left(\frac{|x|}{L}\right) \right) \quad (2.8)$$

where

$$\begin{aligned} x &= \text{longitudinal coordinate with its origin at the point where the design load is applied [mm]} \\ L &= \text{a parameter often denoted the 'characteristic length' [mm], explained by the following expression} \end{aligned}$$

---

1. Esvelde /22/ uses the term *foundation coefficient* for what herein is called track modulus.

$$L = \left( \frac{4EI}{k} \right)^{1/4} \quad (2.9)$$

Some cross sectional data for some rail profiles in common use in Norway are tabulated in Table 2.6 below.

**Table 2.6:** *Cross sectional area, moment of inertia, height from base to neutral axis and mass per meter for some rail profiles in use in Norway, /66/.*

Rail profile	Cross sectional area [mm <sup>2</sup> ]	Vertical moment of inertia [mm <sup>4</sup> ]	Height from base to neutral axis [mm]	Mass per meter [kg/m]
S49	6297	1.819·10 <sup>7</sup>	73.3	49.43
S54	6948	2.073·10 <sup>7</sup>	75.0	54.54
S64	8270	3.252·10 <sup>7</sup>	80.61	64.92
UIC54	6934	2.346·10 <sup>7</sup>	77.5	54.43
UIC60	7686	3.055·10 <sup>7</sup>	80.95	60.34

The reason for the absolute value signs in Eqn. (2.8) is that the deflection for physical reasons has to be symmetric with respect to the axis through which the load acts, i.e.  $x=0$ , for a single axle load.

As a modification of Eqn. (2.7) one may use dimensionless variables. Among others, this was the approach of Tsai and Westmann /79/ when solving the BOEF problem when there is no tension between the sleeper and the foundation.

An alternative to a deflection based approach is to use the *rail moment* as the primary variable in the governing differential equation, Eqn. (2.7), as indicated by Scott /71/.

The rail moment is obtained by twice differentiating the expression for the deflection, i.e. Eqn. (2.8), and multiplying the result with  $EI$ :

$$M(x) = \frac{Q_d \cdot L}{4} \cdot e^{-\frac{|x|}{L}} \cdot \left( \cos\left(\frac{x}{L}\right) - \sin\left(\frac{|x|}{L}\right) \right) \quad (2.10)$$

When the rail moment is known, an estimate of the rail tensile or compressive stresses along the cross sectional symmetry line may be calculated according to the well-known formula

$$\sigma(x) = \frac{M(x)}{I} \cdot h_n \quad (2.11)$$

where  $h_n$  is the distance from the neutral axis. To assess the stresses to a more accurate degree it is important to know the residual (initial) stress distribution, the effect of the rail geometry and longitudinal contributions like temperature stresses and train braking stresses. A more detailed, 'non-FEM'-calculation of rail stresses is described by Esveld /22/.

### 2.3.3 Finding the rail seat load

The rail seat loads between the rail and the sleepers will be of interest as these forces are the cause of the stresses in the ballast layers and in the subgrade. Often the task of finding the rail seat load is considered to be trivial using the following very straightforward expression (as, e.g., Hay /29/ does):

$$S_n = p_n \cdot c = k \cdot y_n \cdot c \quad (2.12)$$

where

$$\begin{aligned} S_n &= \text{rail seat load for sleeper no. } n \text{ [N]}, \\ n &= \text{sleeper no. } n, \\ p_n &= \text{pressure per unit length of rail for sleeper no. } n \text{ [N/mm]}, \\ y_n &= \text{deflection for sleeper no. } n \text{ [mm]}, \\ c &= \text{sleeper spacing [mm]}. \end{aligned}$$

Eqn. (2.12) takes the deflection of each sleeper as a mean value representing the rail length half-way to the neighbouring sleeper on either side. In this way Eqn. (2.12) may be said to be *deflection consistent* because the seat load is calculated on the basis of the BOEF deflection at the coordinate where the sleeper is positioned. However, the shape of the deflection curve (according to Eqn. (2.8)) indicates that the sleeper deflections will *not* exactly be representative for the surrounding rail section. From simple calculus it can be shown that the deflection at the sleeper position is bigger (in absolute value) than the average deflection (taken over a section midway to the neighbouring sleepers) in regions where the second derivative of the deflection is negative<sup>1</sup>. Obviously, in regions where the second derivative is positive the opposite is true. This corresponds to an overestimation of the seat forces for sleepers positioned under or near the wheel load, and an underestimation for sleepers positioned somewhat farther away. In addition, large relative errors in seat loads may be found for sleepers positioned near the points where the calculated deflection is zero. Because most of the load is transferred to the sleepers nearest to the wheel, the net effect in most cases is that the sum of the seat loads will exceed the value of the wheel load and therefore static equilibrium is violated.

If one still assumes lumping of the forces to the sleeper to be justified, the exact (in terms of BOEF theory) expression that satisfies static equilibrium reads

$$S_n = k \cdot y_{max} \cdot \int_{x_n - 0.5c}^{x_n + 0.5c} e^{-\frac{|x|}{L}} \cdot \left( \cos\left(\frac{x}{L}\right) + \sin\left(\frac{|x|}{L}\right) \right) dx \quad (2.13)$$

where

$$\begin{aligned} y_{max} &= \text{maximum rail deflection as given by Eqn. (2.8) with } x=0 \text{ [mm]}, \\ x_n &= \text{coordinate of sleeper no. } n \text{ [mm]}. \end{aligned}$$

Kerr /48/ argues that Eqn. (2.13) is the correct one, while Eqn. (2.12) is an approximation. In Marquis et al. /57/ the expression in Eqn. (2.13) has also been used.

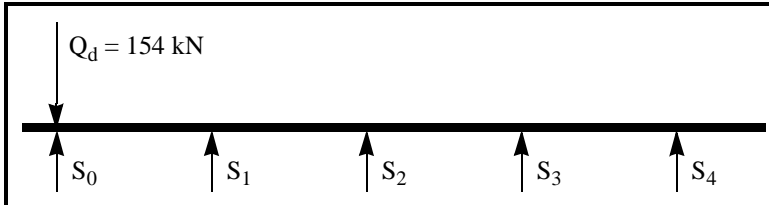
Evaluation of the integral in Eqn. (2.13) may be done with the help of appropriate computer software<sup>2</sup>. Alternatively, one could use numerical integration techniques (e.g. Simpson's rule, Gaussian quadrature). (An analytical solution does exist but is lengthy and separate expressions

1. Here, the deflection is taken to be positive in the downwards direction (as in Eqn. (2.8)).

must be developed when the integral is to be evaluated on an interval with the origin in the interior.)

However, the deviation of the deflection consistent expression in Eqn. (2.12) from the *static equilibrium consistent* expression in Eqn. (2.13) is in most cases acceptable and the former equation should be preferred because of easier calculations. Moreover, the maximum seat force as calculated by Eqn. (2.12) is slightly higher than the static consistent solution and therefore on the safe side. In Table 2.7 the two methods are compared for a given wheel load.

**Table 2.7:** Example of numerical comparison between design seat loads as calculated by the 'standard method' (Eqn. (2.12)) and the 'lumping' method (Eqn. (2.13)). The design load corresponds to that of a typical freight train and is the same as in Table 2.4. The sleeper spacing is assumed to be 600 mm.



Track modulus [N/mm <sup>2</sup> ]	Method	Seat loads [kN] and % deviation from 'lumped' value									
		$S_0$	%	$S_1$	%	$S_2$	%	$S_3$	%	$S_4$	%
Soft $k=30$	Std.	48.0	2.8	35.9	0.56	17.5	-1.6	4.87	-5.8	-0.778	-30
	Lump.	46.7		35.7		17.7		5.17		-0.598	
Medium $k=90$	Std.	63.2	4.8	39.3	-0.11	11.3	-6.0	-0.814	-110	-2.68	-4.5
	Lump.	60.3		39.4		12.1		-0.388		-2.57	
Stiff <sup>a</sup> $k=150$	Std.	71.8	6.1	39.5	-0.91	7.40	-12	-2.65	-18	-2.39	-1.6
	Lump.	67.7		39.9		8.40		-2.24		-2.35	

- a. In practise a  $k$ -value of 150 N/mm<sup>2</sup> may not be obtainable when soft rubber pads are installed between the sleepers and the rails.

As can be seen from Table 2.7 the maximum seat loads,  $S_0$ , are found to be more or less the same for the two methods. On the outskirts of the deflected section the two methods may come up with quite different predictions.

To sum up this section, it is not a trivial task to calculate the rail seat forces accurately, although reasonable results may be obtained for the four to five sleepers nearest to the single axle wheel load<sup>1</sup>. In the case of Eqn. (2.12) the rail seat forces are consistent with the deflection at their

2. The author has made use of Mathcad PLUS 6.0 Professional Edition, a product from MathSoft, Inc. Throughout the present chapter either the abovementioned product or Microsoft Excel 97 spreadsheet has been used for the numerical calculations.

locations (according to Winkler, Eqn. (2.6)), but static equilibrium is not fully satisfied. Eqn. (2.13) predicts rail seat forces that sums up correctly to the applied design wheel load, but the trade off is that the forces are not consistent with the predicted deflections at the positions of the sleepers. These difficulties are fundamentally connected to the usage of a *continuous* deflection model to assess *discrete* rail seat forces. To overcome these shortcomings it is necessary to leave behind the BOEF model and model the track with more discrete rail support. Models with discrete support are described in Section 2.9.

### 2.3.4 Multiple axle loads

The fact that the BOEF model is linear allows us to superpose two or more axle loads and calculate the deformations and reactions as a sum of the corresponding values produced by each load individually. As an example, the resulting deflection at the point of interest, which for convenience is assigned the coordinate  $x=0$ , is given by

$$y_{res} = y(x_1) + y(x_2) + \dots + y(x_i) \quad (2.14)$$

where

$$\begin{aligned} y_{res} &= \text{the resulting deflection} \\ x_i &= \text{the coordinate of axle no. } i \end{aligned}$$

The resulting values of the rail moment and the rail seat loads may be calculated by expressions similar to Eqn. (2.14). It should also be pointed out that multiple axle loads do not add more complexity to the model as compared to the single axle load case (apart from an adding procedure as in Eqn. (2.14)). This is due to the linearity of the model.

For convenience influence coefficients are sometimes introduced for deflection and rail moment. These are simply the damped wave part of the corresponding full expressions of Eqn. (2.8) and Eqn. (2.10). For the rail deflection the influence coefficient reads

$$\eta(x_i) = e^{-\frac{|x_i|}{L}} \left( \cos\left(\frac{x_i}{L}\right) + \sin\left(\frac{|x_i|}{L}\right) \right) \quad (2.15)$$

The corresponding influence coefficient for the rail moment is

$$\mu(x_i) = e^{-\frac{|x_i|}{L}} \left( \cos\left(\frac{x_i}{L}\right) - \sin\left(\frac{|x_i|}{L}\right) \right) \quad (2.16)$$

Because of the oscillating nature of the deflection and moment there are in fact combinations of axle spacings, track moduli and rail flexural rigidities ( $EI$ ) that will reduce the maximum values of deflection and rail moment compared with the single axle case. It may be shown that the maximum reduction for a double axle bogie is approx. 21% for the moment at an axle spacing of  $0.5 \cdot \pi L$ , and for the deflection a maximum reduction of about 4.3% is obtained at an axle spacing of  $\pi L$ .

---

1. Combined number of sleepers on both sides of a single axle load.

### 2.3.5 Fictitious longitudinal sleepers and foundation coefficient

Because the formation of the differential equation, Eqn. (2.7), assumes a continuous foundation support it may be reasonable to ask if there is a way to single out the effect of various geometric sleeper properties (i.e. sleeper dimensions and sleeper spacing) from the effect of track resiliency. The traditional answer to this is to transpose the cross sleepers into two fictitious longitudinal sleepers, one under each rail, as illustrated in Figure 2.3. The idea is that per unit length of track the area giving support to the load should be the same after the transition to longitudinal sleepers.

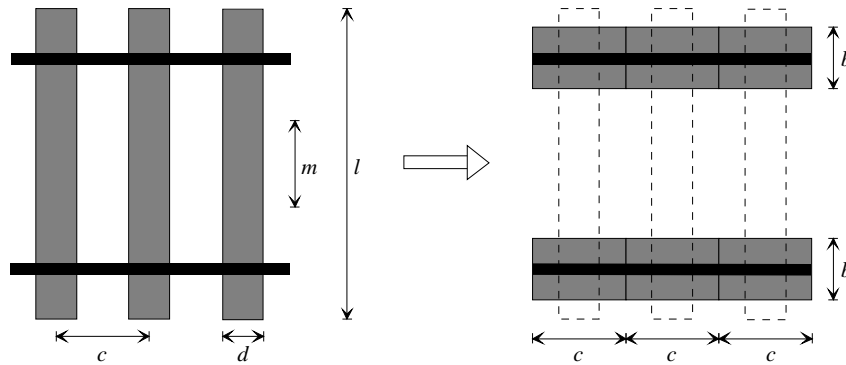


**Figure 2.3:** Transition of cross sleepers into longitudinal sleepers.

Referring to Figure 2.3 the expression for the width,  $b$ , of the longitudinal sleeper is

$$b = \frac{d \cdot (l - m)}{2c} \quad (2.17)$$

where

- $d$  = width of each cross sleeper [mm]
- $l$  = length of each cross sleeper [mm]
- $m$  = length of an assumed unsupported area in the middle of the sleepers [mm]
- $c$  = sleeper spacing [mm]

From a numerical example provided by Eisenmann /18/  $m$  has been assigned a value of 500 mm, but no reason for this particular value is given<sup>1</sup>. A common way to bring some justification to the assumption of an unsupported area is that most of the pressure underneath the sleepers is transferred within the tamped zones, which are located in the vicinity of the rails.

The vertical stress between the sleeper and the ballast for sleeper no.  $n$ , i.e.  $\sigma_n$ , may then be assessed through the expression below, assuming a uniform stress distribution:

$$\sigma_n = \frac{S_n}{b \cdot c} \quad (2.18)$$

1. For twin block sleepers  $m$  should be taken as the length of the connecting steel rod, which should produce more accurate results.

The foundation coefficient  $C$  (with units of  $\text{N}/\text{mm}^3$ ) is defined through the following equation:

$$k = b \cdot C \quad (2.19)$$

In this way the track modulus,  $k$ , is separated into two factors: The longitudinal sleeper width,  $b$ , which accounts for sleeper shape, sleeper spacing and length of unsupported area, while the foundation coefficient,  $C$ , accounts for the resilient properties of the rail pads, sleepers, ballast and subgrade. This split-up makes it possible to separate the effect of changing geometric sleeper properties, including sleeper spacing, from that of changing the resilient properties. This may be convenient in some instances, and in all expressions where the track modulus  $k$  occurs the product  $b \cdot C$  may be used instead.

It should be emphasised that the longitudinal sleeper is only meant to transfer vertical loading, and do not in any way improve the ability of the superstructure to take shear loads or moments. Thus the concept of a 'longitudinal sleeper' is not so much of a real sleeper as of a continuous longitudinal support in the vertical direction.

### 2.3.6 Finding the track modulus

Among others, Selig and Li /73/ and Cai et al. /7/ have described methods for measuring the track modulus  $k$ . The various methods may be categorised as follows:

- (1) Deflection basin test,
- (2) Single axle load test,
- (3) Multiple axle load test, and
- (4) Calculation with the help of other analytical or numerical methods.

**Deflection basin test.** This method is based on the vertical equilibrium of the rail. Allowing multiple axle loads the expression reads

$$\sum_i Q_{di} = \int_{-\infty}^{\infty} p(x) dx = k \int_{-\infty}^{\infty} y(x) dx \quad (2.20)$$

where the left side sums up the design axle loads. The track modulus,  $k$ , is assumed constant.

The integral on the very right side of Eqn. (2.20) expresses the deflection basin area that may be estimated by measuring the deflection of the loaded sleepers taking into account the sleeper spacing. The track modulus is then calculated as

$$k = \frac{\sum_i Q_{di}}{c \sum_{n=1} y_n} \quad (2.21)$$

where  $y_n$  is the deflection of sleeper no.  $n$  and  $c$  is the sleeper spacing.

To improve the accuracy of the method one could take into account only the portion of the load-deflection curve that surrounds the load level for which the calculated  $k$  is to be used. In this case one should subtract the lower load limit and the corresponding deflection basin area from

the equation above. In this way a more representative tangent modulus is obtained from a generally non-linear load-deflection relationship. One major reason for non-linearity of the load-deflection curve is slack in the track, i.e., some sleepers are not in good contact with the ballast (due to, e.g., settlements or inappropriate tamping), and a soft response is expected until those sleepers are pressed down to firm contact. A second reason is that most of the track materials do not in general respond linearly to applied load.

This test requires a large number of sleeper deflection measurements and is therefore quite time-consuming. In addition, as seen for seat load calculations, the accuracy may not necessarily be improved when deflections for more distant sleepers are taken into account, although this can be necessary to satisfy vertical equilibrium. A benefit is that the model is applicable for both single and multiple axle loads.

**Single axle load test.** This test requires only deflection measurements directly beneath a single axle load. In this way a *track stiffness*,  $K$ , may be calculated as follows:

$$K = \frac{Q_d}{y_{max}} \quad (2.22)$$

To account for non-linearity the equation may be revised such that a representative tangent modulus is calculated.

From BOEF theory it can then be shown that the track modulus is calculated as:

$$k = \frac{K^{\frac{4}{3}}}{4 \cdot (EI)^{\frac{1}{3}}} \quad (2.23)$$

where  $EI$ , as before, is the flexural rigidity of the rail.

This method is a simple and efficient one, and performed with some care it should produce reliable results at least for cars equipped with single axles. For cars with trucks the method may be of more questionable accuracy.

**Multiple axle load test.** This method may be seen as an extension of the 'single axle load test' to multiple axle loads. The following iterative procedure is referenced in Cai et al. /7/ and is originally due to Zarembski and Choros /88/:

$$\left| k - \frac{1}{2y_{max}L} \sum_{i=1}^n Q_{di} \eta_i \right| \leq \varepsilon \quad (2.24)$$

where  $\varepsilon$  is a prescribed error of tolerance and  $\eta_i$  is the deflection influence coefficient described by Eqn. (2.15). Note that also  $\eta_i$  is a function of  $k$ .

Also Eqn. (2.24) should be possible to modify such that a more realistic tangent modulus is calculated in case of a non-linear load-deflection relationship.

An alternative to Eqn. (2.24) is to use the BOEF deflection expression for a multiple axle load directly (Eqn. (2.14)) and compare with the measured deflection. One may then iterate on  $k$  until



the two deflections match. The iterations, whether you iterate on Eqn. (2.24) or Eqn. (2.14), are best carried out using computer software, e.g. a spreadsheet.

**Calculation with the help of other analytical or numerical methods.** This group of methods may at first seem superfluous as the track modulus is of limited interest when the BOEF model is not the one to use. In fact, what actually constitutes the concept of track modulus is the BOEF track model. Other track models may be able to calculate the various quantities of interest with no help of the BOEF track modulus. Non the less, a calculated track modulus may be valuable as a quick way of comparing foundation properties of alternative track designs as the track modulus concept is well known to most track design engineers.

The easiest way to find a track modulus from a track model is perhaps to take the calculated deflection together with the applied load as input parameters to the 'single axle load test' equations, alternatively the 'multiple axle load test' equations. In this way the calculated track modulus will be *deflection consistent*, i.e. the predicted deflection will be the same for the BOEF model as for the model initially used for calculating the deflection. This will be a reasonable approach if the  $k$ -value is to be used for deflection calculations.

If the  $k$ -value is to be used for rail moment or seat load calculations it will be more natural to take the calculated rail moments or seat loads as a starting point for calculating the corresponding  $k$ -value consistent with these quantities.

One way of calculating the track modulus is explicitly mentioned here since it may have some practical interest. This method calculates  $k$  as a function of the Young's modulus and the Poisson's ratio. Scott /71/ describes several methods for this, on the basis of work done by Biot, Vesic, Vlasov and Levontiev.

Biot and Vesic have found solutions for an infinite beam resting on a homogenous, linearly elastic and three dimensional continuum and loaded with a point load. Vesic found the following relation for  $k$ :

$$k = \frac{0.65E_f}{1 - \nu_f^2} \cdot \left( \frac{E_f b^4}{EI} \right)^{\frac{1}{12}} \quad (2.25)$$

where

- $E_f$  = Young's modulus for the foundation material
- $\nu_f$  = Poisson's ratio for the foundation material
- $b$  = is the beam width, or fictitious beam width

The difference between a continuum solution compared to a BOEF solution with  $k$  as in Eqn. (2.25) is according to Vesic generally less than 10 percent. Equation Eqn. (2.25) provides an approximate general relation between the foundation parameters, and there is therefore a potential of improving the relation if one wants more accurate correspondence between the two models for a selected track reaction. The cost is then of course that there are different expressions for  $k$  for the various track reactions. Scott provides an example taken from Biot of what  $k$  should be if the maximum moments should be identical in the two models.

In the model of Vlasov and Leontiev  $k$  is given by

$$k = \frac{E_f (1 - \nu_f) b}{(1 + \nu_f)(1 - 2\nu_f)} \int_0^{\infty} (g')^2 dz \quad (2.26)$$

where  $g$  is the assumed function describing the variation of vertical displacement with depth in the foundation layer.  $g$  could for instance be a linearly decreasing function or an exponential decreasing function. The foundation layer may be either finite or infinite in depth. The  $E_f$  and  $\nu_f$  describe the material properties of the foundation in a plane strain problem.

### 2.3.7 Some comments about predictability

Since the BOEF-model is used to calculate a  $k$ -value, one should not be surprised if one gets nearly the same deflections from the BOEF model as from measurements in the track. This is especially so if the  $k$ -value at that location has been measured with nearly the same axle load. Such agreeing results are not, however, to be interpreted as the BOEF model being a good model with a high degree of predictability. In fact, when using the same method for measuring the  $k$ -value and the deflection (or possibly another track reaction), one has lost much of the strength of predicting the overall track behaviour. Such an exercise is therefore very close being tautological, much like a circular definition. On the other hand, one could gain some insight into the *repeatability* if the calculated result is checked against one or more measurements.

If a track model should display a high degree of predictability, it should be able to predict a particular reaction in the track from a means of testing that do not involve measuring the same reaction in the track. For instance, measure the material or component properties in the laboratory and then calculate the response in the track with an appropriate track model. If the reactions in the track as calculated from the track model coincides with the reactions measured in the track, the track model may have a high degree of predictability, but many such tests have to be carried out to be reasonably sure of the method's predictability. Another possible course to follow is to use a track modulus consistent with a particular reaction to calculate another reaction. By way of example, use a *deflection* consistent  $k$ -value when calculating the BOEF rail stress. Compare this calculated value with the measured rail stress. If the BOEF model is really predictive the calculated and the measured stresses should be similar. As can be deduced from this, the main point for real and strong predictability is not to use the very same equation or procedure for calculating a needed parameter and to predict a reaction when the input parameters are else the same.

The comments above place strong requirements on a model to be really predictive. From a theoretical and modelling point of view these requirements are the ideal ones. This is of course also beneficial for the practising engineer, but the practitioner may see this different. She may very well be satisfied with using a deflection consistent  $k$ -value for calculating the maximum deflection as long as the calculated value does not deviate too much from a 'real' (measured) one. In fact, she may get very good results if she happens to have the same load as when the  $k$ -value was measured. But then she does not really need a  $k$ -value, as the original deflection measurement (made to calculate  $k$ ) will suffice. The crucial question is rather what range of loads that could be used while still maintaining a certain accuracy. Therefore,  $k$ -values are even more valuable if the measured track reactions (at least the deflection) and load values are given along with the track moduli. Only then qualified extrapolation may be done.

After all, it is the actual loads and the corresponding real track reactions that are the most valuable quantities, everything else is interpretation. If loads and track reactions are given you also have a possibility of using alternative models if the track design is known. Also, if possible, re-

cordings of the variation of the  $k$ -value (along with corresponding loads and track reactions) through the seasons are most valuable.

### 2.3.8 Limitations of the BOEF model

In addition to the fundamental problem of circular definition when measuring  $k$  there are several more evident limitations that are inherent in the BOEF model. It is important to be aware of these restrictions in an actual design process in order to avoid using the method in situations where it is not appropriate. The most prominent aspects that can be questionable may be described as follows:

**Continuous foundation.** This is a consequence of the formulation of the governing differential equation (Eqn. (2.7)) where a continuous foundation is assumed. Assuming a conventional track design, the rails are discretely supported by the sleepers. As described in Section 2.3.3 this discrete support may cause some trouble when considering the seat loads at some distance from the wheel load. In the vicinity of the load the results are reasonable if the track is not too stiff (with a  $k$  exceeding that of Table 2.7) or if the sleeper spacing is not too wide. The latter effect is also pointed out by Timoshenko /78/.

**Tensile stresses possible.** In those parts of the track that experience upward deflection<sup>1</sup> tensile forces will develop in the foundation according to the BOEF model. This is because we have only made an assumption about resilience, according to Winkler, and not made any reservations concerning the development of tensile stresses. However, by enforcing a non-tensile-stress material model we would have introduced serious trouble because we will then not know *a priori* which parts of the track ladder that are in contact with the foundation. The problem then becomes nonlinear, and is more difficult to solve, see Section 2.5. However, in an actual track construction there might, to a limited extent, be some justification for elastic tensile stresses. Two reasons may be given: The trapezoidal cross-sectional shape of most concrete sleepers, being wider at the base than at the top, may cause uplift of some of the crib ballast material which return into place without loss of energy when the train has passed<sup>2</sup>. This adds weight to the track ladder and may to a certain degree be considered as equivalent tensile forces. Secondly, which probably is a bigger effect, there are small elastic shear strains developing on the interface between the sleepers and the crib ballast and also within the crib ballast itself. The combined effect of these two mechanisms is probably not very big, but together with the dead weight of the track ladder the effect may be sufficient to avoid the development of uplift relative to the original BOEF model (with zero track ladder weight).

**The response of the track is assumed linear.** This is according to Winkler, Eqn. (2.6). Generally speaking, geomaterials do not behave linearly, and the same is also true for most pad and sleeper materials. For frictional materials a hardening behaviour is expected, and for some cohesive materials a softening behaviour is expected. Since most railway tracks are ballasted a hardening behaviour is anticipated. Another factor contributing to the non-linear behaviour is slack (free play) between the sleepers and the ballast as briefly discussed in Section 2.3.6. The slack will cause a hardening behaviour of the track.

**Material behaviour only in the vertical direction - no stress distribution can be predicted.** The Zimmermann method is a one-dimensional model, i.e. it takes into account only the reac-

1. These zones are located periodically out from the point of load application. It can be shown that the period is  $2\pi L$ , and the first tensile zone is at  $x \in \langle 3\pi L/4, 7\pi L/4 \rangle$ .
2. This presumes that no ballast material falls into the gap developing underneath the sleepers during train passage so that the sleepers return exactly into their initial positions.

tions and deflections in the vertical direction. As a consequence the model is not in a position of predicting anything else than the vertical line load  $p(x)$ , or the foundation vertical stress  $\sigma(x)$  if the fictitious longitudinal sleeper width  $b$  is taken into account. However,  $\sigma(x)$  is often assumed constant in the transversal direction. If a constant stress approach is adopted, which in this context is a simple auxiliary theory of stress distribution, the stress between the rail and the pad may be calculated on the basis of contact area.

**Shear deformation in the rails is not included.** These deformations are small compared to the bending deformation. To account for the shear deformation one could use the Rayleigh-Timoshenko beam instead of the Euler-Bernoulli beam.

**Continuously welded rails (CWR) are assumed.** This assumption justifies the ability of the bending moment to be transferred in the rails. However, it is possible to account for the effect of joints, and Esveld /22/ has the expressions for such a track.

**The weight of the rails and sleepers is assumed to be zero.** The plausible reason for this is that the weight of the track ladder will be negligible compared to the forces exerted by the rolling stock. Nevertheless, the effect can easily be taken into consideration by reformulating the governing differential equation:

$$EI \frac{d^4 y}{dx^4} + ky = q \quad (2.27)$$

where  $q$  [N/mm] is the constant line load equivalent to half of the combined weight of the rails and the sleepers. (The *half* makes the equation comply with earlier definitions).

The particular solution of this non-homogenous differential equation is simply given by the constant function  $y = q/k$  so that the general solution is

$$y_q(x) = \frac{q}{k} + \frac{Q_d}{2kL} e^{-\frac{|x|}{L}} \left( \cos\left(\frac{x}{L}\right) + \sin\left(\frac{|x|}{L}\right) \right) \quad (2.28)$$

The particular part of the solution ( $q/k$ ) represents a downward rigid body motion that does neither produce any extra rail moment nor rail stress. Normally the particular part will at most add a few tenths of a millimetre to the deflection.

According to Eqn. (2.28) it may be shown that no tension will occur (i.e.  $y(x) \geq 0 \forall x$ ) if  $q \geq 0.5e^{-\pi} \cdot Q_d/L$  ( $\approx 0.022 Q_d/L$ ). This condition is satisfied in most cases when we are considering common nominal wheel loads on a track with concrete sleepers. Making the evaluation for a design wheel load (taking into account quasi-static and dynamic contributions) may not produce the same conclusion.

**No time dependence.** Finally it may be worth noting that the BOEF model says nothing about time dependent or dynamic behaviour of the track. It is evident that the track is subjected to dynamic loading when trains pass over it, and especially so if the train speed is high and the foundation is soft. A few aspects of dynamic behaviour are discussed in Section 2.11.

## 2.4 The sleeper as a beam on elastic foundation

The sleeper, being of finite length, may also be analysed as a beam on elastic foundation. This will make it possible to more accurately assess the sleeper deflection, the vertical stress distribution between the bottom of the sleeper and the ballast, and also the moment and shear distribution in the sleeper itself. The general procedure is developed by Hetényi /30/ and also described by Timoshenko /78/.

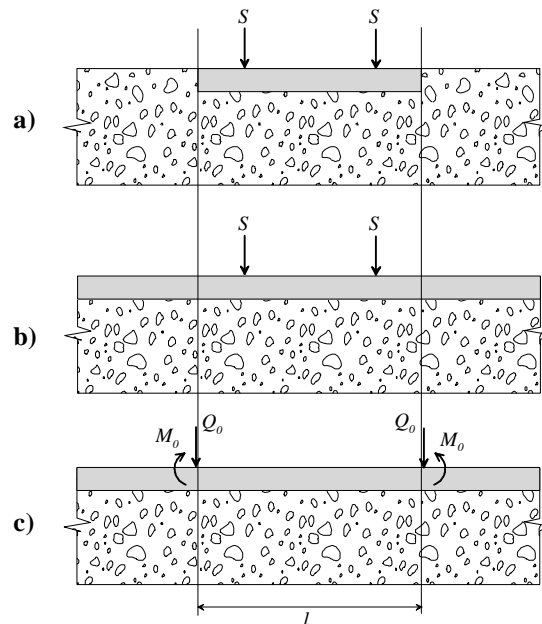


**Figure 2.4:** *Modelling of a sleeper as a beam on elastic foundation (redrawn from /78/). a) Original problem. b) Loads on an infinitely long beam. c) End conditioning force  $Q_0$  and end conditioning moment  $M_0$  applied to the infinite beam.*

Referring to Figure 2.4 the original problem in a) is viewed as a sum of the two problems in b) and c) in the following way:

- (1) First calculate the reactions on an infinitely long beam subjected to the two seat loads  $S$ , as in Figure 2.4 b).
- (2) Calculate the shear forces and the bending moments in the infinite beam at the positions of the sleeper ends.
- (3) Find the end-conditioning forces<sup>1</sup>  $Q_0$  and  $M_0$  by requiring that the total shear force and moment should be zero at the sleeper ends (free ends).
- (4) The sleeper reaction is then a superposition of the reactions of the seat loads and the end-conditioning forces.

The end-conditioning forces are thus imposed to ensure that the middle portion of the infinite beam, i.e. the sleeper, behaves as if it was a beam of finite length. Formally, these end-conditioning forces are applied outside the positions of the sleeper ends on the infinite beam, but still infinitely close to the sleeper ends. The equations involved are given in /30/ and /78/.

1. The term *end-conditioning forces* is used by Hetényi /30/.

A numerical example will be given. Consider a concrete sleeper with  $E=40$  GPa,  $I=2.2 \cdot 10^8$  mm<sup>4</sup>, length  $l=2600$  mm and width  $d=280$  mm. This corresponds approximately to the Norwegian NSB95 sleeper. The sleeper pad has a stiffness of 70 kN/mm, which corresponds to that of a frequently used sleeper pad /28/. The vertical stress distributions beneath the sleeper will be calculated for the loads and track moduli of Table 2.7 on page 13.

To find the  $k$ -modulus for the sleeper (not the same as the track modulus) when the total track modulus is given, one may use a simplification based on linear springs coupled in a series. An assumption is made that only the sleeper pad and the foundation below the sleeper provide vertical resiliency in the structure. Looking at one half of the sleeper, the foundation modulus for the sleeper,  $k_{sleeper}$ , is given by

$$k_{sleeper} = \frac{2c}{l} \cdot \frac{k \cdot K_{pad}}{K_{pad} - k \cdot c} \quad (2.29)$$

where

- $c$  = sleeper spacing
- $l$  = sleeper length
- $k$  = track modulus
- $K_{pad}$  = sleeper pad stiffness

Referring to Table 2.7, the numerical values of  $k_{sleeper}$  are 18.6 N/mm<sup>2</sup> and 182 N/mm<sup>2</sup> for the soft ( $k=30$  N/mm<sup>2</sup>) and medium ( $k=90$  N/mm<sup>2</sup>) track, respectively. For the stiff track ( $k=150$  N/mm<sup>2</sup>) the value of  $k_{sleeper}$  turns out to be negative which indicates that the pad is so soft that such a high overall track modulus would not be possible.

The design loads are taken as the maximum seat loads in Table 2.7, i.e. 48.0 kN for the soft track and 63.2 kN for the medium track. After calculating the deflection, the stresses are calculated by using the Winkler equation (Eqn. (2.6)) and dividing by the sleeper width. The results for the vertical stresses under the sleeper are shown below in Figure 2.5.

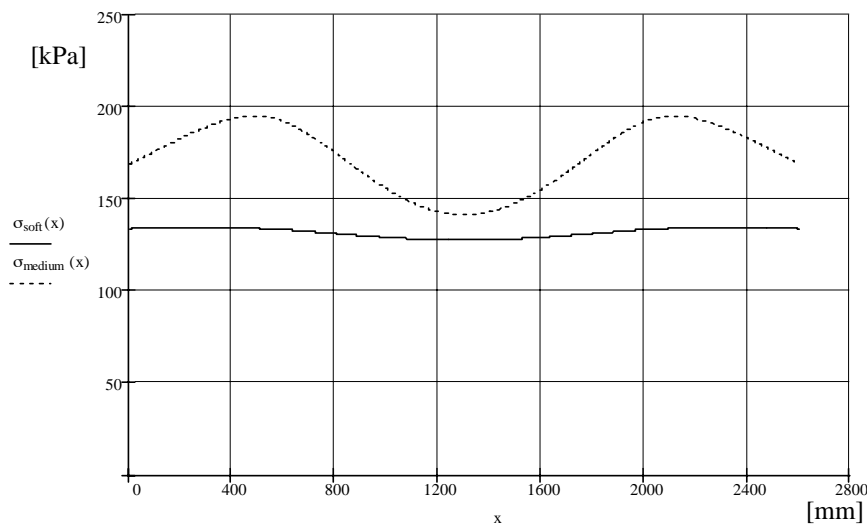


**Figure 2.5:** Vertical stresses between a concrete sleeper and the underlying ballast for a soft track and a medium stiff track. The needed data are given in the text.

From Figure 2.5 it can be deduced that the vertical stresses below the sleeper are more concentrated when the track is stiffer. Also, the overall stress level is higher because of bigger seat loads when the track as a whole is stiffer.

## 2.5 Tensionless BOEF models found in the literature

As described in Section 2.3.8 the BOEF model tacitly assumes that tensile stresses can develop in exactly the same way as compressive stresses on the interface between the sleepers and the rest of the foundation. Since this cannot be physically valid for granular materials, there is a need for tensionless track models. Such models are nonlinear since the length of the contact zone cannot be known in advance and will vary dependent upon the size of the load.

Among others, Tsai and Westmann /79/ and Adin et al. /1/ have described tensionless models based on a Winkler foundation. The two models differ a bit in mathematical approach.

### 2.5.1 Model according to Tsai and Westmann

Tsai and Westmann /79/ arrive at the following differential equation (which is slightly modified to comply with earlier definitions in this thesis):

$$EI \frac{d^4 y}{dx^4} + ky = q + kyH(-y) \quad (2.30)$$

where  $H(\cdot)$  is the Heaviside step function.

When evaluating  $H(-y)$  we notice that  $H(-y) = 0$  when  $-y < 0$ , which occurs when  $y > 0$ . In other words, we get back Eqn. (2.27) when the deflection is positive, i.e. downward.  $H(-y)$  is equal to 1 when the deflection is negative, i.e. upward. In this case the  $ky$  factor cancels from the equation and we arrive at the ordinary beam equation with no continuous support.

Eqn. (2.30) is solved with the help of Green's function, and Tsai and Westmann /79/ arrive at the following general solution for a single axle load (somewhat modified from their dimensionless solution):

$$y(x) = \frac{q}{k} + \frac{Q_d}{2kL} \cdot e^{-\frac{|x|}{L}} \cdot \left( \cos\left(\frac{x}{L}\right) + \sin\left(\frac{|x|}{L}\right) \right) + \frac{1}{2L} \int_{-\infty}^{\infty} e^{-\frac{|x-\xi|}{L}} \cdot \left( \cos\left(\frac{x-\xi}{L}\right) + \sin\left(\frac{|x-\xi|}{L}\right) \right) \cdot y(\xi) \cdot H(-y(\xi)) d\xi \quad (2.31)$$

where  $\xi$  is a parameter introduced through Green's function.

The numerical solution of Eqn. (2.31) is obtained by successive approximations. The zeroth approximation is taken as the classic solution as given by Eqn. (2.28). Higher order approxima-

tions follow by successive substitution. Recognising  $\eta(\cdot)$  as the influence coefficient for the deflection from Eqn. (2.15) we get:

$$\begin{aligned}
 y_0(x) &= \frac{q}{k} + \frac{Q_d}{2kL} \cdot \eta(x) \\
 y_1(x) &= y_0(x) + \frac{1}{2L} \int_{-\infty}^{\infty} \eta(x-\xi) \cdot y_0(\xi) \cdot H(-y_0(\xi)) d\xi \\
 y_2(x) &= y_0(x) + \frac{1}{2L} \int_{-\infty}^{\infty} \eta(x-\xi) \cdot y_1(\xi) \cdot H(-y_1(\xi)) d\xi \\
 &\dots \\
 y_n(x) &= y_0(x) + \frac{1}{2L} \int_{-\infty}^{\infty} \eta(x-\xi) \cdot y_{n-1}(\xi) \cdot H(-y_{n-1}(\xi)) d\xi
 \end{aligned}
 \tag{2.32}$$

Although no complete proof of convergence is presented, it was found that the degree of convergence decreased with increasing values of the load.

/79/ also presents graphs of the deflection for various loads, Figure 2.6. Here  $y_0 = Q_d/(2kL)$  is the deflection directly beneath a wheel and caused by a limit load  $Q_d$  such that uplift just begin. The load must then be  $Q_d = 2e^{\pi}qL$ .

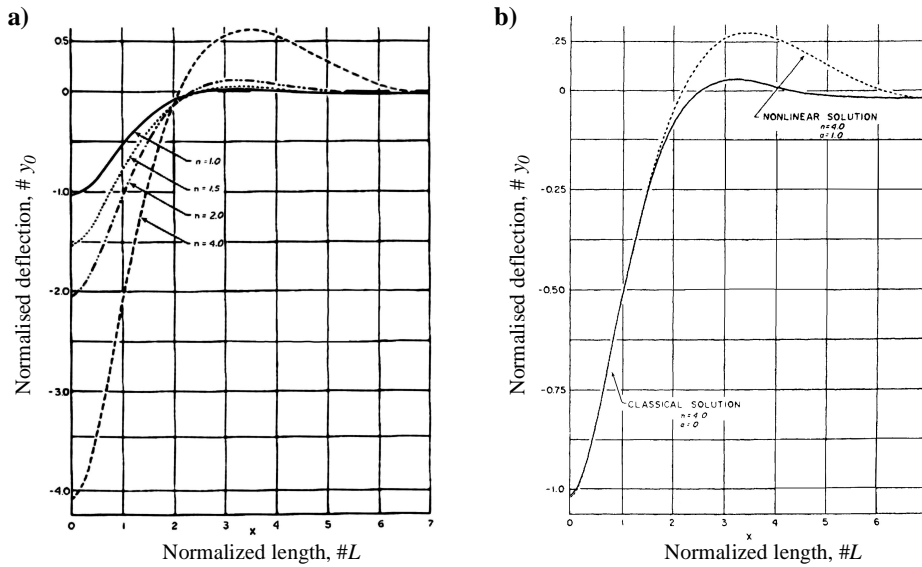


**Figure 2.6:** Deflections for a no tension BOEF model /79/ (slightly modified). a) Effect of load magnitude. b) The no tension effect for equal loads (numerical example).

From Figure 2.6a) it is evident that the uplift effect is rapidly increasing when the load increases ( $n$  in the figure being the number of limit loads). In part b) we see the difference in deflection between the conventional BOEF model and the no tension model when the load is four times the limit load.



### 2.5.2 Model according to Adin et al.

Adin et al. /1/ have solved the no-tension problem by applying the finite element method. They used beam elements with exact stiffness matrices especially developed for a beam on a Winkler foundation.

The problem to be solved is of a more general nature than that of Tsai and Westmann /79/ as several zones of uplift are allowed, Figure 2.7.

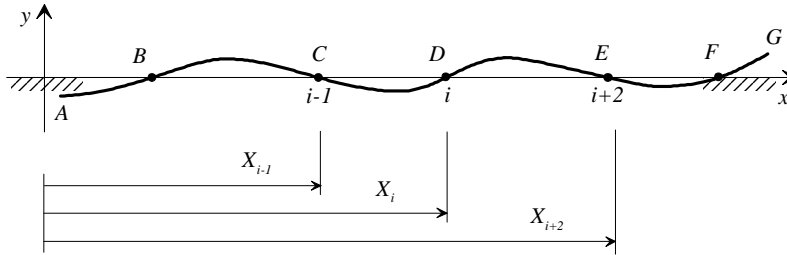


**Figure 2.7:** General deflection of a beam on elastic foundation. (Redrawn from /1/.)

Figure 2.7 illustrates the problem to be solved also from a more analytical, non-FEM viewpoint /1/. If there are  $N$  transition points where the deflection is zero (points  $B$ ,  $C$ ,  $D$ ,  $E$  and  $F$  in the figure) there are  $N+1$  zones of either compression or tension. Two differential equations of the same type as Eqn. (2.27), one with parameters for compression and one with parameters for tension, are solved. When not imposing any boundary conditions at this stage the solutions read:

$$y_j(x) = A_1 \cos(\lambda_j x) \cosh(\lambda_j x) + A_2 \cos(\lambda_j x) \sinh(\lambda_j x) + A_3 \sin(\lambda_j x) \cosh(\lambda_j x) + A_4 \sin(\lambda_j x) \sinh(\lambda_j x) + y_{qj} \quad (2.33)$$

where  $j$  is either  $c$  or  $t$  dependent upon compression or tension,  $A_{1-4}$  are constants to be determined from the boundary conditions for each zone, the  $\lambda$ s equals  $1/L$  and  $y_q$  is a particular solution depending on any line load.

For each zone the number of unknowns sum up to 4 ( $A_{1-4}$ ), hence the total number of unknowns for the beam being  $4(N+1)$  if the coordinates  $X_i$  of the transition points are known. However, the  $X_i$  are *not* known in advance, thus  $N$  more unknowns are added to the problem which now have  $5N+4$  unknowns. In addition the problem is aggravated by the fact that the number of transition points cannot be fully determined before the solution starts. From the examples given it nevertheless seems that the number of transition points in most cases is the same as in the linear elastic solution.

The  $5N+4$  conditions needed to solve for the  $5N+4$  unknowns may be listed as follows:

- (1) continuity of deflection at  $X_i$
- (2) continuity of slope (1st derivative) at  $X_i$
- (3) continuity of moment (2nd derivative) at  $X_i$
- (4) continuity of shear force (3rd derivative) at  $X_i$
- (5) boundary conditions at the beam ends
- (6) at  $X_i$  the deflections are zero

The  $5N+4$  equations are then solved in an iterative process.

Returning to the finite element formulation in /1/ the nodal force-displacement relation is<sup>1</sup>

$$\mathbf{k} \cdot \mathbf{v} = \mathbf{S} \quad (2.34)$$

where  $\mathbf{v}$  is the nodal displacement vector,  $\mathbf{v}^t = \{y_1, \theta_1, y_2, \theta_2\}$ , and  $\mathbf{S}$  is the nodal force vector,  $\mathbf{S}^t = \{F_1, M_1, F_2, M_2\}$ , both explained in Figure 2.8.

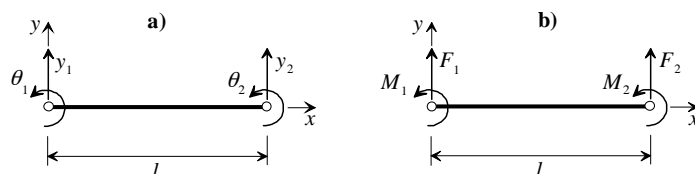


**Figure 2.8:** BOEF element. a) Nodal degrees of freedom. b) Nodal forces. (Redrawn from /1/.)

The exact element stiffness matrices  $\mathbf{k}$  for the tension zone and for the compression zone are given in /1/.

For the bi-moduli foundation (in which the no tension option is a special case) two types of nodes are used: a) Primary nodes are used at points of load application, local supports and discontinuities of the beam or foundation. These nodes remain stationary throughout the solution process, and will contribute to an exact solution when the foundation (or track) modulus is constant. b) Secondary nodes are placed at the points of zero deflection, and their position will vary during the iterative solution process. The iteration is stopped when the coordinates of the secondary nodes remain unchanged within a predefined limit.

Several examples are given in /1/ with different types of point loading including moments. Graphs of deflection, shear force and beam moment are presented.

## 2.6 A compensating load approach to the no tension problem

This section describes a model developed by the author based on adding equal but opposite loads to the BOEF model in the regions where uplift occurs. It will be demonstrated that this approach is equivalent to the more formal method by Tsai and Westmann /79/ and may thus be viewed as a physical interpretation of this formal method.

### 2.6.1 The basic idea and an interpretation of Tsai and Westmann's model

This section describes a model developed by the author based on adding equal but opposite loads to the BOEF model in the regions where uplift occurs. It will be demonstrated that this approach is equivalent to the more formal method by Tsai and Westmann /79/ and may thus be viewed as a physical interpretation of this formal method.

1. Adin et al. /1/ use the notation  $[S]\{d\}=\{A\}$ .

The basic idea of the method goes like this: In areas where the track is lifted up with corresponding tensile stresses, equal but *compressive* stresses is added to the track ladder in such a way that the total vertical stresses between the track ladder and the foundation sum to zero in the uplift regions. Thus the track ladder experiences no stresses from the foundation at these zones (and may therefore be noted tensile free where uplift is taking place). This is more in conjunction with the well established fact that coarse graded granular materials cannot sustain tensile stress.

When adding distributed loads to the rail we need to know how much deflection these loads will cause.

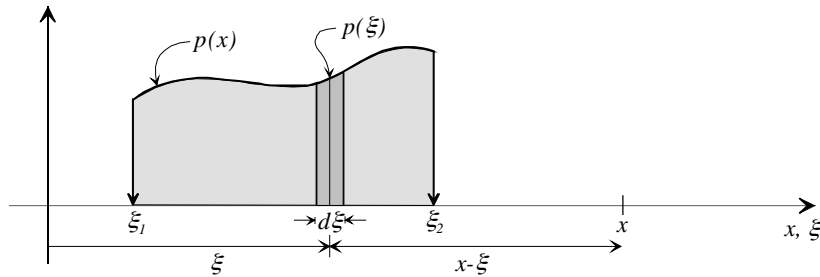


**Figure 2.9:** Definitions used for calculating the deflection of an arbitrary line load.

With reference to Figure 2.9, an infinitesimal load  $p(\xi)d\xi$  will cause the following infinitesimal deflection  $\delta y$  at point  $x$ :

$$\delta y = \frac{p(\xi) \cdot d\xi}{2kL} \cdot \eta(x - \xi) \quad (2.35)$$

Integration over the whole line load, from  $\xi_1$  to  $\xi_2$ , produces the total deflection at point  $x$  (the value of  $x$  is arbitrary):

$$y(x) = \frac{1}{2kL} \cdot \int_{\xi_1}^{\xi_2} p(\xi) \cdot \eta(x - \xi) d\xi \quad (2.36)$$

Normally the convolution integral in Eqn. (2.36) has to be evaluated numerically.

The method of using convolution integrals to calculate deflections from distributed loads has also been utilised by Kerr /49/, although for a different foundation model.

Returning to the no tension problem, the line load function  $p(\xi)$  in the tension zones must be  $p(\xi) = k \cdot y(\xi)$  to fully compensate for the tension load (opposite sign as compared with Eqn. (2.6) on page 10). Thus, an implicit expression may be established for the total deflection when the track ladder weight is included:

$$y(x) = \frac{q}{k} + \frac{Q_d}{2kL} \cdot \eta(x) + \frac{1}{2L} \int_{-\infty}^{\infty} y(\xi) \cdot \eta(x - \xi) \cdot H(-y(\xi)) d\xi \quad (2.37)$$

where  $H(\cdot)$  is the Heaviside step function (as in Eqn. (2.30) and Eqn. (2.31)).

By using the Heaviside step function together with infinite integration limits in the last term one makes sure that only the uplift regions are taken into account and that all of them are included.

When comparing Eqn. (2.37) to Eqn. (2.31) it is evident that they are identical. It has therefore been demonstrated that the formal procedure employed in /79/ is equivalent of applying an exact opposite load in the tension regions.

It should be emphasised that the solution in Eqn. (2.37) is only valid for a single axle load (where  $Q_d$  is half an axle load). If multiple axle loads are considered the deflection cannot be superimposed as the response is not linear. Instead, the whole analysis has to be redone.

Although Eqn. (2.32) and Eqn. (2.37) may do a reasonable job of finding the deflection, some aspects regarding the analysis of railway structures come into play. First, the measurements of the track modulus are probably *not* done with respect to a no tension approach, see Section 2.3.6. As a result the calculated 'no tension' deflection directly beneath the load will not in theory be the same as the one measured when assessing the track modulus! However, the difference is very small and may in practice be neglected. Second, it is not necessary to evaluate the integrals in the abovementioned equations from minus infinity to plus infinity. This is so because the only uplifts that occur in practice are the two nearest to the axle load, one on each side. For the number two uplift from the load to start it can be shown that  $Q_d > 2e^{3\pi}qL$ . Even for the most favourable conditions for this uplift to occur the design wheel load must be far beyond its maximum limits. Thus, it is only required that the integrals are evaluated in the two uplift regions situated symmetrically on either side of the axle load.

### 2.6.2 The main ingredients of the new model

An alternative to the iterative procedure employed by Tsai and Westmann /79/ (as described by Eqn. (2.32)) is to *assume* a compensating pressure in the uplift region and then solve a set of simultaneous equations based on certain conditions that may be established. These equations are nonlinear and must be solved with the help of mathematical software. The method will be demonstrated for a single axle load.

The assumed compensating pressure must be close to the exact one so that the resulting pressure is close to zero, and at the same time this pressure function must be simple to work with. An appealing choice is to pick a deflection function of the same type as the BOEF expression with self weight included (compare with Eqn. (2.28)) and then multiply it with the no tension track modulus  $k_{nt}$ :

$$p(x) = k_{nt} \cdot y_p(x) = k_{nt} \cdot \left\{ \frac{q_p}{k_p} + \frac{Q_p}{2k_p L_p} e^{\frac{|x|}{L_p}} \left( \cos\left(\frac{x}{L_p}\right) + \sin\left(\frac{|x|}{L_p}\right) \right) \right\} \quad (2.38)$$

where subscript  $p$  indicates quantities that are unique for the deflection function  $y_p$  and  $x$  is restricted to the uplift regions.  $E$  and  $I$  are assumed to be the same as for the track in question, so the unknown parameters are  $k_{nt}$ ,  $q_p$ ,  $k_p$  and  $Q_p$ . The  $k_{nt}$  is the track modulus consistent with the no tension approach (to be commented upon below). The roles of the  $q_p$ , the  $k_p$  and the  $Q_p$  are to be curve fitting parameters, as they do not necessarily represent measurable quantities in the track.

The total deflection for a single axle load when no tension is present between the track ladder and the foundation is approximated by

$$y_{nt}(x) = y_q(x) + \frac{1}{2k_{nt}L} \cdot \left\{ \int_{\xi_{01}}^{\xi_{02}} k_{nt} \cdot y_p(\xi) \cdot \eta(x - \xi) d\xi + \int_{-\xi_{02}}^{-\xi_{01}} k_{nt} \cdot y_p(\xi) \cdot \eta(x - \xi) d\xi \right\} \quad (2.39)$$

where  $y_q$  is the deflection according to Eqn. (2.28) (but with  $k_{nt}$ ),  $\xi_{01}$  and  $\xi_{02}$  are the zero intercepts on the  $x$ -axis.

The model is calibrated in a way that makes the maximum deflection caused by *the design load alone* (i.e. the deflection caused by the weight of the track ladder is subtracted) exactly the same as for the traditional BOEF model. However, other schemes of calibration may be possible. The reason for the present calibration is simply to make this new model in agreement with measurements of the maximum deflection, as is the case for the traditional BOEF model. For practical reasons, the measurements of the maximum deflection only involve the deflection caused by the applied axle load (as indicated from the equations given in Section 2.3.6). So, for a single axle load  $k_{nt}$  will always be slightly bigger than the ordinary  $k$ ; and this compensates for the extra deflection beneath the axle caused by the added pressure in the uplift regions. Because of this, the *total* maximum deflection will be slightly smaller for the no tension model, since the deflection caused by track ladder weight will be smaller when the track modulus increases. These differences in track moduli and maximum deflections will be negligible when it comes to railway track behaviour, but the concept may be useful for other applications and thus makes the model more general.

Another feature of the model described by Eqn. (2.39) is that only two potential uplift zones are taken into account, i.e. those nearest to the load on either side. These two symmetrical zones of uplift are the only zones where uplift actually occur (as previously described (page 29)). Because of the nonlinearity of the model the uplift zones will vary both in position and extent when the load is varied. This will also cause  $k_{nt}$  to not being unique for a specific track design as opposed to the BOEF track modulus  $k$ .

### 2.6.3 The set of equations to be solved

The six unknowns in the model are  $k_{nt}$ ,  $q_p$ ,  $k_p$ ,  $Q_p$ ,  $\xi_{01}$  and  $\xi_{02}$ . Therefore, six conditions leading to six equations have to be established. These are:

$$\left. \begin{aligned} (1) \quad & y_{nt}(\xi_{01}) = 0 \\ (2) \quad & y_{nt}(\xi_{02}) = 0 \\ (3) \quad & y_p(\xi_{01}) = 0 \\ (4) \quad & y_p(\xi_{02}) = 0 \\ (5) \quad & y_{max, measured} = \frac{Q_d}{2kL} = y_{nt}(0) - \frac{q}{k_{nt}} \\ (6) \quad & \int_{\xi_{01}}^{\xi_{02}} k_{nt} \cdot \{y_{nt}(x) - y_p(x)\} dx = 0 \end{aligned} \right\} \quad (2.40)$$

As can be seen, the first four equations simply state that the no tension deflection curve along with the compensating deflection curve should be zero at the zero intercepts. The fifth equation does the calibration against measured or calculated maximum values. The sixth equation ensures vertical force equilibrium in the no tension zones as a whole, but pointwise there might still be unbalanced pressures due to the fact that the pressures resulting from  $y_{nt}$  do not com-

pletely cancel the pressure from  $y_p$  (i.e.  $y_{nt}$  is only approximately equal to  $-y_p$ ). From numerical experiments these unbalanced pressures seem to be small.

The equation set in Eqn. (2.40) was solved using mathematical software, and the calculation time was only a few minutes on a standard PC. Some trial and error with the starting values is necessary to ensure convergence of the solution.

It should be pointed out that the solution is only an approximation to the problem - by the very nature of the solution scheme. The reason is that  $y_p$  in the compensating pressure function in Eqn. (2.38) is only approximative.

### 2.6.4 Some results from the new model

To study real track behaviour the position and length of the uplift zone as a function of the BOEF track modulus, see Figure 2.10.

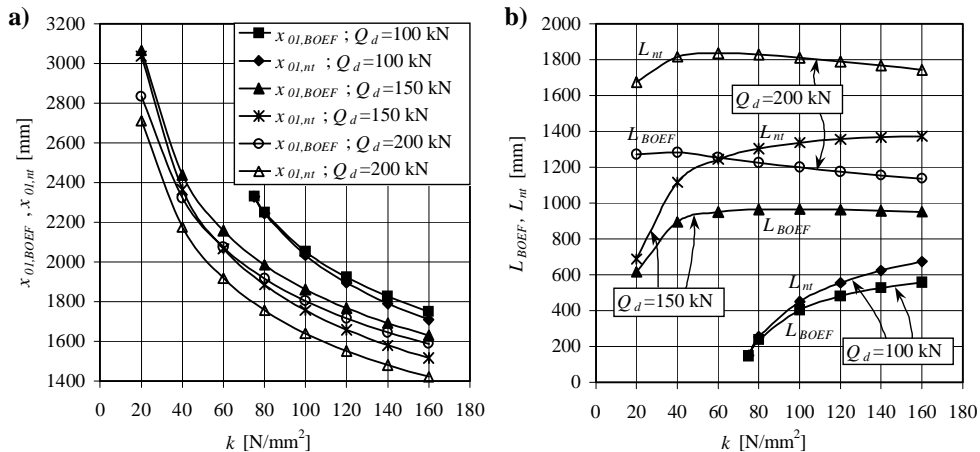


**Figure 2.10:** Numerical example that compares the BOEF model with the new no tension model.  $q = 2.8$  N/mm which corresponds approximately to the half weight of a new track with UIC 60 rails and NSB95 sleepers. a) Distance from load to first uplift. b) Length of the uplift zone.

As can be seen from Figure 2.10 the effect of a no tension model is to lengthen the zone of uplift, especially when the load and track modulus attain large values. Not mentioned in the figure, but the values for a design load of 200 kN and track moduli above 100 N/mm<sup>2</sup> must be viewed as approximate because the residual forces in the uplift zone cannot longer be considered to be negligible.

An example of a deflection curve is shown in Figure 2.11 below. Here the design load is 200 kN and the track modulus is 50 N/mm<sup>2</sup>, and the track parameters are else the same as for Figure 2.10. For comparison the deflection curve for a BOEF model is also shown.

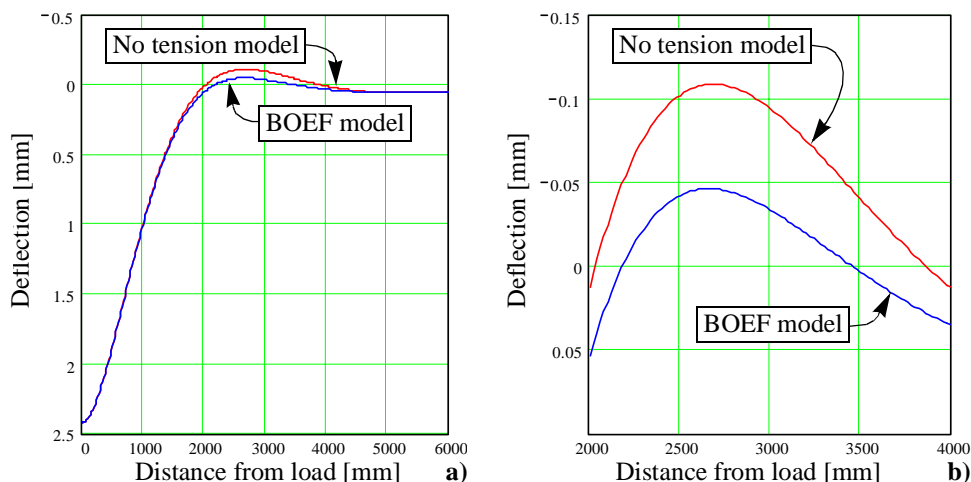


**Figure 2.11:** Example of deflection for the no tension model compared to the BOEF model.  $Q_d = 200 \text{ kN}$ ,  $k = 50 \text{ N/mm}^2$ , other parameters as in Figure 2.10. a) one half of the curve, b) detail of the uplift zone.

### 2.6.5 Conclusions of the new model

To conclude it is evident that when uplift occur in the track, i.e. no tensional forces are active on the interfaces between the sleepers and the ballast, the length of the uplift zones are considerably longer than calculated by traditional BOEF theory. Also, the amplitudes of the uplifts are larger. The two uplift zones near the axle load, one on each side, are the only ones that are likely to occur when considering a railway track.

The usefulness of the model may be demonstrated in at least two cases:

- (1) A buckling-of-rails problem: If there is a buckling-of-rails hazard, it will be very valuable to know the lateral resistance in the track. If the track is loaded, i.e. a train is passing, the lateral resistance will be dependent of how large a portion of the track ladder that is actually in contact with the foundation. What this new method shows is that the zone of contact is smaller than expected from original BOEF theory.
- (2) Contact problems are very computational demanding in terms of a finite element formulation, and besides, a lot of effort has to be put into the modelling if the answers should be reasonable accurate. So, the present method provides a quite simple algorithm, and an alternative, that may solve the problem to an acceptable accuracy.

The present model is hopefully an improvement compared to the traditional BOEF model, as the no tension property of the foundation is taken care of, at least approximately. Also, the weight of the track ladder is incorporated. However, it should be noted that the new model still suffers from the other BOEF limitations as listed in Section 2.3.8.

## 2.7 Dimensionless sensitivity diagrams

A track model is at its best a general and a very comprehensive model. In practical engineering, on the contrary, one is usually interested in the design reaction values, i.e. the maximum track reactions, and where they occur in the track. Furthermore, what is interesting to the track engineer is how do the design values change if the track is changed. An example may be the question of how much the maximum rail deflection changes if the sleeper spacing is increased. More generally, the need for knowing how the track response changes may arise in several situations such as

- (1) Selection of the best performing track design among several alternatives
- (2) Evaluation of effective measures to renovate an existing track
- (3) Increase in permitted axle load and the effect of countermeasures

To meet these needs a tool called 'dimensionless sensitivity diagrams' has been developed. These diagrams respond to questions like 'if track design parameter  $n$  is altered  $x$  percent how many percent will track reaction  $r$  be changed?'. If the nominal values of the new track reactions are wanted, one has to perform a complete calculation on one basis track design, which often will be an existing track design. The effects on track reactions of changing this basis design will then be answered by the dimensionless sensitivity diagrams. The concept of dimensionless sensitivity diagrams has also been described in /74/.

### 2.7.1 BOEF model with a single axle load

A BOEF track model with a single axle load is not a complex system, and may not even justify the use of such diagrams, but will nevertheless provide an easy way of explaining the construction of such diagrams. Eqn. (2.41) gives the fully written out expression for the maximum rail deflection under a single axle load when the weight of the track ladder is ignored:

$$y_{max} = \frac{Q_d}{2bCL} = \frac{1}{2^{3/4} \cdot E^{1/4}} \cdot Q_d \cdot c^{3/4} \cdot I^{-1/4} \cdot d^{-3/4} \cdot (l-m)^{-3/4} \cdot C^{-3/4} \quad (2.41)$$

Figure 2.3 on page 15 explains some of the parameters in Eqn. (2.41). In the present context the  $m$ -parameter (length of unsupported section of the sleepers) should not be considered a design parameter unless more justification to its assessment can be brought forward.

If we divide the written out part of the expression in Eqn. (2.41) with the corresponding parameters for a basis design, equipping these latter parameters with subscript 0, we get the following:

$$\left( \frac{y_{max}}{y_{max,0}} \right) = 1 \cdot \left( \frac{Q_d}{Q_{d,0}} \right) \cdot \left( \frac{c}{c_0} \right)^{3/4} \cdot \left( \frac{I}{I_0} \right)^{-1/4} \cdot \left( \frac{d}{d_0} \right)^{-3/4} \cdot \left( \frac{l-m}{l_0-m_0} \right)^{-3/4} \cdot \left( \frac{C}{C_0} \right)^{-3/4} \quad (2.42)$$

The leading factor 1 indicates that to vary Young's modulus is normally not an option in a design procedure as the various rail steels have almost identical moduli.

If one of the design parameters is varied in Eqn. (2.42), keeping the other parameters the same as in the basis design, the result will tell how the maximum rail deflection depends on that particular parameter. If the other parameters are varied one by one in the same way, the result will show how the maximum rail deflection depends upon the various track parameters. Since Eqn. (2.42) describes the dependencies in a dimensionless way, the same expression may be used for all alternative designs provided that a basis design has been calculated first.



When it comes to this basis design, the BOEF model with a single axle load does not need a specific track design to serve as a basis. This is because the development of Eqn. (2.41) and Eqn. (2.42) was possible through a purely analytical approach without needing any presumptions about the track design. Any track may therefore serve as the basis track design. However, this feature is unique to the BOEF model with a single axle load and does not generally apply to other cases.

In addition to the maximum deflection, diagrams may be constructed for other track reactions as well. Figure 2.12 on page 35 provides dimensionless sensitivity diagrams for maximum values of rail deflection, rail moment, rail tensile stress in rail foot, seat load and vertical ballast pressure underneath the sleepers. The equations for these quantities have been given previously in Sections 2.3.2, 2.3.3 and 2.3.5. It should be noted that the seat load and the vertical ballast pressure are derived from the deflection according to Eqn. (2.18), and that the rail tensile stress in rail foot is derived from the rail moment according to Eqn. (2.11). For the seat load it is emphasised that the diagram in Figure 2.12 e) is based on Eqn. (2.12) (and not the more involved Eqn. (2.13)). More detailed diagrams that can be used in an actual design process are given in Appendix A.

Some comments regarding the diagrams in Figure 2.12 may be appropriate:

- ◆ All the curves traverse through the point (1, 1). Naturally, if no changes are made to the track, no changes in track reactions will occur.
- ◆ All reactions are linearly dependent on the level of the design load. The reason is that the BOEF model is linear.
- ◆ The range of variation of track parameters is wide (up to three times the basis value). This is only needed for some of the design parameters and certainly not for all of them.
- ◆ All the curves are power functions with the parameter ratio as the independent variable. The exponents are typical 1.0, 0.75, 0.25, -0.25 or -0.75 (all of them represented in Figure 2.12, part e)).

As an example of how to use the diagrams consider the following case:

A main line is evaluated for the effect of increasing the design axle load by 20%. The countermeasures to be taken are to change from S49 rails to S54 and to reduce the sleeper spacing from 60 cm to 54 cm. Changing the rails corresponds to an increase in vertical moment of inertia of 14% (according to Table 2.6 on page 11), while the reduction in sleeper spacing is 10%. The parameter ratios are therefore 1.2, 1.14 and 0.9 for the change in design load ( $Q_d$ ), moment of inertia ( $I$ ) and sleeper spacing ( $c$ ), respectively. According to the diagram describing the deflection, the factors to multiply the present deflection by are 1.2 (caused by increased design load), 0.97 (caused by increased rail moment of inertia) and 0.92 (caused by decreased sleeper spacing). Multiplying all these factors will give the total factor of change in deflection:  $1.2 \cdot 0.97 \cdot 0.92 = 1.07$ . I.e., an increase of about 7% in maximum rail deflection for a single axle load should be expected when the load and track is changed as described above. For the rail moment the moment ratios from the diagram are 1.2 ( $Q_d$ ), 1.03 ( $I$ ) and 0.97 ( $c$ ), which produce an increase in maximum rail moment of about 20%.

## 2.7.2 BOEF model with multiple axle loads

The principles of how to use the dimensionless sensitivity diagrams in Figure 2.12 even for multiple axle loads will be considered here. Using such diagrams for multiple axle loads will be an alternative to more direct techniques as described in Section 2.3.4.

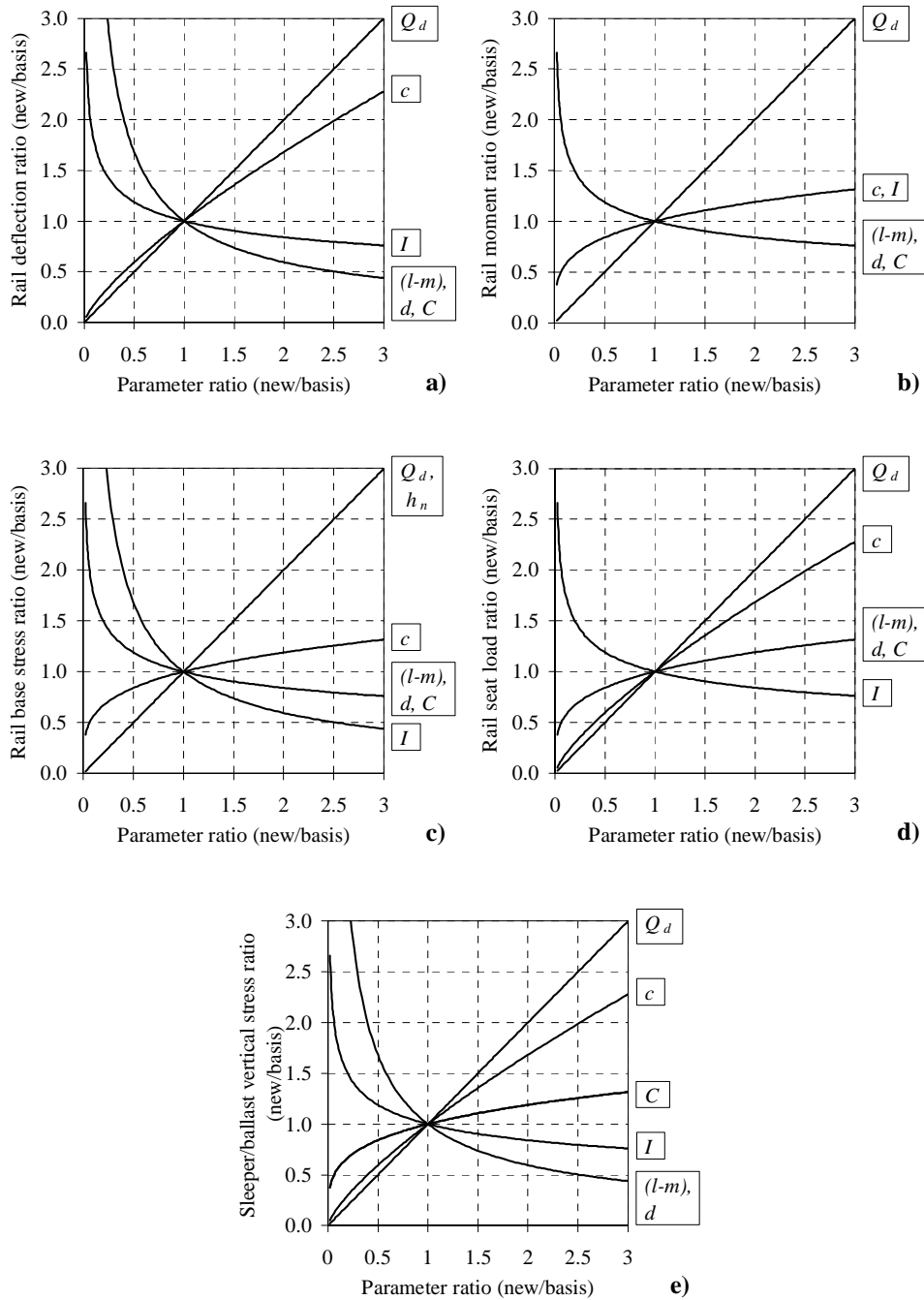


**Figure 2.12:** Dimensionless sensitivity diagrams for a BOEF model with a single axle load. a) rail deflection, b) rail moment, c) tensile stress in rail base ( $h_n$  is the height from rail base to neutral axis), d) rail seat load and e) vertical stress between sleeper and ballast. Larger diagrams can be found in Appendix A.

The ratio of the axle spacing to the characteristic length, the  $a/L$  ratio, will prove useful as a dimensionless length measure in the following. But since  $L$  will change whenever  $I$ ,  $c$ ,  $(l-m)$ ,  $d$  and  $C$  are changed it may be practical to have a diagram that shows the ratio of the new  $L$  to the basis  $L$  as a function of the parameter ratios. Such a diagram is shown in Figure 2.13 below.

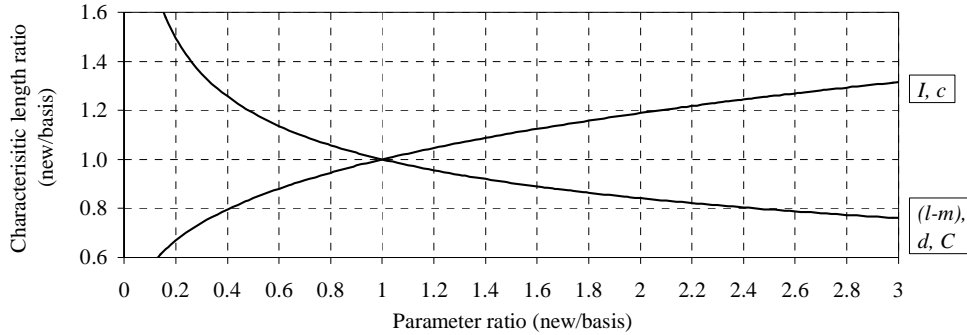


**Figure 2.13:** The characteristic length ratio as a function of track parameter ratios.

For multiple axle loads the values from the diagrams for a single axle load are multiplied with factors that attribute to the multiple axle load effect. With the use of influence coefficients as given in Eqn. (2.15) and Eqn. (2.16) on page 14 for rail deflection and rail moment, respectively, one may establish the factors given in Eqn. (2.43) and Eqn. (2.44).

$$f_d = 1 + \sum_{i=2}^n \frac{Q_{di}}{Q_{d1}} \cdot \eta(x_i) \quad (2.43)$$

$$f_m = 1 + \sum_{i=2}^n \frac{Q_{di}}{Q_{d1}} \cdot \mu(x_i) \quad (2.44)$$

where

- $f_d$  = multiple axle load factor for deflection, rail seat load and vertical ballast stress
- $f_m$  = multiple axle load factor for moment and tensile stress in rail base
- $n$  = no. of axles
- $Q_{di}$  = design load for axle no.  $i$
- $Q_{d1}$  = design load for basis axle (denoted axle no. 1)
- $x_i$  = distance from basis axle to axle no.  $i$

Eqn. (2.44) will provide the factor that multiplied with the maximum reaction ratios from Figure 2.12 will produce the maximum rail moment and rail base stress for a multiple axle load. This is because the maximum rail moments and rail base stresses are always directly beneath the points of load application. Unfortunately, this does not generally apply to deflections and the derived quantities. In this case the maximum values are located directly below the loads only if the axle spacing equals to  $n\pi L$ , where  $n$  is an integer.

For a double axle load where the loads are identical in magnitude, the  $f_d$  and  $f_m$  factors are given in Figure 2.14. Here the axle spacing is denoted  $a$ , and  $L$  is, as before, the characteristic length. As may be seen from the figure, the factors  $f_d$  and  $f_m$  are close to 1.0 when the  $a/L$  ratio exceeds about 3. This implies that for a combination of high track moduli and large axle spacings the reactions for a double axle load are almost the same as for a single axle load.

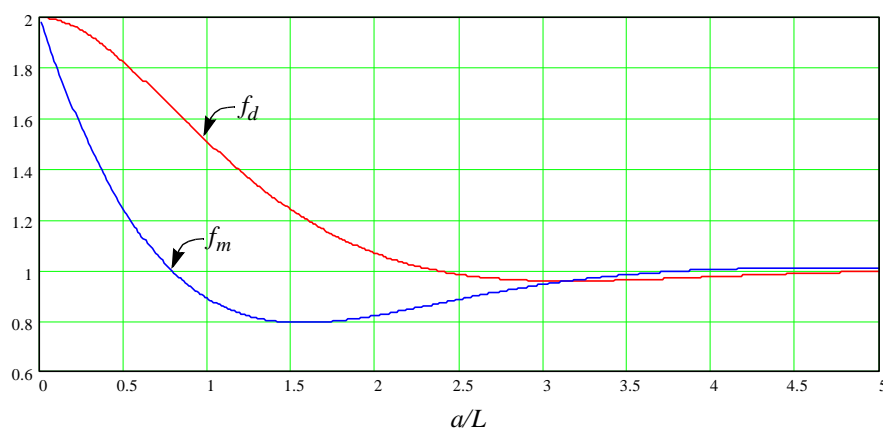


**Figure 2.14:** The factors  $f_d$  and  $f_m$  for a double axle load with the same load on both axles.

To be completely accurate when calculating maximum deflection (and derived quantities) one has to look more into the details. The method described in the following is restricted to a double axle load, with identical design loads, and will prove useful both when using dimensionless sensitivity diagrams and when using more standard methods. For the rail seat load and the corresponding vertical stress on the ballast one has to assume that the axle in question is directly above a sleeper.

To locate the maximas of deflection (and derived quantities) one has to differentiate the deflection function for several combinations of axle spacings and characteristic lengths. Doing this in a systematic way, denoting the distance from one axle to the maximum deflection location as  $x_{max}$ , the result may be displayed in a dimensionless diagram as in Figure 2.15.

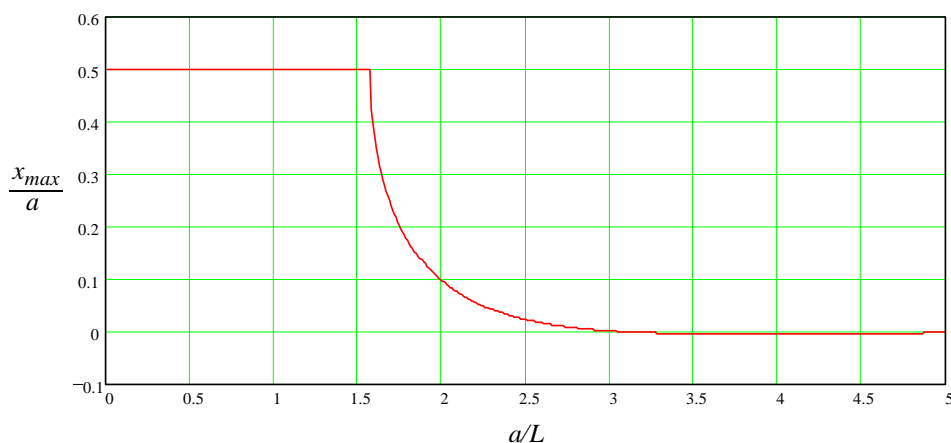


**Figure 2.15:** BOEF, double axle load: The distance  $x_{max}$  from one axle to the point of maximum deflection as a function of  $a/L$ .

In Figure 2.15 the ratio  $x_{max}/a$  is 0.5 as long as the ratio  $a/L$  is below about 1.6 (it turns out that the exact value is  $\pi/2 \approx 1.57$ ), which imply that there is only one maximum deflection point and this is located at the midpoint between the axles. With a higher  $a/L$  ratio the maximum deflec-

tion is nearer to the axles, which means that now there are *two* maximas. The curve crosses zero at an  $a/L$  ratio of  $\pi$  and here the axle load position and the position of the deflection maximum are coincident.

To further illustrate the nature of the deflection caused by a double axle load as a function of the  $a/L$  ratio, see Figure 2.16. Here we clearly see the division of the maximas as the  $a/L$  ratio increases. Also, the maximum value of the deflection decreases as the  $a/L$  ratio increases. This is expected since the additive effect on the deflection the two axle loads have on each other is diminishing as the loads are moving apart (or alternatively, as  $L$  is decreasing).

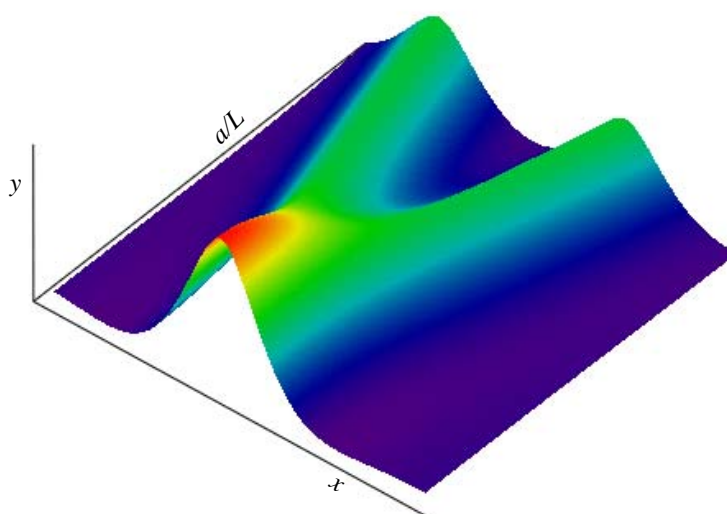


**Figure 2.16:** A 3D-plot of the deflection,  $y$ , for a double axle load as a function of  $a/L$  ratio. Note that the deflection axis is chosen to be positive in an upward direction. The axle spacing ( $a$ ) increase has been symmetrically distributed along the  $x$ -axis.

Knowing where the maximas are located, the crucial question related to the use of the dimensionless sensitivity diagrams is how large the differences are between the maximum values and the values at the point of load application. Figure 2.17 gives an answer to this by displaying a correction factor  $f_{dcorr}$  that the deflection and the derived quantities at the point of load application are to be multiplied by to get the maximum reactions. As can be seen from Figure 2.17 the differences between the reactions at the point of wheel contact and the maximum reactions are normally small and less than 10% for all  $a/L$  ratios. For an  $a/L$  ratio exceeding 2.0 the error is less than 2% and is therefore negligible.

When using the dimensionless sensitivity diagrams for a single axle load to calculate the reactions for a double axle load the following steps should therefore be taken:

- (1) Find the appropriate reaction ratio from the diagrams for a single axle load (Figure 2.12).
- (2) Find the new  $L$  from Figure 2.13.
- (3) Use  $L$  from item (2) to find  $f_d$  and  $f_{dcorr}$  or  $f_m$ , dependent on what reaction that is solved for.
- (4) Multiply the ratio from item (1) by the factors found in item (3).

In order to investigate further the practical accuracy of a double axle deflection calculation it would be interesting to see what values the axle spacing, characteristic length and foundation

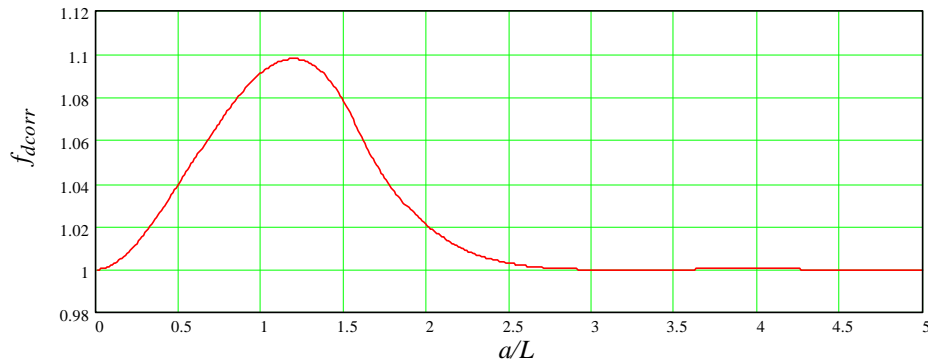


**Figure 2.17:** Finding the maximum deflection. Correction factor,  $f_{dcorr}$  to be multiplied with the values for deflection at the point of load application for a double axle load.

coefficient will take if the error should be less than, say, 2% when taking the deflections at the axle positions as the maximum deflections. According to Figure 2.17 an error less than 2% occurs when  $a/L$  is bigger than 2 (or less than 0.33, but this latter option is of no practical interest). Figure 2.18 tries to illuminate what combinations of  $C$  and  $a$  that may be allowed if the error should be less than 2%.

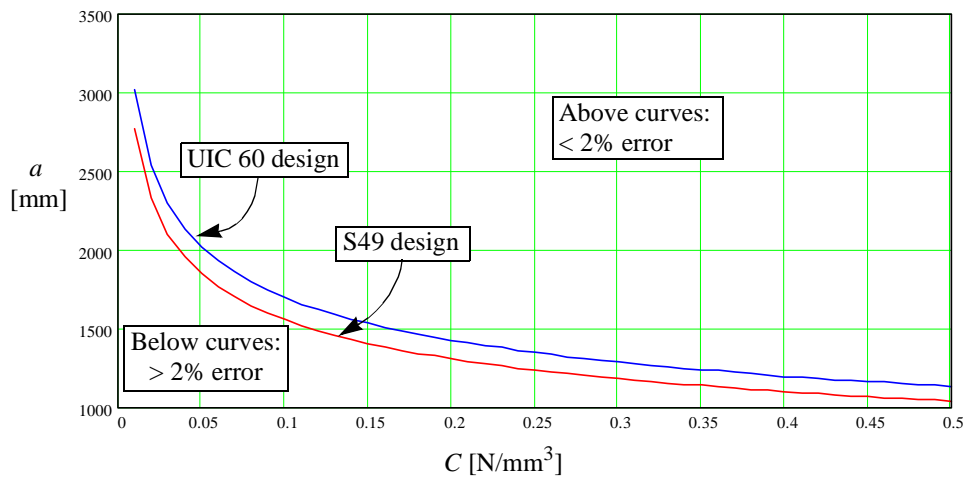


**Figure 2.18:** Double axle load: Combinations of foundation coefficient,  $C$ , and axle spacings,  $a$ , for two common track designs that make the error 2% when taking the deflections at the axle positions as the maximum deflection. The fictitious longitudinal sleeper width,  $b$ , is taken to be 490 mm for the UIC 60 design and 410 mm for the S49 design.

In practice there are very few double axled bogies where the axle separation is below 2000 mm. In that case, if the error of using the deflection at the axle positions as the maximum deflection should exceed 2% then the foundation coefficient must be below approx.  $0.05 \text{ N/mm}^3$ . A consequence of a foundation coefficient lower than  $0.05 \text{ N/mm}^3$  is that the rail deflection will exceed 3 mm for a reasonable design load, which in most cases will be unacceptable. Therefore, combinations of  $C$  and  $a$  that are below the curves in Figure 2.18 are not very likely to occur in a real situation.

So, to conclude, if  $a/L$  is greater than or equal to 2.0 then it is acceptable to take the deflection at the axle positions as the overall maximum deflection for a double axle load. The error of doing this is at most 2%. This also applies to rail seat load and vertical stress between sleeper and ballast as these quantities are derived from the deflection.

The correction curve for the deflection (and derived quantities) has only been calculated for a double axle bogie with the axles equally loaded, see Figure 2.17. Consequently, the description given in this section is not complete for axle configurations consisting of more than two axles or with differing axle loads in a double axle bogie. However, it may be argued that for any axle configuration the difference between the deflection calculated at the axle positions and the global maximums are small, and may be neglected in most cases without significant loss of accuracy. The details of this are considered to be beyond the scope of this thesis.

## 2.8 Other types of continuous models

Kerr /49/ and Scott /71/ review several types of elastic foundation models. A common feature of some of the models is that they try in various ways to tie the springs in the Winkler model together. Other models use a semi-infinite elastic half-space as a starting point. In the Winkler model, see Section 2.3.2, the vertical springs are uncoupled laterally, and the vertical force they exert on the rail is identical to buoyancy in a liquid. In this respect the foundation coefficient  $C$  may be regarded as the specific weight of the liquid, while the track modulus  $k$  is the buoyancy force exerted by the liquid per unit length of the foundation (fictitious sleeper) and per unit deflection. By analogy, any upward deflection is counteracted with a corresponding suction force set up by the liquid. A detail that makes the Winkler model diverge from the 'liquid analogy' is that the pressure exerted by the foundation on the beam is in the same direction as the deflection, while a liquid would exert a pressure normal to the beam regardless how the beam is deformed. This difference comes only into play when the deflection is large or the beam is heavily curved in the vertical direction and is not normally relevant to a railway track.

**Filonenko-Borodich foundation.** In this model the interaction between the foundation springs is obtained by connecting the top ends to a stretched elastic membrane with a constant tension field  $T$ . Taking the equilibrium in the vertical direction of a beam element yields the relation

$$p = ky - T \frac{d^2y}{dx^2} \quad (2.45)$$

where  $T$  is a constant tensional force [N].

**Pasternak foundation.** This foundation model assumes shear interactions between the Winkler springs. The resulting equation in this model is identical with Eqn. (2.45).

Scott /71/ places these two models into a more general framework where the pressure  $p$  from the soil is given by

$$p = ay^{(0)} + by^{(2)} + cy^{(4)} + \dots \quad (2.46)$$

where the superscripts denote the order of the derivatives. The first term to the right is then the Winkler assumption (confer Eqn. (2.6)), while the third term represents the pressure component

resulting from the bending action of a beam. The second term is then the one represented by the stretched membrane. With the sixth and higher derivatives the physical connection diminish.

This stretched membrane approach has a special relevance to railway track design as the tension and compression in the rails vary with temperature when the rails are continuously welded. Hetényi /30/ describes solutions for beams on elastic foundation under both vertical and axial loading. When the rail is subjected to compression, which will be the case on a sunny day during the summer season, the vertical deflection will be larger than when no axial forces are present. On the other hand, the deflections will be smaller when the rail is subjected to tension, which typically occur during winter conditions. According to numerical experiments the effect on the deflection is small when reasonable tension or compression is present in the rails. The effect may be larger if, for instance, a no tension model is loaded axially.

**Reissner foundation.** Reissner uses the equations of a continuum as a starting point. He then assumes the horizontal stresses (in-plane stresses) in the foundation layer to be negligibly small compared to the vertical stresses. Also, the horizontal displacements of the upper and lower boundaries of the foundation layer are assumed to be zero. The resulting relation is then

$$c_1 y - c_2 \frac{d^2 y}{dx^2} = p - \frac{c_2}{4c_1} \frac{d^2 p}{dx^2} \quad (2.47)$$

where  $c_1 = E_f/H$  and  $c_2 = HG_f/3$ . Here  $E_f$  and  $G_f$  are elastic constants for the foundation material, while  $H$  is the thickness of the foundation layer.

It is worth noting that for a constant or linear  $p$ , and redefining  $c_1$  and  $c_2$  to  $k$  and  $T$ , respectively, Eqn. (2.47) will be identical with Eqn. (2.45).

**Vlasov and Leontiev approach.** The displacements are represented by finite series where each term is a product between a dimensionless assumed function and a function to be found in the calculations. The assumed function describes the variation of the displacement with depth, and here some reasoning has to be done both to keep the function simple and to keep it reasonable accurate. The unknown function has the dimension of length and describes how the vertical deflection varies in the  $x$ -direction. Through a variational process a differential equation in the unknown function is arrived at and the solution of this equation will eventually solve the problem.

## 2.9 Classic beam element models for railway track

This is a class of models that makes use of the Finite Element Method with beam elements. The theory behind such simple models can be found in numerous textbooks on structural mechanics and structural finite element method, e.g. in Cook et al. /12/. Herein models where only the rails are discretised as elements will be worked out. The discrete support from the sleepers is then replaced with springs located at the same positions as the sleepers. Contrary to the BOEF models, beam element models will not depend upon the assumption of continuous foundation support, but the other limitations mentioned in Section 2.3.8 also apply here. The quantities to be calculated are the same as for the BOEF model and are mentioned in Section 2.3.1 on page 8.



### 2.9.1 An Euler-Bernoulli beam element model

A simple Euler-Bernoulli beam element model has been developed to model the track behaviour when the rail is discretely supported by the sleepers. Two models have been developed one ordinary model with linear spring support in both tension and compression, and another model with linear spring support only in the compression mode. The latter one could be said to be a 'no tension' model. A sketch of both models is shown in Figure 2.19.

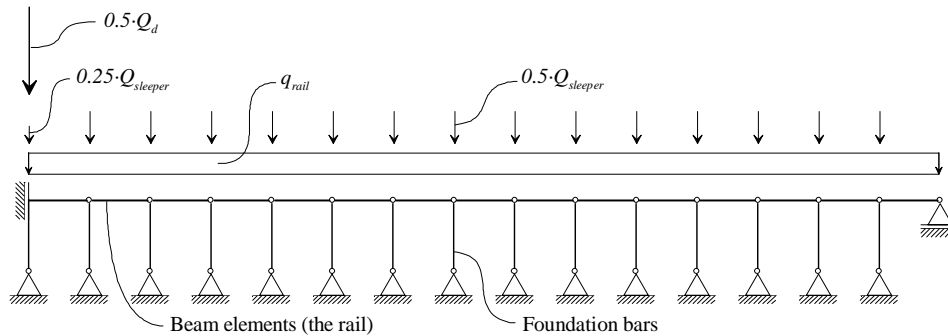


**Figure 2.19:** *Beam element model of a track section.*

In Figure 2.19 the support of the rail at the sleeper positions has been modelled as bars and not as springs which is more common. This is due to the computer software used to calculate the model, which is a computer program named Focus Konstruksjon (ver. 5.6) - a Norwegian structural program for frames. This software allows only bars to have a no tension option. Symmetry considerations allow us to model only a quarter of the track when proper loads and boundary conditions are imposed. The symmetry is the reason why only half the design wheel load and half the sleeper weight (one quarter at the left end) are taken into account. The restrained degrees of freedom at the left end are also a result of symmetry considerations. At the right end the type of restraining is not that important, provided no change in the other boundary conditions, when the focus is on how the track nearest to the load performs. This is so because there is a sufficient number of sleeper spacings from the point of load application to the right boundary, and almost no part of the load will be counteracted at the right end.

The stiffness of the foundation bars is given by an analogy to the BOEF model as the foundation coefficient  $C$  (defined by Eqn. (2.19) on page 16) collocated at the centre of the rail-sleeper contact area will give the spring stiffness,  $k_{spring}$ :

$$k_{spring} = b \cdot C \cdot c = k \cdot c \quad (2.48)$$

As before,  $b$  is the width of the fictitious longitudinal sleeper,  $c$  is the centre to centre sleeper spacing and  $k$  is the track modulus. Eqn. (2.48) is valid for a beam element model where the foundation springs have the same stiffness in tension as in compression.

When a no tension option is imposed, the spring stiffness is modified in the following way:

$$k_{spring,nt} = \begin{cases} k \cdot c & ; y \geq 0 \\ 0 & ; y < 0 \end{cases} \quad (2.49)$$

### 2.9.2 Comparison between beam element models and BOEF models

For the purpose of comparison, deflections for a single axle load for four different models were calculated. The models are the following:

- ◆ The BOEF model with track ladder weight included (Eqn. (2.28)).
- ◆ The new no tension model developed on the basis of the BOEF model (Section 2.6 and Eqn. (2.40)).
- ◆ The Euler-Bernoulli beam element model with the same spring stiffness in tension as in compression (Eqn. (2.48)).
- ◆ The Euler-Bernoulli beam element model with zero spring stiffness in tension and a stiffness of  $kc$  in compression (Eqn. (2.49)).

A design load of 200 kN was chosen as this load will be big enough to reveal any differences between the models. At the same time this load may be considered a practical upper bound on the design wheel loads. The track parameters are listed as follows:

- ◆ UIC60 rails with mass 60.34 kg/m, equivalent to a  $q_{rail}$  of 0.59 kN/m. The moment of inertia of the rail is  $I = 3.055 \cdot 10^7 \text{ mm}^4$ .
- ◆ NSB95 sleepers weighing 270 kg. The corresponding halfweight of the sleeper,  $0.5 \cdot Q_{sleeper}$  is 1.32 kN.
- ◆ Sleeper spacing,  $c$ , is 600 mm.
- ◆ Track modulus,  $k$ , is 50 N/mm<sup>2</sup>.
- ◆ Track ladder weight,  $q$ , for the BOEF model is 2.8 N/mm.

The overall deflection curves for the four models are depicted in Figure 2.20.

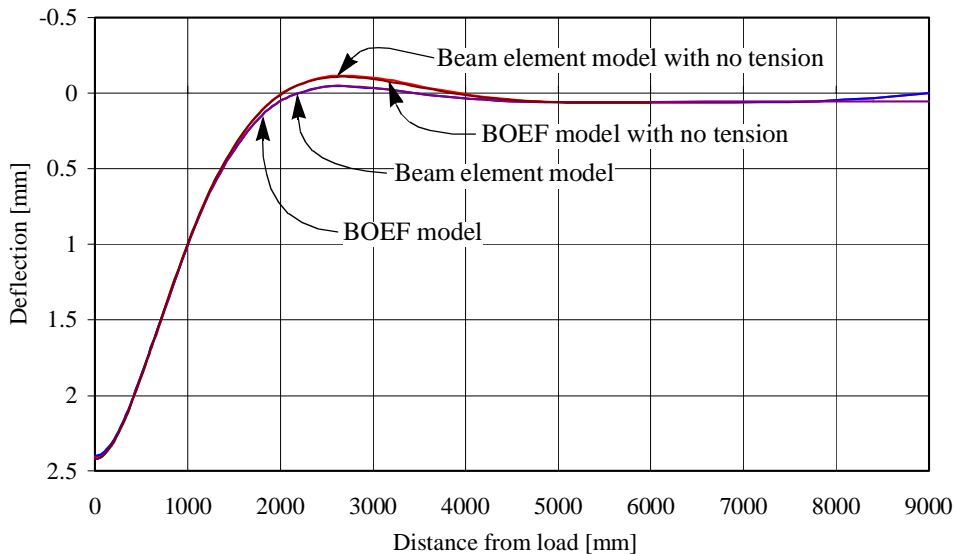


**Figure 2.20:** Example of deflection curves for three different track models. Track parameters and loading level given in the text.

The two BOEF models have been made deflection consistent; i.e. the maximum deflections are identical. The two beam element models have not been made consistent to the maximum deflection. But as can be seen from the deflection pattern in Figure 2.20 the maximum values are very similar.

The ordinary beam element model and the BOEF model produce an almost identical deflection pattern as can be seen from Figure 2.20. Only at the right end the beam element model seems to have a smaller downward deflection, but this is entirely due to the boundary condition at this end. The tensionless beam element model and the tensionless BOEF model also have very similar deflections. As expected, the tensionless models produce bigger upward deflections than the other two. At the right end the tensionless beam element model behaves similarly to the ordinary beam element model.

A more detailed picture of the part of the beam that is subjected to upward deflection is given in Figure 2.21.

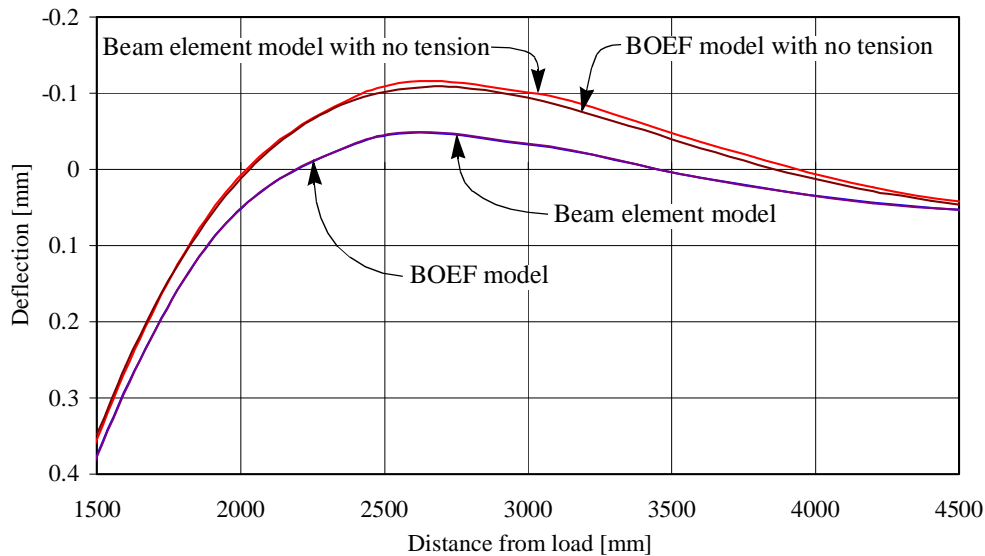


**Figure 2.21:** The upward deflection part of the three models given in Figure 2.20.

Again, from Figure 2.21, it is difficult to differ the deflection of the BOEF model from that of the ordinary beam element model. The difference between the two deflection curves for the tensionless models are now clearly visible, but still the two curves agree with each other to a large extent.

A conclusion to be drawn from this particular example, with track parameters as on page 43, is that there is very little difference in deflection between the models with continuous foundation compared with the models with discrete support. Whether this conclusion is also valid for other track parameters and for other track reactions is not obvious and further work has to be done. The part of this question that deals with the two types of linear foundation is addressed in Section 2.9.3.

### 2.9.3 Dimensionless sensitivity diagrams for an Euler-Bernoulli beam element model

When not dealing with the ordinary BOEF model a basic track design has to be specified. In Norway the following design is common for all new lines and major realignments /43/:

- ◆ UIC 60 rails

- ◆ NSB 95 sleepers
- ◆ 600 mm sleeper spacing
- ◆ ballast thickness of at least 350 mm beneath the sleepers<sup>1</sup>

Together with this track design a track modulus of  $50 \text{ N/mm}^2$  is assumed for the basic track design. Eqn. (2.48) will transform the track modulus into a foundation spring stiffness, thus assuming the same behaviour both in tension and compression. The design wheel load is set to 200 kN in the basic model. The same model as in Figure 2.19 is utilised, but with the modification that  $q_{rail}$  and  $Q_{sleeper}$  both are set to zero. This modification is necessary when the resulting diagrams are to be compared with the ones from the ordinary BOEF model (Section 2.7). The calculation of these diagrams has also been described in /74/.

In the same way as for the BOEF model the diagrams are constructed by taking one parameter at a time and vary its value to see the effect on the various track reactions. The track reactions are then made dimensionless by dividing them with those of the basic design before the result is plotted in the diagram. The various values used in the analysis are given in Table 2.8.

**Table 2.8:** *The values used for loading and track parameters in an Euler-Bernoulli beam element model to establish dimensionless sensitivity diagrams.*

Quantity to be varied	Basis model	Other values used in the analyses								
		50	350							
$Q_d$ [kN]	200	50	350							
$k$ [N/mm <sup>2</sup> ]	50	10	20	30	40	60	70	80	90	100
$c$ [mm]	600	450	500	550	650	700	750			
$I$ [10 <sup>7</sup> mm <sup>4</sup> ] <sup>a</sup>	3.055	1.3675	1.819	2.073	2.308	2.346	3.252			

a. Values from actual rails in use, confer Table 2.6.

In contrast to the BOEF model the values of  $(l-m)$ ,  $d$ ,  $C$  and  $h_n$  have for simplicity not been explicitly treated in the analyses with the Euler-Bernoulli beam element model. The first three parameters are actually included in the track spring stiffness, through the track modulus (see Eqn. (2.48)). To evaluate their separate effect one could use Eqn. (2.17) and Eqn. (2.19).  $h_n$  is only present in the calculation of rail bending stresses, and its effect may be treated separately by using Eqn. (2.11) together with the appropriate rail moment. This is in fact the same approach to  $h_n$  as in the BOEF model.

In Figure 2.22 only the three most fundamental dimensionless sensitivity diagrams for the Euler-Bernoulli beam element model are given, i.e. the diagrams for deflection, rail moment and rail seat load. The solid lines in the diagrams represent the BOEF sensitivity lines, while the filled circles represent the beam element mode. In diagram b) (for the rail moment) open circles have been used for the moment of inertia in order to avoid confusion with other parameters. Also, the regression coefficients for regression functions of the power type are shown, but the actual regression curves are, however, not shown here. The regression was done with the 'Trend line' option in a Microsoft Excel spreadsheet. For comparison, the corresponding parameters

1. The regulations /43/ actually specifies a minimum total height of 750 mm from the base of the ballast to the top of the rail, and this makes the depth of the ballast layer beneath the sleepers approx. 350 mm.

for the BOEF sensitivity lines are also given. As for the ordinary BOEF model, more detailed diagrams are provided in Appendix A.

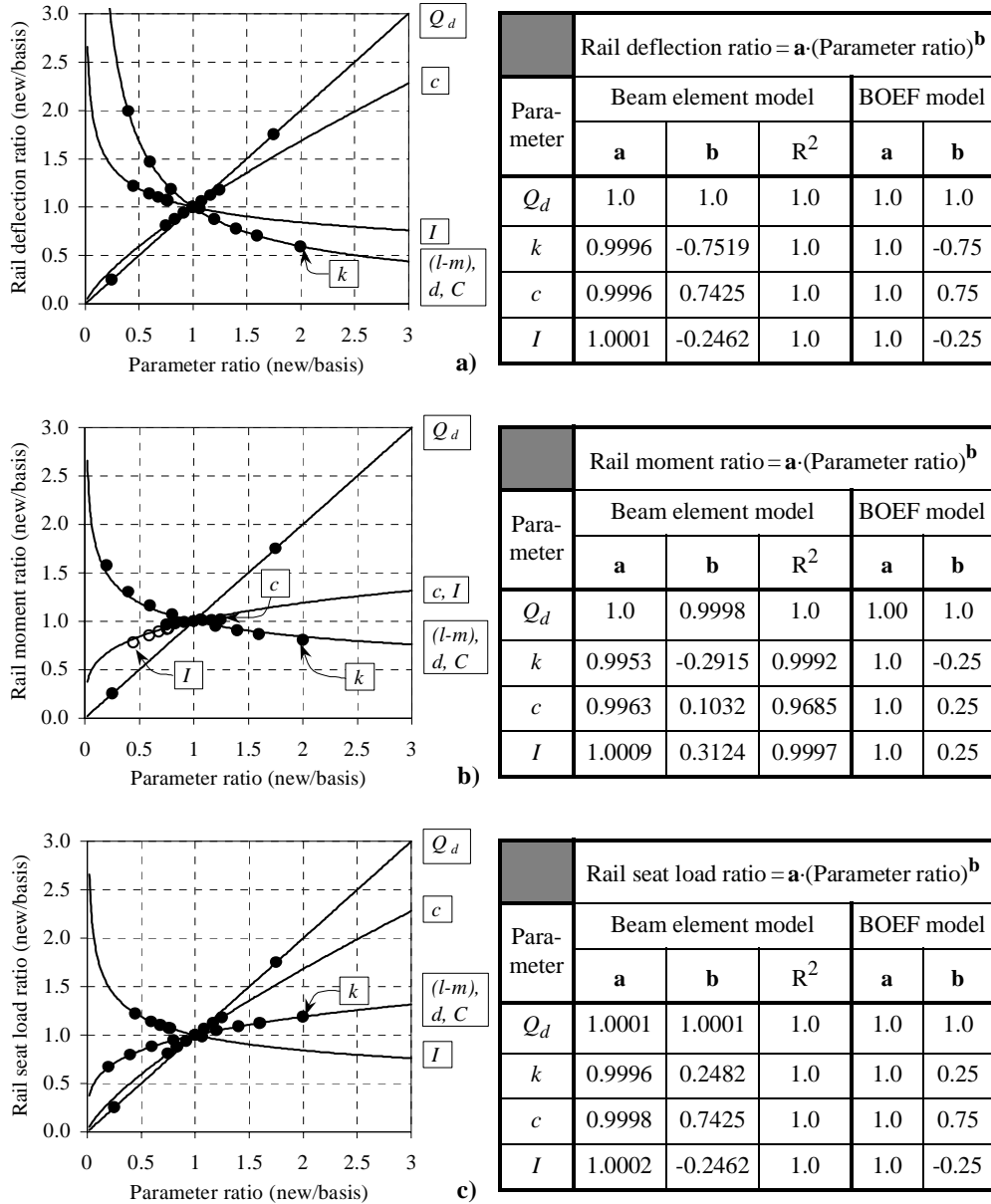


**Figure 2.22:** Dimensionless sensitivity diagram for a beam element model (filled or open circles) compared with the BOEF model (solid lines). Regression coefficients for the beam element model given along with the corresponding coefficients for the BOEF model. Larger diagrams can be found in Appendix A.

As can be seen from Figure 2.22 there is a very good correspondence between the BOEF sensitivity lines and the corresponding beam element markers when it comes to rail deflection and rail seat load. This is also reflected in the tables next to the diagrams. For the rail moment there

are some differences, especially for the moment of inertia and sleeper spacing. It is worth noting that all the reactions are linear with respect to the design load both in the BOEF model and in the beam element model. This is of course due to the fact that both models actually are linear and also were intended to be linear.

With reference to the discussion at the end of Section 2.9.1 the general conclusion must be that for the rail deflection there are almost no differences between the ordinary BOEF model and the beam element model. For the rail moment there are some differences as the impacts from the track modulus and rail moment of inertia are bigger for the beam element model, while the impact from the sleeper spacing is smaller.

Another interesting property of the regression lines of the beam element model is that the power functions describe these lines very accurately since the  $R^2$ -values are very close to 1.0 in all cases. This also implies that the curves traverse very close to the coordinate (1,1), which represents the basis model. The physical meaning of these considerations is that the basis model for a linear beam element model with a single axle load does not matter much. In other words, the dimensionless diagrams for this type of model have a quite general validity, and they should not be regarded just as regression lines for those particular values used in the analyses. In practical engineering, for a single axle load, these diagrams could be used in precisely the same way as the diagrams for the BOEF model.

As an illustration of the differences between the current diagrams and the ones described for the BOEF model (Section 2.7) the same example as on page 34 will be recalculated. As before, the parameter ratios are 1.2 ( $Q_d$ ), 1.14 ( $I$ ) and 0.9 ( $c$ ). According to the new diagram describing deflection, the deflection ratios are 1.2, 0.97 and 0.92 which are the same as for the BOEF model. Hence the deflection is increased by 7 %. For the rail moment the ratios are 1.2, 1.04 and 0.99, and the rail moment is then about 24 % greater than the basis rail moment. For the BOEF case the rail moment was increased by 20 %, so the new diagram predicts a slightly greater rail moment in this particular case.

## 2.10 Outline of a new beam element model with nonlinear support

### 2.10.1 The relationship between wheel load and maximum deflection

This model developed by the author is motivated by the fact that the load-deflection curve for a railway track is often, if not always, nonlinear. The nonlinear behaviour is usually of the hardening type with increasing track stiffness<sup>1</sup> as the load increases. In such a model the track stiffness must be regarded as the derivative of the load with respect to deflection. This type of load-deflection relationship is schematically shown in Figure 2.23 below.

The load as a function of deflection may then be modelled as in Eqn. (2.50) for a single axle load:

$$Q_m = A \cdot \left( \frac{y_m}{y_{ref}} \right)^B \quad (2.50)$$

where

---

1. See Eqn. (2.22) on page 17 for the definition in the linear case.

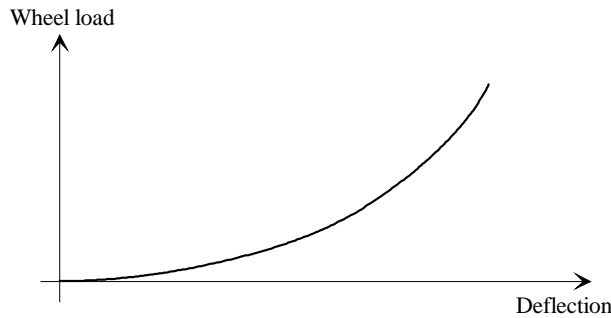


**Figure 2.23:** Sketch of a typical relationship between wheel load and rail deflection.

- $Q_m$  = measured or known wheel load [N]
- $y_m$  = measured deflection of the rail directly below the wheel load [mm]
- $y_{ref}$  = a reference deflection, set equal to 1.0 mm
- $A$  = regression constant with same unit as  $Q_m$
- $B$  = regression constant

The nonlinear track stiffness,  $K_{nl}$ , is given as the derivative of the expression in Eqn. (2.50):

$$K_{nl}(y) = \frac{dQ}{dy} = AB \left( \frac{y}{y_{ref}} \right)^{B-1} \quad (2.51)$$

To establish the relation in Eqn. (2.50) one only needs to measure the load and deflection at two different load levels. An easy way of doing this, with acceptable accuracy, is to measure the rail deflection for passing trains at low speed. When the speed is low the wheel loads are approximately the nominal wheel loads given in the specifications from the rolling stock manufacturers. These loads are quite accurate provided that the cars are empty. Preferably the two load levels should be quite different in magnitude and this may require that some of the railway cars be loaded. When more than two measurements of deflection and loads are carried out one may perform a statistical regression to obtain the constants  $A$  and  $B$ .

The expression in Eqn. (2.50) may also apply to cases of two or more axles. Then  $Q_m$  is still the wheel load, while  $y_m$  is the maximum deflection measured. There may be a risk that the maximum deflection  $y_m$  is not directly below a wheel load when you have multiple axle loads. This phenomenon is more articulated when the track response is soft (confer the discussion in Section 2.7.2). Since the track stiffness in the current model increase with load, confer Eqn. (2.51), the track is also soft when the load is small. The difference between the deflections below the wheel loads and the maximum deflections are in most cases small and may be neglected. Another important property with a nonlinear model is that a summation of the rail deflections or moments is not possible when these reactions are produced by multiple axles. Instead, a separate analysis has to be made for each axle configuration.

There is no direct physical interpretation of the parameters  $A$  and  $B$ . However, as can be seen by inspection of Eqn. (2.50), the track behaves linearly if  $B = 1$ , it hardens if  $B > 1$  and if  $B < 1$  the track shows a softening behaviour. The reason why an expression like the one in Eqn. (2.50) was chosen was that this expression would give a sufficient nonlinear behaviour at a cost of only one more parameter compared with the linear model. As argued above this imply that only two measurements of deflection at different load levels are needed. As will be evident later, this lim-

ited number of parameters will also be beneficial for the beam element model as only two additional equations in addition to the ordinary stiffness relations have to be established.

### 2.10.2 Establishing and solving the model equations

The crucial question next is how to transfer from an overall track stiffness model to a beam element model. The rail will, as before, be modelled as Euler-Bernoulli beam elements with only one element per sleeper spacing if there are no loads between the sleepers. The rail support will be modelled with the same model as for the overall track but, of course, with other parameters  $\alpha$  and  $\beta$ , i.e.:

$$S_n = \alpha \cdot \left( \frac{y_n}{y_{ref}} \right)^\beta \quad (2.52)$$

where

$$\begin{aligned} S_n &= \text{rail seat load for sleeper no. } n \\ \alpha, \beta &= \text{regression parameters analogous to } A \text{ and } B \text{ in Eqn. (2.50)} \\ y_n &= \text{deflection for sleeper no. } n \end{aligned}$$

It is emphasised that Eqn. (2.52) represents an *assumption* on the behaviour of the rail support. There have not been made any tests to establish this relation. However, Eqn. (2.52) was an appealing choice since the overall track behaviour was modelled by the same type of expression. If the rail was completely stiff and of finite length,  $\alpha$  would equal  $A$  divided by the number of rail supports and  $\beta$  would be identical with  $B$ . The numerical values of  $\alpha$  and  $\beta$  will be found as part of the analysis.

The next step is to establish the element model for the track. As ordinary structural frame computer codes normally cannot deal with this problem, it is necessary to establish the equations manually. This is done by applying ordinary stiffness relations from structural mechanics, but with the model in Eqn. (2.52) for the rail support. In structural mechanics this process is known as the *direct method*. The stiffness relations provide as many equations as there are unspecified degrees of freedom (dofs), but two more concurrent relations have to be established in order to solve also for  $\alpha$  and  $\beta$ . One additional equation is established by using the ordinary stiffness relation for the specified dof, i.e. the known overall deflection. It is then necessary that this relation contains the two unknowns  $\alpha$  and  $\beta$ , and the only requirement for this to be satisfied is that the known deflection is measured at a sleeper position.

The last necessary equation is established by equilibrium between external energy applied by the load and internal energy stored in the track model. The external energy supplied by a single wheel load is

$$E_{ext} = \int_0^{y_m} Q(y) dy = \frac{A}{B+1} \cdot \left( \frac{y_m}{y_{ref}} \right)^{B+1} \quad (2.53)$$

The energy stored internally in the track because of the wheel load is a sum of the energies stored in the nonlinear support springs,  $\Sigma E_n$ , and the bending energy of the rail,  $E_{rail}$ :



$$E_{int} = \sum_n E_n + E_{rail} = \sum_n \frac{\alpha}{\beta + 1} \cdot \left( \frac{y_n}{y_{ref}} \right)^{\beta + 1} + \frac{1}{2EI} \int_{rail} [M(x)]^2 dx \quad (2.54)$$

where  $n$  is rail support no.  $n$  and  $M(x)$  is the rail moment.

As the principle of conservation of energy forms one of the model equations the model is energy consistent. This also provides uniqueness to the model, i.e. there is a one-to-one correspondence between load and deflection. As such the model could be said to be nonlinear elastic.

Currently the model has 14 unknowns, six deflections, six rotations, and  $\alpha$  and  $\beta$ . A general-purpose calculation programme run on a PC was used to solve the resulting set of nonlinear equations. The software utilises a kind of Newton-Raphson technique to solve the equation set.

### 2.10.3 Some results for the new beam element model

From various analyses of a single wheel load the  $\alpha$  and  $\beta$  are found to be reasonably constant for different load levels within the same overall model (same  $A$  and  $B$ ). A calculation with  $A = 20000$  N,  $B = 1.5$  and with S54 rail elements spanning six sleepers on each side of the load shows that the variation is at most around 1 % for both parameters, but they deviate in opposite directions. The deviation in the support load (seat load) by using  $\alpha$  and  $\beta$  from different load levels is thus only in the order of 0.2 %. That  $\alpha$  and  $\beta$  being constant for any load is important for Eqn. (2.54) to be valid.

Some results from analysing a single axle load are given. In all cases there were a single wheel load  $Q = 100\,000$  N with  $A = 25\,000$  N,  $B = 2.0$ , and with maximum deflection  $y_0 = 2.0$  mm. The track consists of UIC60 rails and the sleeper spacing was 600 mm. Analysed track length was 3600 mm to each side of the wheel load, but only the half to the right of the wheel load was analysed, as the two parts are symmetric.  $\alpha$  and  $\beta$  was calculated to be 7650 N and 2.32, respectively. The deflection consistent track modulus was calculated to be 24.8 N/mm<sup>2</sup>. Rotation, but no vertical deformation is allowed at the rightmost sleeper. In Figure 2.24 the deflection distribution of the new model is compared with the BOEF model.

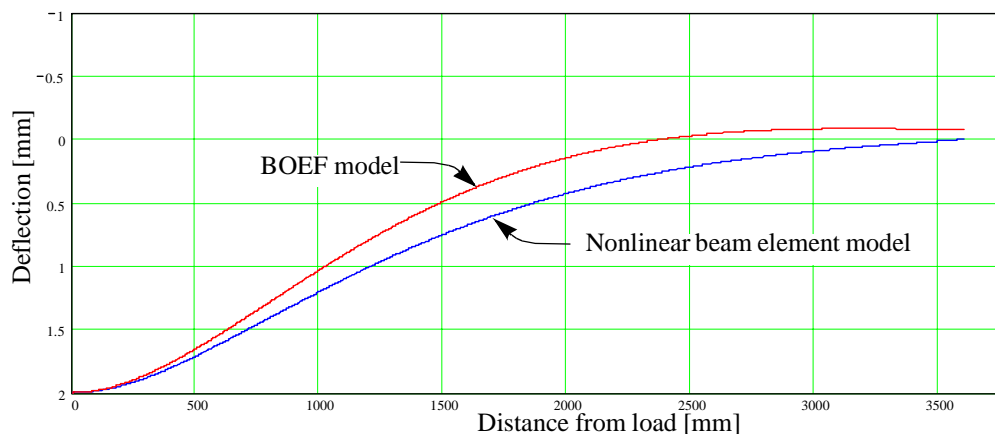


**Figure 2.24:** Deflection distribution for the new nonlinear beam element model compared with the ordinary BOEF model with the same maximum deflection.

The corresponding rail moment distribution is depicted in Figure 2.25.

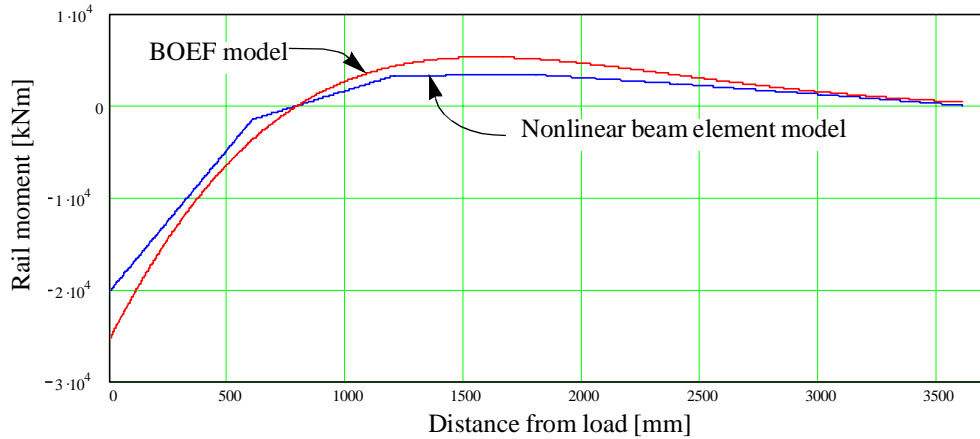


**Figure 2.25:** Rail moment distribution for the new nonlinear beam element model compared with the ordinary BOEF model with the same maximum deflection.

As can be seen from the diagrams in Figure 2.24 and Figure 2.25, there are no big differences either in rail deflection or in rail moment between the BOEF and the current new model, especially near the point of load application. It seems however that the new model has an impact on the track farther away from the load than that of the BOEF model, confer Figure 2.24. In 'linear response terms' this should imply a softer behaviour for the new model. But with regard to the seat loads, the new model concentrates these loads nearer to the axle load, as can be seen from Figure 2.26. The seat loads for the new model thus indicates a stiffer behaviour near the point of load application. All in all it can be said that the new model gives a track that is stiff where the load is applied, but soft farther away from the load.

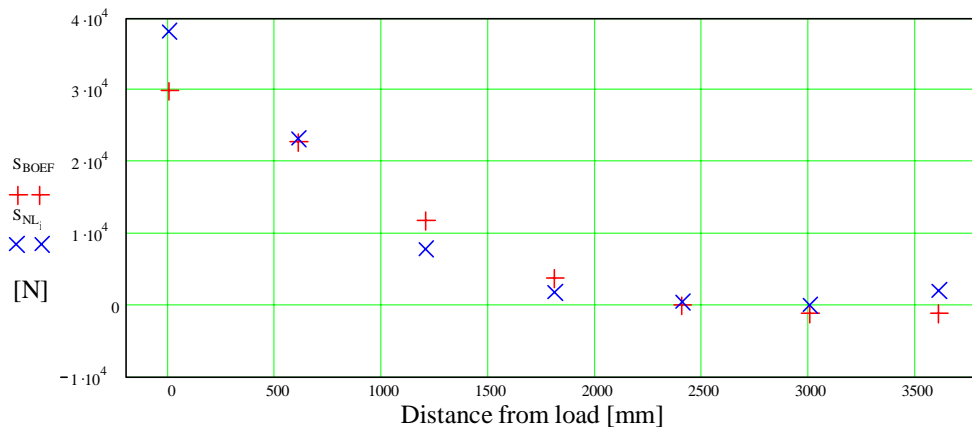


**Figure 2.26:** Seat load distribution for the new nonlinear beam element model compared with the ordinary BOEF model with the same maximum deflection. The BOEF seat loads are calculated using Eqn. (2.12).

The seat load for the new model at the very right end in Figure 2.26 seems to be substantially higher than for the neighbouring sleeper, but this is an error due to the end support conditions. If more elements were added to the right end this erroneous seat load would diminish.

Analyses made with also the vertical deflection at the rightmost sleeper as a free dof revealed unrealistically big upward deflection at this position. For the same data as those used in the figures above, the upward deflection is calculated to be 0.56 mm. It is believed that this behaviour is due to the relatively short model and also the fact that any preloading from the rails and sleepers has not been accounted for. However, a somewhat bigger upward deflection is expected because the track is very soft when the deflection is around zero, and this also complies with the fact that ballast materials cannot sustain tension.

#### 2.10.4 Concluding remarks

The new model represents a 'top down' approach in the sense that you first establish the overall track model (Eqn. (2.50)) then you proceed to the element reactions by calculating the various responses and the needed nonlinear spring data in the same operation. In principle, this is much the same approach as the ordinary BOEF method. In the BOEF method you establish the overall model by assuming a Winkler foundation and solving the resulting differential equation. Then you measure the track modulus, which is a parameter created by the BOEF model, and you may then calculate the various reactions. The main difference in the general solution procedures is that for the BOEF model it is only needed to solve the differential equation once and for all, while for the new nonlinear model you have to solve the equation set each time you change the input data.

Normally a finite element analysis is a 'bottom up' approach as the element properties (geometric properties and material properties) are used to build a total model. The deflection of the point of load application is not known, in fact this deflection is often the one that is important to find by such an analysis. This is also true for a nonlinear analysis. But in a nonlinear analysis it is often required to incrementally apply the load on the structure and perform the analysis stepwise. For the current model, however, when by some means  $\alpha$  and  $\beta$  are known a priori one may calculate the dofs by applying the whole load to the model and using the stiffness relations only.

The capabilities of the new model have not been fully explored, hence the notion 'outline' in the heading of this section. Some of the most important facets of the model that need further exploration may be summarised as follows:

- (1) The model has to include more rail and spring elements especially when one wants to model the response from multiaxial loading.
- (2) More data from track measurements, especially deflections, but also rail stresses and seat loads, are needed to explore the usefulness and reliability of the model. To get reliable data for rail stresses and seat loads is however more challenging than for the deflections.
- (3) The effect of the track ladder weight may be advantageous to include in the model.
- (4) It may be possible to separate the effects from the rail pads and the sleepers and then deduce from the overall behaviour what behaviour should be left with the ballast and substructure.

In the future, this method will hopefully provide a conceptually simple but still a more accurate tool for the railway track engineer. Especially when the track shows a clear nonlinear load-deflection relationship the present model will be advantageous, and in particular when it comes to

seat load calculations. The fact that the method may be based on measuring the rail deflection only, makes the data capturing as easy as for the BOEF method. To measure the rail deflection one may use one or more LVDTs (Linear Variable Differential Transformers).

## 2.11 Dynamic models

According to Clough and Penzien /11/ a dynamic load is defined as a load where its magnitude, direction or position varies with time. As a result, the structural response, i.e. deflections and stresses, is also dynamic or time-varying. Hence a dynamic model aims at describing the dynamic response to dynamic loading. By examining the loading of a railway track we will soon find that there is dynamics involved when a train moves along the track.

The field of dynamics of railway tracks is vast, and only a scratch on the surface will be made here. Because of its complexity, dynamic analyses of railway tracks are not made on a routine basis even today. However, dynamic analyses of railway cars within the rolling stock industry are now feasible with an acceptable accuracy. Examples hereof are the software packages of ADAMS Rail/Medyna, Gensys, Nucars, Simpack and Vampire /40/. These packages also have simplified models of the track itself, but the main objective of the computer codes is to calculate the responses of various rolling stock items.

In a certain respect one may say that the loading of the track is 'more dynamic' than the loading of the rolling stock. This may be evident when a train at constant speed moves along a tangent track with perfect geometry and with uniform vertical resiliency along the track. Apart from any hunting behaviour the individual cars experience very small dynamic loads. On the other hand, a location in the track will undergo several onloadings and offloadings during the time it takes for the total number of train axles to pass. The crucial question in a design process is whether a dynamic analysis of the track is necessary to get reliable response data for the critical stresses and strains. It is likely that dynamic track analyses will be more common in the future because of higher train speeds, better material data and more accurate numerical tools. The present-day problem of high speed trains travelling at velocities that at some places exceed the critical soil velocity may show the usefulness of dynamic analyses also in practical engineering.

Clough and Penzien /11/ mention two basically different types of structural dynamic loading, namely a *prescribed* dynamic loading and a *random* dynamic loading. In the former case the structure can be analysed in a deterministic manner, whereas in the latter case a nondeterministic, or stochastic, analysis has to be performed. A deterministic analysis normally leads to a displacement-time history that corresponds to the prescribed loading history, and the other responses, such as stresses and strains, are normally calculated in a secondary phase on the basis of the displacements. However, in a stochastic analysis the variation of the displacements with time is not known, and all responses have to be evaluated independently from separate stochastic analyses. In the proceeding sections only prescribed dynamic loading and deterministic analyses are addressed.

In addition to /11/, which is a good general textbook for the introduction to dynamics of structures, Frýba /25/ is more specific on moving loads. The latter textbook<sup>1</sup> is often referenced by researchers in the field of railway track dynamics.

---

1. The 1972 edition (1st ed.)

### 2.11.1 Models with given loading

An example of a simple dynamic model of an Euler-Bernoulli beam is given by Esveld /22/. Such a beam loaded at  $x=0$  with a concentrated harmonic load

$$F(t) = Q_0 \cdot e^{i2\pi ft} \quad (2.55)$$

may be modelled with the following differential equation:

$$EI \frac{\partial^4}{\partial x^4} [w(x, t)] + m \frac{\partial^2}{\partial t^2} [w(x, t)] + c \frac{\partial}{\partial t} [w(x, t)] + w(x, t) = 0 \quad (2.56)$$

where  $i$  is the complex unit,  $f$  is the loading frequency,  $t$  is the time variable,  $w(x, t)$  is the deflection function,  $m$  is the track vibrating mass and  $c$  is the track damping.  $m$  and  $c$  are in this context given per unit length of track. The left-hand side of this differential equation is describing a foundation model that is known as the *Kelvin model*.

With similar boundary conditions as for Eqn. (2.7) on page 10 the solution of Eqn. (2.56) has the form:

$$w(x, t) = y(x) \cdot e^{i2\pi ft} \quad (2.57)$$

Hence Eqn. (2.56) can be rewritten to a form similar to Eqn. (2.7) for the statically loaded BOEF:

$$EI \frac{\partial^4}{\partial x^4} [y(x)] + [k - 4\pi^2 f^2 m + i2\pi fc] \cdot y(x) = 0 \quad (2.58)$$

The track modulus in the static case must however be replaced by a complex track modulus,  $k^*$ :

$$k^* = \sqrt{[k - 4\pi^2 f^2 m]^2 + 4\pi^2 f^2 c^2} \cdot e^{i \operatorname{atan} \left\{ \frac{2\pi fc}{k - 4\pi^2 f^2 m} \right\}} \quad (2.59)$$

An alternative version of the same model is provided by El-Sibaie /20,21/ on the basis of Frýba /25/. Here the load is assumed to be moving at steady speed along the track, and the governing differential equation is modified to

$$EI \frac{\partial^4}{\partial x^4} [w(x, t)] + m \frac{\partial^2}{\partial t^2} [w(x, t)] + c \frac{\partial}{\partial t} [w(x, t)] + w(x, t) = Q(t) \cdot \delta(x - v_0 t) \quad (2.60)$$

where  $Q(t)$  is a load that varies with time,  $\delta$  is the Dirac delta function and  $v_0$  is the constant velocity by which the load  $Q(t)$  moves along the track. /21/ also shows the solution of the simplified problem when the load is constant, i.e. do not vary with time. The advantage of Eqn. (2.60) over Eqn. (2.56) is that the effect of moving loads is taken into account.

A typical deflection shape is shown in Figure 2.27 below. Note that the deflection and rail moment are not perfectly symmetric as in the static case. This is caused by the velocity of the moving load and the foundation damping.

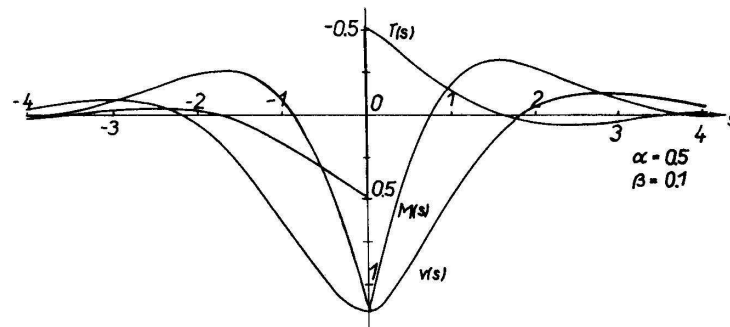


**Figure 2.27:** Rail deflection  $v(s)$ , rail moment  $M(s)$  and rail shear force  $T(s)$  when inertial and damping characteristics are included. Light damping ( $\beta=0.1$ ) and subcritical speed ( $\alpha=0.5$ ). From Frýba /25/.

With advanced computer software it is possible to make a model where no track loads are given explicitly but rather come out of an analysis of the total track-train system. The wheel loads are then a result of the vehicle weight, track irregularities (misalignments), track curving, wheel irregularities (i.e. wheel flats) coupled with track and train characteristics.

### 2.11.2 Static versus dynamic analysis

The question whether a static or dynamic analysis of a track section should be performed is dependent upon several factors:

- ◆ Accuracy
- ◆ What data are needed
- ◆ Train speed
- ◆ Foundation characteristics

If, for instance, data are needed for damping characteristics for a track on soft ground trafficked by high speed trains, a dynamic analysis should be performed.

Another way of deciding whether a dynamic analysis has to be carried out is to measure the deflection in the track when a train passes. If the deflection is reasonably symmetric with respect to the maximum deflection it is likely that a static analysis will capture most of the reaction effects in the track.



---

## CHAPTER 3 Elements of constitutive modelling of railway ballast

---

### 3.1 Introduction

In this chapter some facets of the modelling of mechanical behaviour of frictional soil will be looked upon more closely. The focus will be on elasto-plasticity, repeated loading and friction - with a view to railway engineering. The use of the finite element method is also briefly discussed.

Railway track dynamics and track-train interaction will not be focused upon as the track loads are assumed to be of a quasi-static nature. With respect to the loads, reference is made to Section 2.2.

While Chapter 2 deals with the reactions in the upper part of the railway structure, the present chapter will be relevant when looking upon the complete structure - from subgrade to rail. It may therefore be pertinent to define the various parts of a railway structure in more detail, see Figure 3.1. This figure is taken from Selig and Waters /72/ and is more relevant to American conditions than to Norwegian conditions. For instance, in Norway we do not differ between top ballast and bottom ballast, and the subballast layer and the placed soil fill will be one layer and frequently made up of rock-fill material. Also note the term 'superstructure' only includes the rails, the fastening system, the sleepers and the crib ballast, while the term 'substructure' covers the ballast layers beneath the sleepers, the placed soil fill and the natural ground.

### 3.2 Some comments on modelling

#### 3.2.1 General requirements to a mathematical model

In general, a good mathematical model should have high standards regarding the following aspects:

- ◆ Answer the posed question(s).
- ◆ Generality.
- ◆ Accuracy.
- ◆ Few parameters needed, easy to use.

As an example to the first item, the BOEF model discussed in Chapter 2 cannot answer the question about strains in the ballast layer given only those data needed by the model. There might be a chance of getting a very rough estimate when some layer thicknesses and some ad hoc hy-



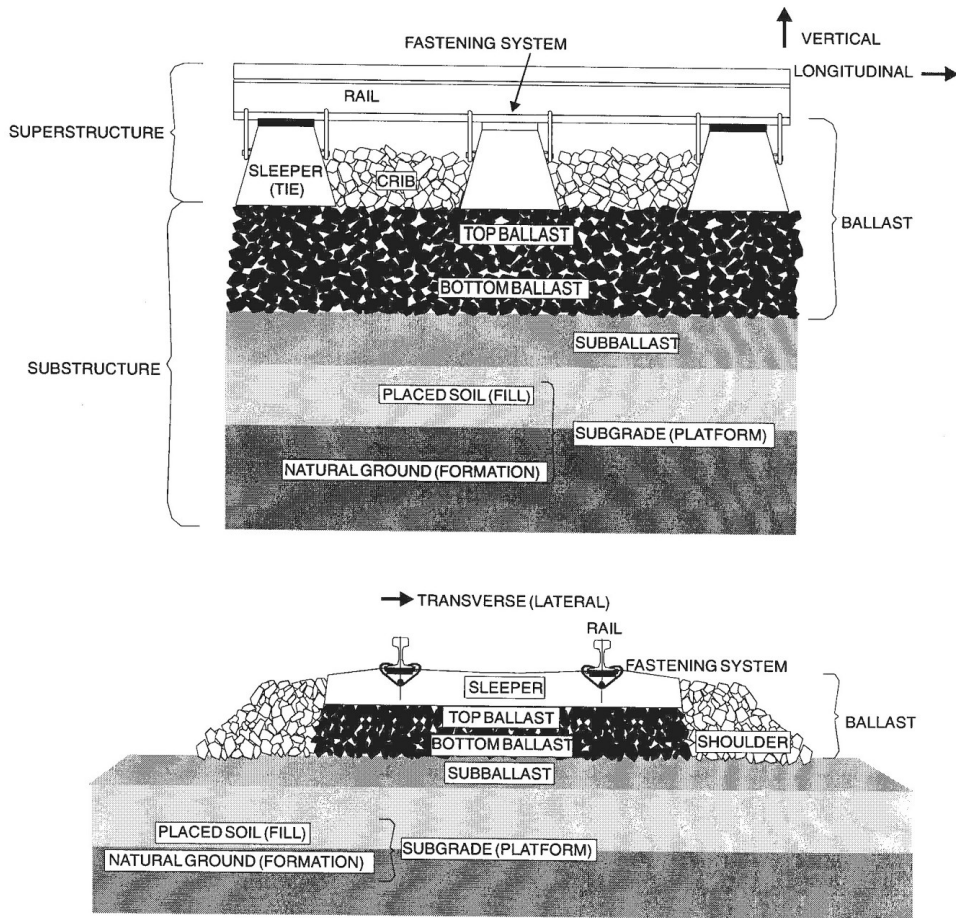


**Figure 3.1:** The various parts of a conventional, ballasted railway track structure. From Selig and Waters /72/.

potheses of load distribution in granular layers are given. These extra pieces of information do not, however, interact with the rail behaviour; rather, this information is used for post processing the original output from the BOEF model. As such, the BOEF model describes the track behaviour from the rail point of view.

The second item on the list is of profound importance in all modelling. A good model should be so general that it will make reasonable predictions of track behaviour for a broad range of input data. Since this is difficult to achieve the recommended range of the input data should be described. If the model is not well known it should be described when results from model predictions are reported. In some cases the model employed is actually mentioned implicitly when requesting the input. This is the case for linear elastic models, where Young's modulus  $E$  and Poisson's ratio  $\nu$  are required input (alternatively, the bulk modulus  $K$  and the shear modulus  $G$ ). Also the BOEF model falls into this category, since a track modulus  $k$ , in addition to rail parameters, is required.

Further, the requirement of high accuracy may seem obvious, but gives rise to certain fundamental problems. One of the more serious ones is the question of strains and stresses in the granular layers. Certainly, the material in coarse granular layers is of a discrete nature with

individual particles assembled together, and this does not encourage a continuum mechanics approach for strains and stresses. Moreover, this discrete nature of the material makes it difficult to measure the exact strains and stresses beneath a passing train. Generally speaking, one may divide the problem of accuracy into two parts: One that consider the accuracy of the material modelling and a second that consider the accuracy of the geometrical model of the object to be analysed. One of the major pros of the finite element method is its ability to handle both material behaviour and geometry accurately.

The generality and the accuracy requirements may be combined to a *predictability* requirement. Some comments regarding predictability has also been given in Section 2.3.6, although with the emphasis on the BOEF model. It should also be mentioned that the first three aspects listed above regarding modelling are most often interrelated. A very general model will lose much of its *raison d'être* if it is not able to answer frequently asked questions in track design or if it is not reasonably accurate.

Considering the final point, the requirement of simplicity may be contradictory to the first three points. However, a model with many parameters may be tailored especially for one purpose and therefore loses its generality. Furthermore, an easy-to-use model will attract more users and may in the future form the framework for more advanced models.

The advent of the finite element method (FEM) has enabled engineers to put more effort into material modelling than into classical solution techniques. This shift of perspective has brought about major progress in material modelling, while solution techniques like the FEM work in the background and produce the answers without bothering the engineer with the computational details. Consequently, the requirement of simplicity may focus on the material behaviour part of the model. A greater responsibility is however put on the engineer to evaluate the results from the finite element analysis as this is a numerical approximation to the problem.

### 3.2.2 Strain and stress measures

When talking about strain and stress there exist several definitions. Here an assumption of small strains and deformations is taken, as the railway embankment structure is assumed to perform satisfactorily. Generally it should be noted that the assumption of small strains do not necessarily imply small deformations, confer, e.g., a cantilever beam with a transversal tip load, but for our purposes the deformations could also be considered small.

When not otherwise stated the strain measure is the Cauchy strain /15/, i.e. strain based on the original configuration. In one dimension the Cauchy strain,  $\varepsilon$ , reads

$$\varepsilon = \frac{l - l_0}{l_0} \quad (3.1)$$

where  $l_0$  is the original length and  $l$  is the deformed length. This strain measure is also called the *engineering strain*.

Also, the stress measure is based on the original configuration, i.e. the numerical values of the stresses are calculated on the basis on unchanged areas. Hence it is assumed that the stresses are *engineering stresses*.

The geotechnical sign convention is used, i.e. compressive stresses and strains are positive while tension and elongation is negative.

### 3.2.3 Types of nonlinearities

Many common metallic materials behave linearly, at least for moderate strains. Hence, there is a linear relationship between stresses and strains. Soils, on the other hand, are generally known to exhibit a nonlinear behaviour.

Generally a mechanics problem is nonlinear if the stiffness matrix or the load vector depends on the displacements /12/. Three important sources of nonlinear behaviour are briefly discussed below /3/: Material nonlinearity, geometric nonlinearity and boundary nonlinearity.

**Material nonlinearity** is associated with changes in material properties when the material is deformed. Plastic behaviour will in any case give rise to nonlinearities, but also elastic behaviour may be nonlinear. The foundation spring model of Section 2.10 is an example of a nonlinear elastic model. Plasticity is treated later in the present chapter.

**Geometric nonlinearities** occur when the deformations are large during an increase of forces from zero to the final values. These deformations will change the geometric shape of the structure so that the behaviour for the first load steps are significantly different from the behaviour when the load approaches its final value. What in effect is analysed is a series of geometrically different structures. Examples hereof are buckling of columns, snap-through buckling of curved beams or shells, squeezing of soft layers between stiff layers. This type of nonlinearity is not treated any further in the present thesis.

**Boundary nonlinearities** may be regarded as a special type of geometric nonlinearity as certain nonlinear effects occur only at the boundary. The source of any boundary nonlinearity is that the boundary conditions change during the analysis. Contact problems are in this category, e.g. the track models described in Sections 2.5 and 2.6. The theory of boundary nonlinearities will be left here as it is considered to be beyond the scope of the thesis.

## 3.3 The finite element method

### 3.3.1 Introduction

The finite element method is inextricably tied to constitutive modelling as this method makes it possible to numerically solve boundary value problems where a constitutive model is an ingredient. There also exists other methods, but the finite element method seems to be the most popular and therefore it deserves a brief description as it is still not so much used by railway track engineers.

The finite element method was invented in the late 50s and early 60s as a means of calculating stresses and strains in structural mechanics. After this initial stage of development it was recognised that the method could also be employed more generally to solve a broad range of boundary value problems. Nowadays the method has evolved to a more or less standard numerical tool in almost every branch of engineering science. In railway technology the method is utilised in as various fields as aerodynamics, electrical engineering and acoustics in addition to numerous structural analysis applications.

The scope of this section is not to give a thorough description of the finite element method (which is hardly possible even for standard textbooks), but rather to provide a glimpse of insight to readers not familiar with this method. More in-depth descriptions can be found in numerous textbooks on general FEM, among which are the books of Cook et al. /12/, Zienkiewicz and Taylor /91/, and Bathe /3/, just to mention a few. The following description is limited to stress and strain computations in static structural mechanics.

### 3.3.2 The finite element method for structural mechanics

An analytical solution procedure takes as a starting point the governing differential equations together with boundary conditions. In principle an analytical solution, when correctly carried out, will provide a closed form solution where the stresses and strains are functions of some position coordinate in addition to material and loading parameters. In more involved cases, as in elastic layer theory, numerical solutions have to be invoked to solve the exact equations. The latter case may therefore be denoted semi-analytical. But in both cases pointwise (or particle-wise) static equilibrium is assumed, and any errors must therefore be due to erroneous solution techniques in addition to numerical noise in the case of a semi-analytical approach. In other words, the stresses and strains at every point in the structure are the exact correct ones, assumed that the material behaviour is exactly described in the model, and exact static equilibrium in every point is assured.

However, when the material in the structure behaves more complex and the geometry of the structure is irregular, an analytical solution is very difficult, if not impossible, to find. And here the finite element method shows to advantage.

Simplistically speaking, the finite element method is a piecewise approximation to the actual stress and strain fields. As such the finite element method generally provide neither exact solutions nor static equilibrium for every particle in the structure (in contrast to analytical solution techniques). Instead of equilibrium for every particle, the method offers equilibrium in a piecewise manner throughout the structure. To be more accurate, the structure is divided into a number of pieces of finite size, not necessarily of equal size, called finite elements (hence the name of the technique). The individual element is assured to be in static equilibrium by the techniques inherent to the method<sup>1</sup>. Certainly, every point within an element is not in equilibrium, but the element as a whole is. Since the whole structure is made up of elements in equilibrium, the structure itself is in equilibrium. The advantage of using this piecewise approximation is that within each element the approximation is carried out with very simple functions.

When the structure is divided into elements the individual elements are assigned a set of nodes in-between which the internal deformation of the element is interpolated. This suggests that the deformations are known at the nodes, which in fact is true when the analysis is completed. At the level of element analysis the nodal deformations (often referred to as *degrees of freedom*, abbr. dof(s)) constitutes the set of unknowns for the element. At the structure level all nodal dofs constitute the total number of unknowns in the analysis. These unknown dofs are found by solving a system of simultaneous equations provided by the method.

The nodal degrees of freedom are typically a selection of the x-, y- and z-deformations at that node (Cartesian coordinate system assumed). The ones to pick are of course dependent of the dimensionality of the problem - a 2D problem do not need the third nodal dof (e.g. the dof in z-direction). All or most of the nodes are placed at the borders of the element, although internal

1. One of the frequently used methods is the principle of virtual work, in which FEM may be recognized as a calculus of variations procedure.

nodes are perfectly OK and may also be beneficial in some cases. To get high accuracy many nodes at each element is necessary, but the penalty is that this would occupy a lot of CPU and storage in the computer during analysis. The simplest element for practical use in structural mechanics is the two-noded bar element with two dofs, and one of the most complex is the 27-noded 3D element with 81 dofs. These and other examples of types of finite elements are shown in Figure 3.2 below.

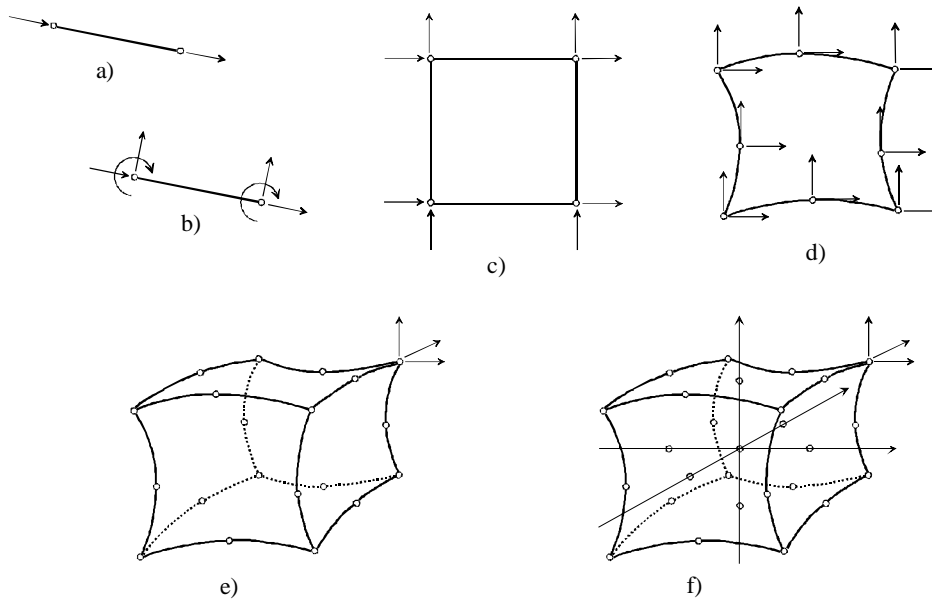


**Figure 3.2:** *Examples of different types of finite elements (nodes and dofs indicated by small circles and small arrows, respectively): a) Two-noded linear truss element (for axial loads only), b) Beam element that allows axial, transversal and moment loads, c) Four-noded 2D element, d) Eight-noded 2D element, e) 20-noded 3D element and f) 27-noded 3D element (with local coordinate system indicated through the centre node). (Elements e) and f) with only three of the dofs displayed.)*

The accuracy of the method depends mainly upon two factors. First, the size of an element decides how large a ‘particle’ must be to assure equilibrium. If we want to look at a region that is smaller than the element size, we may find that the static equilibrium conditions are violated. However, if we choose to divide our structure into smaller elements, equilibrium is satisfied at more and smaller subregions within the structure. This will in most cases improve the accuracy. Second, the way the deformations are allowed to vary within an element will also affect the accuracy. This is closely related to the number of dofs of each element. Assuming polynomial interpolation and with reference made to Figure 3.2 it may be argued that with two dofs at an element edge, the variation of deformation between the nodes can at most be linear, with three dofs the deformation may vary parabolic, and so on. If the deformations are only allowed to vary linearly, so that the corresponding strains and stresses are constant within an element, the accuracy is poorer than if the deformations are allowed to vary with functions with a somewhat higher order. This is so because we cannot in advance know exactly how strains and stresses vary (this is actually something we want to calculate during the analysis!), and the more intricate variations we allow the greater is the chance that we actually are close to the right one. However, the functions that provide this interpolation within an element must also take care of cases where

the solution requires lower order interpolation functions (i.e., the polynomials must be *complete*).

A consequence of the accuracy problem is that in regions of the structure where the strains and the stresses are expected to vary greatly over small distances, there should be more and smaller elements. If possible, you will also benefit from substituting simple elements with more advanced elements with more nodes and dofs. Again, any improvement of accuracy gained in this way must be balanced against increased computing costs.

A more mathematical approach to the finite element method may be found in numerous textbooks as mentioned in Section 3.3.1.

### 3.4 Elastic models for transportation structures

There are numerous elastic models that have been used for transportation structures. Here a brief review is given for some of the most common models. Many of the models are tailored for road-building materials but the concepts may be equally applicable to railways. A general reference on constitutive laws for geologic materials is the book by Desai and Siriwardane /15/.

#### 3.4.1 Linear, isotropic elasticity

The elastic model may come in several versions, but the one that assumes isotropic conditions is the one described here and is adopted from /64/. When the constitutive matrix is denoted  $\mathbf{D}$ , the generalised Hooke's law reads:

$$\boldsymbol{\sigma} = \mathbf{D}\boldsymbol{\varepsilon} \quad (3.2)$$

where

$$\boldsymbol{\sigma}^T = [\sigma_{11}, \sigma_{22}, \sigma_{33}, \sigma_{12}, \sigma_{13}, \sigma_{23}] = [\sigma_x, \sigma_y, \sigma_z, \tau_{xy}, \tau_{xz}, \tau_{yz}] \quad (3.3)$$

$$\boldsymbol{\varepsilon}^T = [\varepsilon_{11}, \varepsilon_{22}, \varepsilon_{33}, 2\varepsilon_{12}, 2\varepsilon_{13}, 2\varepsilon_{23}] = [\varepsilon_x, \varepsilon_y, \varepsilon_z, \gamma_{xy}, \gamma_{xz}, \gamma_{yz}] \quad (3.4)$$

$$\mathbf{D} = \frac{E}{(1+\nu)(1-2\nu)} \begin{bmatrix} 1-\nu & \nu & \nu & 0 & 0 & 0 \\ \nu & 1-\nu & \nu & 0 & 0 & 0 \\ \nu & \nu & 1-\nu & 0 & 0 & 0 \\ 0 & 0 & 0 & \frac{1-2\nu}{2} & 0 & 0 \\ 0 & 0 & 0 & 0 & \frac{1-2\nu}{2} & 0 \\ 0 & 0 & 0 & 0 & 0 & \frac{1-2\nu}{2} \end{bmatrix} \quad (3.5)$$

Here,  $E$  is Young's modulus and  $\nu$  is Poisson's ratio.

The various stress components in Eqn. (3.3) are defined as stresses on the surfaces of a cubical material element:

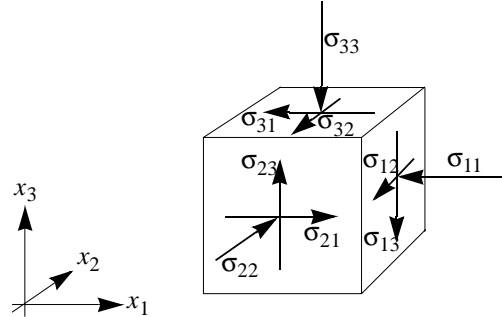


**Figure 3.3:** Stress components.

The strain components, Eqn. (3.4), may be illustrated similarly as in Figure 3.3.

The flexibility matrix, the inverse of the constitutive matrix, is sometimes useful for manual strain calculations:

$$\mathbf{D}^{-1} = \frac{1}{E} \begin{bmatrix} 1 & -\nu & -\nu & 0 & 0 & 0 \\ -\nu & 1 & -\nu & 0 & 0 & 0 \\ -\nu & -\nu & 1 & 0 & 0 & 0 \\ 0 & 0 & 0 & 2(1+\nu) & 0 & 0 \\ 0 & 0 & 0 & 0 & 2(1+\nu) & 0 \\ 0 & 0 & 0 & 0 & 0 & 2(1+\nu) \end{bmatrix} \quad (3.6)$$

The strain is then given by

$$\boldsymbol{\varepsilon} = \mathbf{D}^{-1} \boldsymbol{\sigma} \quad (3.7)$$

Using the bulk modulus,  $K$ , defined by

$$K = \frac{E}{3(1-2\nu)} \quad (3.8)$$

and the shear modulus,  $G$ , defined by

$$G = \frac{E}{2(1+\nu)} \quad (3.9)$$

the constitutive matrix  $\mathbf{D}$  reads

$$\mathbf{D} = \begin{bmatrix} K + \frac{4}{3}G & K - \frac{2}{3}G & K - \frac{2}{3}G & 0 & 0 & 0 \\ K - \frac{2}{3}G & K + \frac{4}{3}G & K - \frac{2}{3}G & 0 & 0 & 0 \\ K - \frac{2}{3}G & K - \frac{2}{3}G & K + \frac{4}{3}G & 0 & 0 & 0 \\ 0 & 0 & 0 & G & 0 & 0 \\ 0 & 0 & 0 & 0 & G & 0 \\ 0 & 0 & 0 & 0 & 0 & G \end{bmatrix} \quad (3.10)$$

The bulk modulus,  $K$ , connects the volumetric strain,  $\epsilon_v$ , defined by

$$\epsilon_v = \epsilon_{11} + \epsilon_{22} + \epsilon_{33} \quad (3.11)$$

and the mean stress,  $\sigma_m$ , defined by

$$\sigma_m = \frac{1}{3}(\sigma_{11} + \sigma_{22} + \sigma_{33}) \quad (3.12)$$

through the following equation

$$\sigma_m = K\epsilon_v \quad (3.13)$$

Likewise, the shear modulus,  $G$ , connects the deviatoric strain,  $\mathbf{e}$ , and the deviatoric stress,  $\mathbf{s}$ . The deviatoric strain is defined by

$$\mathbf{e} = \boldsymbol{\epsilon} - \epsilon_m \quad (3.14)$$

where

$$(\epsilon_m)^T = \frac{1}{3}[\epsilon_v, \epsilon_v, \epsilon_v, 0, 0, 0] \quad (3.15)$$

The deviatoric stress is defined by

$$\mathbf{s} = \boldsymbol{\sigma} - \sigma_m \quad (3.16)$$

where

$$(\sigma_m)^T = [\sigma_m, \sigma_m, \sigma_m, 0, 0, 0] \quad (3.17)$$

The deviatoric strain and the deviatoric stress is then linked as follows:

$$\mathbf{s} = 2G\mathbf{e} \quad (3.18)$$

In some cases it is convenient to have expressions for  $E$  and  $\nu$  in terms of  $K$  and  $G$ :



$$E = \frac{9K}{1 + 3\frac{K}{G}} = \frac{9KG}{3K + G} \quad (3.19)$$

$$\nu = \frac{1}{2} \left( 1 - \frac{1}{\frac{K}{G} + \frac{1}{3}} \right) = \frac{1}{2} \left( \frac{3K - 2G}{3K + G} \right) \quad (3.20)$$

Linear, isotropic elasticity is well suited for metals subjected to moderate stresses within the working range. For soils this model is less suited because of anisotropy, stiffening or softening behaviour and the lack of tensile strength, just to mention a few facets of soil behaviour not coherent with linear and isotropic elasticity.

### 3.4.2 Cross anisotropic elasticity

Transportation structures made of granular materials are often compacted vertically during the construction phase. After construction the service loads act mostly in the vertical direction and may have an additional compactive effect. However, in the horizontal direction neither active compaction effort nor much service loading is applied. The constituent granular material may therefore behave differently in the vertical direction than in the horizontal direction, thus giving rise to a behaviour termed *cross anisotropic elasticity* or *transversal elasticity*. Another source of anisotropy is flaky or elongated material particles as these will tend to orientate with a long axis in the horizontal direction. Both the compaction effect and the particle shape effect will cause a higher stiffness in the vertical direction than in the horizontal direction. Assuming the  $x_3$ -axis as the vertical one, the flexibility matrix for such a material reads /87/

$$\mathbf{D}^{-1} = \begin{bmatrix} \frac{1}{E_H} & -\frac{\nu_{HH}}{E_H} & -\frac{\nu_{VH}}{E_V} & 0 & 0 & 0 \\ -\frac{\nu_{HH}}{E_H} & \frac{1}{E_H} & -\frac{\nu_{VH}}{E_V} & 0 & 0 & 0 \\ -\frac{\nu_{HV}}{E_V} & -\frac{\nu_{HV}}{E_V} & \frac{1}{E_V} & 0 & 0 & 0 \\ 0 & 0 & 0 & \frac{2(1 + \nu_{HH})}{E_H} & 0 & 0 \\ 0 & 0 & 0 & 0 & \frac{1}{2G_{VH}} & 0 \\ 0 & 0 & 0 & 0 & 0 & \frac{1}{2G_{VH}} \end{bmatrix} \quad (3.21)$$

where

- $E_H$  = Young's modulus for horizontal compression
- $E_V$  = Young's modulus for vertical compression
- $\nu_{HH}$  = Poisson's ratio for expansion in one horizontal direction due to compression in the other horizontal direction
- $\nu_{VH}$  = Poisson's ratio for expansion in the horizontal plane due to vertical loading
- $\nu_{HV}$  = Poisson's ratio for expansion in the vertical plane due to horizontal loading

$G_{VH}$  = shear modulus for shear deformation in a vertical plane

Usually the matrix in Eqn. (3.21) is considered to be symmetric with five independent parameters to measure  $\nu_{64}$ , as  $\nu_{VH}$  is set equal to  $\nu_{HV}$ .

### 3.4.3 Nonlinear resilient models for pavement design

An overview of some of the most popular models is given in Hoff /34/. These models are based on conventional triaxial testing on unbound road building materials, i.e. natural gravel or crushed stone aggregates.

**The  $K$ - $\theta$ -model.** This model is described by Hicks and Monismith /31/ based on their own research and earlier works by others. The model calculates the resilient modulus  $M_r$ , which is the ratio of deviator stress to the recoverable axial strain, in the following way:

$$M_r = K_1 \theta^{K_2} \quad (3.22)$$

where

$\theta$  = mean stress =  $\sigma_m$

$K_1$  and  $K_2$  are regression coefficients from regression analyses of triaxial test results.

To avoid problems with the units, a version with dimensionless coefficients may be preferred:

$$M_r = K_1^* \sigma_a \left( \frac{\theta}{\sigma_a} \right)^{K_2} \quad (3.23)$$

where  $K_1^*$  is a regression coefficient (a modification of  $K_1$ ) and  $\sigma_a$  is a reference pressure which often is set to 100 kPa (approx. 1 atm.).

The resilient modulus is typically used as an effective Young's modulus along with a measured or assumed Poisson's ratio, the latter being constant. When used in a boundary value problem, e.g. in a finite element formulation, this approach is known to have convergence difficulties /32/.

**The Uzan model.** Uzan /80/ modified the  $K$ - $\theta$ -model to include the effect of the deviatoric stress. The resilient modulus is then

$$M_r = A \theta^B q^C \quad (3.24)$$

where  $A$ ,  $B$  and  $C$  are regression coefficients and  $q$  is the deviatoric stress:

$$q = \sigma_1 - \sigma_3 \quad (3.25)$$

**The Pappin and Brown model.** Pappin and Brown /67/ divided the mechanical behaviour into a volumetric and a deviatoric part. A modified form of the model is given /58/:

$$\epsilon_v = \left[ \left( \frac{p}{A} \right)^B (1 - C\eta^2) \right] \quad (3.26)$$

$$\varepsilon_s = \left(\frac{p}{D}\right)^E \eta \quad (3.27)$$

where

$$\begin{aligned} \varepsilon_v &= \text{resilient volumetric strain} \\ \varepsilon_s &= \text{resilient shear strain} \\ p &= \text{mean stress} = \sigma_m \\ \eta &= q/p \\ A, B, C, D \text{ and } E &\text{ are regression coefficients.} \end{aligned}$$

The bulk and shear moduli can now be calculated as

$$K = \frac{p}{\varepsilon_v} \quad (3.28)$$

$$G = \frac{q}{3\varepsilon_s} \quad (3.29)$$

**The Boyce model /5/.** The volumetric strain is given by

$$\varepsilon_v = p^{B_1} \left[ \frac{1}{B_3} - \frac{1 - B_1}{6B_2} \eta^2 \right] \quad (3.30)$$

while the shear strain is given by

$$\varepsilon_s = \frac{p^{B_1}}{3B_2} \eta \quad (3.31)$$

where  $B_1$ ,  $B_2$  and  $B_3$  are material parameters from triaxial testing.  $B_2$  and  $B_3$  may be interpreted as nonlinear shear and bulk moduli, respectively. The secant bulk and shear moduli can be calculated by using Eqn. (3.28) and Eqn. (3.29).

Hornych /37/ reports a potential function that the Boyce model can be derived from. This potential has the form of a complementary strain energy function.

The Boyce relations have also been modified to include anisotropy /19, 37/.

### 3.4.4 Nonlinear hyperelastic models

Hyperelastic models are defined in terms of a strain energy function from which the stress-strain relation is derived. These type of models are also denoted *Green elastic models*. The main advantage of hyperelastic models is that there is a one-to-one correspondence between stress and strain, i.e. the same stress-strain path is used for unloading as for loading. As such, Hooke's law represents a linear hyperelastic model, and the nonlinear elastic models described in Section 3.4.3 are also meant to be hyperelastic although this was not always explicitly stated in the literature.

The hyperelastic models assume that a strain energy density  $U$  can be defined in terms of strains:

$$U = U(\boldsymbol{\varepsilon}) \quad (3.32)$$

Since an infinitesimal change in strain energy may be accomplished by multiplying the stress by an infinitesimal change in strain, the stress itself may be calculated by differentiating the strain energy with respect to strain:

$$\boldsymbol{\sigma} = \frac{\partial U}{\partial \boldsymbol{\varepsilon}} \quad (3.33)$$

The individual stress component is calculated by taking a partial derivative of the strain energy function with respect to the strain component corresponding to the stress component.

Two nonlinear hyperelastic models are presented in the following. They have in common a coupling property between shear and volumetric deformation that accounts for shear deformation and pressure-dependent behaviour.

**Model according to Hjelmstad and Taciroglu /32/.** Given the strain matrix  $\mathbf{E}$

$$\mathbf{E} = \begin{bmatrix} \varepsilon_{11} & \varepsilon_{12} & \varepsilon_{13} \\ \varepsilon_{21} & \varepsilon_{22} & \varepsilon_{23} \\ \varepsilon_{31} & \varepsilon_{32} & \varepsilon_{33} \end{bmatrix} \quad (3.34)$$

and the deviatoric strain matrix  $\mathbf{E}'$

$$\mathbf{E}' = \begin{bmatrix} e_{11} & e_{12} & e_{13} \\ e_{21} & e_{22} & e_{23} \\ e_{31} & e_{32} & e_{33} \end{bmatrix} = \begin{bmatrix} \varepsilon_{11} & \varepsilon_{12} & \varepsilon_{13} \\ \varepsilon_{21} & \varepsilon_{22} & \varepsilon_{23} \\ \varepsilon_{31} & \varepsilon_{32} & \varepsilon_{33} \end{bmatrix} - \frac{1}{3} \begin{bmatrix} \varepsilon_v & 0 & 0 \\ 0 & \varepsilon_v & 0 \\ 0 & 0 & \varepsilon_v \end{bmatrix} \quad (3.35)$$

where  $\varepsilon_v$  is given by Eqn. (3.11), a deviatoric strain measure  $e$  is defined as the square root of the second deviatoric strain invariant  $J_2^e$ :

$$e = \sqrt{J_2^e} = \sqrt{\frac{1}{2} \text{tr}(\mathbf{E}'\mathbf{E}'^T)} = \sqrt{-e_{11}e_{22} - e_{11}e_{33} - e_{22}e_{33} + e_{12}^2 + e_{13}^2 + e_{23}^2} \quad (3.36)$$

The square of the strain energy density function is then assumed to be a product of a bulk strain energy  $\mathcal{U}(\varepsilon_v)$  and a deviatoric strain energy  $\mathcal{V}(e)$ :

$$U(\boldsymbol{\varepsilon}) = \sqrt{2\mathcal{U}(\varepsilon_v)\mathcal{V}(e)} \quad (3.37)$$

The stress is obtained by the help of Eqn. (3.33):

$$\boldsymbol{\sigma} = \frac{\mathcal{U}'\mathcal{V}}{U} \mathbf{I} + \frac{\mathcal{U}\mathcal{V}'}{U} \mathbf{n} \quad (3.38)$$

where  $\mathbf{I}$  is the identity matrix and  $\mathbf{n}$  is a tensor representing the direction of the deviatoric strain:

$$\mathbf{n} = \frac{\partial e}{\partial \boldsymbol{\epsilon}} = \frac{\mathbf{e}}{2e} \quad (3.39)$$

The tangent constitutive matrix  $\mathbf{D} = \partial \boldsymbol{\alpha} / \partial \boldsymbol{\epsilon}$  can be evaluated from Eqn. (3.38).

/32/ gives examples of the use of the present model. It is concluded that the model is well suited for FEM application and it is amenable to large-scale computation. The shear dilatancy is well captured, but the lack of tensional strength of granular materials is not taken into account.

**Model according to Hoff et al. /35/.** The soil model described herein is the model developed by Hoff and co-workers at the Norwegian University of Science and Technology.

The model is developed for coarse graded unbound granular materials and describes how the dilatancy of the material can be taken into account in a way that actually shows to advantage in describing the behaviour of the aggregate. It turns out that when including the dilatancy the unrealistic tensile stresses calculated using isotropic elastic theory are substantially reduced or even eliminated. A hyperelastic description is used to assure path independence. The strain energy function reads

$$U = \frac{1}{2} K (I_1^\epsilon)^2 + D \cdot I_1^\epsilon J_2^\epsilon + 2G J_2^\epsilon \quad (3.40)$$

where

$$\begin{aligned} I_1^\epsilon &= \text{the first strain invariant} = \epsilon_v \\ D &= \text{a parameter accounting for the dilatancy of the material, determined through} \\ &\quad \text{triaxial tests, with units of Pa.} \\ J_2^\epsilon &= \text{the second deviatoric strain invariant} \end{aligned}$$

The stresses are found by taking the partial derivatives of the strain energy with respect to the corresponding strains. For instance is the constitutive relation between the principal stresses and the principal strains as follows

$$\begin{bmatrix} \sigma_1 \\ \sigma_2 \\ \sigma_3 \end{bmatrix} = \begin{bmatrix} K + \frac{4}{3}G + D\epsilon_1 & K - \frac{2}{3}G - \frac{1}{2}D\epsilon_3 & K - \frac{2}{3}G - \frac{1}{2}D\epsilon_2 \\ K - \frac{2}{3}G - \frac{1}{2}D\epsilon_3 & K + \frac{4}{3}G + D\epsilon_2 & K - \frac{2}{3}G - \frac{1}{2}D\epsilon_1 \\ K - \frac{2}{3}G - \frac{1}{2}D\epsilon_2 & K - \frac{2}{3}G - \frac{1}{2}D\epsilon_1 & K + \frac{4}{3}G + D\epsilon_3 \end{bmatrix} \cdot \begin{bmatrix} \epsilon_1 \\ \epsilon_2 \\ \epsilon_3 \end{bmatrix} \quad (3.41)$$

The correct constitutive relation for a triaxial case, where  $\sigma_2 = \sigma_3$  and  $\epsilon_2 = \epsilon_3$ , in terms of  $\sigma_d$  and  $\sigma_m$  is

$$\begin{bmatrix} \sigma_d \\ \sigma_m \end{bmatrix} = \begin{bmatrix} 3 \cdot G & \frac{3}{2} \cdot D \cdot \epsilon_q \\ \frac{3}{4} \cdot D \cdot \epsilon_q & K \end{bmatrix} \cdot \begin{bmatrix} \epsilon_q \\ \epsilon_v \end{bmatrix} \quad (3.42)$$

where

$$\begin{aligned} \sigma_d &= \sigma_1 - \sigma_3 \\ \epsilon_q &= \frac{2}{3}(\epsilon_1 - \epsilon_3), \text{ the work consistent deviatoric strain} \end{aligned}$$

The non-symmetry of the constitutive matrix in Eqn. (3.42) is simply due to the definitions of the stresses and strains used. The more general constitutive matrix in Eqn. (3.41) is symmetric.

Traditionally, there exist several ways of getting around the problem of tensional stresses<sup>1</sup> in the bottom of granular layers described by isotropic soil parameters. Hoff et al. /35/ describe some of the most frequently used strategies used to avoid the tensional stresses:

- (1) Permanent horizontal compressive stresses from compaction are assumed
- (2) Using Poisson's ratio larger than 0.5
- (3) Anisotropic stiffness
- (4) Stress adjustment using the Mohr-Coulomb failure criterion

Researchers relying on item (1) anticipate high levels of initial stresses so that the soil never faces tensile stresses during loading. Using a Poisson's ratio larger than 0.5 has as a consequence a peculiar material behaviour where the material expands when subjected to isotropic compressive stress. The fourth alternative represents an ad hoc procedure that 'repairs' the stresses but violates the original boundary value problem with its elastic constitutive assumption. The third alternative is a fruitful one that does not make any additional assumptions beyond that of anisotropy. However, this alternative does not always display material parameters that are consistent with those found in triaxial testing /35/. The model described by Hoff et al. is therefore a conceptually very promising alternative.

One major disadvantage of the model by Hoff et al. is that it will fail if

$$3GK - \frac{9}{8}D^2\varepsilon_q^2 = 0 \quad (3.43)$$

## 3.5 Features of elasto-plasticity

### 3.5.1 Introduction

For transportation structures like railway tracks and highways there are numerous models when it comes to calculating the elasto-plastic behaviour. For the railway part, the models generally fall into two categories:

- ◆ Overall models which try to describe the settlement of the track ladder. This type of approach tries to simulate a measured settlement as a function of mainly the axle load and the number of axles. Some models also take into account the state of the track, increased settlement after tamping and a nonlinear effect of differing axle loads. A review of this type of models is done by Dahlberg /14/ and is not treated further in this thesis.
- ◆ Continuum models that calculate the plastic strain at a micro level, in essence for every soil particle, and the summation to a total settlement is often done by a finite element code. The material data needed are normally obtained by laboratory testing of the various materials that constitute a railway track. These models are generally expensive in computer time, and especially so if repeated loading is to be taken into consideration.

The latter category of models may be subdivided further, as will be evident later.

---

1. When fines are present there may be suction in the interstitial pore water corresponding to an apparent tensile strength.

The types of strains that may occur in a material may be resilient, permanent or even time dependent. Table 3.1 displays two grouping schemes based on time dependence and permanency of the strains.

**Table 3.1:** Strains: Two grouping schemes and the relation between them.

	Resilient, $\varepsilon^e$	Permanent, $\varepsilon^p$
Instantaneous, $\varepsilon^i$	Instantaneous elastic, $\varepsilon^{ie}$	Instantaneous plastic, $\varepsilon^{ip}$
Time dependent, $\varepsilon^t$	Time dependent elastic, $\varepsilon^{te}$	Time dependent plastic (viscous), $\varepsilon^{tp}$

A material subjected to a constant stress during a limited period of time may expose a one-dimensional behaviour like the one in Figure 3.4.

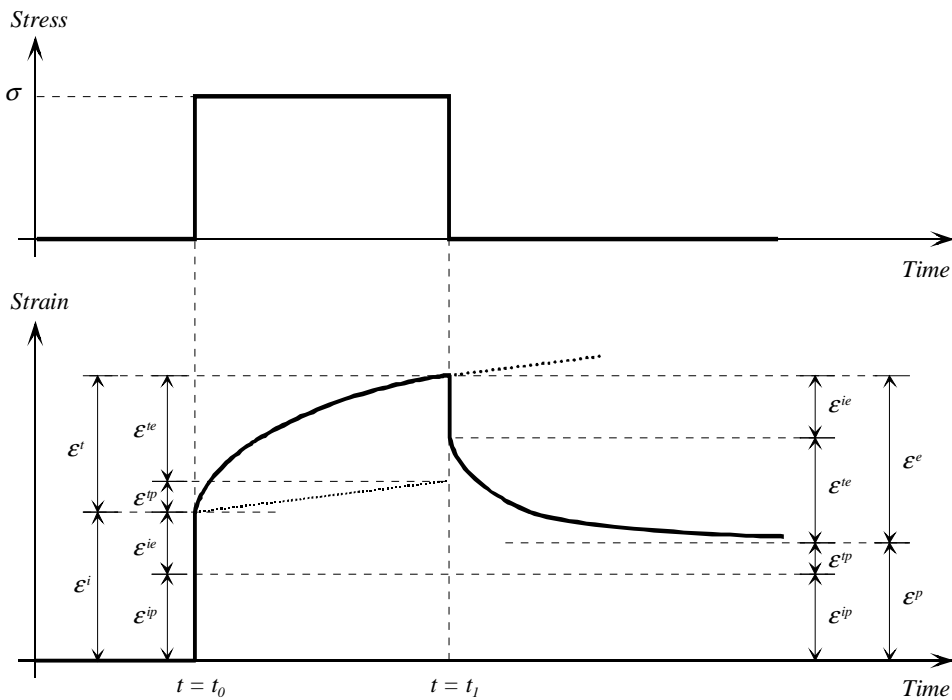


**Figure 3.4:** Relationships between various types of strain. The dashed line continuing from the peak of the curve indicates that if the load is long lasting the growing part of the deformation will be the time dependent plastic part (assumed linear) as the elastic time dependent part will stop increasing.

If  $t_1$  is large enough compared to  $t_0$  the time-vs.-strain-curve will become linear for many materials when approaching  $t_1$ , as the time dependent plastic strain is the only contributing strain component. This is indicated by the upper dotted line around  $t_1$  that is parallel to the lower dotted line from  $t_0$  to  $t_1$ .

In the further discussion, when not otherwise stated, only strains and stresses corresponding to an instantaneous response will be treated. For brevity, the superscripts  $e$  and  $p$  will be used solely for instantaneous response. The reason why the time dependent behaviour is left at this point is that in a railway track, apart from the subgrade, the structural materials are not considered to have a time dependent response. Time dependent behaviour is thus beyond the scope of the present work.

In order to get a feeling for the order of magnitude of the plastic deformation compared to the elastic and total deformation in a railway track it may be pertinent, at this stage, to make a qualified estimation. Let us define the problem as finding the plastic deformation in the granular layers per load cycle (or axle) when the total plastic deformation from one tamping action to the next should be kept within reasonable limits. We assume that this total plastic deformation is 10 mm over a period of 1100 days (3 years), the latter being a normal tamping interval for the Norwegian railway network. Further, let the daily number of trains be 20, each train having an average of 50 axles - which could be reasonable numbers for a Norwegian mainline carrying both passenger and freight traffic. Thus the number of axles in the 1100 day period totals 1 100 000. The plastic deformation per load cycle is then on average about  $1 \cdot 10^{-5}$  mm. If the elastic deformation on top of the granular layers is about 1 mm, which is actually a low number, the plastic deformation is not more than 1/100 000 of the elastic deformation.

The average plastic deformation mentioned above may hide substantial variation, for instance is it reasonable to believe that the development of plastic deformation is more rapid directly after tamping than later on (Dahlberg /14/). Also, one should be aware of that the measured plastic deformation in the track is the *net* deformation; it may be possible that larger contributions almost cancel when summed. By way of example, it is likely to believe that horizontal plastic deformation that occur in the track when the axle load is positioned on one sleeper is counteracted by the corresponding plastic deformation when the axle load is transferred to the next sleeper. Although the numbers in the example above could be questionable, it is to be hoped that the example gives the right picture of the order of magnitude of the net plastic deformation per axle. If the plastic deformation on average should be substantially larger, say 5 or 10 times, the cumulative plastic deformation would not be acceptable and the track would find itself in a failure condition with respect to its practical use. But still, even with this latter deformation, the plastic deformation per axle would only be a tiny fraction of the total deflection. The conclusion to be drawn on a *per axle level* is that the plastic or permanent deformation could be neglected in a structural analysis without significant loss of accuracy if the track is else assumed to have a normal plastic deformation rate. On a *cumulative level*, however, the plastic deformation is relevant as most conventional tracks needs lifting and tamping from time to time. Yet, on the cumulative level, it may be necessary to do calculation on the per axle level in order to get the correct total plastic deformation for all axles. The fact that the plastic strain per axle passage is so small compared to the total strain may lead to a simplified model for the development of cumulative plastic deformation.

Since the plastic deformation per axle load is so small, there are practical difficulties of measuring it with more or less standard deformation measuring devices, where undoubtedly limited precision comes into play. This problem is even more pronounced when it comes to describing the path of the plastic strain with respect to some stress quantity for one load cycle. One may therefore be forced to deduce from the course of the cumulative deformation what the average plastic deformation per loading cycle should be.

In the following some of the most well known approaches to elasto-plasticity are described. A closer look into the existing theories motivates a simplified approach to the problem of calculating the accumulated cyclic strains. It is emphasised that the focus is quite practical, i.e. the calculation of (engineering) stresses and strains when the structure is fully loaded and the plastic



strains after one or more loading cycles. What happens during one particular cycle is explored in more detail in Section 3.7.

### 3.5.2 Classic elasto-plastic continuum theory

The general framework for classic elasto-plastic continuum models can be found in numerous textbooks, e.g. in Chakrabarty /10/, Mendelson /59/ or Khan and Huang /47/. A good introduction to elasto-plasticity for soils is found in Scott /71/. In the development of this framework researchers like Coulomb, St. Venant, Lévy, von Mises, Prandtl, Reuss and Drucker are often mentioned. What we today know as *Classic Plasticity* was finalised by the works of Drucker around 1950. Much of the general framework was worked out with a view to metal plasticity.

The description in the following is adopted from Nordal /64/. To help further description reference is made to Figure 3.5 that describes uniaxial behaviour.

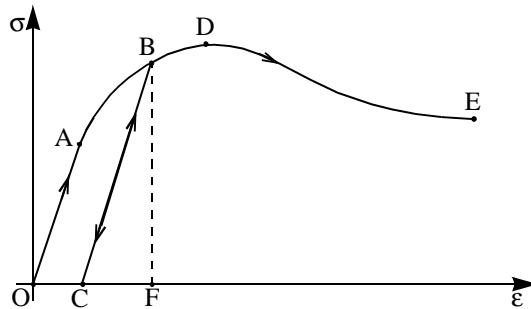


**Figure 3.5:** Stress-strain relationship in a uniaxial test.

With reference to Figure 3.5 the part of the curve denoted OA is said to be *linear elastic*. After the *yield point* at A the material *hardens* until the *failure point* at D. From D to E the material *softens*. The failure point D represents the maximum stress point, and point E represents a residual strength in the material after failure. Unloading and reloading at any point are assumed to be purely linear. Loading beyond the yield point A produces permanent strain, which in the figure is represented by the distance OC. The recovered, elastic strain is the distance CF. When reloading from C a new yield point is met at B and the material returns to the curve towards D and E.

In a three dimensional context the yield point A will be generalised to a yield surface in a stress space. This surface originates from all different combinations of stress that produces yielding in the material. Likewise it is possible to define a failure surface.

Within the yield surface the response is purely elastic, much in the same way as in Figure 3.5 between O and A. When the stress is increased and an equilibrium state cannot be found within the elastic region, i.e. within the yield surface, a stress state that lies on the outside of the original yield surface is the only possibility. This corresponds in the uniaxial case to go from a point on the OA-line to a point B beyond the original elastic region. But in the process of 'hitting' the yield surface and trying to reach for a stress state on the outside, the *yield surface itself is pulled along by the increasing stress*; it may translate or expand or both. In other words, when plastic flow develops the stress state always lies on the yield surface. Consequently, any unloading will be in the elastic region and reloading to the prior stress state will not produce any additional

plastic strain. During such an unloading-reloading loop the yield surface remains unchanged. These considerations are analogous to the uniaxial case, e.g. traversing the points OABCB for the curve in Figure 3.5.

More mathematically the following ingredients are needed in a classic elasto-plastic stress strain model:

- (1) A principle for adding elastic and plastic strains:

$$d\boldsymbol{\varepsilon} = d\boldsymbol{\varepsilon}^e + d\boldsymbol{\varepsilon}^p \quad (3.44)$$

where  $d\boldsymbol{\varepsilon}$  is the total strain,  $d\boldsymbol{\varepsilon}^e$  is the elastic strain and  $d\boldsymbol{\varepsilon}^p$  is the plastic strain. This is the same principle for addition as in the uniaxial case.

- (2) A relationship that governs the elastic contribution:

$$d\boldsymbol{\varepsilon}^e = \mathbf{D}^{-1} d\boldsymbol{\sigma} \quad (3.45)$$

where  $\mathbf{D}$  is the elastic constitutive matrix, e.g. the one given by Eqn. (3.5). If isotropic linear elasticity is assumed then Eqn. (3.45) is the Hooke's law generalised to three dimensions.

- (3) Ingredients to control the plastic contribution:

- (a) A yield criterion.
- (b) A flow rule.
- (c) A hardening rule.

The third item above will be examined further, as the two former are explained by their very definitions. The three ingredients that control the plastic contribution will answer the following three questions:

- ◆ (The yield criterion) Where in the stress space does the yield start?
- ◆ (The flow rule) What direction in the stress space will the yield follow?
- ◆ (The hardening rule) What is the numerical size of the plastic strain contribution?

As argued above *the yield criterion* is implemented as a yield surface in a stress space,

$$F(\boldsymbol{\sigma}, \kappa) = 0 \quad (3.46)$$

where  $\kappa$  is a state variable. It is possible to have more than one state variable, but for simplicity only one is assumed here. The state variable controls the size of the yield surface. Examples of state variables may be the degree of mobilisation,  $f$ , and the preconsolidation pressure for over-consolidated clays,  $p_c$ .

For soils the Mohr-Coulomb and the Drucker-Prager yield criteria are frequently used.

*The flow rule* determines the direction of the plastic flow. The yield surface is pulled along by the increasing stress, consequently  $dF=0$ , which implies that during loading

$$\left\{ \frac{\partial F}{\partial \boldsymbol{\sigma}} \right\}^T d\boldsymbol{\sigma} + \frac{\partial F}{\partial \kappa} d\kappa = 0 \quad (3.47)$$

In Eqn. (3.47) the term  $\{\partial F/\partial \boldsymbol{\sigma}\}$  is recognised as the outward normal to the yield surface. Eqn. (3.47) is called the *consistency equation*. Yielding occurs only when  $\{\partial F/\partial \boldsymbol{\sigma}\}^T d\boldsymbol{\sigma} > 0$ , if

$\{\partial F/\partial \sigma\}^T d\sigma = 0$  neutral loading is taking place (corresponds to loading tangentially to the yield surface) and if  $\{\partial F/\partial \sigma\}^T d\sigma < 0$  we have elastic unloading. The component of  $d\sigma$  that is parallel to the outward normal  $\{\partial F/\partial \sigma\}$  is denoted *the plastifying stress component*,  $d\sigma^p$ , and is in this context considered as the real cause of the plastic strain increment. Since the consistency equation only applies to neutral and plastic loading (softening not being considered) one may use the plastic stress component,  $d\sigma^p$ , instead of the total stress,  $d\sigma$ , in Eqn. (3.47).

Eqn. (3.47) will describe an *isotropic* kind of hardening, i.e. the yield surface expands by the same amount in all directions in stress space. An alternative is the *kinematic* type of hardening where the yield surface translates in stress space without changing size. Kinematic hardening is also termed the *Bauschinger effect*, especially for uniaxial loading. In *mixed hardening* the yield surface both expands and translates in stress space. Most materials, included soil, may be described by a kinematic or mixed type of hardening, leaving isotropic hardening as a limiting case that is convenient mathematically.

If we assume direct proportionality between  $d\sigma^p$  and  $d\epsilon^p$ , and assume as above that  $d\sigma^p$  is parallel to  $\{\partial F/\partial \sigma\}$  the plastic strain increment may be written

$$d\epsilon^p = d\lambda \frac{\partial F}{\partial \sigma} \quad (3.48)$$

where  $d\lambda$  is a scalar proportionality factor to be determined by the hardening rule. Eqn. (3.48) is a flow rule that is associated with the yield surface, hence the notion *associated flow rule*. However, the plastic strain may be connected to a separate surface called *the potential surface*  $Q$ , and if  $Q \neq F$  the flow rule is said to be *nonassociated*. To wit,

$$d\epsilon^p = d\lambda \frac{\partial Q}{\partial \sigma} \quad (3.49)$$

In case of a nonassociated flow rule the consistency equation is still valid, i.e. the yield surface is still pulled along by the stress increment, but the actual calculation of the plastic strain increment is not connected with the yield surface but rather with the plastic potential surface. Granular materials often obey the nonassociated flow rule.

*The hardening rule* defines the size of the scalar  $d\lambda$  in the flow rules Eqn. (3.47) and Eqn. (3.48). To calculate  $d\lambda$  the consistency equation for *strain hardening* may be reformulated to

$$\left\{ \frac{\partial F}{\partial \sigma} \right\}^T d\sigma + \left( \frac{\partial F}{\partial \kappa} \frac{d\kappa}{d\bar{\epsilon}^p} \frac{d\bar{\epsilon}^p}{d\lambda} \right) d\lambda = 0 \quad (3.50)$$

where  $\bar{\epsilon}^p$  is a scalar measure of cumulative plastic strain which is expressed by

$$\bar{\epsilon}^p = \sum |d\epsilon^p| = \sum \sqrt{(d\epsilon^p)^2} = \sum d\lambda \sqrt{\left( \frac{\partial Q}{\partial \sigma} \right)^2} \quad (3.51)$$

for a nonassociated flow. The term  $(d\kappa/d\bar{\epsilon}^p)$  is available from a laboratory curve where  $\kappa$  is plotted as a function of  $\bar{\epsilon}^p$ .  $(d\bar{\epsilon}^p/d\lambda)$  is available through Eqn. (3.51).

Likewise, for *work hardening* the consistency equation may be written as

$$\left\{ \frac{\partial F}{\partial \sigma} \right\}^T d\sigma + \left( \frac{\partial F}{\partial \kappa} \frac{d\kappa}{dW^p} \frac{dW^p}{d\lambda} \right) d\lambda = 0 \quad (3.52)$$

where  $W^p$  is a measure of the dissipated energy that cumulates during the yielding process:

$$W^p = \sum \sigma^T d\epsilon^p = \sum d\lambda \sigma^T \left\{ \frac{\partial Q}{\partial \sigma} \right\} \quad (3.53)$$

In Eqn. (3.52) the term  $(d\kappa/dW^p)$  is given from a laboratory curve relating  $\kappa$  and  $W^p$ , while  $(dW^p/d\lambda)$  is obtained from Eqn. (3.53).

Formally, the two consistency equations in Eqn. (3.50) and Eqn. (3.52) may be written in terms of a plastic resistance number  $A$  (also denoted *plastic modulus* /90/):

$$\left\{ \frac{\partial F}{\partial \sigma} \right\}^T d\sigma - A d\lambda = 0 \quad (3.54)$$

where for strain hardening

$$A = - \frac{\partial F}{\partial \kappa} \frac{d\kappa}{d\bar{\epsilon}^p} \frac{d\bar{\epsilon}^p}{d\lambda} \quad (3.55)$$

and for work hardening

$$A = - \frac{\partial F}{\partial \kappa} \frac{d\kappa}{dW^p} \frac{dW^p}{d\lambda} \quad (3.56)$$

The consistency equation Eqn. (3.54) is now used to isolate  $d\lambda$ , thus arriving at the final hardening rule:

$$d\lambda = \frac{1}{A} \left\{ \frac{\partial F}{\partial \sigma} \right\}^T d\sigma \quad (3.57)$$

What type of hardening Eqn. (3.57) describes is decided by the nature of  $A$ , of which two examples are given in Eqn. (3.55) and Eqn. (3.56).

By introducing Eqn. (3.57) into Eqn. (3.49) and putting this result into Eqn. (3.44) together with Eqn. (3.45) one gets for the total strain increment

$$d\epsilon = \mathbf{D}^{-1} d\sigma + \frac{1}{A} \left\{ \frac{\partial Q}{\partial \sigma} \right\} \left\{ \frac{\partial F}{\partial \sigma} \right\}^T d\sigma \quad (3.58)$$

As before, the  $Q$  symbolises a nonassociated flow and could be interchanged by  $F$  if associated flow is assumed. Also, observe that the vector product  $\{\partial Q/\partial\sigma\}\{\partial F/\partial\sigma\}^T$  makes a full matrix. The elasto-plastic compliance matrix  $\mathbf{D}_{ep}^{-1}$  may now be written

$$\mathbf{D}_{ep}^{-1} = \mathbf{D}^{-1} + \frac{1}{A} \left\{ \frac{\partial Q}{\partial\sigma} \right\} \left\{ \frac{\partial F}{\partial\sigma} \right\}^T \quad (3.59)$$

so that the relation in Eqn. (3.58) may be abbreviated to

$$d\epsilon = \mathbf{D}_{ep}^{-1} d\sigma \quad (3.60)$$

However, in most finite element codes the constitutive matrix will be needed; in other words,  $\mathbf{D}_{ep}$  and not  $\mathbf{D}_{ep}^{-1}$  will be the useful one. Simply inverting the latter one is not the recommended practise as cases where  $A=0$  (perfect plasticity) will cause trouble. Therefore an other procedure, due to Yamada et al. (published 1968) and Zienkiewich et al. (published 1969), is normally adopted. The details of the derivation may be found in Nordal /64/, and only the resulting elasto-plastic stiffness matrix is given:

$$\mathbf{D}_{ep} = \mathbf{D} - \frac{\mathbf{D} \left\{ \frac{\partial Q}{\partial\sigma} \right\} \left\{ \frac{\partial F}{\partial\sigma} \right\}^T \mathbf{D}}{A + \left\{ \frac{\partial F}{\partial\sigma} \right\}^T \mathbf{D} \left\{ \frac{\partial Q}{\partial\sigma} \right\}} \quad (3.61)$$

Hence the general stress-strain relationship is

$$d\sigma = \mathbf{D}_{ep} d\epsilon \quad (3.62)$$

During the derivation of Eqn. (3.61) an alternative expression for  $d\lambda$  was arrived at. This expression assures that  $d\lambda$  also has a specific value even for perfect plasticity ( $A=0$ ), which is not the case in Eqn. (3.57):

$$d\lambda = \frac{\left\{ \frac{\partial F}{\partial\sigma} \right\}^T \mathbf{D} d\epsilon}{A + \left\{ \frac{\partial F}{\partial\sigma} \right\}^T \mathbf{D} \left\{ \frac{\partial Q}{\partial\sigma} \right\}} \quad (3.63)$$

The framework of classic elasto-plastic theory is of an incremental nature, i.e. the theory relates increments of stress to increments of strain, and may therefore be denoted a *hypoplastic* theory.

Some of the disadvantages of the classic elasto-plastic theory (at least for isotropic hardening behaviour) may be stated as follows:

- (1) The theory requires an elastic region, bounded by a yield surface, where no plastic strains can develop.
- (2) When several identical load cycles are applied to the track structure, only the first cycle produces any plastic strain while the other cycles produce only elastic strains. This is a consequence of the first item.

- (3) On a per axle level the plastic deformation in a well conditioned track is very small (see the discussion in Section 3.5.1) and it is questionable whether this behaviour can be modelled by classic elasto-plasticity. One main reason for this is the need of a yield surface, which has to be established by experiment. Since the plastic deformations are very small no yield in the classical sense may be observed.
- (4) For computational purposes you have to follow each cycle very accurately. This necessitates huge computational resources when the cumulative effect of all load cycles during the service life of an embankment is to be evaluated.

Note the practical consequences of the first two items in the list above: During construction only one pass with a static compaction roller would be sufficient and no further compaction (i.e. plastic strain) occurs when additional passes are employed. When the track is put into service no additional plastic deformation would take place if the traffic loads are smaller than the compaction loads. In reality none of these predictions of the classic elasto-plastic theory are true.

### 3.5.3 Other plasticity theories

A few other commonly known classes of models are briefly mentioned below; a more thorough treatment of them may be found in the references given.

**Generalised plasticity.** This framework is directly based on classic elasto-plasticity as described in Section 3.5.2., and the classic plasticity theory may be considered as a particular case of generalised plasticity. The theory described here is from Zienkiewicz et al. /90/ but using a slightly different notation. The concept was initially proposed by Mróz and Zienkiewicz /61/ and by Zienkiewicz and Mróz /92/ in 1985. Later extensions are referenced in /90/.

In generalised plasticity there is no need to define explicitly any surfaces for yield or failure. In case of nonassociated flow, no potential surface needs to be defined. Instead, *normalised direction vectors* are defined. These direction vectors are generalisations of the gradient vectors in classic plasticity defined by  $\{\partial F/\partial \sigma\}$  and  $\{\partial Q/\partial \sigma\}$ . One vector is defined for separating loading from unloading (plays the role of  $F$ ), while two vectors are defined for the plastic contribution - one for loading and one for unloading (play the role of  $Q$ ). Also, no hardening rules are needed in generalised plasticity.

**Multiple surface plasticity.** This model was introduced by Mróz /62/ in 1967 as an extension of the classic elasto-plastic framework. Independently Iwan /39/ developed a similar model on the basis of rheological models with springs and frictional elements. Modifications have since been made to the model and is briefly reported in /90/. The model by Mróz /62/ utilise several yield surfaces where each surface embrace possible inner surfaces and is itself surrounded by possible outer surfaces. The model is to a certain degree able to model stress-strain history included the effect of stress induced anisotropy. More on the use of multiple surface plasticity and the Iwan model may be found in Section 3.7.2, but then with a view to cyclic loading of frictional systems.

**Bounding surface model.** In this model the number of surfaces is limited to two, and a field of hardening moduli is described by prescribing the variation between the two surfaces. The model was independently proposed by Krieg /53/ and Dafalias and Popov /13/ in 1975. Some of the subsequent modifications are described in /90/.

**Endochronic theory.** Valanis proposed in 1971 /82/ endochronic plasticity as an alternative to classic plasticity in the description of rate independent but still history dependent response of materials. There are three main features that differ endochronic theory from classic plasticity theory /81/: (a) A yield surface is not required, (b) the physical assumptions have their origin in irreversible thermodynamics of internal variables, (c) the material memory is defined in terms of an intrinsic time scale as a material property.

### 3.6 Simplifying approaches to elasto-plasticity in cyclic loading

The motivation for looking at elasto-plasticity in cyclic loading with new eyes was the feeling that the classic elasto-plasticity, or its generalisation in the generalised theory of plasticity, was far too complex when it came to cyclic loading. As pointed out before, a numerical calculation for some thousands of cycles would not be possible within reasonable limits when it comes to computer costs even today. Also, classic elasto-plasticity theory will not generate additional plastic strains beyond the first load cycle.

#### 3.6.1 The use of classic and generalised plasticity in cyclic loading

Despite the limitations of the basic theories, as stated on page 78, some adjustments may be done in order to get some information even for cyclic development of plastic strain. The idea is to circumvent the need for calculating all cycles (as stated in item (4) on the list on page 79) by calculating the stresses and strains for one representative cycle and then applying the result for an interval of cycles that may be represented by the cycle investigated. An assumption that has to be made is that the yield and potential surfaces are possible to construct on the basis of measurements on monotonic loading and, optionally, unloading.

Referring to Figure 3.6 an elasto-plastic loading-unloading cycle OABC has been applied repeatedly to model cyclic loading with development of accumulated plastic strain (a phenomenon often referred to as *ratcheting* or *cyclic creep*).

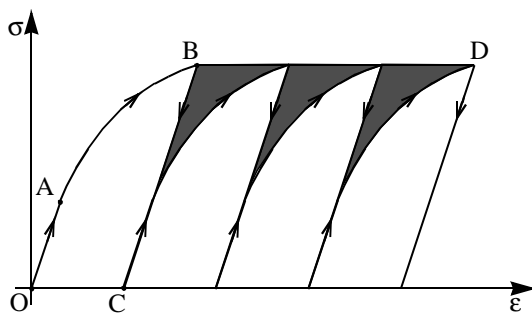


**Figure 3.6:** Using classical elasto-plasticity for cyclic loading in the uniaxial case.

The shaded areas in Figure 3.6 represent the saved energy by cycling the load as opposed to a (fictitious) monotonic loading OABD. This violates the condition of 'stability in the large' as formulated by Drucker and is not considered to be good modelling practise /27/. Generally it should be noted that Drucker stability requirements is more of a classification scheme as observed behaviour is not always coherent with them. Also, these requirements are not a conse-

quence of thermodynamical considerations. From a practical standpoint, where the total accumulated plastic strains together with the peak stresses are wanted, the type of modelling described by Figure 3.6 may nevertheless be approved.

However, it is almost impossible to establish the yield and potential surfaces from one cycle only when considering the small plastic strain in the service state of transportation structures. A regression or back-calculation of the strains based on the accumulated plastic strain over several cycles is therefore necessary. Also, the method only works when all the loads, for the sequence that is to be modelled, are identical.

### 3.6.2 The elastic approximation

Another way of calculating cyclic behaviour is to split the strain after each cycle into an elastic part and a plastic part as in classic plasticity. But instead of doing a complete analysis with total strain and total stress, the elastic strain is connected with the stress, while the plastic strain is modelled on basis of laboratory measurements. In terms of uniaxial behaviour this approach is explained in Figure 3.7 both for elastic-perfectly-plastic behaviour, and elastic-linear-elasto-plastic behaviour with unloading in both cases.

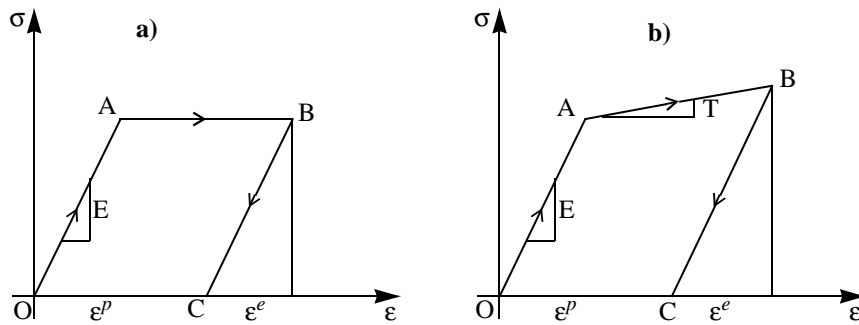


**Figure 3.7:** Two simple cases of elasto-plasticity. a) Elastic-perfectly-plastic, b) Elastic-linear-elasto-plastic.

In Figure 3.7 a), at point A we may apply a zero increment of stress, i.e.  $d\sigma=0$ , to get unlimited plastic strain. Applying instead a finite increment of strain we may have a stable stress-strain state at point B. When unloading from point B, assuming the unloading modulus being the same as when loading, both the plastic strain and the elastic strain reveal their numerical sizes. When the elasto-plastic part is monotonically increasing, as in Figure 3.7 b), the applied stress increment will only cause a finite amount of plastic strain. As in part a) of the figure, the elastic and plastic strain components are measurable after unloading.

In both cases the total stress  $\sigma$  at the point of load reversal (point B) can be calculated using the unloading modulus of elasticity and the elastic strain only - hence no dependence on  $\epsilon^p$ . Since the point of load reversal is arbitrarily chosen a general relation exist for all points on the two cyclic stress-strain curves in Figure 3.7:

$$\sigma = E\epsilon^e \quad (3.64)$$



One assumption must here be taken for both cases: That the unloading is purely elastic, i.e. no plastic strains develop during unloading. In other words, the plastic strains are identical at the peak point (B) and at the unloaded point (C), but the numerical value reveals itself at the unloaded point.

Both  $\epsilon^p$  and  $\epsilon^e$  for point B are known when unloading to point C, provided that proper measurements have been taken during the loop OABC. In these simple models there is no need to model the plastic strain contribution in a way suggested by the classical framework as its numerical value will be apparent from laboratory tests when unloading.

This motivates to separate an elasto-plastic stress-strain analysis for cyclic loading into two parts for such simple models as above:

- (1) A part that calculates the stress. The stress is given by the elastic model only.
- (2) A part that calculates the plastic strain based on measurements in the laboratory and the results from (1).

Since the stress level is so important for the calculation of plastic strains, as may be seen from Figure 3.7, it is important that the elastic model in item (1) above is accurate.

From Figure 3.7 it is also seen that it is the elastic response that provide the resistance against plastic deformation. In a) the material has no further elastic response - it is purely plastic - and there is no resistance against the development of plastic strain. In b) some elastic response is still possible after point A and the development of plastic strains are limited.

The energy absorbed in the uniaxial model of Figure 3.7 will however not be correctly calculated when using only the elastic stress-strain curve. The total volumetric energy absorbed until point B is represented by the area under the curve OAB, while an elastic model only will absorb the energy under the curve BC. The energy absorbed by the models on loading may be divided into a dissipative part and an elastically stored (conservative) part:

$$W = \int_0^B \sigma(\epsilon) d\epsilon = \int_0^B \sigma(\epsilon) d\epsilon^e + \int_0^B \sigma(\epsilon) d\epsilon^p \quad (3.65)$$

The elastic models neglect the dissipative part of the energy, only the elastic part is taken into account.

The extension to a multidimensional stress-strain space will be made with a comparison to classic elasto-plastic theory. First it is important to note that classic theory relates stress increments  $d\sigma$  to total strain increments  $d\epsilon$ , conf. Eqn. (3.62). Second it is worth noting that the procedure of calculating  $\mathbf{D}_{ep}$  may be interpreted as an attempt to calculate  $d\epsilon^p$ , which makes it possible to calculate the stress from the elastic strain and the elastic constitutive matrix. This may be demonstrated by inserting  $\mathbf{D}_{ep}$  (Eqn. (3.61)) and  $d\lambda$  (Eqn. (3.63)) into Eqn. (3.62). Hence the incremental stress-strain relation Eqn. (3.62) may now be written

$$d\sigma = \mathbf{D} d\epsilon - \mathbf{D} d\lambda \left\{ \frac{\partial Q}{\partial \sigma} \right\} = \mathbf{D} d\epsilon - \mathbf{D} d\epsilon^p \quad (3.66)$$

or

$$d\sigma = \mathbf{D} d\epsilon^e \quad (3.67)$$

which is the same relation as Eqn. (3.64) but extended to a multidimensional stress-strain space. This exercise shows that to calculate the stress from a purely elastic theory is in perfect agreement with the classic elasto-plastic theory *provided that the elastic strains are known*.

To find the correct elastic strains in a structure is however not only a function of the elastic properties but also a function of the plastic properties. Hence, using Eqn. (3.67) to calculate the stresses in a structure where some parts yield will not produce the correct solution. The reason, in short, is that yielding will redistribute stress from volumes suffering from large plastic strains to volumes experiencing less plastic strains in a way that assures static equilibrium at every point in the structure. In a displacement based finite element analysis the resulting algebraic equations are derived from a principle of stationary potential energy, thus needing all parts of the energy to be taken into account when a correct solution is aimed at. The consequence of neglecting the plastic contribution will be an underestimation of the deformations /61/.

The energy (work) absorbed by the material in the multiaxial case is a straightforward extension from the uniaxial case. At an infinitesimal level this energy is expressed as

$$dW = dW^e + dW^p = \boldsymbol{\sigma}^T d\boldsymbol{\epsilon}^e + \boldsymbol{\sigma}^T d\boldsymbol{\epsilon}^p \quad (3.68)$$

The plastic part of the energy is the same as the one encountered in Eqn. (3.53) and represents the dissipated part of the energy on loading. More on energy exchange in cyclic loading is provided in Sections 3.7.1 and 3.7.2.

When only a small portion of the energy is dissipated during a load cycle an elastic approximation may be justified. As in the one-dimensional case the net  $\boldsymbol{\epsilon}^e$  and  $\boldsymbol{\epsilon}^p$  after each cycle are measured directly instead of being calculated by more indirect use of laboratory data as in classic elasto-plastic theory. The measuring of these strains requires that the stress path used for loading is exactly reversed for unloading.

When doing an elastic approximation like this there is no need for any yield surface, potential surface or hardening parameters in the sense of classic elasto-plasticity. Instead the plastic strain is modelled by itself on the basis of, among other factors, the stress from an elastic calculation. Thus, the split up of the analysis in two stages is also valid for a multi-dimensional stress-strain state, i.e. one analysis for the stress, using elasticity only, and one analysis for the plastic strains.

### 3.6.3 Definitions of loading and unloading. The cause of the plastic strain.

In classic elasto-plasticity the definition of loading is that of a stress increment having an outward component normal to the yield surface, thus producing a plastic strain increment. During loading the yield surface is displaced outward in the direction of the outward normal so that the stress increment still lies on the surface. For neutral loading the stress increment is tangential to the yield surface, and for unloading the stress increment is bringing the stress state away from a yielding state thus producing elastic response only. These definitions are shown in Figure 3.8.

As mentioned in Section 3.5.2 on classic plasticity, the component  $d\boldsymbol{\sigma}^p$  of  $d\boldsymbol{\sigma}$  is parallel to the outward normal  $\{\partial F/\partial \boldsymbol{\sigma}\}$  and is denoted the real cause of the plastic strain increment. The plastic strain is at its maximum when  $d\boldsymbol{\sigma}$  is parallel to  $d\boldsymbol{\sigma}^p$ , and both pointing in the direction of  $\{\partial F/\partial \boldsymbol{\sigma}\}$ , and zero when perpendicular to  $d\boldsymbol{\sigma}^p$ . However, it should be noted that also elastic strain develops as long as the yield surface is expanding, even for a stress increment causing maximum, but limited, plastic strain. In a chain of causes and effects it may be pertinent to ask

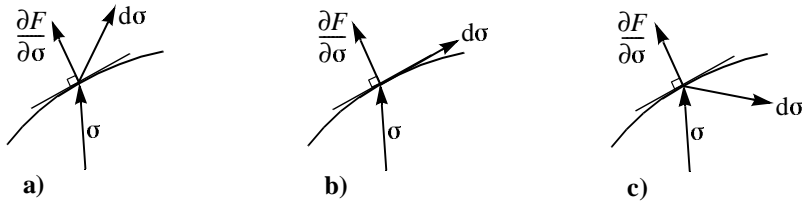


**Figure 3.8:** Definition of loading and unloading in classic elasto-plasticity. a) loading, b) neutral loading and c) unloading.

what is the cause of  $d\sigma^p$ . As for the uniaxial case in Section 3.6.2 the answer is that it is the elastic properties in the material that is responsible for  $d\sigma$  and hence the component  $d\sigma^p$ .

When dealing with definitions of loading and unloading it may be relevant to consider a simple uniaxial case as in Figure 3.9.

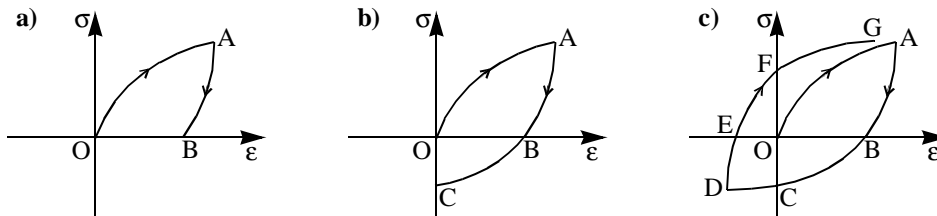


**Figure 3.9:** Loading, unloading and reloading in the uniaxial case. a) Loading and unloading to  $\sigma = 0$ , b) Loading and unloading to  $\varepsilon = 0$ , c) a loading-reloading-loop.

Referring to Figure 3.9 one may distinguish between two types of loading and unloading:

- (1) Loading and unloading in terms of the stress. This is depicted in part a) of the figure.
- (2) Loading and unloading in terms of the strain. This is depicted in part b) of the figure. A better terminology would perhaps be that of straining and unstraining.

The definition of item (1) will be used in the present work as this definition is more natural when it comes to structures like railways and highways. This definition will also make sense when the development of plastic strain is not ruled out for any load increment as no part of the stress space is a priori considered to be a purely elastic region.

In a multidimensional stress space a pure unloading must be considered as traversing the stress path in exactly the opposite direction as that of loading. Hence when dealing with moving loads, the loading and unloading do not follow the same stress path. This is due to the rotation of the principal stress directions during a passage of a wheel. Applying the stress-strain relation in Figure 3.9 c) some components of stress may then follow a stress-strain path OA upon loading and a path ABCDE upon unloading.

### 3.6.4 Relations for plastic strains

There exist numerous relations for plastic strains in the literature. Lekarp /56/ has described some of them. In his study he states that the permanent deformation response of granular materials is affected by the following factors:

- ◆ Stress level
- ◆ Principal stress rotation
- ◆ Number of load applications
- ◆ Moisture content
- ◆ Stress history
- ◆ Density
- ◆ Grading and aggregate type

Some of these factors will be addressed later in the thesis. For now, a consequence upon the plastic strains when using the elastic approximation is discussed.

Using the elastic approximation, where the plastic strain has been detached from the calculation of stress, does not imply that the calculation of plastic strain has been detached from stress. The stress is in fact an important parameter in calculating the plastic strain, although other parameters contribute as stated above. Since the stress and the elastic strain are tied together through Eqn. (3.67), the stress may be interchanged by the elastic strain when calculating the plastic strain. Schematically this can be shown as in Figure 3.10.

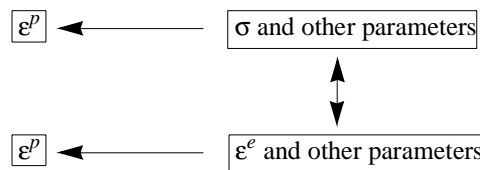


**Figure 3.10:** When calculating  $\varepsilon^p$ ,  $\sigma$  or  $\varepsilon^e$  may be used.

**Veverka.** Most researchers use the stress as a parameter to calculate the plastic strain in granular materials in addition to the number of cycles. The possibility of using of the elastic strain when calculating the plastic strain has been used by Veverka /84/:

$$\sum \varepsilon^p = a \varepsilon^e N^b \quad (3.69)$$

where  $N$  is the number of load repetitions and  $a$  and  $b$  are material parameters. The model of Veverka has not been confirmed by other researchers, according to /56/, but the concept of using elastic strain instead of stress should be valid when an elastic response is able to approximate the real response.

**Hoff and Nordal /33/.** From the measurements the plastic strains have to be interpolated in order to cover the possible stress ranges and cyclic stress peaks. Also, the number of load repetitions is an important parameter.

Hoff and Nordal /33/ have developed a model that describes the total vertical plastic strain on the basis of triaxial test results on crushed well graded aggregates. According to this model the plastic strain,  $\varepsilon_1^p$ , is:

$$\varepsilon_1^p = \frac{d \cdot N \cdot f}{d_0 + N \cdot f} + l \cdot Sm \cdot g(N) \quad (3.70)$$

where

- $d$  = measured permanent vertical strain after 10 000 load cycles for a chosen degree of shear mobilisation.
- $d_0$  = reference strain set equal to 1 ‰
- $Sm$  = calculated degree of shear mobilisation in the material point
- $N$  = number of equal load repetitions
- $f$  = shape factor for the plastic strain development with respect to  $N$ , evaluated on the basis of triaxial tests.
- $l$  = coefficient for long-term strains due to wear and other long term effects
- $g(N)$  = a function responsible for the long-term strain's dependence upon  $N$ , for the time being set equal to  $N$ .

### 3.7 Cyclic loading of frictional systems

As the mechanical behaviour of granular materials are substantially governed by friction, a closer look into frictional systems are pertinent. Stress-strain curves for some simple rheological models are presented, along with some energy considerations. A principle will emanate that divides the stress into a dissipative part and a conservative part, and this will show to advantage when hysteresis is considered.

#### 3.7.1 Basics of cyclic loading of a frictional system

In cyclic loading, as for monotonic loading, the total energy supplied to the material during loading is transformed into recoverable energy and dissipated energy (in addition a small part of the energy may be stored). According to classic elasto-plasticity, with linear unloading, the recoverable energy is entirely connected with the elastic response, while the dissipated energy is entirely connected with the plastic response. However, some researchers claim that this is not so for cyclic loading of frictional materials. Jefferies /42/ reported that some part of the plastic strain energy is recovered on unloading of a dilatant sand. This part of the energy was connected with the recoverable part of the dilatancy. Mróz and Zienkiewicz /61/ and Mróz /60/ concluded that during unloading recoverable plastic strains developed. Furthermore, the purely elastic unloading response could be constructed by taking initial moduli of small loading-unloading cycles at consecutive points along the overall unloading curve. Not stated in /60/, but the difference between the actual unloading curve and the constructed elastic unloading curve shows that plastic strain energy is recovered during unloading.

The dissipated energy is assumed to be connected with internal friction in the material, which may or may not lead to net plastic deformation during a load cycle. A rubber-like material may show large hysteresis loops, but the net plastic deformation is close to zero. The energy dissipated will partly increase the internal kinetic energy of the material (resulting in a temperature increase) and partly transfer to ambient material as heat. For a frictional soil there may also be net plastic deformation after a load cycle.

For a closer look into cyclic behaviour, consider the model of Figure 3.11 where a) represents a phenomenological model and b) and c) represent its rheological alternatives with b) as the

most direct representation. This model will be useful as a basic model when discussing frictional soil behaviour. The model may be viewed as a St. Vénant model where linear hardening has been added /68/.

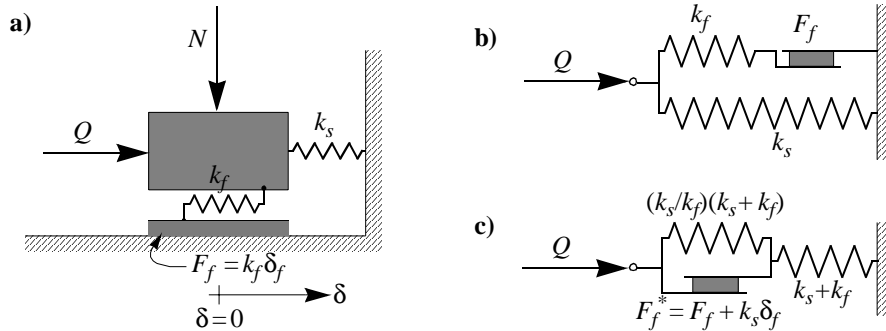


**Figure 3.11:** a) A phenomenological model, b) direct rheological model of a), c) St. Vénant rheological model with additional parallel spring representing the model in a).

With analogy to a frictional soil, the grey box of Figure 3.11 is an individual soil grain.  $k_s$  represents the volumetric elastic stiffness of the grain,  $k_f$  represents a combined stiffness consisting of the shear stiffness of the grain and a stiffness in the contact point resisting tangential forces.  $F_f$  is the sliding force in the frictional element. A more complete model would involve the two springs and the frictional element on all sides of the grain that are in contact with other grains, but the configuration in Figure 3.11 a) will suffice for the uniaxial behaviour that is described in the following.

In Figure 3.11 a) the applied horizontal force  $Q$  is counteracted by a spring force  $k_s \delta$  and a friction force  $F_f$  or a spring force  $k_f \delta$ . When the deformation of the system is  $\delta_f$  the friction element cannot withstand the applied force and will for increasing force and deformation slide with constant force  $F_f$ . When  $F_f$  has been mobilised, the spring with stiffness  $k_s$  will be the only one that can counteract the increased load. The normal force  $N$  will be the cause of the  $F_f$ , but will not enter the rheological models in b) and c).

If the system of Figure 3.11 is subjected to cyclic loading a picture of the force-deformation relationship like the one in Figure 3.12 will result. Only compressional loading is considered as frictional soil is not capable of resisting tensional loading.

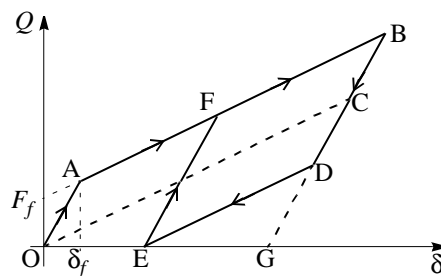


**Figure 3.12:** Behaviour of the rheological model in Figure 3.11.

From Figure 3.12 the first loading cycle will be the path OABDE where OE represents the net plastic deformation. Note that at C the  $F_f$  will change direction when unloading, and at D the

frictional element starts sliding and will continue to do so until E. Upon subsequent loading-unloading cycles there will not be produced any extra net plastic deformation, hence the cycles will traverse the path EFBDE. In classical elasto-plastic terms, on loading along OA the behaviour is entirely elastic while from A to B an elasto-plastic behaviour is encountered. Upon unloading an elastic behaviour is obtained along BD while an elasto-plastic behaviour is seen from D to E. If the unloading was purely elastic the path BDG would be traversed, and the distance from E to G may be considered as the recovered plastic strain. The plastic strain after unloading (net plastic strain) is therefore not the same as on top of the load cycle. The system of Figure 3.11 actually possesses a pure kinematic type of hardening with the dotted line OC as the mid points between the yield lines AB and DE.

Considering the energies involved it is seen that the recoverable energy is the area under BDE, while the area inside OABDE represents the dissipated energy. However, not all the dissipated energy is connected with the development of net plastic strain. An alternative path OAFE would have produced an equivalent plastic strain as the path OABDE. Hence the energy constrained by the path EFBDE is not involved in producing any net plastic strain but must be dissipated by frictional sliding which results partly in an increase in internal kinetic energy and partly as a heat transfer to the surroundings. The consequence is that the net plastic strain is not connected with the plastic work in a one-to-one correspondence, something which makes work hardening with respect to the net plastic strain less meaningful in cyclic loading of the model in Figure 3.11.

Likewise, within a classical elasto-plastic framework, not all the energy that is recovered can be denoted elastic strain energy as some of the recovered energy may be interpreted as recovered plastic strain energy, the latter represented by the area EGD in Figure 3.12. The conjectures of recovered plastic strain and plastic strain energy have probably evolved because the unloading path is not linear. However, the recovered plastic strain energy seems to have the same properties as the recovered elastic strain energy. In particular, this energy is also capable to do work on an external system in the same way as the elastic recovered energy. This leads to a rather confusing conclusion: On unloading we may differ between the plastic recovered energy and the elastic recovered energy, but they both seem to have identical intrinsic properties in terms of doing work on an external system. This illustrates the problem of the concept of plastic recovered energy and the recovered plastic strain.

The notion of recovery of plastic strains and of plastic strain energy may also be explained on the backgrounds of two quite different views on loading and unloading. In a kinematic hardening regime the unloading from D to E actually is considered as *loading* since plastic strain starts to develop (irrespective of the direction of the strain). On the other hand, when taking an everyday or practical approach, the unloading is defined as removing loads from an already loaded state. This latter definition is adopted in the present thesis, as also stated in Section 3.6.3. Within a mechanical framework this is the *hypoelasticity* approach and considers all recovered strain and strain energy as elastic. In hypoelasticity the unloading curve may be different from that of loading. It is however admitted that some researchers, e.g. Kolymbas and Herle /52/, argue that when unloading is different from loading the stress-strain relationship should be denoted hypo-plastic as such models are so-called incrementally nonlinear.

The kinematic hardening approach is nevertheless useful for a physical understanding of what happens when the external load is (gradually) removed. At point B of figure Figure 3.12 both springs of the model are compressed. When removing load from point B these internal springs will continue to apply internal loads to the grey box, i.e. we have an internal unloading mechanism when removing external load from point B. From B to D there is frictional locking so the response is entirely elastic. (Strictly speaking, in kinematic hardening plasticity there is unloading from B to C (C is a neutral state), but after C there is loading.) From D to E plastic strains develop as the friction element no longer locks but slide with constant force, and this process is

identical to the one from A to B (the unloading path BDE turned upside down is exactly the same as the loading path EFB). Note that when sliding the friction increase (here in one step from 0 to  $F_f$ ), and the stiffness drops. This is caused by the deactivation of the spring connected to the frictional element thus leaving the spring with stiffness  $k_s$  as the only one capable of moving the grey box. The box will move until the external load is zero, and then the friction force equals the spring force.

The analogy to a frictional soil is quite straightforward at this stage: Considering a soil particle, comprising several individual grains, the internal elastic stresses together with the friction will resist the external stresses at the point of maximum load. When unloading the (gradual) removal of the external stresses will make the internal stresses cause a (reverse) loading of the particle. These stresses originate from the storage of elastic strain energy upon loading. After some point of internal loading plastic strains start to develop - and will not stop to develop before the internal elastic stress is entirely balanced by the friction when the external load is zero. This effect will cause the unloading curve being different from the loading curve, but in a real soil particle there may also be other factors causing differences in the shape of the loading curve from that of the unloading curve.

At the unloaded point E a permanent deformation OE has been produced which is also the deformation of the spring with stiffness  $k_s$ . The spring with stiffness  $k_f$  is deformed  $\delta_f$  but in the opposite direction of the other spring. The deformations and corresponding forces, the latter being self-equilibrating, may be denoted initial deformations and initial forces, respectively. When constructing a soil structural component the placing and compaction would have brought the structure to a state similar to point E prior to any service loads. The energy stored in the model when unloaded to point E is shown as the shaded area in Figure 3.13. The energy amount stored is not big, and in a soil layer component this energy is not easily released. Heavy vibrations or earthquakes may release some of the energy with soil expansion as a result. More on initial stresses and strains may be found in Section 3.8.

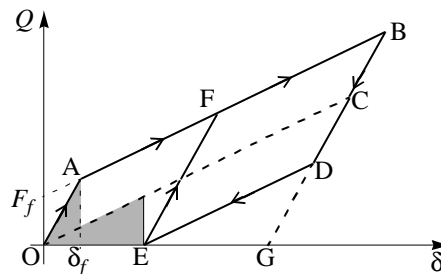


**Figure 3.13:** Energy stored in the model after cyclic loading to E (shaded area).

One may state that in kinematic hardening plasticity, as also in most elasto-plasticity theories, one focuses on the development of plastic strains at the cost of simplifying the elastic response (often with one set of values for Young's modulus and Poisson's ratio). The plastic strains may be calculated at any stage during a load cycle. In a hypoelastic theory one focuses on how the elasticity varies through loading and unloading and plastic strains develop during load cycles only. Theoretically, hypoelasticity and plasticity models may be both be viewed as ways of describing plastic (or viscoplastic) phenomena /93/. If the net strain after a load cycle is of primary importance, as it is in the present thesis, a hypoelastic approach could be pursued.



### 3.7.2 Modelling cyclic behaviour by adapting the Iwan model

The objectives of the present section are to demonstrate a more refined phenomenological model capable of taking care of some additional effects. The simple model described in the previous section was adequate in describing a simple phenomenological understanding of frictional soil behaviour subjected to cyclic loads. However, to achieve a deeper understanding the following additional effects should be included:

- (1) The net plastic strain should increase as the maximum load increases.
- (2) Cyclic creep, i.e. ratchetting, should be possible.
- (3) Increasing stiffness with increasing medium stress.
- (4) Reduced cyclic creep as the number of load cycles increases.

Only item (1) will be fully explored here.

There are more advanced rheological models that more closely can follow a hysteretic stress-strain curve for real materials. One example is the Iwan model /39/. The model is similar to the multiple surface model by Mróz /62/ but has as a starting point a rheological model. The Iwan model have several units consisting of a parallel spring and a frictional element, as in the left part of Figure 3.11 c), coupled in a series with a single spring at one end. The frictional elements have different limiting friction forces and are thus activated in turn as the external force increases. The resulting stress-strain curve is more curved but still piecewise linear. An example is shown in Figure 3.14 for a model with three spring-and-friction units and a single spring - all coupled in a series. The mechanical behaviour is much the same as for the more simple model in Figure 3.11, but depending on the number of elements the model is able to model increasing net plastic strain for the first cycle with increasing stress level (item (1) above). This behaviour may allow a relation between the work put into the system and the plastic strain (work hardening) for the first cycle, but will fail on subsequent cycling of the load as no plastic strain develop. It is also seen that on reloading the behaviour is much stiffer than that of initial loading. Connecting to plasticity theory it is seen that the Iwan model is a rheological representation of a pure kinematic model with multiple yield surfaces.

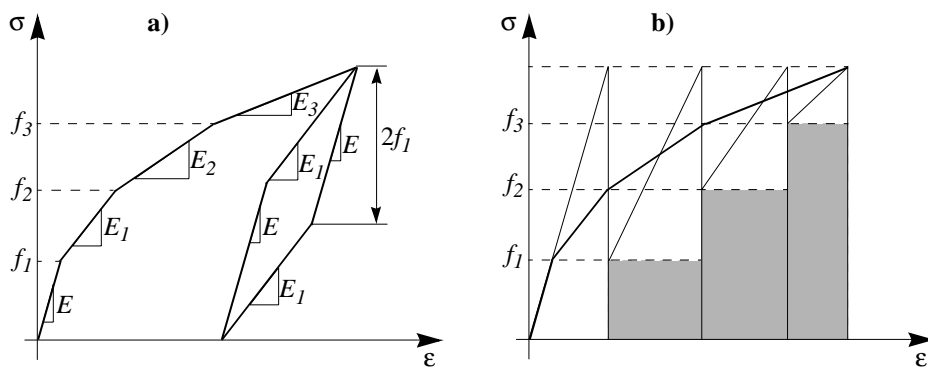


**Figure 3.14:** Stress-strain curve for an Iwan model with three spring-and-friction units and a single spring coupled in a series. a) Stress-strain curve of loading, unloading and reloading, b) Elastically stored energy (white) and dissipated energy (shaded) during loading

From a graphical procedure on the loading curve of Figure 3.14 the energy has been divided into stored elastic energy and dissipated energy, see Figure 3.14 b). The stored elastic energy of each of the four elements is shown as white triangles, while the dissipated energy is shown as shaded

rectangulars. Upon unloading the elastically stored energy is the only part that is available to the mechanical part of the system, as coupling between thermal and mechanical properties is not considered. When unloading the stored elastic energy is transferred into three parts (as was also the case for the simpler model of Figure 3.11):

- (1) Recovered elastic energy
- (2) Dissipated energy
- (3) Stored elastic energy

The stored elastic energy after the first unloading will not change during subsequent loading cycles, thus remaining at the level from the first unloading. Consequently, the elastic energy supplied upon reloading will only be transferred to recovered and dissipated energy during unloading; no part will be stored. This effect is due to the present model setup and is not generally valid.

It is, despite the limitations of the current model, interesting to note the different behaviour of the first cycle, the response being softer, compared to the subsequent cycles. This is due to the fact that initially no energy is stored in the model, i.e. no springs are strained. In a real soil specimen this is not the case due to, e.g. overburden loads in situ or compaction. It is however not probable that in situ loading or compaction will eliminate the present effect completely since these prior loading mechanisms are not likely to be identical of the laboratory loading during the first loading cycle. Therefore, a somewhat different behaviour during the first loading cycle compared with subsequent cycles should be expected even for real soil specimens. Within kinematic hardening plasticity, one may say that at the outset of the first loading of the model the stress state is in the centre of the elastic region, but on subsequent unloading and reloading the stress state is always at the yield surface when unloading or reloading starts.

From Figure 3.14 it is evident that the dissipative energy increase its share of the total energy input as the model approaches a failure state. At failure all or most of the extra energy input is dissipated through friction. If additional elements with a spring and a frictional slider in parallel are added to the model the model could be refined. Provided that the new friction sliders have a frictional slip force between those of the basic model, the response curve would approach a continuous and smooth curve if a sufficient number of additional elements are added. Also the frictional curve would approach a continuous and smooth curve. These curves for unloading are shown schematically in Figure 3.15 where the dissipated energy is shaded.

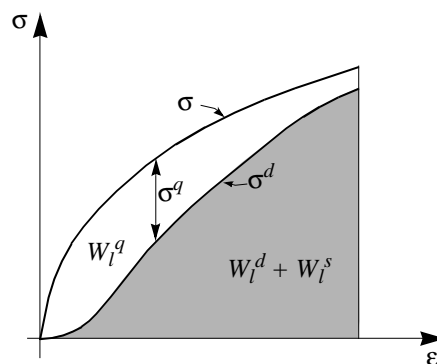


**Figure 3.15:** Smooth elastic and frictional stresses when loading. Elastic energy is white, dissipated and permanently stored energies are shaded.

In Figure 3.15 superscript  $q$  has been applied when the quantity it belongs to is connected with the elastic energy, while superscript  $d$  is used for dissipative quantities. Subscript  $l$  denotes loading and subscript  $u$  will later denote unloading.

Generally during loading the external applied energy  $W^{ext}$  will partly be temporarily stored as elastic energy ( $W_l^q$ ), partly dissipated ( $W_l^d$ ) and partly stored more permanently ( $W_l^s$ ):

$$W^{ext} = W_l^q + W_l^d + W_l^s \quad (3.71)$$

The stored contribution,  $W_l^s$ , may be defined in a way such that it is not released upon unloading along a stress path exactly opposite that of loading. It may, as stated before, be released by other loading events not following the same stress path.  $W_l^s$  is, however, difficult to measure. When the amount  $W_l^s$  is absorbed by the material during loading it may be interpreted as a dissipative part of the energy, and when it is released by the material during unloading it is likely to be interpreted as recovered elastic energy. It may also be possible that  $W_l^s$  is released during subsequent loading or absorbed during unloading. With a possible exception for initial loading where no prior energy is stored within the material, the  $W_l^s$  may probably be considered small and may be neglected. Still, from a phenomenological point of view, the notion of a stored part  $W_l^s$  may be fruitful, although its definition may be debated.

When unloading, only the elastic energy part,  $W_l^q$ , may at the very best be recovered. Usually some of it is dissipated and some of it may be stored more permanently. Considering the internal loading mechanism when unloading,  $W_l^q$  is the only energy available to the system. Then

$$W_u^q = W_u^q + W_u^d + W_u^s \quad (3.72)$$

from a loaded state to an unloaded state. Comparing Eqn. (3.71) and Eqn. (3.72) it is seen that

$$W_u^q \leq W_l^q \quad (3.73)$$

The energy conversion during unloading, as stated by Eqn. (3.72), is illustrated in Figure 3.16 a) while the total dissipated and stored energy is depicted in part b) of the figure. In part b)  $W^d$  and  $W^s$  is the sum of their contributions in loading and unloading.

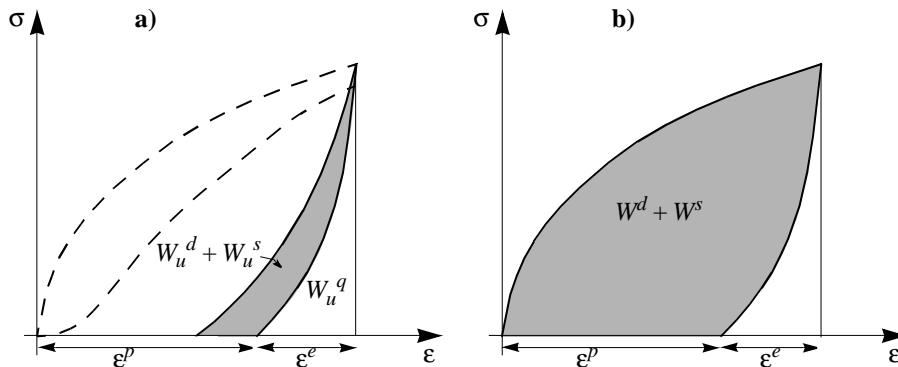


**Figure 3.16:** a) Energy conversion during unloading, b) total amount of dissipated and stored energy.

Note the consequences of a high degree of dissipation also when unloading: The rebound will be stiff in the sense of a steep curve, thus producing a higher resilient modulus (defined on page 67) than a material exhibiting the same total strain but with a bigger elastic strain. In such a case the material with the least modulus should be preferred as this material dissipates less energy and has a higher resistance against permanent deformation. In other words, there is a pit-fall when choosing materials only on the basis of their resilient moduli.

In the limit, where an infinite number of springs and frictional sliders constitutes the Iwan model, the curves in Figure 3.15 will be completely smooth. This represents a pure kinematic model with an infinite number of yield surfaces and where the purely elastic region shrinks to a point. The of movement of the yield surfaces during loading, unloading and reloading is illustrated in Figure 3.17, though for a limited number of yield surfaces.

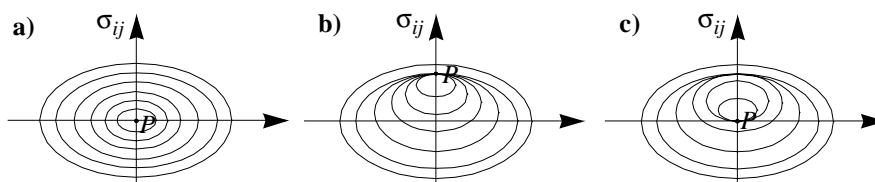


**Figure 3.17:** Pure kinematic yielding in stress space during cyclic loading. a) Initial material state, stress (represented by point  $P$ ) equal to zero, b) material state at maximum stress during the stress cycle, c) unloaded state when stress is equal to zero.

It is seen from Figure 3.17 that during initial loading more yield surfaces are activated than during unloading. During an unloading-reloading cycle only the two inner surfaces are activated, so during cyclic loading the material states will oscillate between the two states of b) and c) in the figure. Thus, in a soil particle the loading has changed the material properties in the loading direction, something that is known as *stress induced anisotropy*. Note also that the two outer surfaces have not been activated. These surfaces will only come into play when the load is sufficiently increased, i.e. the model has a memory of the maximum load level.

The discussion above leads to a division of the stress component into a part where the corresponding part of the applied work is stored elastically, and is thus available to the system on rebound (unloading), and a part whose related energy is dissipated. On unloading the stress can be partitioned in a similar way. The sum of these two components must form the total stress:

$$\sigma = \sigma^q + \sigma^d \quad (3.74)$$

where  $\sigma^q$  is the stress that is capable of storing and releasing mechanical energy and  $\sigma^d$  is the stress that is responsible for dissipating energy. The strain associated with these stresses is in both cases the total strain. For a drained, frictional material the total stress is to be considered the effective stress. A thermomechanical justification of this partitioning of the stress is given by Ziegler /89/ and is briefly reproduced in Appendix B. What herein has been called elastic stored energy is in thermomechanical terms similar to the *free energy*.

Eqn. (3.74) is also valid for other types of stress that is of a dissipative nature; hence  $\sigma^d$  may also be a viscous stress component dependent upon the strain rate. Viscous behaviour is generally recognised by the fact that the maximum stress occurs prior to the maximum strain in cyclic loading.

To establish from experiment the numerical values of the two components of stress is difficult for a soil specimen subjected to loading in a conventional triaxial cell with standard instrumentation. Therefore this split-up of the stress is more of a phenomenological framework that may prove to be useful when considering dissipation effects and else cyclic behaviour.

### 3.7.3 Basic modelling of the conservative and dissipative stresses

According the discussion above, the friction is very low at the outset of loading but increases when unloading and becomes the dominant part near failure. It is also reasonable to believe that the ratio of the frictional stress to the total stress is monotonically increasing or constant with the strain. Otherwise, incrementally negative dissipative energy contributions could result provided the other material properties remain constant. On this background a function is defined that describes the ratio of dissipative stress to total stress with respect to strain:

$$r^d(\varepsilon) = \frac{\sigma^d(\varepsilon)}{\sigma(\varepsilon)} = \begin{cases} 0 & ; \varepsilon = 0 \\ 0 < r^d(\varepsilon) < 1 & ; 0 < \varepsilon < \varepsilon_f ; r^d(\varepsilon) < r^d(\varepsilon + d\varepsilon) \\ 1 & ; \varepsilon = \varepsilon_f \end{cases} \quad (3.75)$$

where  $\varepsilon_f$  is the minimum strain where no elastic stresses are present (static failure) and  $d\varepsilon$  is a positive strain increment. The  $r^d(\varepsilon)$  is supposed to be smooth and continuous over its total domain. Eqn. (3.75) is monotonically increasing and has the value 1 at  $\varepsilon = \varepsilon_f$  thus being slightly more restricted than necessary.

Likewise, it is possible to define a function where the ratio of elastic stress to total stress is described:

$$r^e(\varepsilon) = \frac{\sigma^e(\varepsilon)}{\sigma(\varepsilon)} = 1 - r^d(\varepsilon) \quad (3.76)$$

By way of example, without any experimental justification, an assumed linear relation would produce the following ratios for the first loading:

$$r^d(\varepsilon) = \frac{\varepsilon}{\varepsilon_f} \quad (3.77)$$

$$r^e(\varepsilon) = 1 - \frac{\varepsilon}{\varepsilon_f} \quad (3.78)$$

Hence the dissipative stress and the elastic stress are

$$\sigma^d(\varepsilon) = \frac{\varepsilon}{\varepsilon_f} \cdot \sigma(\varepsilon) \quad (3.79)$$

$$\sigma^e(\varepsilon) = \left(1 - \frac{\varepsilon}{\varepsilon_f}\right) \cdot \sigma(\varepsilon) \quad (3.80)$$

For unloading a pure kinematical approach may be pursued. Then the sizes of the yield surfaces are constant and hence the frictional slip stress connected with the individual springs will be constant. But when it comes to the elastic part, the modulus will double because each infinitesimal spring will take twice as much stress and strain before the associated frictional element and the next spring are activated.

### 3.8 Initial stresses and initial strains

Initial stresses and initial strains represent a stress-strain state that is present in the structure prior to the structural load case that is to be analysed. Thus there are no relations between the present structural load case and the initial stress-strain state, and the causes behind this stress-strain state must be sought in the history records of all contributing effects experienced by the structure. However, any substantial initial stresses may affect the subsequent deformation due to loading since the mechanical behaviour of granular materials is generally stress dependent.

In structural mechanics initial stresses and strains may be the effects of change in temperature (according to the degree of thermal expansion allowed), swelling (e.g. because of moisture), misfit of structural members or material working (especially working of metals). Freeze-thaw cycles is a special case of combined thermal and swelling effects, as the problems connected with such processes are mainly related to the phase transition of the interstitial soil water. Thermal (apart from freeze-thaw effects) and misfit effects (at a macro level) on initial stresses in unbound granular materials may normally be neglected. Swelling action may in some cases produce substantial initial pressures, but is not a frequent encountered problem as it is dependent upon the presence of certain types of clay minerals (e.g. montmorillonite). In granular materials like soil a frequent cause of initial stresses and strains is compaction during construction, by traffic loads or by other means. This compaction process may at a micro-level be regarded as misfit forces between individual grains. Another likely source is freeze-thaw cycles. Gravity forces can be treated separately (as an additional structural load) although the stresses and strains originating from gravity may very well be viewed as initial stresses and strains because they are present prior to any service loading for which the structure is to be analysed.

In general a material may be subjected to both initial stresses and initial strains. The ratio between those two is decided by the constraints that the particular material point is subjected to. If the material is fully constrained the material will display zero initial strain but fully developed initial stress. On the other hand, if there are no constraints around the material there will be no initial stresses and fully developed initial strains. Of course, these two extremes are rarely found and the material finds itself in an intermediate state. A pertinent example of extremes may be continuously welded rails vs. bolted rails. In the first case there are almost no strains, while large stresses may arise. For the bolted rails case the rails are allowed to move freely (within the limits of rail spacing in the joints) causing considerably strain and little stress.

Initial strains may be converted to initial stresses, and vice versa, with the help of the constitutive relation that exists for the material. If one assumes the condition of the structure at the start of the analysis to be the undeformed/reference condition the initial strains are by definition zero. Consequently only the initial stresses have to be dealt with.

Although the causes of an initial stress-strain state may be known to a certain extent, the numerical values of these stresses and strains are difficult to obtain for an existing railway embankment. To numerically quantify the initial stress and initial strain one has to have a relation between the actual cause and the resulting stress or strain. In the case of compaction, assuming

sufficient side support, it has been argued that the compaction creates large passive stresses, i.e. a situation where the maximum principal stress is horizontal when the compaction device is removed /80/. Deep ditches may counteract this effect, at least partly and in regions where the initial stresses are most wanted.

An estimate of the initial stresses (or residual stresses) in a railway or road embankment can be considered to be important for several reasons:

- ◆ The soil behaviour is stress dependent and therefore also dependent on the initial stresses. Stress dependent soil models are described in Section 3.4 for the elastic case.
- ◆ Justification of elastic soil models - avoiding tensile stresses.
- ◆ Failure calculations.

Despite the difficulties in measuring or calculating the initial stresses there are, however, some important features of initial stresses in a coarse graded unbound aggregate that should be emphasised. The following points are postulated, partly based on the discussion above:

- (1) Initial stresses are always to some extent present in a material where the material particles are not allowed to move freely. This implies that fluids in a static state do not have any initial stresses, while solid materials do.
- (2) Initial stresses are self-equilibrating, no external action has to be applied to satisfy equilibrium (this is actually a part of the very definition of initial stresses!).
- (3) The initial stresses can not possibly be larger than the strength of the material. (The material strength is here considered as a failure state where unlimited plastic strains will occur<sup>1</sup>, which is a state that may change during the life of the structure (e.g., because of hardening or softening behaviour)). This implies that materials with high strengths may demonstrate high initial stresses, while weak materials do not.
- (4) The initial stress tensor generally consists of normal stresses (both compressive and tensile) and shear stresses. If no tensional stresses are allowed in the material, as in a cohesionless unbound granular material, the initial stresses may not be tensional either.
- (5) The consequence of item (2) and (4) above for a granular material is that any initial compressive stress has to be equilibrated by shear stresses, not by tensional stresses (as may be the case for metallic materials). This leads to *lower compressive* stresses in another part of the structure, but never to tensile stresses as in metals. The shear stresses transfer the difference in compressive stresses between the two areas. (The stress state cannot possibly be both compressive and tensional within the same material particle.)
- (6) According to classical geotechnics, e.g. /65/, initial shear stresses are not possible in a cohesionless and weightless material. But if the material weight is added shear stresses may be mobilised proportional to the normal compressive stresses<sup>2</sup> (which for a half space are identical with the gravitational pressure).
- (7) Consequently, if no cohesion is present, the (compressive) initial stresses are zero at the top of the embankment and may grow gradually in the downward direction. (Not to be confused with the horizontal resting pressure).
- (8) If the maximum initial stresses according to item (6) and (7) are present in an embankment, the embankment will be at the edge of a failure condition. Certain load patterns (dependent upon magnitude and placement) will then produce failure earlier than a case with small initial stresses present.

1. This definition of strength is in most cases not acceptable for a road or railway in service - here some bounds on the magnitude of plastic deformations must be imposed.

2. According to Coulomb.

- (9) The horizontal pressure at rest is a consequence of gravity and is, at least conceptually, best treated as a separate load. There may, however, be arching effects in part of the structure that leads to higher horizontal pressures than the ones according to gravity. These arching effects are similar to those of stone arches, e.g. in bridges. The resulting *excess* stresses must then be acknowledged as initial stresses. In a granular structure these arching effects may be regarded as variability in compaction and they have probably a random occurrence throughout the structure.
- (10) Any reinforcement embedded in the granular material, like geosynthetics, will alter the strength characteristics of the material. Since the material is strengthened, mostly in the tensile region, one may expect that more residual stresses are imposed.

This description of initial stresses and strains is rather qualitative, although some bounds on magnitude have been pointed out. The actual numerical values of the initial stresses and strains in road or railway pavements are very difficult to measure, not to mention to calculate accurately. It should also be emphasised that for our purpose the horizontal initial stresses, or those parallel to the granular surface, have been focused herein and also in the literature /80/. These stresses are perhaps easier to conceive as proper side confinement and arching effects can explain their origin. Vertical initial stresses are also possible, but to be useful these stresses have to be transmitted to the structure through shear stresses at the sides. These shear stresses must point in a downward direction so that the vertical compressive stress will increase inside the structure. It may be questionable whether such shear stresses are able to transmit over long distances in granular materials.

To conclude, it is not likely that the initial stresses are substantial in the unbound granular parts of a road or railway pavement. Compaction processes do induce initial stresses and strains. But as far as strengthening of the material is concerned it is probably the densification itself that contributes most to the strengthening process and not any presence of initial stresses. In fact, as pointed out in item (8) above, high initial stresses may lead to an earlier failure of the structure and are not always beneficial. To utilise initial stresses of a magnitude that counts in a design process will therefore be dubious, if not risky. In a design process it is also a question whether the initial stresses at the time of construction will last during the lifetime of the structure.

### 3.9 Using constitutive models and FEM for a railway track

If the railway track is stable in the sense that the plastic strain accumulation is reasonable and not accelerating the net plastic strain from each cycle can be viewed as very small compared to the elastic ones. This argument has been discussed in more detail in Section 3.5.1, and is a necessary but not sufficient condition to use elasticity to model the behaviour. As seen in Section 3.7 the hysteresis can be noteworthy for each cycle even for frictional systems, thus the stress-strain relationship is not unique. The hysteresis being small, which actually also imply that the net plastic strain is small, is a sufficient condition for approximating the behaviour with an elastic model. The elastic model is then of a hyperelastic type, which imply that there exists a free energy that interrelates the stresses and strains.

On the other hand, if the track is sufficiently unstable or the materials involved show large hysteresis loops, then an elastic approximation may be doubtful. An elasto-plastic analysis must then be carried out, but a calculation for thousands of load cycles is not performed on a routine



basis today. A calculation for one representative load cycle may then be an alternative as a means to get a feeling for the order of magnitude of the deformations on a per cycle level.

The constitutive model must be based on testing the materials that the actual track section consists of. Some part of this material testing is focused in Chapter 4. In addition to a material model with the right parameters one needs a tool to solve the boundary value problem. As mentioned in Section 3.3 this tool is often the finite element method. Unlike roads and airfields the railway track is not possible to approximate with an axisymmetric model where the axis of symmetry is vertical. In the finite element method an axisymmetric model is considered to be two-dimensional. A railway track must be modelled as a three-dimensional problem and this makes the analysis considerably larger than a two-dimensional one.

---

## CHAPTER 4    **Triaxial equipment and testing of railway ballast**

---

### **4.1 Introduction**

Triaxial testing is nowadays carried out on a routine basis in traditional geotechnics to obtain strength parameters for soils. But triaxial testing of granular materials is also a field of research, e.g. in traditional geotechnics, in road pavement design and in assessing railway ballast properties.

Judging by the name of the test method, the objective is to determine the material properties by varying the stresses on three perpendicular planes in the specimen. If the stresses are to be varied independently on all three planes at the same time one has to use a *true triaxial testing unit*. This kind of testing unit uses cubical specimens and is mainly intended for research purposes. More information on such devices may be found in /16/.

The most commonly used device for triaxial testing is the *conventional triaxial cell* that uses cylindrical specimens. The soil specimen is covered with a membrane and subjected to a confining stress applied through a pressure fluid (air, water or oil) and an axial pressure transmitted through end platens attached to the specimen. Because of the cell pressure two of the three principal stresses are equal, typically  $\sigma_3 = \sigma_2$ , while  $\sigma_1$  is in the axial direction. The present chapter describes these kind of devices with a focus on the testing of railway ballast.

As with the true triaxial testing unit the *hollow cylinder device* is mainly used for research purposes. This device is similar to the conventional triaxial cell but uses tubelike specimens and may also impose shear stresses by applying torsion to the end platens. The outer cell pressure may for some devices be different from the pressure on the inner side of the specimen. A review of some of the types of hollow cylinder devices is given in /70/.

### **4.2 Conventional triaxial testing units found in the literature**

The review here focuses on the conventional triaxial cell intended for testing coarse grained materials. Nowadays ballast materials for railway purposes are commonly made of crushed rock with a maximum particle size in the range of 50-80 mm. Section 4.4 contains more on the requirements for railway ballast.

Because of the size of the material the specimens to be tested need to be large. Typically a minimum diameter of the specimen is 5-7 times the maximum grain diameter. Also, to obtain a height to diameter ratio of 2:1 or more, as recommended by /4/ and /17/, it is clear that the specimens have to be substantially larger than the ones normally encountered in traditional geotech-

nics. As a result, there are quite few studies on triaxial testing on railway ballast, but large triaxial cells have also been used to study more well graded materials for, e.g. constructing road pavements, high embankments and earth dams.

**Knutson et al.** /50/ at the University of Illinois at Urbana-Champaign, USA, describe a triaxial cell with the capability for testing specimens with a diameter of 203 mm (8 inches) and a height of 406 mm (16 inches). Several types of ballast were tested, but the maximum particle size was that of the AREA no. 4 ballast (see Section 4.4.2) which is 51 mm. The confining pressure was supplied by means of air pressure and was constant during the tests. The deviatoric stress was repeated and applied by a hydraulic actuated piston. 50 haversine load pulses per minute, each of 0.15 seconds duration, were applied. The maximum deviatoric and confining pressures in the standard test sequence were 827 kPa (120 psi) and 103 kPa (15 psi), respectively. For one preliminary test the confining stress was 138 kPa (20 psi) for the same maximum deviator stress. The axial deformations were measured both by an LVDT at the top of the hydraulic actuator and by two electronic-optical scanners. Collimators measured the vertical motion of black and white targets placed at the upper and lower quarter points of the specimen. The outer LVDT was primarily measuring the permanent deformation, while the electronic-optical system primarily measured the resilient deformation.

**Institut für Geotechnik at ETH** in Zürich, Switzerland, has performed a series of triaxial tests on railway ballast to determine the mechanical properties as a function of the level of fouling /23/. The specimen size is 262 mm of diameter and approx. 500 mm of height. A broad range of gradations have been investigated, from a new ballast with maximum grain size of 63 mm and minimum size of 31.5 mm to a heavily fouled ballast with maximum grain size of 22.4 mm and 40% passing the 0.5 mm sieve. A hydraulic actuated piston supplied the deviatoric stress with a frequency of up to 25 Hz, but 10 Hz seems to have been the normal testing frequency for the repeated part of the test. The maximum deviatoric stress during testing was 260 kPa (for the least fouled materials). The confining stress was applied through pressurised water and was held at 30 kPa during all tests. The axial deformation was recorded by a displacement transducer in the deviator piston, and in addition there was one external displacement transducer (no information on where this later transducer was placed). No lateral displacement measurements were made, instead volume changes were measured by weighing the flow of water in and out of the cell. Due to inertia of the water, the changes of volume were not possible to detect during the repeated tests, but only during the quasi-static tests with a frequency of 0.01 Hz.

**Kolisaja** /51/ describes a triaxial cell capable of testing 300 mm by 600 mm specimens that has been developed at Tampere University of Technology, Finland. Most of the materials tested, and reported in /51/, have a broad gradation and a maximum particle size of 32 mm or less. Two of the materials are open-graded with a  $C_u$  around 2-3 and a maximum particle size of 64 mm which makes these materials similar to a railway ballast. Only the deviator load is cycled, and this loading system is servo-hydraulic. The maximum deviator stress is about 2.8 MPa and the maximum frequency is 20 Hz, while a 5 Hz loading frequency seems to have been the maximum (during preconditioning). The maximum deviatoric stress during the testing is not given but is probably considerably lower than the one achievable by the actuator. During the resilient testing, procedures with haversine pulses with 0.1 sec. duration and a resting period of 0.9 sec. have been applied. The confining stress is applied by using air pressure and it seems that the maximum confining pressure has been 138 kPa, i.e. the maximum confining pressure according to SHRP Protocol P46 /77/. Generally, the testing has been conducted using the three procedures of SHRP, CEN and NGI<sup>1</sup>. Axial deformation is measured by two to four strain gauge transducers mounted on the 200 mm central part of the specimen. Radial strain is measured by two dia-

---

1. SHRP - Strategic Highway Research Program, CEN - European Committee for Standardization, NGI - Norwegian Geotechnical Institute

metrically placed proximity transducers at one third from top of specimen. These transducers measure the distance to small metal plates glued to the specimen. For the 300 mm specimens a strain gauge instrumented ring also measures the radial strain at one third from the base end.

**Norwegian Geotechnical Institute (NGI)** has built a triaxial apparatus capable of testing specimens with a diameter of 625 mm and a height of 1250 mm /86/. Six materials were tested in the study, four of which were well graded and two were uniformly graded. The maximum particle size varied between 32 and 120 mm, the latter being valid for one of the uniformly graded materials. The equipment and software originate from MTS, USA. The deviatoric stress capacity is about 2.6 MPa, but only 600 kPa was used in the tests. The loading procedure used implied a cosine-shaped deviatoric load pulse with duration 0.1 sec. with a resting period of 0.9 sec. The confining stress was applied by using a constant partial internal vacuum, equivalent to a maximum confining stress of 80 kPa. Five instruments (not mentioned which type) are used for measuring the vertical deformation, and are fixed on the central half of the specimen. Two of the instruments measure repeated strains while the remaining three measure the permanent strain. It seems that strings are fixed to the specimen and the change of length (height) is measured at the base of the cell. Three instruments are used to measure change in specimen circumference with the help of spring loaded strings.

**Lekarp and Isacsson** /54/ describe the development of a large triaxial apparatus at the Royal Institute of Technology in Stockholm, Sweden. The specimen size is 500 mm by 1000 mm and the maximum particle size is 100 mm. However, the materials tested so far have a quite non-uniform gradation as the uniformity coefficients ( $C_u = d_{60}/d_{10}$ ) are around 10 with a maximum particle size of 90 mm. The apparatus is capable of cycling both the deviatoric and the cell pressure. The frequency of load application is normally 1 Hz when both stresses are cycled (normally in phase), but is increased to 10 Hz when only the deviatoric stress is cycled. The loading system consists of servo-hydraulic actuators from MTS that provide up to 1270 kPa of deviator stress and 620 kPa of confining stress. The maximum frequencies of the equipment is 20 Hz for the deviator stress and 2-3 Hz for the confining stress, but these frequencies seems not to have been used in testing of the materials. The confining fluid is silicone oil and the confining stress is applied by a hydraulic actuator that operates on a separate pressure cylinder that is connected to the cell chamber through a 1-inch bore tube. The strain measurements are done by LVDTs. Vertically three LVDTs measure the strain in the 600 mm mid portion of the specimen, and they are fixed to the specimen with expandable roller plugs in predrilled holes into the specimen material. The horizontal strain measurements are carried out with a 'string of wheels' mounted around the specimen at mid height and with one LVDT mounted at the junction of the string. The 15 sets of wheels are supposed to roll freely on the membrane surface thus providing an average measurement of the horizontal strain.

**Van Niekerk et al.** /83/ report on a large triaxial cell capable of testing specimens of 300 mm by 600 mm (diameter by height) developed at the Delft University of Technology, The Netherlands. The material tested seems to be well graded with an upper particle size of 45 mm. A hydraulic actuator applies the deviatoric stress, and the maximum stress is about 2.1 MPa, while the maximum frequency is 5 Hz. The confining stress is applied by partial internal vacuum, thus limiting the confining stress between 0 and 90 kPa. There are no means of applying repeated confining pressure. The deformations are measured by on-sample LVDTs. At 1/3 and 2/3 of the specimen height small blocks are glued to the membrane. On these blocks two self-centring rings are laid which serve as a local reference basis for three axial and two sets of three radial LVDTs.

**Smaller triaxial cells for testing coarse graded unbound aggregates.** There are several research institutions that operate conventional triaxial cells for testing coarse graded aggregates. These materials are mainly intended for base course layers in roadwork construction. Among

others, Hoff /34/, Galjard et al. /26/ and Hornyach and Gerard /36/ describe triaxial cells that test specimens with smaller maximum diameters, typically up to 150 mm. Such devices cannot be used for testing of railway ballast in the natural gradation, although there have been reports on testing scaled-down ballast material in cells that can take specimens with diameters of 100 and 150 mm /41/.

### 4.3 The triaxial testing unit used in the present study

The equipment used in the present study is a conventional large scale triaxial cell for repeated loading, which comprises three main parts

- ◆ The triaxial cell with loading actuators
- ◆ The load control unit
- ◆ The data capture unit

The two latter units consist of a PC, an amplifier and two controllers.

What makes the present triaxial unit a bit special is its capability of cycling both the deviatoric stress and the confining stress. The unit is made for testing railway ballast, thus requiring large specimens of 300 mm of diameter and 600 mm of height.

#### 4.3.1 The triaxial cell with loading actuators

The triaxial cell used in the present work has also been described in /75/. Reference is made to Figure 4.1 on page 103 for a sketch of the triaxial cell. When studying the figure, bear in mind that the total height of the apparatus is nearly 3.6 m, and the steel table is square with side lengths of approximately 1.0 m.

As can be seen from the figure, the cell chamber itself is mounted on a steel table. Others, like Kolisoja /51/ and Lekarp and Isacsson /54/, place the cell on or near the floor which enables easy access for instrumentation and for dismantling operations. However, the present design provides space for the confining stress actuator, which together with the bellows arrangement, transmit pressure to the confining fluid. Especially when it comes to variable confining pressure, where rapid response is important, a design like the one in Figure 4.1 will be beneficial because of the direct and easy way of applying the confining stress.

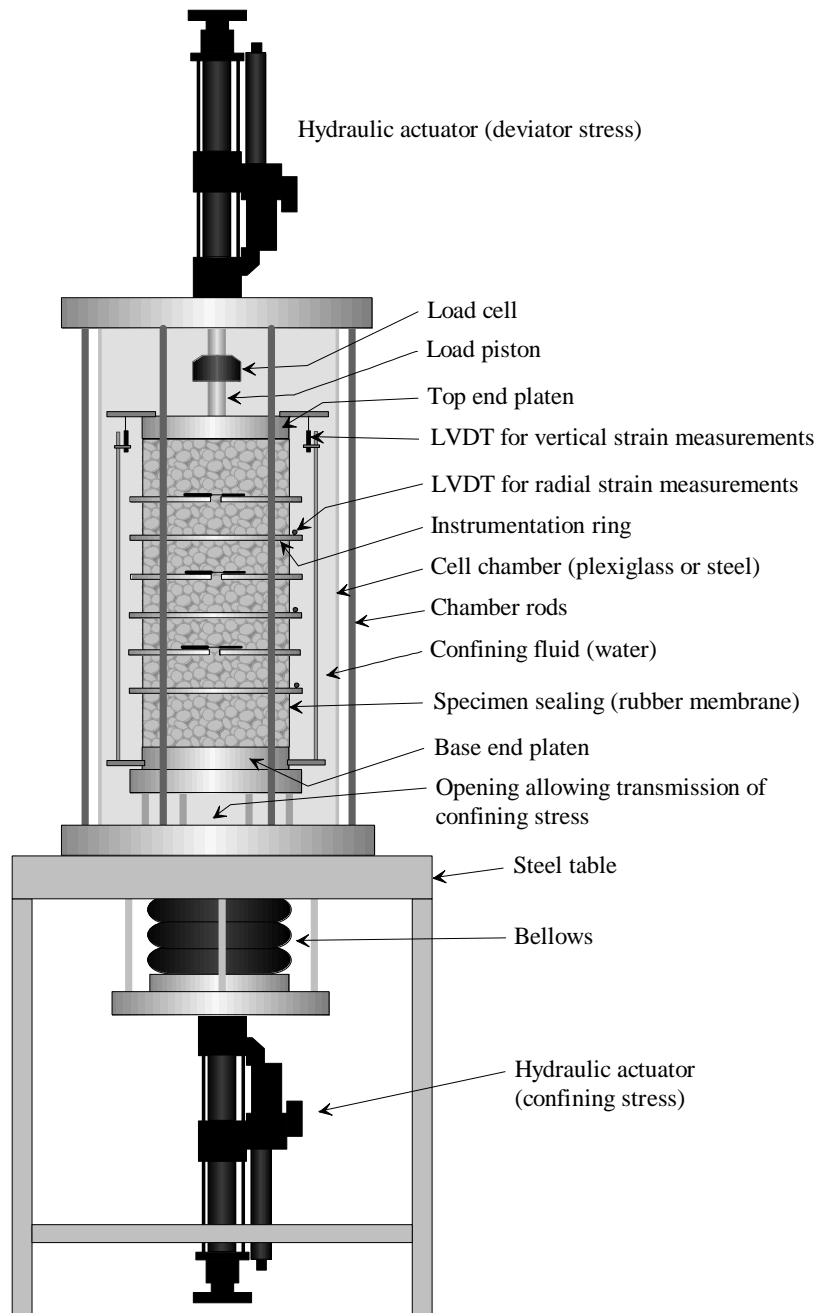


**Figure 4.1:** *The triaxial cell apparatus with specimen (cables not shown).*

A hydraulic actuator mounted on top of the cell chamber provides the deviatoric stress. The load is transmitted through a piston to the top end platen of the specimen. The technical specifications of the hydraulic actuators, which are manufactured by MTS Systems Corp., USA, are given in Table 4.1.

**Table 4.1:** *Data of the hydraulic actuators from MTS used in the triaxial apparatus.*

	<b>Deviatoric actuator</b>	<b>Confining actuator</b>
<b>Type of actuator</b>	MTS Model 244.22	MTS Model 244.21
<b>Nominal repeated force capacity</b>	±100 kN	±50 kN
<b>Standard piston stroke</b>	±75 mm	±75 mm

The hydraulic power supply is provided by a unit from MTS designated MTS Model 510.10D. This unit provides 40 l/min. of flow at 210 bar continuous pressure. The oil reservoir is 142 litres and the electric power requirements are 220V, 3 phase, 50Hz and 18 kW. This unit was located in a separate room to avoid some noise.

Converted to stresses, the hydraulic system can apply deviatoric stresses up to about 700 kPa and confining stresses up to about 400 kPa. The working frequency of the repeated stresses is 5Hz, if the full piston stroke length is not used. For small stresses a frequency of 10Hz may be achieved.

The vertical forces applied to the specimen (both deviatoric and confining) are counteracted through tensional forces in the chamber rods. A more usual way of dealing with these forces is to have a strong outer frame that takes the deviatoric force, while the chamber rods only take the vertical component from the confining pressure. Since both the stresses and the deformations are measured inside the cell, our design should be no source of error.

Water was used as the confining medium. Distilled water was supposed to give less resilience upon loading compared to water taken directly from the tap. But some tests after the completion of the ballast testing showed that it is acceptable to use ordinary water. It is however recommended that the water is allowed to adjust to ambient temperature before testing begins. Then the water will also reach an equilibrium air content. A low air content is beneficial to the confining pressure actuator because the increased stiffness causes the stroke length of the piston to be smaller, thus allowing faster loading. Further, water is 'clean' to work with. A cotton filter cartridge is mounted between the water storage tanks and the triaxial cell to remove contaminant particles that have entered the water from the laboratory environment or because of punctured specimen membranes.

However, water conducts electricity and contributes to corrosion of steel parts. The electrical conductivity of water is hazardous to any electrical signals where any live part is in contact with the water. As a consequence, all current carrying parts have to be waterproof. Corrosion inside the cell is avoided by choosing non-corrosive materials like aluminium, brass and stainless steel.

One of the frequently used alternatives as a confining medium is silicone oil. This liquid insulates electric live parts, but is in nearly every other aspect more troublesome to work with. In addition to being more expensive, it is more 'dirty' in the sense that you have to treat it as special waste when you replace the oil. When it comes to mechanical properties, the high viscosity compared to water makes rapid flow of the oil more difficult in variable confining stress tests.

Air may also be used as the confining fluid in triaxial testing. However, air is very compressible, thus requiring long stroke lengths of the confining pressure actuator. This will limit the maximum repeated confining pressure. Since air stores considerably more energy for the same pres-

sure compared to oil or water there is a bigger safety hazard if the cell chamber is punctured or fragmented. Air as a confining medium is normally limited to constant confining stress tests.

### 4.3.2 The load control unit

The deviator actuator is connected to an MTS Model 407 controller, while an MTS Model 406 controller takes care of the confining pressure actuator. The hydraulic system is controlled by a PC program that runs the tests and collects pressure and deformation data. The PC program is written in LabWindows CVI, and runs under Win95. The system can define different load sequences for specimen testing. Each sequence consists of a static load with a dynamic cyclic load on top. The dynamic load signal is normally sinusoidal (haversine) with no rest time between the cycles, but other signal forms can easily be applied. The load sequences for the deviator and the confining pressure are controlled independently, but on the same time basis. This enables support for arbitrary phase difference between the load cycles applied to the actuators. In addition to specifying any phase difference in the load sequences, it is possible to adjust the phase difference during testing. This is convenient if the one wants to accurately adjust the phase difference on the basis of the continuously *measured* values of the loads. When testing a sample, several load sequences can be run in succession to define a load program.

For the current adjustments of the load control unit the horizontal load is smaller in the beginning of each load step than the one actually specified. The deviator load has the correct value straight away. After a 30-60 cycles, the loads are adjusted to the specified ones.

### 4.3.3 The data capture unit

The deformations of the specimen are measured by eight LVDTs (Linear Variable Differential Transformers) manufactured by the British company RDP Electronics. The LVDTs used, which have designation MD5/500W, are submersible and can withstand pressures up to 35 bars (3.5 MPa). The stroke length of the LVDTs is  $\pm 12.5$  mm. Submersible LVDTs make it possible to use water as the confining medium. Compared to ordinary LVDTs, that are neither submersible nor can withstand pressure, our LVDTs are about 3 times as expensive. A total of eight LVDTs are used, and the positioning of them is approximately as in Figure 4.1. Six of the LVDTs are used for horizontal deformation measurements while the remaining two are used to measure the axial deformations. In addition, data are collected from internal LVDTs in the actuators, but this data are intended for internal controlling of the piston positions. The deviatoric stress is measured by a load cell mounted on the deviatoric piston and the cell pressure is measured by a pressure transducer in contact with the confining water. More on mounting the LVDTs on the specimens is found in Section 4.5.3.

The specimen LVDTs are connected to HBM SPIDER8 4.8 kHz carrier frequency amplifiers (made by Hottinger Baldwin Messtechnik GmbH, Germany). As the SPIDER8 amplifiers only support inductive transducers in full or half bridge mode, the primary (excitation) input leads on the LVDTs are not used. Instead the secondary (response) output leads are connected to the amplifiers together with the centre tap, in a half bridge connection. As this could lead to decreased linearity in the LVDT response, the LVDTs are calibrated against a micrometer rig through a procedure producing a polynomial calibration curve of third order. This gives very good sensor linearity, and it is the PC control program that does the linearisation. The measuring system has a resolution of about  $1\mu\text{m}$  over the whole LVDT stroke length.



The control program reads deformation data from the SPIDER8 amplifiers and force signals from the MTS controllers at a rate of minimum 200Hz. For a number of load cycles, the PC computes the maximum and minimum signal values for each sensor by a regression procedure. Regression over five load cycles has been used for the tests reported in Chapter 5, apart from the first few seconds where only two cycles have been used for regression to enable faster computation. This regression procedure calculate sinus functions that approximates the actual signals the best through a least square fit. The program further averages the calculated deformation signals to compute strain values for axial and radial directions, and combines them with the stresses to compute Young's moduli and Poisson's ratios (the latter two are not stored at the PC's hard disk, but only displayed at the screen during testing). The maximum and minimum values from these regression curves, the strain being the average, are the ones that are reported in Chapter 5 and Appendix D as the results of the tests. Regression values from each sensor are however stored at the PC's hard disk to enable later verification of proper sensor function. The interval for which data are stored varies from about 10 to 20 cycles. It is also possible at up to 10 times for each load step to save the sensor signals as they are read by the system, i.e. in a non-processed form.

## 4.4 Specifications for ballast material

The emphasis is put on the Norwegian requirements as these are the one applicable for the material tested. Some of the requirements from other parts of the world are described.

### 4.4.1 Norwegian specifications

According to The Norwegian National Rail Administration (Norw. *Jernbaneverket*, abbr. JBV) the ballast material delivered should comply with the specifications put forward in /44/. The overall functional requirements state that the ballast should

- ◆ have sufficient bearing capacity
- ◆ drain water
- ◆ be clean (i.e. be free from contaminants and fine grained material)
- ◆ ensure a suitable and uniform resilience along the track

In Norway the railway network is divided into 5 priorities according to the number of passengers and the freight tonnage, but this division do not reflect in the ballast requirements. Only one quality is asked for, but a smaller sized grading is allowed at yards.

Crushed rock with a nominal grading of 25 to 63 mm is used as ballast material. Up to 10% by weight of the material may be less than 25 mm, and up to 10% of the material may be between 63 and 73 mm of size. 73 mm is the maximum size. Not more than 0.5% of the material should be less than 1.6 mm. The resulting gradation limit curves are shown in Figure 4.2.

A Los Angeles test is performed for determining the resistance against abrasion and impact. 5 kg of sample of one of the three fractions 25-32 mm, 32-40 mm or 40-50 mm<sup>1</sup> is placed in a Los Angeles testing machine with a charge of 12 steel spheres each weighing approx. 440 g. The machine rotates its total load for 500 revolutions. The percentage material crushed to less than

---

1. Only the fraction 32-40 mm is tested at routine controls, according to /45/.

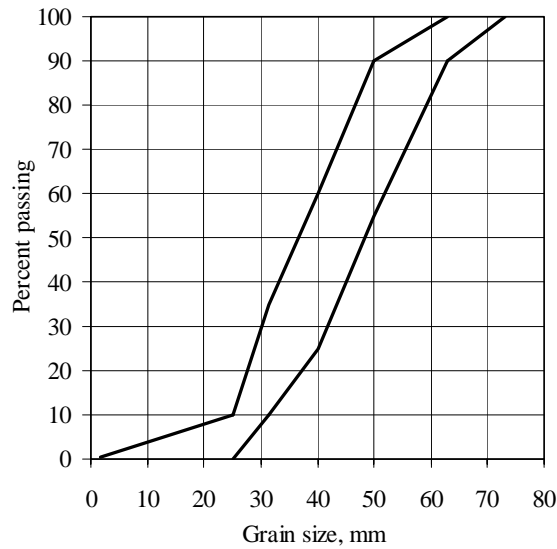


**Figure 4.2:** Gradation limit curves for Norwegian railway ballast.

2 mm is reported as the Los Angeles value. The ballast fulfils the requirements if the LA-value plots in the 'Good' or 'Very good' sectors of the diagram in Figure 4.3.

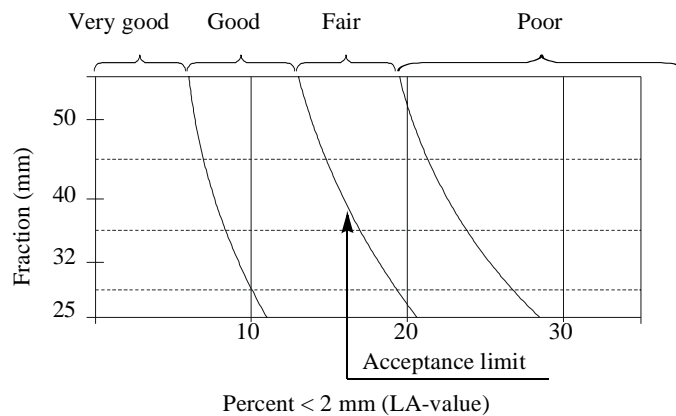


**Figure 4.3:** Classification diagram for LA-values according to JBV (translated and slightly changed from /44/).

The requirement for particle shape is that the material should be as cubical as possible. A test where 100 particles are picked at random and classified as cubical, flat or elongated is performed. Here, a flat particle is defined as being more than twice as wide as it is thick, whereas an elongated particle is said to be more than twice as long as it is wide. The number of particles in each category is counted and the percentages calculated and plotted as a single point in a diagram as the one in Figure 4.4. The particle shape of the material is accepted if at least 65% of the particles are cubical.

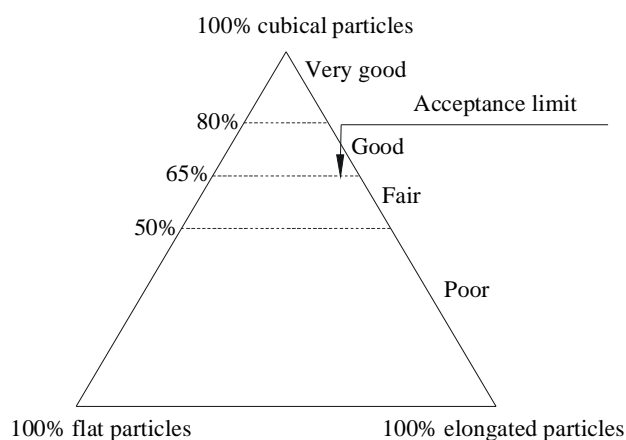


**Figure 4.4:** Classification diagram for particle shape according to JBV (translated and slightly changed from /44/).

#### 4.4.2 Ballast specifications of some other railway administrations

**Sweden /85/.** Banverket, the Swedish railway track authorities, owns most of the railway network in Sweden and is also responsible for the Swedish ballast requirements. The requirements are not dependent upon the annual tonnage, but a separate quality, class 2 ballast, may be used on yard areas. Class 1 ballast, used on most of the railway network, has a nominal grading of 32-63 mm. At most 4% by weight may be finer than 31.5 mm, while at most 10% may be between 63 and 80 mm, the latter being the maximum size. Class 2 ballast for yards has a nominal gradation of 11-32 mm. Regarding mechanical properties, Banverket prescribes impact values (according to Swedish FAS Method 210) and Los Angeles values (according to ASTM C535, but with some deviations).

**Finland /85/.** Also in Finland the state owns most of the railway network through VR Track, a part of the VR Group. VR has divided the railway network into four different categories dependent upon annual tonnage and number of passengers. The ballast requirements for mechanical properties are relative to the classification of the specific line, while the gradation requirements are not. The gradation has the nominal size 32-64 mm. From the limit curves given in /85/ it seems that 70 mm is the maximum size and that up to 15% by weight of the material may be retained on the 64 mm sieve. Also, up to 7% of the material may pass the 32 mm sieve with 1 mm as a lower limit. The mechanical properties are tested with a Los Angeles-like test and with an impact test, but the test procedures are not the same as in Sweden. For both tests there are given different limit values that correspond to the line category.

**CEN /8/.** The European Committee for Standardisation (CEN) has proposed a European standard for railway aggregates /8/. This standardisation proposal suggests five gradings where three of them have nominal sizes 32-50 mm and the remaining two have 32-63 mm. For all gradings maximum 3% is allowed to be finer than 22.4 mm. Also, more than 50% of the material shall be within 32-50 mm (for one grading the upper limit is 63 mm). When plotted it is seen that the five gradations are quite similar, and one gradation (designated E in /8/) contains the other four as subsets. Additional limits on fines content may be imposed. The standard opens up for specifying the particle shape by using flakiness index, shape index and the particle length. When it comes to mechanical properties the aggregate may be tested by a modified Los Angeles test, by

a modified impact test or a modified micro-Deval test. When the present CEN proposal is approved it will also be valid for Norway.

**AREA /2/.** AREMA, former AREA (see footnote 1 on page 6), is an organisation formed by the North American railway industry. Among other tasks, AREMA submits an annually updated design and maintenance manual for the member railways, the AREMA Manual. This manual also provides detailed specification of ballast material. There are seven various gradations specified, ranging from two finer gradations primarily for yards to five more conventional coarse gradations. Gradation no. 4 is one of the frequently used coarser gradations for main lines /50/. This gradation has a maximum size of 51 mm, with maximum 10% of the material larger than 38 mm. Maximum 15% should be smaller than 19 mm, while less than 5% should be smaller than 9.5 mm. The content of fines smaller than 0.075 mm should be less than 1%. Thus, AREMA gradation no. 4 is finer than Nordic ballast gradations, but coarser AREMA gradations do exist. Also, the specifications used by the individual railway company may vary from those of AREMA. When it comes to mechanical properties the Los Angeles value according to ASTM C 535, and the degradation value limits (LA-values) ranges from 25% to 40% dependent upon parent rock type. AREMA also specify other types of tests, e.g. the Sodium Sulphate Test (ASTM C 88), Percent of Flat and/or Elongated Particles (ASTM D-4791-89).

## 4.5 Specimen preparation

The specimens tested in this study had a cylindrical shape with a diameter of 300 mm and an intended height of 600 mm, thus occupying about 42.4 dm<sup>3</sup> of volume and weighing about 75-80 kg. The ballast materials were split and the fractions used to compose gradings complying with the curves in Section 4.6.

In order to test the performance of the equipment various tests have been conducted. These include tests of compaction procedures, actuator loading, instrumentation, toughness of the membranes and other tests that are necessary to be able to run a material test with reliable accuracy. In short one may say that the present equipment and procedures originate from numerous tests, sometimes aided by calculations, but very often carried out along a 'trial and error' scheme.

### 4.5.1 Fractioning and blending

The material from the quarry was sieved into individual fractions using large quadratic sieves with side edges of 500 mm. The nominal apertures were 1.6 mm, 11.2 mm, 25 mm, 31.5 mm, 40 mm, 50 mm and 63 mm and 75 mm. To avoid clogging of the sieves not more than about 12 kg of material was sieved at once. The sieves were placed on a vibrating table, and the vibration time was about one minute. Afterwards, based on visual inspection, some of the particles were manually angled through the sieves without using force; this could apply to at most three or four particles on each sieve, and especially to flaky or elongated particles. Visual observation confirmed that the sieving procedure did not wear the material much. The fractions less than 11.2 mm and larger than 63 mm were not used in the specimens. The fractions left were blended into the predetermined gradations, see Section 4.6.

The specimens were made of six equal layers of material. To ensure a uniform gradation all the layers have been blended according to the specified gradation. From each layer two medium

sized and cubical stones were selected as instrumentation stones. The instrumentation would later be glued to these stones, and a smooth face of each stone was marked.

#### 4.5.2 Compaction of specimens

In the literature several methods of compaction are described. Hoff /34/ presents some of the most common methods, and his tabulated examples are reproduced below in Table 4.2.

**Table 4.2:** *Compaction methods utilised in the preparation of triaxial specimens of unbound granular materials /34/.*

Source	Specimen diameter [mm]	Method of compaction	No. of layers	Materials tested
NTNU, previously	100	Vibrating table + static load	5	Natural gravel
NTNU, Hoff /34/	150	Gyrator	1	Gravel, crushed rock
SHRP standard	150	Hand held pneumatic hammer	Vary	
Recommended by the SCIENCE project	150	Static load + vibration of mould	1	Gravel, crushed rock
Pappin and Boyce, Nottingham, UK	150	Vibrating table	7	Gravel, crushed rock
Technical University of Tampere, Finland	300	Vibrating tamper	6	Gravel, crushed rock
Arkansas	150	Triaxial apparatus	5	
NGI, Norway	625	Vibrating hammer	8	Gravel, crushed rock

In the present study the material is compacted in a dry state, any moisture is added after the specimen is installed in the triaxial cell, see Section 4.5.6. The aggregate material is compacted in an unimpaird steel tube mould with an inner diameter of 300 mm and a height of 1000 mm. The compaction device consists of two vibrating motors mounted on top of a steel shaft with the compaction steel platen welded to the lower end. This compaction plate has the size of the full cross section of the tube, thus eliminating the need for moving the compactor around on top of each layer. Figure 4.5 shows a sketch of the compactor device. The two steering plates are screwed together and, because there are holes made in them for the shaft, they can glide vertically. When compacting, the upper steering plate will be at the top end of the mould, while the lower one will be just inside the mould preventing the shaft from moving horizontally relative to the mould. The axles of the two vibrating motors are rotating in opposite directions which cancels out the horizontal force component when the rotations are synchronised. The synchronisation takes place automatically, without any external regulation, when the motors have reached their working speed after start-up. In this way the useful vertical component becomes the sum of the two components from each motor.

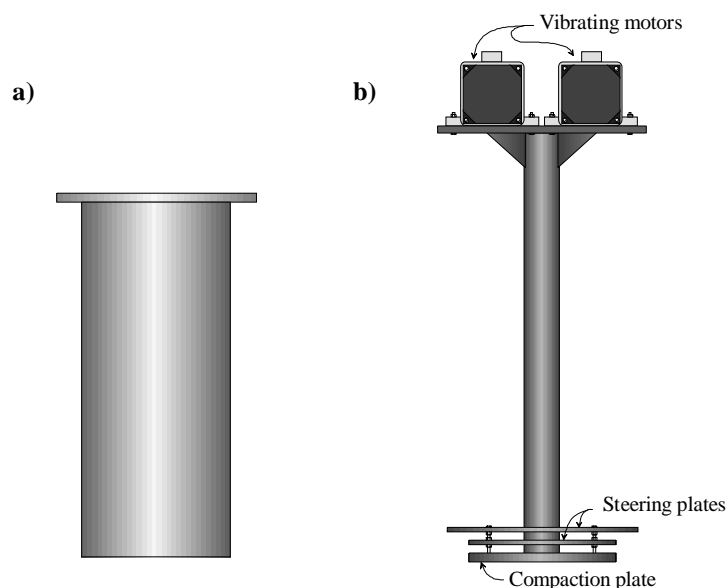


**Figure 4.5:** *Sketches of equipment for making specimens. a) The steel tube mould (300 x 1000 mm). b) The vibrating plate compactor.*

The motors of the compactor are produced by Svedala/Dynapac and have designation ER 705. In our tests we employed a maximum centripetal force of 12 kN (the combined effort of the two motors). The achievable maximum force is 32 kN. The adjustment of the centripetal force is easily done by adjusting the position of the excentric weights mounted on the motor axles. The frequency is 2870 rpm, which corresponds to about 48 Hz, and the power consumption is 1500 W each. The total mass of the compaction device is approximately 220 kg.

The material for each layer is split into two parts. The first part provides a base for the instrumentation stones, the latter being placed with the marked face outward at midlayer height. Then the second part is placed in the mould and levelled before compaction starts.

The total compaction time is 1 second per centimetre specimen height, i.e. 60 seconds for a 600 mm triaxial specimen, hence the six equally thick layers are compacted for 10 seconds each. Some crushing has been observed, but the amount is limited to about 2-3% of the stones by weight and is not considered a serious problem for good quality railway ballast. The major part of the crushing consists of splitting one particle into two pieces.

The compaction procedure and the compaction equipment used in the present study have also been described in /75/.

### 4.5.3 Instrumentation and mounting of specimens into the triaxial cell

After compaction the specimen is pushed out of the mould by a hydraulic piston, and at the same time the inner rubber membrane is pulled on at the specimen surface. Suction (pressure below the atmospheric pressure) of at least 60-70 kPa, provided by a vacuum pump, is applied inside the specimen in order to avoid collapse. This suction must be applied until the triaxial cell has been filled with water and pressurised.

After demoulding the specimen is placed in the triaxial rig for instrumentation. The membrane is punctured at the positions where the instrumentation is to be fixed to the sample, i.e. on the preplaced instrumentation stones. The holes in the membrane should not be bigger than a couple of millimetres in diameter to avoid drop in interior suction. Adhesive tape or small pieces of thin rubber membrane may be necessary as a temporary sealing of the holes. Epoxy is put into the holes and onto the stones. An epoxy 'rosette' of 20-25 mm in diameter on each instrumentation stone is aimed at. After ensuring that the epoxy is hardened and the specimen is air tight, holes equivalent to the diameter of the mounting plates, which is 15 mm, are made in the rubber membrane where the epoxy 'rosettes' were placed. The mounting plates are thereafter glued to the instrumentation stones with epoxy. The instrumentation ring, the arrangement for fixing the ring to the specimen and a detail of an LVDT with spring loaded armature are shown in Figure 4.6.

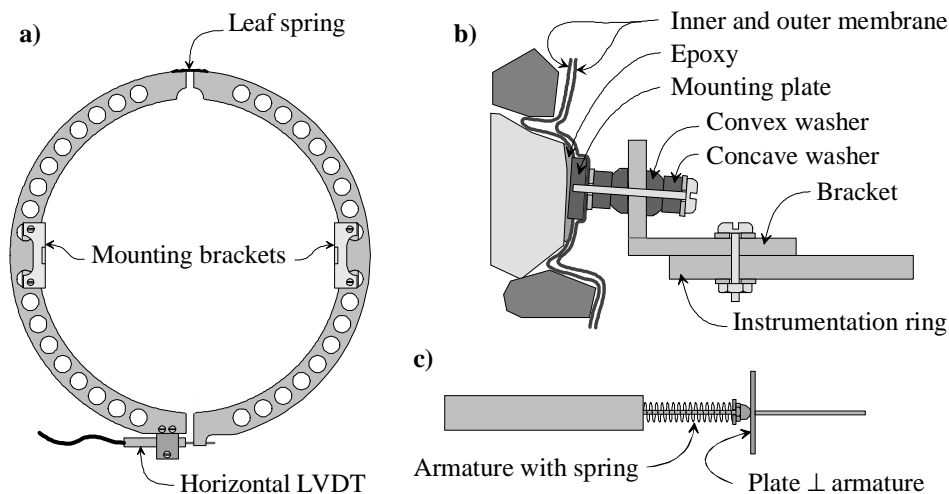


**Figure 4.6:** a) Instrumentation ring, b) arrangement for fixing the instrumentation rings to the specimen, c) LVDT with spring loaded armature.

When all the mounting plates have been fixed to the specimen a second, outer rubber membrane is placed onto the specimen to seal it properly. This membrane will cover the mounting plates, and it must be punctured at the locations of the threaded holes in the mounting plates to allow the instrumentation rings to be fastened. Leakage is avoided by pressing a washer against the rubber membrane by tightening the screw that holds the instrumentation ring in place. Then the LVDTs are mounted on the instrumentation rings and adjusted. Because of the rugged surface of the instrumentation stones and a possible tilting of them during compaction there is a need of adjusting the fastening arrangement so that the instrumentation rings remain horizontal. This has been accomplished by using convex and concave washers as in Figure 4.6 b). By loosening the brackets it is also possible to adjust the position horizontally and vertically.

Six instrumentation rings and LVDTs are used for horizontal deformation measurement. As can be seen from Figure 4.6 a) the rings use a 'caliper principle' for measuring the deformations. The heights from the bottom platen to the ring fixation points on the specimen are intended to be approx. 5 cm, 15 cm, 25 cm, 35 cm, 45 cm and 55 cm, i.e. at mid layer heights. Every other ring is turned 90 degrees horizontally so that measurements are equally taken at perpendicular diameters. The exact placing of the rings is somewhat dependent upon reliable fixing to the specimen.

The fastenings for the vertical LVDTs may now be screwed to the end platens, see Figure 4.1. The vertical rods, on which the LVDTs are to be clamped, are fastened to the bottom end platen of the specimen. If the rods were fastened to the top end platen more sideways movements of the rods and LVDTs had to be anticipated during loading (specimens A, B and C actually had this configuration). Two rods and LVDTs are used for vertical deformation measurements and they are placed at diametrically opposite sides of the specimen.

In order to adjust for any specimen tilting (central axis is out of vertical position), adjustment platens are needed between the base end platen of the specimen and the cell pedestal. It is important that the specimen is vertical so that deviatoric force is applied at the centre of the top end platen. The fully instrumented specimen is shown in Figure 4.7 b).

Finally the chamber is filled with water and pressurised. The specimen is no longer dependent on internal suction. The work involved in material processing, specimen making and instrumentation will normally take about three working days for one person.

#### 4.5.4 Discussion of the selected instrumentation concept

The particular choice of instrumentation concept results from several preliminary tests and has proven to work satisfactorily in the present study but is not claimed to be *the optimal solution*. Generally, experience from Hoff /34/ and results described by Gaaljord /26/ showed that instrumentation with LVDTs is reliable in triaxial testing of unbound granular materials.

**Avoiding membrane effects.** Hoff /34/ used three rings and LVDTs mounted on the central third of the specimen for horizontal deformation measurements and two LVDTs mounted between the two outer rings for vertical deformation measurements. The rings were clamped to the specimen by spring load, with curved plates on the outside of the membranes as the only part in contact with the specimen. Any deformation of the membranes during testing will then be included in the measurements. However, Hoff used constant cell pressure during his tests so the deformation of the membranes was of no significance. For the new triaxial apparatus, where cyclic confining pressure is also applied, it was evident that the instrumentation had to be placed on the material itself and not on the outside of the membranes.

The choice of gluing the instrumentation directly to the stones was taken in favour of using studs embedded in the material, which has been done for finer graded material /26/. The reason for this was mostly practical as it was considered difficult for the open graded ballast material to keep any studs in place without adding some binding material (cement or equivalent) at the intended spots. Also, the use of any added material was regarded unfavourable for the material that should be tested. This method of fixing the instrumentation directly to individual particles is probably a new way of instrumenting triaxial specimens. Gluing the instrumentation to the outer membrane is however quite common /26/.

**Horizontal deformation measurements.** It was decided to use six rings for this new triaxial apparatus. This is mainly due to the nature of the material tested. Railway ballast is considerably coarser than the materials tested by Hoff and this challenged us with the problem of representativity of the deformation measurements. Certainly, one measurement of the deformation between two diametrically opposite particles cannot be taken as representative of the total deformation. But with more measurements the average deformation will be closer to the correct one. Also, if something should happen to one or more LVDTs during testing it is reassuring to have a certain degree of redundancy. In Hoff's research /34/ the curved plates that fixed the



rings to the specimen embraced more particles and a single measurement thus represented more material particles.

The trade off with six hoops is that some of the measurements are taken nearer to the ends of the specimen than is usually recommended, as the two nearest are located 5 cm from the ends. This implies that any end effects will be more pronounced for this kind of instrumentation than for central third instrumentation. However, we do believe that the adverse effect of doing this is small, particularly when the repeated stresses are not close to a failure load.

The use of string-of-wheels for horizontal deformation measurements, as reported by Lekarp /54/, was not considered appropriate because of the rugged surface of the specimens, see Figure 4.7.

**Vertical deformation measurements and the problem of particle rotation.** Measuring the vertical deformation over the whole height of the specimen, as in the present study, is not the recommended practise either. However, trials with on-sample instrumentation over the mid third did produce quite scattered results for the vertical deformations. Occasionally the deformation signal from one or more sensors was 180 degrees out of phase with the deviatoric load, something that normally indicates erroneous sensor definition in the data capture program. An alternative explanation is that the specimen is elongated when the deviatoric stress is compressive, something which normally gives no sense. It was nevertheless found that the sensors functioned properly but the reason for the strange results was *resilient particle rotation*. The mechanism behind the particle rotation is probably the varying stiffnesses of the supportive contacts, in addition to the positions of the support points relative to the axis of the applied force on the stone. As a result the instrumentation stones tilted when they were subjected to repeated loads.

With a small mirror fixed to the mounting plate at the instrumentation stone, and a laser beam, the angle was possible to measure. The rotation of one of the instrumentation stones was measured to be in the order of 0.1-0.2 degrees about a horizontal axis parallel to the circumference at about 200 kPa of repeated deviator stress and 90 kPa of confining stress. A preliminary conclusion for constant confining stress is that the vertical measurements suffered the most from this phenomenon. Also, the problem is probably more pronounced when the specimen, including the instrumentation stones, consists of large particles because the rotary arm out to the LVDT is longer.

The conclusion of the investigation was that it was better to measure deformations over the full specimen height, taking the risk of any end effects, than to try on-specimen instrumentation with very scattered results. Another argument is that it is desirable with a long measurement basis when the material is as coarse as the railway ballast material.

**The choice of measuring principle for the LVDTs.** As shown in Figure 4.6 c) the armature is spring loaded so that it exerts a small force on the plate mounted on the other half of the instrumentation ring. Hence there is no moment transferred through the contact point. Any lateral force transferred is frictional and is thus some fraction of the normal force at the point of contact. If the spring is not too stiff the normal force will be small and consequently the frictional or lateral force will be small. To grease the contact point will also be beneficial. With this type of arrangement the locking of LVDTs during testing is avoided, which is beneficial for the resilient deformation measurements. Also, any initial locking is easily avoided by only tapping the instrumentation ring gently. Then the armature and the LVDT automatically adjust to a released position. This type of connection has also the advantage of a short construction length.

One major problem with this type is the difficulties of keeping the plate, against which the armature is pressed, perpendicular at all times. If the armature moves relative to the plate, and the plate is not perpendicular to the armature, then the permanent deformation recorded will be somewhat erroneous. However, the elastic deformation in repeated tests should not suffer too much from this.

Alternative arrangements for the LVDTs have been considered /75/ but the present principle was found to perform the best. The main problem of the alternatives was that they were able to transfer moment, thus having a higher tendency of locking the LVDTs.

**The weight of the on-sample instrumentation.** The total mass of the on-sample instrumentation, which is the instrumentation for horizontal deformation, is about 2400 g excluding the LVDT cables. Roughly 30% of the weight is compensated for by buoyancy when the cell chamber is filled with water. Because the LVDTs are heavier than the leaf springs on the other side of the rings, there are some unbalanced weights. Therefore the LVDT cables have been tied to vertical rods placed inside the cell, thus relieving most of the unbalanced weights. The instrumentation weight that is left over to the specimen to bear should not in any case cause any significant errors as these loads are very small compared to the load applied during testing. This conclusion holds even if one considers the forces on the instrumentation stones alone: Assume that a force equivalent to the weight of 1500 g is born by the specimen. This equals 125 g or 1.23 N per instrumentation stone. A small instrumentation stone has a mass of about  $(3.0 \text{ cm})^3 \cdot 3.0 \text{ g/cm}^3$  which equals approximately 80 g, the equivalent weight being 0.78 N. The minimum stress applied to the specimen is 20 kPa, which for an instrumentation stone with a face area of  $9.0 \text{ cm}^2 (= 3.0 \cdot 3.0 \text{ cm}^2)$  is equivalent to a force of about 18 N. Even with these unfavourable assumptions the external force and the weight of the stone is about 15 times greater than the weight applied by the instrumentation.

In some cases, due to movements during compaction, the instrumentation stones may not be very well embedded in the rest of the material. In such cases the weight of the instrumentation may influence somewhat on the measurements. Because of this it is important that the instrumentation stones are supported and embedded properly when placed during specimen making.

#### 4.5.5 Membranes and sealing

The selection of reliable membranes and of proper sealing is of outmost importance as a major water leakage into the specimen will make it collapse. The particular choice for membranes and sealing in the present study is a result of several preliminary trial-and-error tests.

Initially 1 mm latex membranes from Polymer Dipping Center (PDC), Sweden, were used. These were perfectly adequate for well graded materials with no large voids and were also used for the first two specimen in the test series, specimen A and B, see Table 4.5. Figure 4.7 a) shows specimen A covered with a 1 mm latex membrane as the inner one. Note the stretch over some of the voids. Unfortunately, these membranes punctured so for the rest of the test series (specimen C-G) 2 mm membranes in para rubber was used. These latter membranes were made of sheets of para rubber that were butt glued to the required cylindrical shape and with a rubber band glued on top of the joint as reinforcement. The para rubber membranes performed well with no major leakages.

A third type of membrane was also tested, a 2 mm latex membrane from PDC, but was not used in the test series reported here. The approximate strengths of the membranes for repeated load

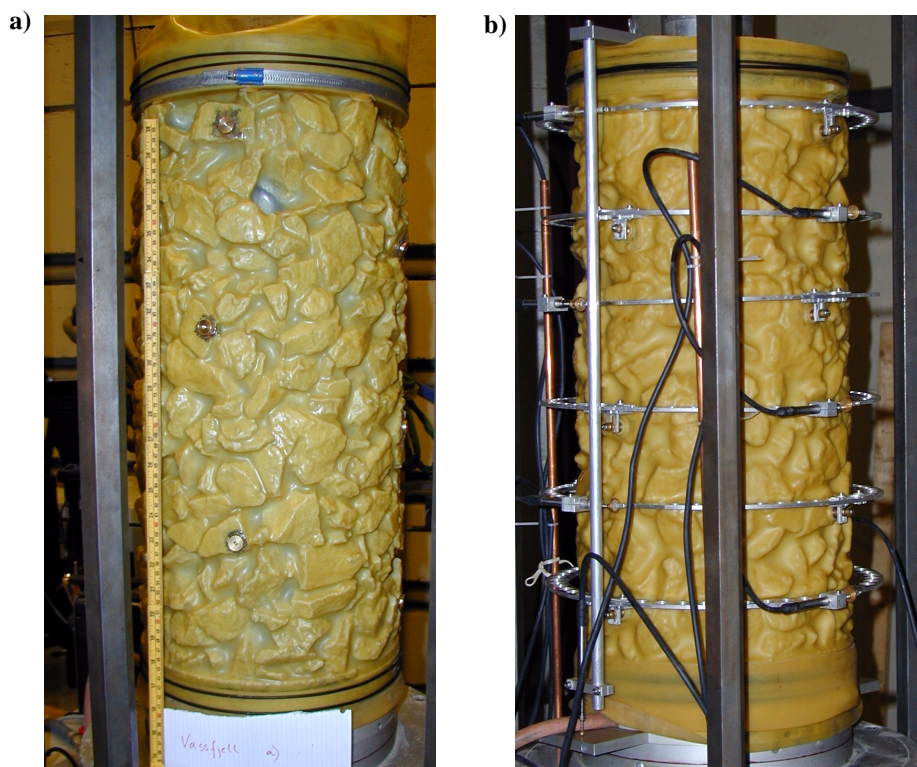


**Figure 4.7:** a) Specimen covered with 1 mm latex as an inner membrane; mounting plates are glued to the instrumentation stones. b) Outer membrane and instrumentation fixed to the specimen.

triaxial testing of railway ballast as experienced during preparatory testing are given in Table 4.3.

**Table 4.3:** Approximate strengths of some membrane types valid for repeated load triaxial testing of railway ballast complying with Norwegian grading specifications. The cell pressure is repeated.

Type of membrane	1 mm latex	2 mm latex	2 mm para rubber
Failure cell pressure [kPa]	110	230	270

For finer and more well graded material the values of Table 4.3 are not valid. For such materials the membranes do not need to bridge large voids and can thus withstand considerably higher cell pressure before failure.

To seal the membranes to the end platens one or two rubber o-rings and one hose clamp were used at each platen for each membrane. For the outer membrane the hose-clamp for the base end platen should be fastened below the o-ring for the inner membrane, while the hose clamp for the top end platen should be fastened above the inner o-ring. The hose clamp on the base end platen for the inner membrane is fastened in the beginning of the demoulding process and it is important that this hose clamp is well tightened so that the membrane stays in place.

As the inner membrane one may reuse an outer membrane from a previous test if there are no big holes in it. The small holes from the screws that fasten the instrumentation rings to the mounting plates can be sufficiently sealed by small sheets of thin rubber attached to the membrane by grease. A complete airtight inner membrane is in fact not ideal, as this would prevent the outer membrane from adhering to the inner one. The outer membrane must be new and unimpaired when placed on the specimen.

#### 4.5.6 Adding moisture to the specimens

In the present study moisture has been applied to some of the specimens after their installation into the triaxial rig with a confining stress applied. It was felt that the compaction effect could be different if the water was added prior to compaction. Also, more crushing could probably be expected. The wetting of the specimens was done by entering water through the inlet in the base end platen normally used for the vacuum pump. A hole in the top end platen connected with a tube to the outside of the cell allowed the air to escape when the water entered the specimen. It was important to allow the water to enter slowly, otherwise pressure buildup might have caused the specimen to collapse. When water flooded through the tube attached to the top end platen the water supply was closed. For the tests conducted in the present study the intention was only to moisturise the material to the natural retention capacity, consequently the specimens were drained after flooding. Small amounts of fines were carried out by the draining water. The moisture content was not measured but is believed to be below 1% for such uniform and coarse grained materials as railway ballast.

### 4.6 Materials tested in the present study

Seven specimens were made and tested in the present study. They have designations A to G in the following. Specimen no. D was tested twice, first in a dry state then in a wet state.

#### 4.6.1 Parent material

The material used in the present study is designated Vassfjell and is taken from a quarry situated some 15 km southeast of the town centre of Trondheim, Norway. The parent rock type is gabbro with a serpentine content; the colour is greyish to light green. The quarry produces the railway ballast in a two stage crushing process. The material used in the present study was delivered from the quarry in December 1997. The grading of the delivered material was slightly to the coarse side of the limit curves for Norwegian railway ballast.

The material has the properties as described in Table 4.4. The Los Angeles values are obtained by using the procedures described in Section 4.4.1, while the particle density is obtained by a method specified by Norwegian road authorities (method 14.422) /76/. The particle shape was found by a slightly different method than the one described in Section 4.4.1: Instead of choosing 100 random particles, a sample of 10 kg complying with the JBV gradation was analysed. When evaluating the particle shape result in table Table 4.4, bear in mind that the method used will emphasise the shape of the smaller particles as these outnumber the larger ones in a representative sample. The values of Table 4.4 comply with the requirements stated in Section 4.4.1, and the material may therefore be used as railway ballast in Norway.

**Table 4.4:** *Los Angeles values, particle shape and specific density of the material used.*

Los Angeles value (two samples)	Particle shape % flat, elongated and cubical particles	Specific density [g/cm <sup>3</sup> ]
11.4 10.1	20, 3.8, 76	3.02

#### 4.6.2 Material meeting the requirements

Five specimens, i.e. specimens A-E, were made with a gradation fulfilling the requirements for railway ballast specified for the Norwegian railway network. These requirements are given in Section 4.4. The gradation for these specimens is given in Figure 4.8. The target mass of specimens A and B was 72 kg, while for specimens B-E it was 75 kg.

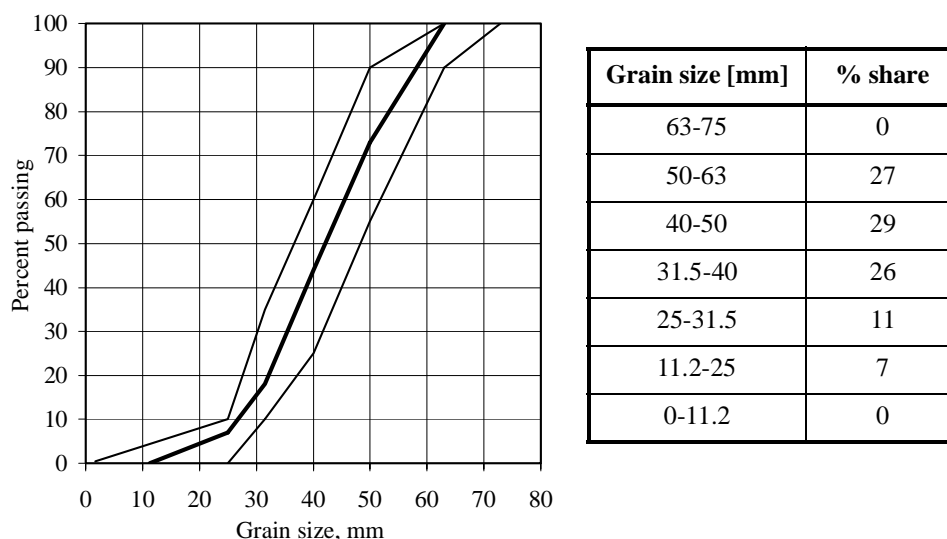


**Figure 4.8:** *The grain size distribution for the material tested that complied with the requirements, indicated by the thick line. Thin lines indicate the limit curves. Data for the gradation is also given in the table to the right.*

#### 4.6.3 Material with increased amount of smaller grains

Two specimens, i.e. specimens F and G, were made with a gradation with an increased amount of smaller grains than allowed by the requirements for railway ballast specified for the Norwegian railway network. The gradation for these specimens is given in Figure 4.9. The target mass of these specimens were 78 kg.

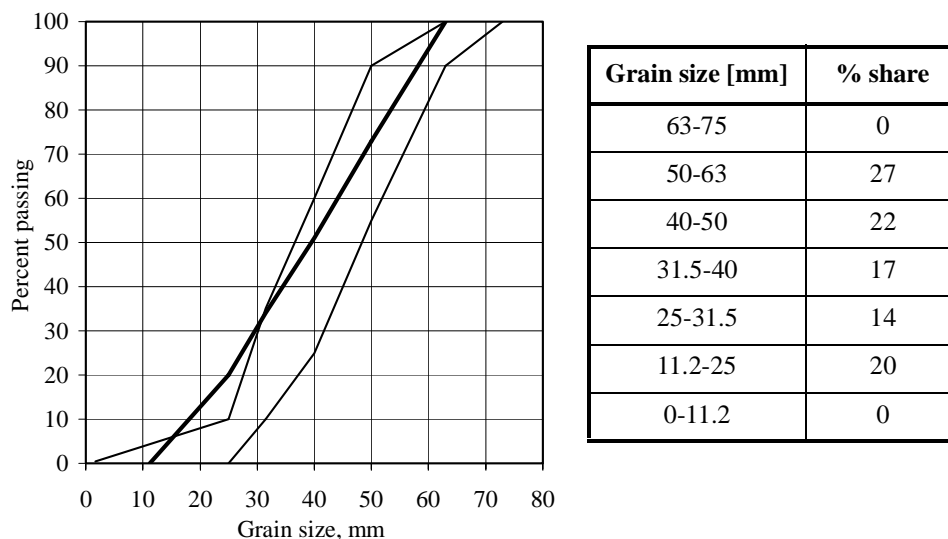


**Figure 4.9:** *The grain size distribution for the material tested that had a higher content of smaller grains, indicated by the thick line. Thin lines indicate the limit curves. Data for the gradation is also given in the table to the right.*

#### 4.6.4 Moisture content

Moisture was added to specimens E-G before loading and also to specimen D after a load series when the specimen was dry. There are two reasons why moisture was added to some of the specimens. First, it was felt that a moist state of the ballast is more critical to the ballast behaviour, and this is also a state frequently encountered especially in the western and northern parts of Norway. It is known that the parent rock is weaker when the micro cracks are filled with water. Tests have shown a reduction of roughly 30%, but strength reductions up to 50% have also been measured /63/. Second, it is valuable to compare the behaviour of the dry ballast with the moist ballast. Since the specimens were drained after flooding, refer to the procedure described in Section 4.5.6, the moisture content is that of a natural retention capacity for the ballast material. The amount of moisture retained was not measured but is believed to be less than 1%.

When the material is only moist or partially saturated, suction comes into play. For partially saturated sand it is known that the shear strength is higher than for a dry sand. This is the effect experienced on a sandy beach where the dry sand feels looser than the wetted one. Kolisoja /51/ reports on studies done by others that the strengthening effect is also valid for coarse and open graded materials up to 10 mm of particle size. But for the tests on the ballast like materials he included in his own research, there was no evident strength change due to any moisture content.

### 4.6.5 Summary of specimen data

A summary of the specimen data is given below in Table 4.5.

**Table 4.5:** *Summary of specimen data.*

Specimen no.	Dry mass [kg]	Initial height [mm]	Bulk density [kg/dm <sup>3</sup> ]	Grading	Moisture	Membrane
A	72.0	579	1.76	JBV	Dry	1 mm latex
B	72.0	574	1.77	JBV	Dry	1 mm latex
C	75.0	610	1.74	JBV	Dry	2 mm para rubber
D dry	75.0	596	1.78	JBV	Dry	2 mm para rubber
D wet	75.0	596 <sup>a</sup>	1.78	JBV	Moist	2 mm para rubber
E	75.0	602	1.76	JBV	Moist	2 mm para rubber
F	78.0	605	1.82	Denser	Moist	2 mm para rubber
G	78.0	612	1.80	Denser	Moist	2 mm para rubber

a. Not measured; value for D dry given.

## 4.7 Triaxial testing procedures found in the literature

### 4.7.1 Introduction

For conventional triaxial testing there are many stress paths that may be followed. One way of dividing the various stress paths is whether confining stress is constant or variable. Another and even more fundamental categorising is whether the deviatoric stress is negative or positive. In the case of negative deviatoric stresses the deviatoric load system has to be made for tensional loads. In the present study both variable and constant confining stress tests have been performed, all of which with a zero or positive deviatoric load.

When dealing with repeated triaxial testing it is customary to use the deviator stress  $q$  or  $\sigma_d$  defined by

$$q = \sigma_d = \sigma_1 - \sigma_3 \quad (4.1)$$

and the mean stress  $p$  defined by

$$p = \frac{1}{3} \cdot (\sigma_1 + 2 \cdot \sigma_3) \quad (4.2)$$

where  $\sigma_1$  and  $\sigma_3$  is the major and minor principal stresses, respectively.  $p$ - $q$  plots are often used to represent the stress paths. The stress paths are characterised by their starting and ending

points in stress space, e.g. a  $q$ - $p$ -space. In variable confining stress tests one may in addition refer to the various paths by their  $q/p$  ratio, or, more correctly, to their  $\Delta q/\Delta p$  ratio. For brevity, the term  $q/p$  ratio may be used in the following instead of the  $\Delta q/\Delta p$  ratio.

#### 4.7.2 Procedures found in the literature

To the knowledge of the author, no internationally accepted standard exists that describes the testing procedure for a railway ballast aggregate in a triaxial apparatus. However, there do exist triaxial testing standards for quarry aggregates of smaller size, and some of the features in these standards may be adopted even for railway ballast.

**prEN 00227413**, a draft for a European standard, describes cyclic load triaxial tests for unbound and hydraulic bound mixtures for roads /9/. The proposal describes procedures for both constant confining stress, limited to materials with maximum particle size of 63 mm, and variable confining stress, limited to materials with maximum particle size of 31.5 mm.

For the variable confining stress tests a conditioning of 20 000-100 000 cycles is first specified. Here,  $\sigma_1 = 0$ -600 kPa and  $\sigma_3 = 0$ -100 kPa, thus the  $q/p$  ratio is 2.0. Alternatively  $\sigma_3 = 10$ -110 kPa for weaker specimens.

The resilient testing is performed for  $q/p$  ratios/maximum deviatoric loads (units of kPa) of 0.5/150, 1.5/600, 2.0/600 and 2.5/300. The deviatoric load is increased in steps until the maximum load for each path is reached. First a series with  $\sigma_3 = 0$  is performed, then a series with  $\sigma_3 = 10$  kPa. For each load step the strains must stabilise before the recordings are taken (at cycles 90 to 100 after stabilisation). The two series with slightly differing confining pressures are actually very close and it may be pertinent to ask whether any differences in material behaviour is due to the load difference. More likely the stress-strain history effect will cause such differences.

For permanent strain testing a separate specimen has to be made. One of the abovementioned stress paths is run for 80 000 cycles.

For the constant confining stress tests the different stress paths are created by increasing  $\sigma_3$  in steps of 10 kPa. The confining pressures/top deviatoric loads are (units of kPa) 10/70, 20/140, 30/210, 40/280. For each  $\sigma_3$  the repeated deviatoric loads are increased step by step until the top load is reached. The recordings are taken for the last 10 cycles after strain stabilisation. Also these loading paths are quite close to each other and stress-strain history effects may overshadow the stress difference effect. There are no procedure specified for the permanent stress behaviour for constant confining stress.

A revised version of the prEN has recently been worked out. The details are not known to the author.

**SHRP Protocol P46 /77/**. This procedure is valid for unbound materials below 37.5 mm of particle size. The protocol differentiates between subgrade soils and base/subbase materials. The description herein is limited to base/subbase materials as the stresses are higher and more relevant even for ballast materials. All the stress paths have a constant confining stress, and the load pulses are haversine shaped with a duration of 0.1 sec. with a 0.9 rest period. First a conditioning of 500-1000 cycles is applied. Here the constant + cyclic deviatoric load is equivalent to 10.3 + 93.1 kPa, while the confining stress is kept at 103.4 kPa. The testing then begins; the confining pressures/top deviatoric loads are (units of kPa) 20.7/62.1, 34.5/103.4, 68.9/206.8, 103.4/206.8



and 137.9/275.8. The deviatoric load is increased in steps until the maximum load for each path is reached. 100 cycles is performed for each load step and the resilient deformation is the average deformation for these cycles. The permanent strain is recorded after the resilient test sequence, and permanent strain testing is not specified. If possible, a rapid shear test is performed on the specimen after the resilient testing is performed.

The load paths of the P46 are more distant to each other than in the prEN proposal and may therefore cover a broader range of stress states. Also, the present test is not so susceptible to stress-strain history effects.

NGI /86/ reports on a procedure used for coarse materials with specimens of 625 mm of diameter and 1250 mm of height. Partial internal vacuum was used as an equivalent confining pressure of 80 kPa. 1000 haversine cycles with a load pulse duration of 0.1 sec and a resting period of 0.9 sec. were performed for each load step. The lowest deviatoric load is 40 kPa and is increased in steps of 20 kPa or 40 kPa (the latter used for some of the specimens) until a maximum deviatoric load of 600 kPa or a permanent axial strain of 2.5% was reached.

## 4.8 Triaxial testing procedure used in this study

### 4.8.1 The objectives and outlines of the testing

First it may be pertinent to state the main objectives of the laboratory investigations. These may be summarised in the following points:

- (1) To test the feasibility of testing ballast materials in the triaxial apparatus developed.
- (2) If possible, to find material properties of the Vassfjell railway ballast:
  - ◆ To establish the possible range of the ratios between  $\sigma_3$  and  $\sigma_1$
  - ◆ Determine the elastic properties
  - ◆ Determine the permanent or plastic properties

The latter item must be viewed relative to the two material parameters *gradation* and *moisture* as specified in Section 4.6.

The testing procedure may be outlined as follows:

- ◆ An isotropic loading which also serve as a conditioning
- ◆ Variable confining stress tests
- ◆ Constant confining stress tests
- ◆ Static load tests

The order of the bulleted list indicates the chronological order of the tests performed on each specimen. The intended loads are tabulated in Appendix C and may also be read from Figure 4.11. The actual applied loads may be read from the curves in Appendix D.

### 4.8.2 A discussion of stresses for variable confining stress tests

To establish the possible range of the ratios between  $\sigma_3$  and  $\sigma_1$  imply that the testing must adopt a procedure that is able to state whether a certain ratio between these principal stresses is possible without failure or other stress-strain states that cannot be achieved in a real structure. Herein, a constant stress ratio will be adopted for each loading step, which more specifically implies that the repeated stresses are varied *in phase* and *proportionally*. Proportional loading implies that the stress paths can be extended through the origin in a stress space.

Why is this stress ratio important? The answer is obvious when considering a three dimensional stress state: Normally, all the principal stresses will change if the material element is loaded. For a linear elastic material, not necessarily granular, this do not apply when the material has a Poisson's ratio equal to zero and when the material element is not constrained in one or two directions orthogonal to the load. In the latter case the material element will be subjected to larger strains in the unconstrained directions.

To conclude, if the conventional triaxial cell should simulate the stress regime in a granular layer one may assume that

$$\sigma'_3 = \sigma'_{30} + K \cdot \Delta\sigma'_1 \quad (4.3)$$

where

$$\begin{aligned} \sigma'_3 &= \text{minor principal effective stress after loading} \\ \sigma'_{30} &= \text{minor principal effective stress prior to loading} \\ K &= \text{principal stress ratio} \\ \Delta\sigma'_1 &= \text{major principal effective stress increment after loading} \end{aligned}$$

The definition of  $K$  is

$$K = \frac{\Delta\sigma'_3}{\Delta\sigma'_1} \quad (4.4)$$

where

$$\Delta\sigma'_3 = \text{minor principal effective stress increment after loading}$$

Hereafter the primes (') are omitted, as the stresses considered are always the effective ones.

The possible values of  $K$  can be determined through triaxial tests. But it may be useful to use some physical argument to limit the values that  $K$  may attain. Assuming a non-softening behaviour, a negative  $K$  is not physically meaningful as an *increase* in  $\sigma_1$  leads to a *decrease* in  $\sigma_3$ . The case in which  $K$  is zero corresponds to a constant confining stress test as the applied confining stress ( $\sigma_3$ ) does not vary with the applied major principal stress ( $\sigma_1$ ). If  $K$  equals 1.0 the stress increase is isotropic since the stress increase is equal in all directions. A  $K$  bigger than 1.0 implies that we are performing some sort of extension test. Depending upon the value of  $K$  and the values of  $\sigma_{10}$  and  $\sigma_{30}$  this may lead to a swap of the principal directions. The conclusion is that for a conventional triaxial compression test the  $K$ -value is between 0 and 1.0.

The  $q/p$  ratio may be expressed in terms of  $K$ :

$$\frac{\Delta q}{\Delta p} = \frac{3(1 - K)}{1 + 2K} \quad (4.5)$$

The inverse is

$$K = \frac{3 - \frac{\Delta q}{\Delta p}}{2 \frac{\Delta q}{\Delta p} + 3} \quad (4.6)$$

Using these formulas, a range of  $K$  from 1 to 0 corresponds to a  $\Delta q/\Delta p$  range of 0 to 3. The relation between  $K$  and  $\Delta q/\Delta p$  is illustrated in Figure 4.10.

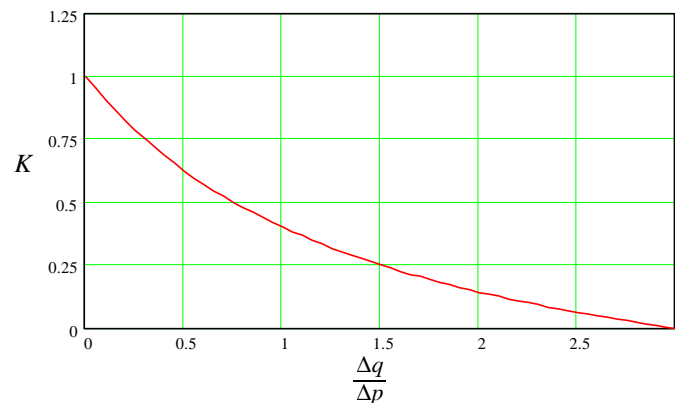


**Figure 4.10:** *The relation between  $K$  and  $\Delta q/\Delta p$ .*

As can be seen from Figure 4.10 the curve is steepest near the isotropic end. This justifies somewhat smaller  $q/p$  increments for  $K$  near 1.0 than elsewhere in order to cover a broad range of stress states with few tests. Initially the  $q/p$  ratios were chosen to be 0.0, 0.3, 0.7, 1.2, 1.8 and 2.2. The last  $q/p$  ratio was chosen also on the basis of the low minimum confining stress. Based on the test results for specimen D, which was the first to reach a complete load series, it was also decided to test for  $q/p$  ratios of 1.5 and 2.0. The reason for introducing these additional load paths was that a failure state approached when the  $q/p$  ratio was around 1.8 so that a  $q/p$  ratio of 2.2 was possibly not achievable for all specimens.

### 4.8.3 The stresses used in the test

Reference is made to Appendix C for the intended stresses used. The stresses appear in chronological order. Appendix D shows the actual applied loads.

The minimum confining pressure was set to 20 kPa at the middle of the specimen for two major reasons:

- (1) The specimen should experience sufficient confining stress to prevent it from falling apart.
- (2) The variation in confining stress should not be too big over the height of the specimen.

Considering the latter item, it is seen that when the specimen height is 600 mm the confining water pressure is 6 kPa higher (approx. 35%) at the base of the specimen than at the top. This

difference will of course diminish when the confining stress is increased during a load cycle. Some of the loading paths have higher confining stresses.

The stress paths used are shown in a  $p$ - $q$  plot in Figure 4.11. 10 000 continuous haversine pulses (no rest period) have been applied for each load step for all the repeated loading stress paths unless failure required the test to be stopped. Failure was defined as 0.25% permanent vertical strain for one complete stress path.

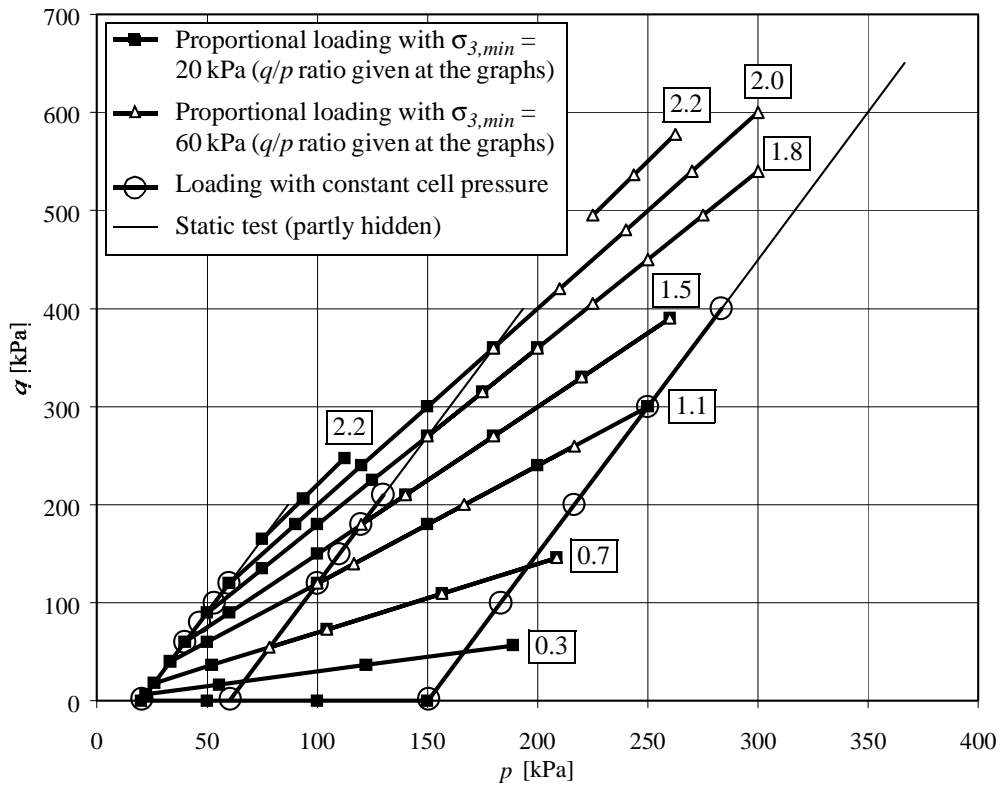


**Figure 4.11:** Stress paths used for triaxial testing.

If all the stress paths of Figure 4.11 is to be applied to one specimen the test run will take about 10-12 working days. Some instants of remoisturing the specimen to ensure that it is moist at all time are included, and so are a few events of draining the cell and removing the cell chamber to adjust instrumentation etc. Included 2-3 days of specimen making the total time spent for one specimen is about 15 working days.



---

## CHAPTER 5 Results and discussion of results from triaxial testing

---

### 5.1 Introduction

The test series described in Section 4.6 is limited and it is not possible to draw conclusions on all the aspects of the Vassfjell ballast behaviour. However, indications on the behaviour of the material may be obtained, and the graphs of the following pages illustrate some important characteristics of the behaviour of the Vassfjell railway ballast. Even so, more tests are necessary to map the behaviour of this material in order to obtain a more complete prediction of its behaviour in a railway track.

The obtained triaxial test results show that the triaxial equipment is well suited for testing railway ballast. This was also one of the objectives with the tests as mentioned in Section 4.8.1. Thus, a major goal of the project has been reached.

The curves from the testing, calculated as described in Section 4.3.3, are displayed in Appendix D in chronological order. These curves are the basis for the graphs displayed in Sections 5.3 and 5.4 and for the static strength parameters in Section 5.5.

### 5.2 Interpreting the test results

#### 5.2.1 Introduction

The limited number of tests does not motivate advanced modelling at this stage. Instead the resilient properties are interpreted within an isotropic linear elastic framework, while the plastic properties are displayed as permanent strains. Despite the deficiencies of linear elasticity, it is hoped that some of the characteristics of the material may be displayed. Linear elasticity is also a well known framework. For the plastic behaviour there exists no obvious framework within which the results could be interpreted. Consequently the strains are displayed as they are measured.

Generally speaking the Young's modulus and the Poisson's ratio from triaxial tests will be secant values calculated on the basis on two stress states, namely the minimum and maximum stresses during a load cycle. This is illustrated in Figure 5.1. When the load differences are big, i.e. for the last load steps in a loading path, the values for the elastic parameters will cover many stress states. Testing with a broader variety of minimum stress states would therefore be beneficial for the accuracy, but more tests would then have to be carried out.

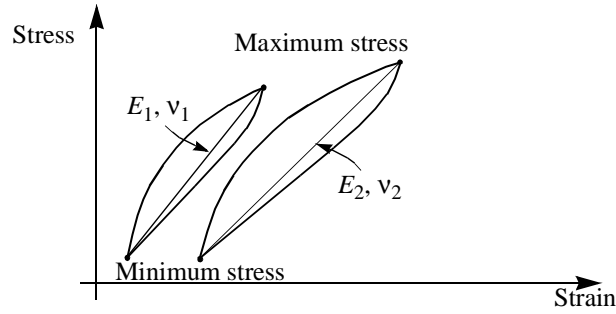


**Figure 5.1:** *The elastic parameters interpreted as secant values.*

### 5.2.2 Expressions for Young's modulus and Poisson's ratio

When the results from the triaxial testing are to be explained by a linear elastic behaviour, expressions for Young's modulus and Poisson's ratio are needed. Their simplest definitions are given in terms of a uniaxial test, but for a three dimensional stress state their values have to be calculated on the basis of the generalised Hooke's relation, i.e. Eqn. (3.2) and (3.5) on page 63. In triaxial testing for highway engineering purposes the Young's modulus,  $E$ , is normally referred to as the resilient modulus,  $M_r$  (conf. Section 3.4.3), in order to be a reminder of any non-linear (stress dependent) behaviour.

Fortunately, in constant confining pressure (CCP) tests, the definitions of these parameters are identical with the ones in the uniaxial case:

$$M_r = \frac{\Delta\sigma_d}{\epsilon_1^e} \quad (5.1)$$

$$\nu = -\frac{\epsilon_3^e}{\epsilon_1^e} \quad (5.2)$$

Where  $\Delta\sigma_d$  is the change in deviator stress during one load cycle.

In variable confining pressure (VCP) tests, however, one has to take the 3D stress-strain state into consideration:

$$M_r = \frac{(\Delta\sigma_1 - \Delta\sigma_3)(\Delta\sigma_1 + 2\Delta\sigma_3)}{(\Delta\sigma_1 + \Delta\sigma_3) \cdot \epsilon_1^e - 2\Delta\sigma_3 \cdot \epsilon_3^e} = \frac{3\Delta q \Delta p}{3\Delta p \epsilon_1^e - \Delta\sigma_3 \epsilon_v^e} \quad (5.3)$$

$$\nu = \frac{\Delta\sigma_3 \cdot \epsilon_1^e - \Delta\sigma_1 \cdot \epsilon_3^e}{(\Delta\sigma_1 + \Delta\sigma_3) \cdot \epsilon_1^e - 2\Delta\sigma_3 \cdot \epsilon_3^e} = \frac{\Delta\sigma_3 \epsilon_d^e - \Delta q \epsilon_3^e}{3\Delta p \epsilon_1^e - \Delta\sigma_3 \epsilon_v^e} \quad (5.4)$$

where  $\epsilon_d^e$  is the direct deviatoric strain,  $\epsilon_d^e = \epsilon_1^e - \epsilon_3^e$

The first parts of the Equations (5.3) and (5.4) have also been reported by Lekarp et al. /55/.

An alternative is to calculate the bulk modulus,  $K$ , and the shear modulus,  $G$ , according to the following formulas valid for conventional triaxial testing:

$$K = \frac{\sigma_m}{\varepsilon_v} = \frac{E}{3(1-2\nu)} \quad (5.5)$$

$$G = \frac{\sigma_1 - \sigma_3}{2(\varepsilon_1 - \varepsilon_3)} = \frac{E}{2(1+\nu)} \quad (5.6)$$

Young's modulus,  $E$ , and Poisson's ratio,  $\nu$ , may then be solved for by using Equations (3.19) and (3.20) on page 66.

### 5.2.3 From sensor signals to elastic and plastic parameters

As explained in Section 4.3.3 the signal of each sensor is transformed to maximum and minimum values through a regression procedure. The details of this are found in the same section. This procedure always leaves the repeated part positive, as the repeated part is the difference between the maximum and minimum values. The minimum part is for strains the permanent part. This concept is shown in Figure 5.2.

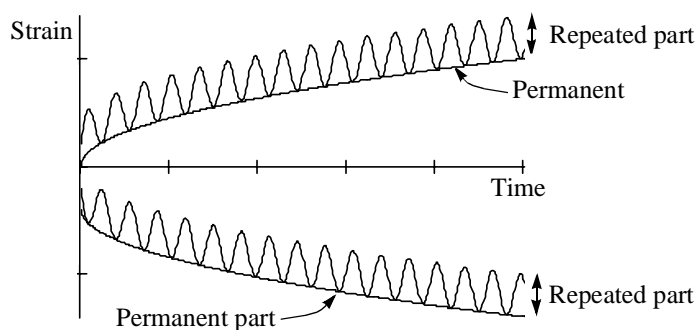


**Figure 5.2:** *The definition of repeated part and permanent part of the processed sensor signals.*

To decide whether the resilient  $\varepsilon_3$  is 180 degrees out of phase with the resilient  $\varepsilon_1$  one has to look into the logged sensor signals for individual cycles. Unfortunately the deformation signals were not logged properly. It seems that the calculated sinusoidal deformation signals have been written to the files instead. It is therefore not possible to judge from the data when the resilient  $\varepsilon_3$  is reversed compared with  $\varepsilon_1$ . For the constant confining stress tests the sign of  $\varepsilon_3$  has been reversed manually in the logging files, as a positive compressive strain is physically unlikely when the deviator is at a maximum. For the variable confining stress tests with a  $q/p$  ratio equal to 1.5 or more, the  $\varepsilon_3$  may also have been reversed for some load steps but this is not possible to verify. No sign corrections have therefore been made for these  $q/p$  ratios.

As a first step to adjust the data the recordings from any malfunctioning LVDTs are removed. The only cause of malfunctioning which is considered to justify this data correction is when the armature has ejected from the coil. Any LVDT locking is however included in the data set, as it is impossible to differ locking from a correct zero strain measurement.



The following steps are then taken to calculate Young's modulus and Poisson's ratio:

- (1) The processed stress values (only one sensor each) and the average of the strain values, adjusted for any malfunctioning LVDTs, are the basis for the calculations (these values are displayed in Appendix D).
- (2) From the stresses and strains in item (1) the values of Young's modulus and Poisson's ratio are calculated using the equations in Section 5.2.2. Values of  $K$  and  $G$  are calculated first and from them the  $E$  and  $\nu$  are calculated.
- (3) The values representing the load step are taken as the median values of the Young's modulus and Poisson's ratio calculated in item (2).
- (4) Occasionally the median value is not defined because one of the values in the domain is a division by zero. This happens when  $\epsilon_v = 0$  and when  $\epsilon_1 - \epsilon_3 = 0$ . Then the undefined values are substituted by dummy values. The resulting median value is then inserted as dummy values in an iterative process. The convergence is usually fast.

Using the median values in favour of the average values in item (3) above is an effective way of filtering extreme values that are not physically possible, results from numerical noise or results from temporarily instrumentation malfunctioning.

The following steps describes the calculation of the permanent strain for each load step:

- (1) A zero level for the load step is calculated in either of two ways: a) If the load step starts a load sequence, the logging immediately before 10 seconds after start is taken as the zero level. In this case there is partial vacuum inside the specimen that must allow draining out. This is of course a debatable practise, but the reason is to avoid including permanent strains that are due to the release of the internal vacuum in the specimen. b) The last recorded permanent strain from the previous load step.
- (2) The permanent strain for the current load step is the last recorded permanent strain in the load step minus the zero level strain from item (1).

The partial vacuum mentioned in item (1) above is a precaution to avoid distortion of the specimen in the beginning of the loading when the loads are ramping up to the correct level. This ramping is not necessarily smooth for the deviator stress and the confining stress.

Values of  $E$  and  $\nu$  have not been calculated for all diagrams and load steps shown in Appendix D, but only for those with intended loads and with repeated load steps that have some duration. The display of permanent strains has been even more restricted as these strains require an almost completed load step to be valid.

#### 5.2.4 Uncertainties in results because of the testing procedure

The main reasons for uncertain results caused by the testing procedures can be tracked down to the following factors (quantities with least assumed accuracy in parentheses):

- ◆ Removal of internal suction at the beginning of the first load step (permanent strains).
- ◆ Not completing the load step because of excessive permanent axial strains (permanent strains).
- ◆ Disturbance of the specimen causing excessive deformation, e.g. when accidentally no confinement was applied to the specimen (both resilient and permanent strains are affected). Some of these disturbances have been reported in Appendix D.

### 5.3 Results from the variable confining stress tests

The results displayed herein also include the isotropic stress tests (Figure 5.3 below).

The error bars in the diagrams for Young's modulus and Poisson's ratio show the statistical 10th percentile and the 90th percentile.

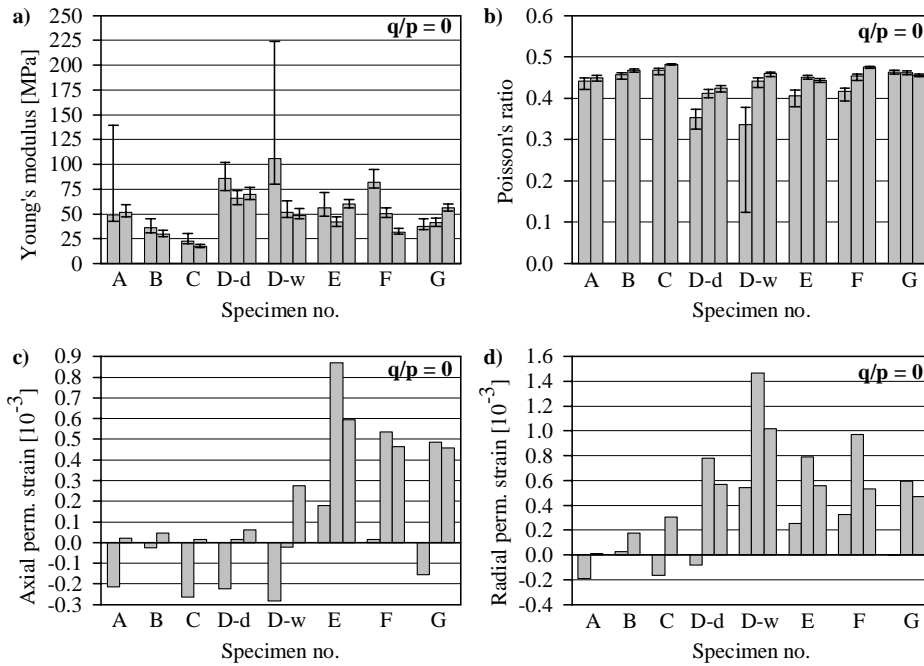


**Figure 5.3:**  $q/p = 0$ . a) Young's moduli, b) Poisson's ratios, c) axial permanent strain per load step, d) radial permanent strain per load step. For specimens A and B the repeated confining stress was 85 kPa for the second load step, while it was 100 kPa for the other specimens.

From Figure 5.3 it is seen that:

- ◆ The Young's modulus is smaller for specimens A, B and C. The results show some scatter and no trends with regard to the test variables are seen. The value of the Young's modulus is about 50 kPa.
- ◆ The Poisson's ratio is similar for all specimens and with a high value of about 0.45.
- ◆ Since only the bulk modulus is defined for isotropic loading if the material is isotropic the values of Young's modulus and Poisson's ratio should not be possible to calculate. The results therefore show that the material is anisotropic.
- ◆ Both permanent strains are higher for specimens E, F and G than for the others. Specimen D wet should be similar in properties as specimen E apart from that D wet have been tested previously in a dry state.

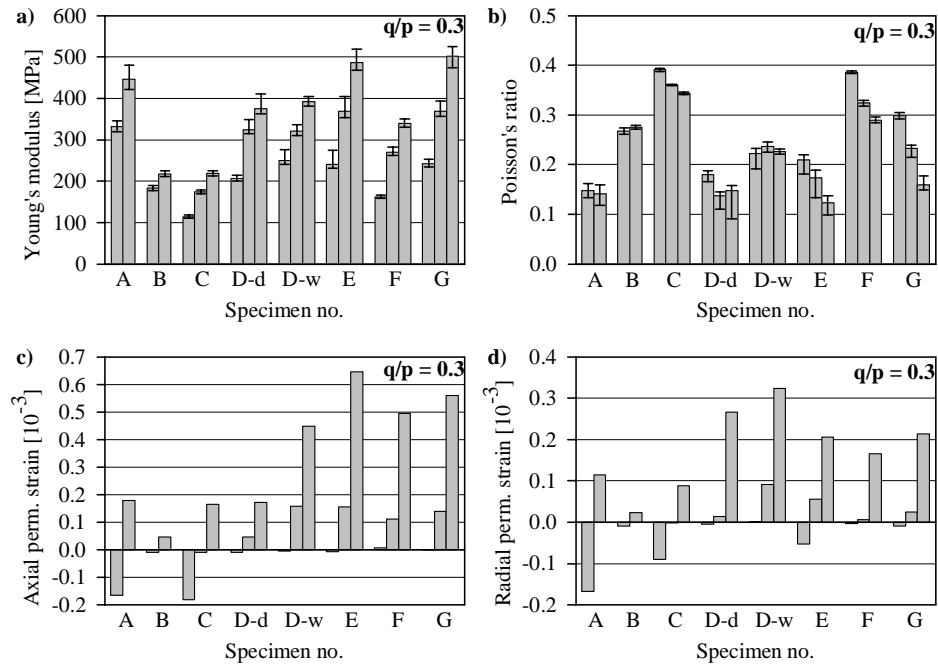


**Figure 5.4:**  $q/p = 0.3$ . a) Young's moduli, b) Poisson's ratios, c) axial permanent strain per load step, d) radial permanent strain per load step.

From Figure 5.4 it is seen that:

- ◆ Young's modulus is considerably higher than for the isotropic tests, around 400 kPa. Also, the modulus increases with increasing load steps. Some scatter in the results, especially specimen B and C show lower moduli.
- ◆ Poisson's ratio is quite scattered, but when removing specimens B and C a trend of lower Poisson's ratios for open graded materials is indicated. A trend of decreasing values with increasing loads is indicated. The values are lower than for the isotropic test.
- ◆ Axial and radial permanent strains are higher for the moisturised specimens than for the dry ones. The radial permanent strain is still mainly compressive, indicating that the load step is mainly isotropic.

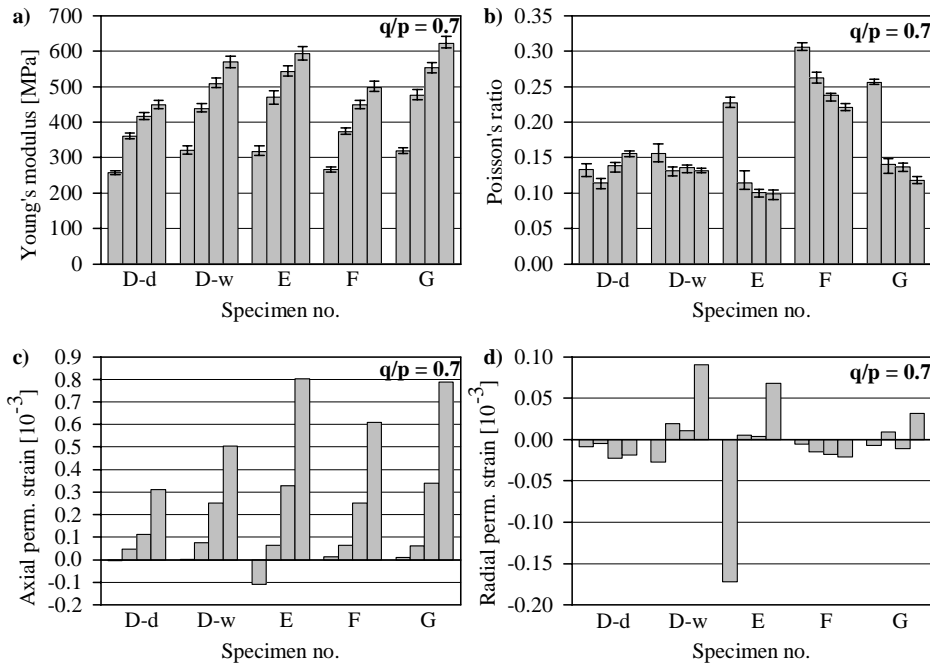


**Figure 5.5:**  $q/p = 0.7$ . a) Young's moduli, b) Poisson's ratios, c) axial permanent strain per load step, d) radial permanent strain per load step.

From Figure 5.5 it is seen that:

- ◆ Similar Young's moduli for all specimens, the value for the dry specimen is being somewhat smaller. Increasing modulus with increasing stress. The value is a bit higher than for the previous load step.
- ◆ Poisson's ratios are somewhat higher for the denser graded specimens (F and G), and also for the first load step for specimen E. Poisson's ratios are either constant with load or decreasing, the latter being typical for specimens E, F and G. The values are lower than for the preceding  $q/p$  ratio.
- ◆ The dry specimen (D dry) seems to have smaller axial strain than the wet ones including those with denser grading.
- ◆ The horizontal permanent strains are small, thus indicating that a transformation from compressive strains to expansional strains may be taking place. Horizontal permanent strain for specimen E, first load step, seems to be larger than for the other specimens. This may be due to the procedure of subtracting some of the strains in the beginning of the first load step. Referring to Appendix D it is seen that most of the strain occurs in the beginning of the first load step.

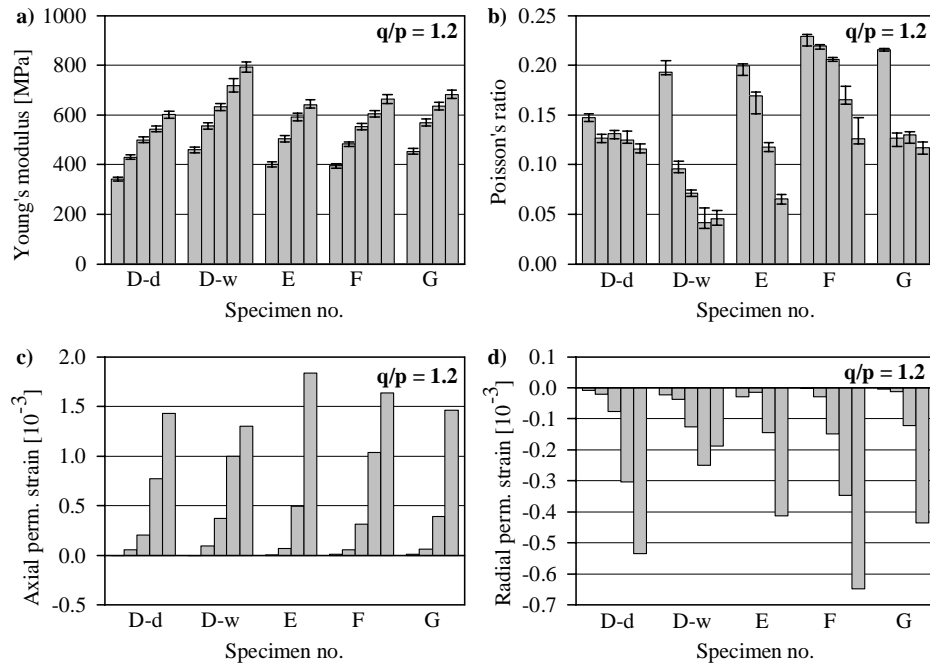


**Figure 5.6:**  $q/p = 1.2$ . a) Young's moduli, b) Poisson's ratios, c) axial permanent strain per load step, d) radial permanent strain per load step.

From Figure 5.6 it is seen that:

- ◆ Very agreeing results for the Young's modulus, specimen D wet is a little bit stiffer. Very good repeatability. Increasing moduli for increasing loads. The value is still increasing compared to the previous load step.
- ◆ The Poisson's ratio variation may perhaps be divided into three groups: a) The dry specimen displaying an almost constant ratio, b) the wet open graded specimens D wet and E displaying decreasing ratios with load, c) the wet dense graded specimens F and G are also showing decreasing ratios with increasing loads but with higher numerical values for the Poisson's ratio than for case b).
- ◆ Similar permanent axial strains for all specimens. The value is about twice the value for the preceding load step.
- ◆ Permanent radial strains are for the first time clearly expansional. Quite similar results.

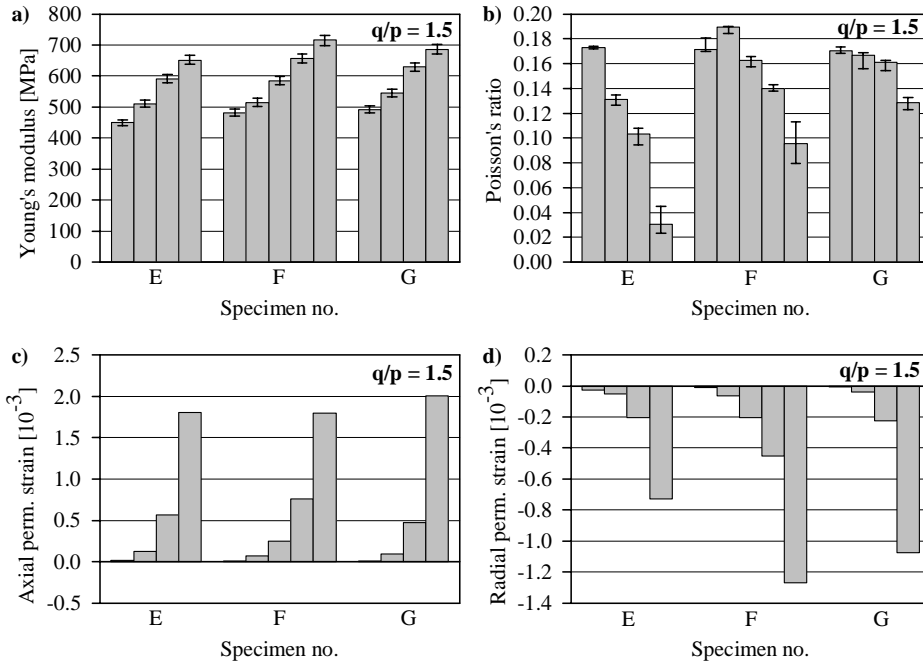


**Figure 5.7:**  $q/p = 1.5$ . a) Young's moduli, b) Poisson's ratios, c) axial permanent strain per load step, d) radial permanent strain per load step.

From Figure 5.7 it is seen that:

- ◆ The Young's modulus is again very agreeing among the specimens. The numerical value is not increasing much from the previous load step.
- ◆ The Poisson's ratios have similar values, but the values for specimen E is decreasing more rapidly.
- ◆ Similar values for both permanent strains. The radial expansional strains have approximately doubled compared to the preceding load step.

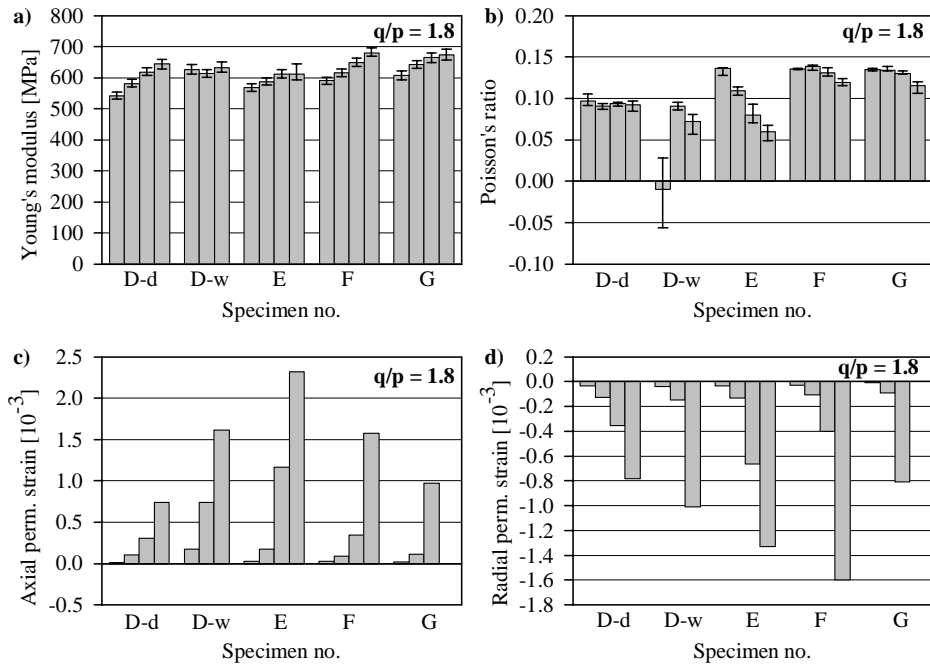


**Figure 5.8:**  $q/p = 1.8$ . a) Young's moduli, b) Poisson's ratios, c) axial permanent strain per load step, d) radial permanent strain per load step.

From Figure 5.8 it is seen that:

- ◆ Young's modulus is very agreeing for all the specimens. The value is about the same as for the previous load step, but the tendency of increasing modulus with increasing stress is now diminishing.
- ◆ The Poisson's ratio is a little bit less for specimens E, F and G than for the previous  $q/p$  ratio, but else with the same pattern. The Poisson's ratio for specimen D wet, for the first load step, is negative and with wide variation. This is due to the near zero values in denominator in the expression for calculating Poisson's ratio.
- ◆ The axial permanent strain is biggest for the wetted specimens. Note that the latter load step for specimen G has been interrupted so early that no permanent axial and radial strains are given.

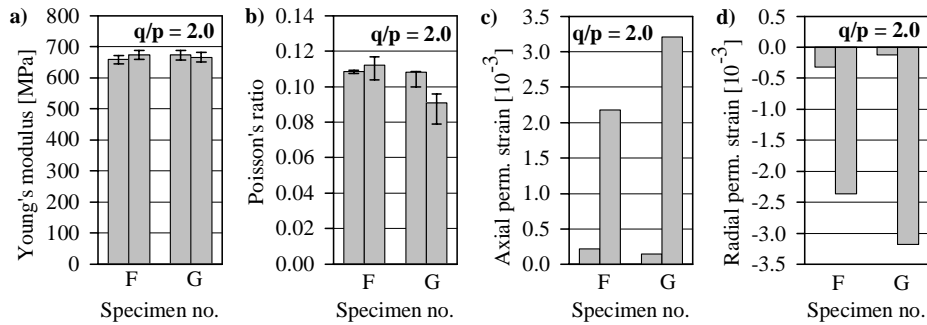


**Figure 5.9:**  $q/p = 1.8$ . a) Young's moduli, b) Poisson's ratios, c) axial permanent strain per load step, d) radial permanent strain per load step.

From Figure 5.9 it is seen that:

- ◆ Specimens F and G are the only ones that have been tested with  $q/p = 2.0$ , but the strength of the specimens D dry, D wet and E from testing with  $q/p = 1.8$  could also justify testing with  $q/p = 2.0$  as the testing with  $q/p = 2.2$  was not successful.
- ◆ The Young's modulus is almost identical for the two specimens, and it is also similar to the modulus for the previous load step. It does not increase with load any more.
- ◆ The Poisson's ratio agrees well too, and is a bit smaller than the one from the previous step.
- ◆ The permanent strains show that the specimens are approaching failure as only two load steps could be performed. The variation in permanent strain from one load level to the other seems to have little effect on the resilient properties.



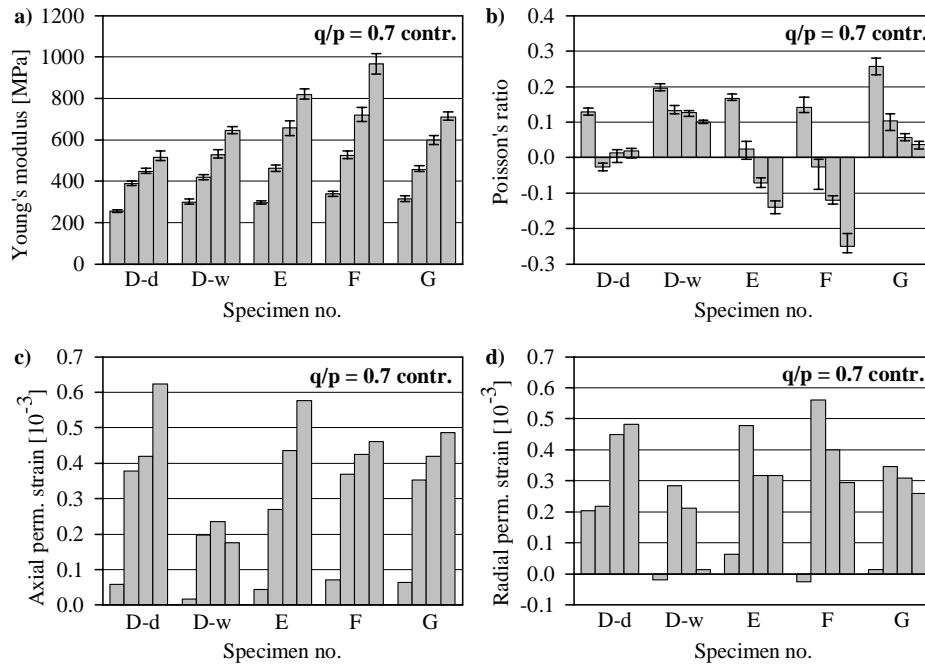


**Figure 5.10:**  $q/p = 0.7$  control step. a) Young's moduli, b) Poisson's ratios, c) axial permanent strain per load step, d) radial permanent strain per load step.

From Figure 5.10 it is seen that:

- ◆ The Young's modulus has increased somewhat compared to the first time the same  $q/p$  ratio was applied.
- ◆ For the Poisson's ratio the results for the control path is more scattered than for the first loading.
- ◆ The permanent axial strains seem to have a stabilising tendency at larger load steps for the control loading.
- ◆ The permanent radial strains are clearly compressive for the control run, while they were around zero for the first run.
- ◆ All in all, the changes since the first run with  $q/p = 0.7$  shows that a stress-strain history effect is present.

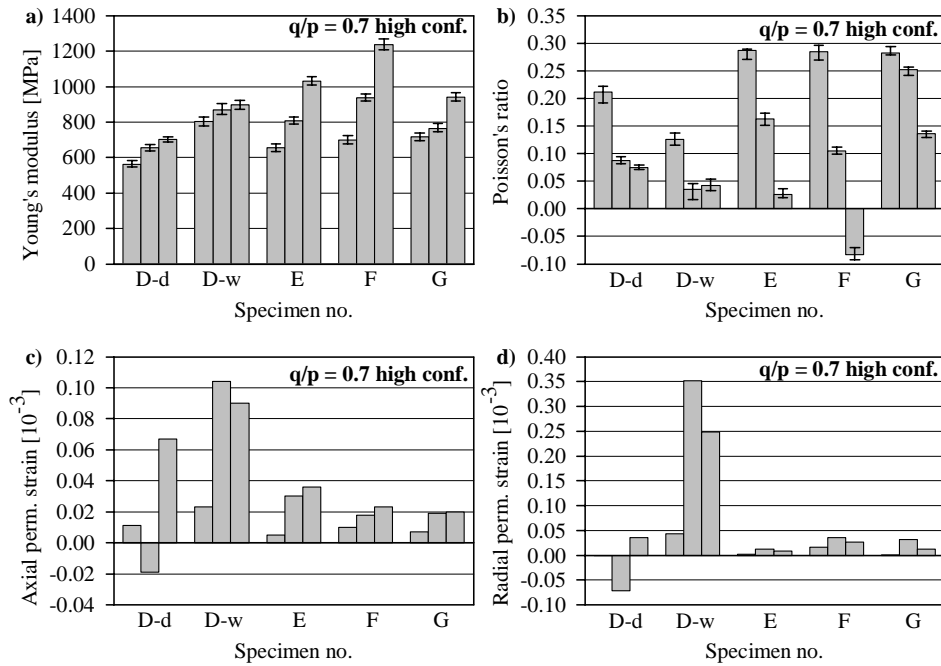


**Figure 5.11:**  $q/p = 0.7$  with high confining stress. a) Young's moduli, b) Poisson's ratios, c) axial permanent strain per load step, d) radial permanent strain per load step.

From Figure 5.11 it is seen that:

- ◆ The Young's modulus increase compared to the same  $q/p$  ratio with lower confining stress.
- ◆ Poisson's ratio almost stays constant at the level from the previous load step.
- ◆ The permanent strains are small compared to the preceding loading.

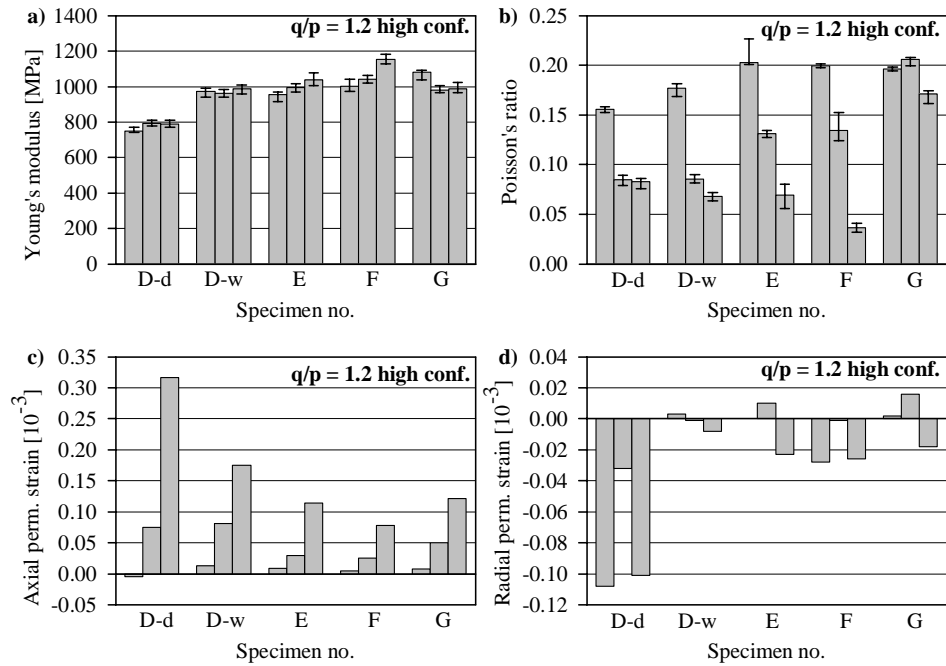


**Figure 5.12:**  $q/p = 1.2$  with high confining stress. a) Young's moduli, b) Poisson's ratios, c) axial permanent strain per load step, d) radial permanent strain per load step.

From Figure 5.12 it is seen that:

- ◆ The Young's modulus is almost doubled compared to the run with lower confining stress. Also, the modulus does not increase with load.
- ◆ The Poisson's ratio is comparable with the one from the run with lower confining stress.
- ◆ The permanent strains are lower. Almost no radial permanent strain occurs.

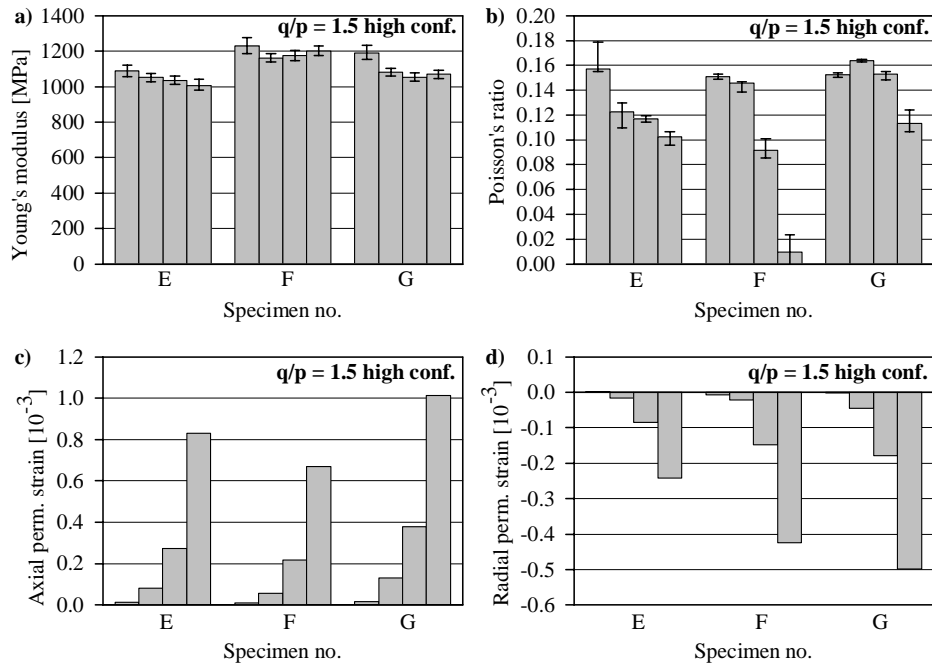


**Figure 5.13:**  $q/p = 1.5$  with high confining stress. a) Young's moduli, b) Poisson's ratios, c) axial permanent strain per load step, d) radial permanent strain per load step.

From Figure 5.13 it is seen that:

- ◆ For the resilient properties the same conclusion as for the previous loading applies.
- ◆ The permanent strains are lower than in the run with lower confining stress and same  $q/p$  ratio.

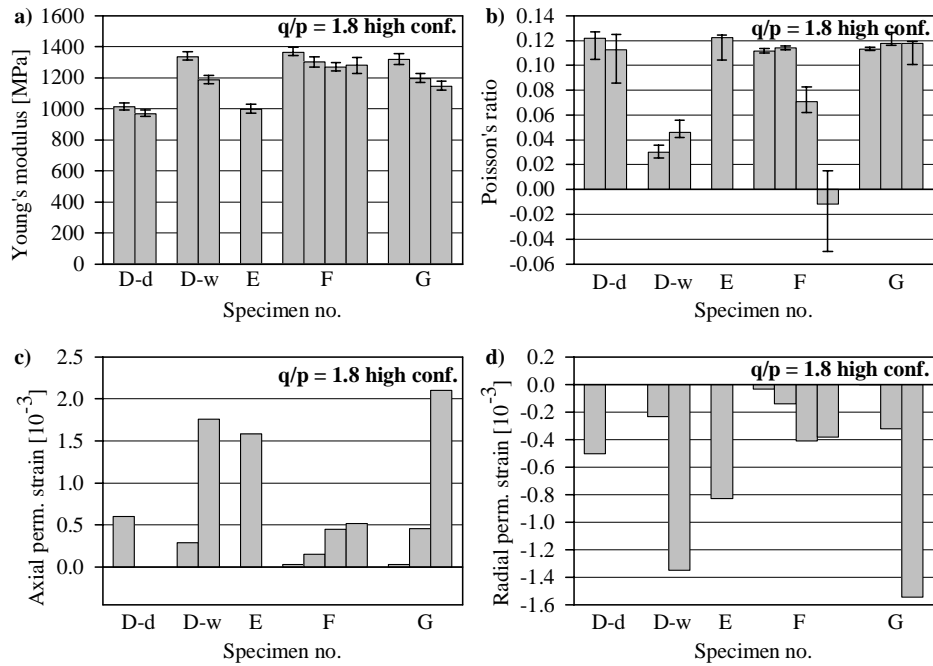


**Figure 5.14:**  $q/p = 1.8$  with high confining stress. a) Young's moduli, b) Poisson's ratios, c) axial permanent strain per load step, d) radial permanent strain per load step.

From Figure 5.14 it is seen that:

- ◆ Again, a doubling of the Young's modulus is seen when increasing the confining stress, while the Poisson's ratio is essentially the same.
- ◆ The permanent strains are of a similar magnitude as when lower confining stress.

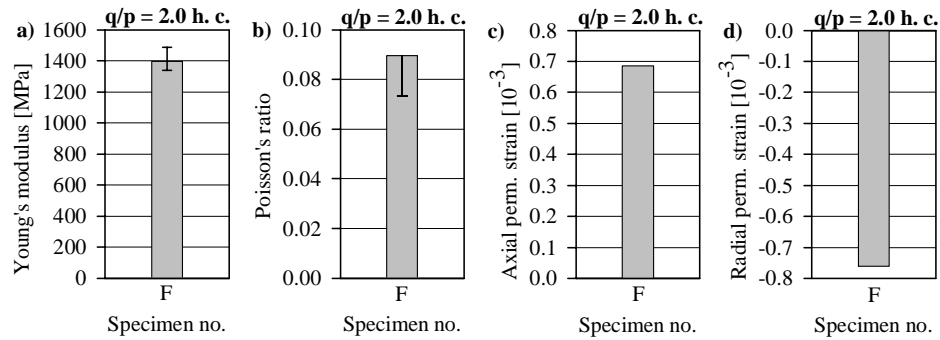


**Figure 5.15:**  $q/p = 2.0$  with high confining stress. a) Young's moduli, b) Poisson's ratios, c) axial permanent strain per load step, d) radial permanent strain per load step.

From Figure 5.15 it is seen that:

- ◆ It is difficult to make fair comparisons when there is only one specimen, but the tendency from the preceding loading seems to be valid here as well.

### 5.4 Results from the constant confining stress tests

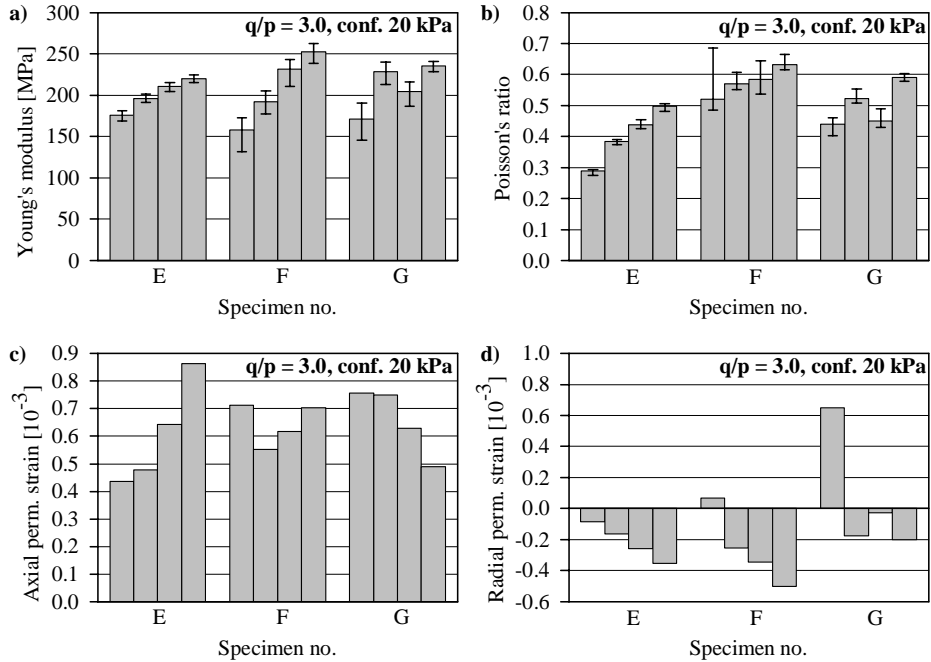


**Figure 5.16:**  $q/p = 3.0$  with confining stress of 20 kPa. a) Young's moduli, b) Poisson's ratios, c) axial permanent strain per load step, d) radial permanent strain per load step.

From Figure 5.16 it is seen that:

- ◆ The Young's modulus is agreeing between the specimens. It also increases with load. Compared to the tests with variable confining stress the modulus is lower.
- ◆ Quite agreeing results also when it comes to the Poisson's ratio. The value increases with increasing loads. Note that Poisson's ratio is above 0.5 for some load steps. This indicates expansion of the specimen.
- ◆ Also the permanent strains shows similar results among the specimens. Note that the radial strain is a bit to the expansional side.

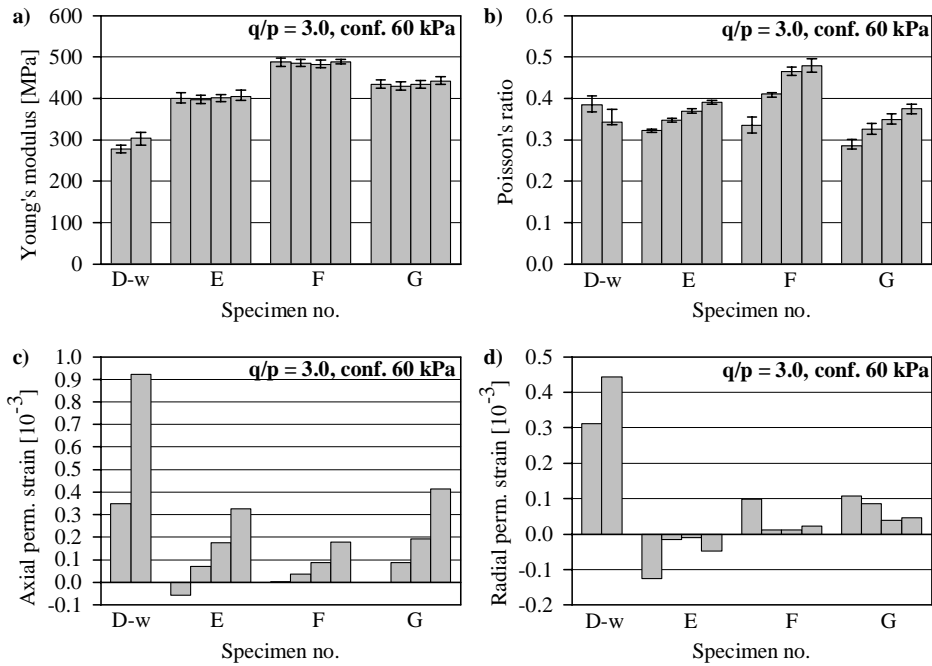


**Figure 5.17:**  $q/p = 3.0$  with confining stress of 60 kPa. a) Young's moduli, b) Poisson's ratios, c) axial permanent strain per load step, d) radial permanent strain per load step. For specimen D wet the repeated deviatoric load was 100 kPa for the first load step, while for the others it was 118 kPa.

From Figure 5.17 it is seen that:

- ◆ The Young's modulus is independent of load within the stress path. The modulus is approximately doubled compared to the preceding tests.
- ◆ The Poisson's ratio has still high values, but is below the expansion limit of 0.5. The values increase with increasing loads.
- ◆ The permanent strains are moderate.



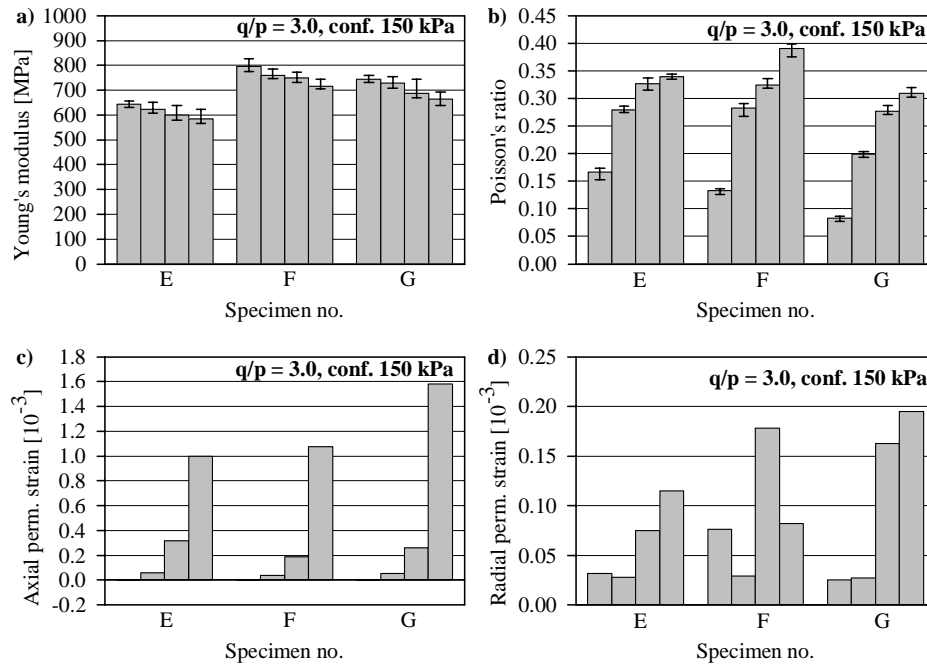


**Figure 5.18:**  $q/p = 3.0$  with confining stress of 150 kPa. a) Young's moduli, b) Poisson's ratios, c) axial permanent strain per load step, d) radial permanent strain per load step.

From Figure 5.18 it is seen that:

- ◆ The Young's modulus is increased since the previous loading path but the modulus decreases slightly with loading in the present loading path.
- ◆ The Poisson's ratio is smaller than for the previous loading path, but still increases with loading in the present loading path.
- ◆ Axial permanent strain is growing, but the radial permanent strains are moderate.

## 5.5 Results from the static tests

Static tests were performed for specimens D wet, E, F and G, see Appendix D. The tests were stress controlled and unnecessary large datafiles were created. Table 5.1 gives the results in a Mohr-Coulomb setting. The attraction  $a$  is the intercept with the normal stress axes. For some of the loadings the failure was surprisingly visible on the curves, while for other loadings a gradual evolvement towards failure was seen.

As can be seen from Table 5.1 it seems as specimens F and G have a somewhat higher strength ( $\tan\phi$ ) while the attraction is higher for specimens D wet and E. The higher shear strength for specimens F and G was expected as these have a bit higher bulk density and a broader gradation.

It is admitted, however, that the results from the static tests are somewhat dependent upon subjective judgement of where the failure occurs. Hence some uncertainty regarding these results remains.

**Table 5.1:** *Results from the static tests.*

Specimen	Confining stress [kPa]	Deviatoric stress at failure [kPa]	$\phi$ [degrees]	$\tan \phi$	Attraction $a$ [kPa]
D wet	100	490	34	0.69	88
	150	620			
E	20	235	35	0.70	74
	60	380			
	150	590			
F	20	255	40	0.85	55
	60	450			
	150	740			
G	20	235	37	0.75	62
	60	385			
	150	635			

## 5.6 Summary of test results

The indicative conclusions from the tests can be summarised as follows:

- (1) Generally the tests show that good repeatability is achieved. The equipment performs quite well and is suited for triaxial testing of railway ballast.
- (2) The tests give valuable information regarding possible stress combinations. Failure appears to occur around a  $q/p$  ratio of 1.8 to 2.0 for the tests with 20 kPa as confining stress. For 60 kPa the  $q/p$  ratio may increase to 2.0 to 2.2.
- (3) Poisson's ratio shows more scatter than Young's modulus from specimen to specimen. But within each load step the scatter is remarkably low, as shown by the error bars indicating the 10th percentile and the 90th percentile; some exceptions exist though.
- (4) The scatter of the Poisson's ratio could in some cases be interpreted as the Poisson's ratio having a greater sensitivity to the test variables than being the case for the Young's modulus.
- (5) For the VCP tests with minimum confining pressure of 20 kPa the Young's modulus increases with load within the same stress path for all  $q/p$  ratios except for  $q/p = 2.0$ . For the VCP tests with minimum confining pressure of 60 kPa the Young's modulus increases with load only for  $q/p = 0.7$ , which is the lowest  $q/p$  ratio for this minimum confining pressure.
- (6) From a variable confining stress test with 20 kPa as minimum confinement to a test with 60 kPa of confining stress the Young's modulus typically doubles.
- (7) An increase in minimum confining stress for the variable confining stress tests seem to increase the Young's modulus while the Poisson's ratio remains the same.
- (8) The presence of moisture seems to have little effect on the resilient properties. The permanent strains are slightly smaller for  $p/q$  ratios not exceeding 1.2.

- (9) Denser grading seems to increase slightly the Poisson's ratio for  $p/q$  ratios not exceeding 1.2, while the situation for Young's modulus seems to be constant. The permanent strains were not significantly changed by a denser grading. A conclusion is then that the grading should be changed more if any significant impact on the material behaviour should be measured.
- (10) For the CCP tests all the specimens were moist. No clear dependency on grading was encountered for any of the parameters analysed.
- (11) The need of a partial internal vacuum for the first load step should be eliminated.
- (12) The PC program deficiency that makes it impossible to find the real sign of the repeated radial strains must be corrected.
- (13) Static tests are in this study performed with stress control. Strain control may have been easier, and the amount of data may then have been reduced.

---

## CHAPTER 6    **Conclusions and recommendations**

---

### **6.1 Conclusions**

The main conclusions of the work done can be summarised as follows:

- (1) For the beam-on-elastic-foundation model (BOEF model) and for a simple linear beam element model a tool called dimensionless sensitivity diagrams has been developed. These diagrams are claimed to be a powerful tool to assess the impact on the track reactions when changing the track parameters. For the BOEF model the method may be used both for a single axle load and for a double axle load, while for the beam element model the method may be used for a single axle load.
- (2) A new track model has been developed where no tension is assumed between the track ladder and its foundation. The no tension property has successfully been implemented by adding compressive stresses in the uplift regions of the track ladder. Compared to the BOEF model, the predicted length of uplift is longer, the uplift deflection is bigger and the uplift begins closer to the load. The deflection of the track with this continuous no tension model is similar to that of a beam element model where the discrete support cannot take tension.
- (3) A beam element model with nonlinear discrete support has been suggested. The model takes advantage of a measured nonlinear force-deflection relationship, which is modelled as a power function with two parameters. Also the discrete support is modelled with a power function with two parameters; the two parameters being solved for during the analysis. The model displays promising results, but needs to be further explored.
- (4) For frictional materials subjected to cyclic loading the concept of reclaimed plastic strain must be rejected. The basis for this conclusion is the energy balance and the dissipation of energy during cyclic loading.
- (5) It is concluded that initial stresses cannot contribute substantially to the bearing capacity in structures made of unbound granular aggregates. This is mainly due to the lack of tensional strength in such materials.
- (6) A large scale triaxial device for testing normally graded railway ballast materials has successfully been developed. Both the deviatoric and confining stresses can be cycled. The direct way of applying the confining stress works very well. The new method of gluing the fastenings for the instrumentation for horizontal deformation measurements directly to aggregate particles seems to work well, one major advantage being the avoidance of any membrane effects.
- (7) The mechanism of resilient particle rotation made it difficult to fix the vertical deformation transducers directly to individual aggregate particles. Instead the vertical deformation had to be measured over the whole length of the specimen.

- (8) In general, the performed triaxial tests show that good repeatability is being achieved. The equipment performs quite well and it seems also well suited for triaxial testing of railway ballast.
- (9) For the Vassfjell railway ballast material the cumulative plastic strains grew rapidly when the  $q/p$  ratio was 1.8-2.0 or more when the specimen was subjected to proportional loading.
- (10) The Young's modulus and Poisson's ratio were in general found to be stress dependent.
- (11) In the tests the Poisson's ratio showed more scatter than the Young's modulus from specimen to specimen. It is not clear whether this scatter is due to the test conditions or can be related to real material behaviour.
- (12) The impact on the material behaviour from moisture and the denser grading is small and limited to  $q/p$  ratios not exceeding 1.2. The Poisson's ratio seems to increase slightly because of denser grading, while the permanent strains tend to be slightly smaller when moisture is added.

## 6.2 Suggestions for further work

- (1) For the new tensionless track model (Section 2.6) only deflection has been calculated. Further developments of the model should also include the rail moment and rail shear forces.
- (2) The beam element model with nonlinear support (Section 2.10) needs further developments. The most urgent one is to make the model able to analyse longer track sections. Also, the incorporation of the track ladder weight should be explored. By this, perhaps the uplift regions of the track ladder could be treated better in the model so that more of the tension is avoided.
- (3) In connection with cyclic loading of frictional materials (Section 3.7) it would have been interesting to see if there are some possibilities to identify mechanisms that can explain the cyclic ratcheting without leaning on any viscous behaviour. More literature review is here necessary.
- (4) A more thorough look into the thermomechanics for frictional granular materials would be useful for a better understanding of the constitutive behaviour. It is felt that thermomechanics forms a very profound and sound basis for the constitutive modelling. More literature review is then necessary.
- (5) It is possible to modify the triaxial device in a quite simple manner in order to test specimens with a diameter of 400 mm and a height of 800 mm. This would be beneficial for increasing the ratio of the diameter of the specimen to the maximum diameter of the particles. Hopefully a higher accuracy would be obtained.
- (6) The testing procedure could preferably be altered so that ramping of the stresses in the beginning of the load sequence is avoided. From theoretical considerations the response of the first load cycle is very different from that of the subsequent cycles. A change in loading procedure also requires data logging through the first cycle. The practical way of getting the stresses correct even for the first cycle may be to have a very low frequency so that automatic stress correction schemes are able to follow the intended stress curves. If the stresses are reliable from the very beginning, it will not be necessary to have internal suction in the specimen in the start of loading (as the confining pressure applied by the loading system may then be relied on). If internal suction is avoided the permanent stresses for the first load step will be more accurate.

- (7) The test series conducted was very limited. Other types of rock, different gradings and different loading patterns should be tested to map a broader range of materials and loading conditions.
- (8) If a broader test series is conducted more advanced constitutive models could be justified. A broader basis for modelling also the permanent behaviour would then be at hand.
- (9) The deficiency in the PC logging program prevented us from ascertain the stress states where the repeated horizontal strain changes its sign. From physical reasoning it can be argued that the repeated horizontal strains should always be tensional when a wheel load passes directly over the material element considered. In the future the testing may preferably be concentrated on stress states that make the horizontal strains tensional.
- (10) A further step based on this thesis as a whole is to utilise the data from the triaxial tests in a more advanced constitutive model and apply the finite element method to a track section in order to calculate the track reactions, e.g. in order to do a parametric study. It would also be of interest to compare finite element analyses with the track models from Chapter 2. This requires more triaxial testing.



---

## References

---

- /1/ Adin, M. A.; Yankelevsky, D. Z. and Eisenberger, M: Analysis of beams on bi-moduli elastic foundation, *Computer Methods in Applied Mechanics and Engineering*, Elsevier Science Publishers B.V., vol. 49, 1985, pp 319-330.
- /2/ American Railway Engineering Association: *Manual for Railway Engineering*, Washington D. C., 1996.
- /3/ Bathe, K.-J.: *Finite element procedures*, Prentice-Hall, Inc., New Jersey, USA, 1996.
- /4/ Bishop, A. W. and Green, G. E.: The influence of end restraint on the compression strength of a cohesionless soil, *Géotechnique*, vol. 15, pp 243-266.
- /5/ Boyce, H. R.: A non-linear model for the elastic behaviour of granular materials under repeated loading, *Proceedings of the international symposium on soils under cyclic and transient loading*, Swansea, 7-11 Jan. 1980, G. N. Pande and O. C. Zienkiewicz (eds.), Balkema, pp 285-294.
- /6/ Brandl, H.: *Geotechnics of rail structures, Geotechnics for Roads, Rail Tracks and Earth Structures*, A. Gomes Correia and H. Brandl (eds.), Balkema, Lisse, The Netherlands, 2001, pp 271-288.
- /7/ Cai, Z.; Raymond, P. and Bathurst, R. J.: Estimate of Static Track Modulus Using Elastic Foundation Models, *Transportation Research Record 1470*, Transportation Research Board, Washington D. C., 1994, pp 65-72.
- /8/ CEN: Aggregates for railway ballast, Draft, *prEN 13450*, Brussels, 1999.
- /9/ CEN: Unbound and hydraulic bound mixtures for roads - Test methods - Cyclic load tri-axial test, *prEN 00227413*, Brussels, 1997.
- /10/ Chakrabarty, J.: *Theory of Plasticity*, McGraw-Hill Book Company, Singapore, 1987 (2nd printing 1988).
- /11/ Clough, R. W. and Penzien, J.: *Dynamics of Structures*, McGraw-Hill, USA, 1975.
- /12/ Cook, R. D., Malkus, D. S. and Plesha, M. E.: *Concepts and applications of finite element analysis*, third ed., John Wiley & Sons, Inc., New York, 1989.
- /13/ Dafalias, Y. F. and Popov, E. P.: A model of non-linearly hardening materials for complex loadings, *Acta Mechanica*, vol. 21, 1975, pp 173-192.



- 
- /14/ Dahlberg, T.: Some railroad settlement models - a critical review, paper submitted to *IMEchE Journal of Rail and Rapid Transit*, accepted for publication September 2000, revised October 16, 2000.
- /15/ Desai, C. S. and Siriwardane, H. J.: *Constitutive laws for engineering materials. With emphasis on geologic materials*, Prentice-Hall Inc., Englewood Cliffs, New Jersey, USA, 1984.
- /16/ Donaghe, R. T.; Chaney, R. C. and Silver M. L. (eds.): *Advanced Triaxial Testing of Soil and Rock*, STP 977, ASTM, Philadelphia, 1988.
- /17/ Duncan, J. M. and Dunlop, P.: The significance of cap and base restraint, *ASCE Journal of the Soil Mechanics and Foundation Division*, vol. 94, no. SM1, 1968, pp 271-290.
- /18/ Eisenmann, J.: Die Schiene als Träger und Fahrbahn - theoretische Grundlagen und praktische Beispiele, in Fastenrath, F. (ed.) *Die Eisenbahnschiene*, Verlag von Wilhlem Ernst & Sohn, Germany, 1977, pp 9-78 (in German).
- /19/ Elhannani, M.: *Modélisation et Simulation Numérique des Chaussées Souples*, Ph.D. thesis, University of Nantes, France, 1991 (in French).
- /20/ El-Sibaie, M.: On the component of track damping resistance and related damping measurements, *Applied Mechanics Rail Transportation Symposium 1988, Winter Annual Meeting of ASME*, pp 59-68.
- /21/ El-Sibaie, M.: A beam on elastic foundation track model for use in a multi-body system simulation, *Transportation Systems 1990, Winter Annual Meeting of ASME*, pp 149-156.
- /22/ Esveld, C.: *Modern Railway Track*, MRT-Productions, Duisburg, Germany, 1989.
- /23/ European Rail Research Institute (ERRI): *Unified assessment criteria for ballast quality and methods for assessing the ballast condition in the track. Determining the criteria for ballast durability using triaxial tests*, Report No. D 182/RP 3, European Rail Research Institute, Utrecht, The Netherlands, 1994.
- /24/ Finansdepartementet (Ministry of Finance): *Storingsproposisjon nr. 1 (2001-2002). For budsjetterminen 2002. Den kongelige proposisjon om statsbudsjettet medregnet folketrygden for budsjetterminen 1. januar - 31. desember 2002. Samferdselsdepartementets fagproposisjon*, Finansdepartementet, Oslo, 2001 (in Norwegian).
- /25/ Frýba, L: *Vibration of Solids and Structures under Moving Loads*, 3rd edition, Thomas Telford, London, 1999.
- /26/ Gaaljord, P. J.; Paute, J. L.; Dawson, A. R. and Gillett, S. D.: Comparison and performance of repeated load triaxial test equipment for unbound granular materials, *Proceedings Euroflex 93 Symposium*, LNEC, Lisbon, 1993, pp 1/1-1/26.
- /27/ Ghaboussi, J., Pecknold, D. A. W. and Wu, X.: *Nonlinear analysis in structural mechanics*, class notes from a graduate course at the Dept. of Civil Engineering, Univ. of Illinois at Urbana-Champaign, USA, 1996.
- /28/ Gåsemyr, H.: *Dimensjonering av overbygningen*, Baneteknikkurs, Jernbaneskolen, Oslo, 1995 (in Norwegian).

- 
- /29/ Hay, W. W.: *Railroad Engineering*, John Wiley, New York, 1982.
- /30/ Hetényi, M.: *Beams on elastic foundation. Theory with applications in the fields of civil and mechanical engineering*, The University of Michigan Press, Ann Arbor, 1946 (sixth printing 1961).
- /31/ Hicks, R.G. and Monismith, C.L.: Factors influencing the resilient response of granular materials, *Highway Research Record No. 345*, Highway Research Board, Washington D. C., 1971, pp 15-31.
- /32/ Hjelmstad, K. D. and Taciroglu, E.: A Coupled Hyperelastic Constitutive Model for Resilient Response of Granular Materials, *Proceedings: Aircraft/Pavement Technology in the Midst of Change*, Seattle, Washington, August 17-20, 1997, pp 178-189.
- /33/ Hoff, Inge and Nordal, R. S.: *Permanente deformasjoner i granulære lag i dekkekonstruksjoner*, report no. STF22 A00451, SINTEF, Trondheim, Norway, 2000.
- /34/ Hoff, I.: *Material Properties of Unbound Aggregates for Pavement Structures*, doctoral thesis, Department of Road and Railway Engineering, The Norwegian University of Science and Technology, Trondheim, Norway, 1999.
- /35/ Hoff, I., Nordal, S. and Nordal, R.: New hyperelastic model for granular materials in pavement structures, *Proceedings of the Fifth International Conference on the Bearing Capacity of Roads and Airfields*, Trondheim, Norway, July 6-8, 1998, pp 1315-1324.
- /36/ Hornych, P. and Gerard, A.: A pneumatic repeatd load triaxial apparatus for unbound granular materials and subgrade soils, *Workshop on Modelling and Advanced Testing for Unbound Granular Materials 21-22 January 1999*, organised by IST, Lisbon, Portugal (preprint).
- /37/ Hornych, P.; Kazai, A. and Piau, J.-M.: Study of the resilient behaviour of unbound granular materials, *Proceedings of the Fifth International Conference on the Bearing Capacity of Roads and Airfields*, Trondheim, Norway, July 6-8, 1998, pp1277-1287.
- /38/ Hunt, G. A.: Track Loading and Damage, paper 2 in *Vehicle/Track Interaction*, lecture to Nordic Seminar on Permanent Way Technology, Report No. LR TSM 003, British Rail Research, Derby, 1994.
- /39/ Iwan, W. D.: On a class of models for the yielding behaviour of continous and composite systems, *ASME Journal of Applied Mechanics*, vol. 34, 1967, pp 612-617.
- /40/ Iwnicki, S. D. (ed.): The Manchester Benchmarks for Rail Vehicle Simulation, contributions from 'International Workshop on Computer Simulation of Rail Vehicle Dynamics', Manchester June 23-24 1997, printed as a supplement to *Vehicle system dynamics*, vol. 31,1999.
- /41/ Jacobsson, L.: *A Plasticity Model for Cohesionless Material with Emphasis on Railway Ballast*, licentiate thesis, Department of Solid Mechanics, Chalmers University of Technology, Göteborg, 1999.
- /42/ Jefferies, M.: Plastic work and isotropic softening in unloading, Technical Note, *Géotechnique*, vol. 47, no. 5, 1997, pp 1037-1042.

- 
- /43/ Jernbaneverket (Norwegian National Rail Administration): JD 530 Overbygning, Regler for prosjektering, *Teknisk regelverk*, submitted by Hovedkontoret, Jernbaneverket, Oslo, 1998 (in Norwegian).
- /44/ Jernbaneverket (Norwegian National Rail Administration): *Teknisk spesifikasjon. Krav til ballastpukk*, m/vedlegg, versjon 2.0, Hovedkontoret, Teknisk avdeling, Oslo, 1998 (in Norwegian).
- /45/ Jernbaneverket (Norwegian National Rail Administration): *Jernbaneverkets rutiner for testing av ballastpukk*, JBV Ingeniørtjenesten, Oslo, 1997 (in Norwegian).
- /46/ Jernbaneverket (Norwegian National Rail Administration): A/S Franzefoss Bruk, Vassfjellet pukkverk. Vurdering av pukkprøve, *saksref. 97/537 JI 722*, Ingeniørtjenesten, Oslo, 1997 (in Norwegian).
- /47/ Khan, A. S. and Huang, S.: *Continuum theory of plasticity*, John Wiley & Sons Inc., New York, 1995.
- /48/ Kerr, Arnold D.: *On the stress analysis of rails and ties*, Report no. FRA-OR&D-76-284, Federal Railroad Administration, U.S. Department of Transportation, Washington D.C., 1976.
- /49/ Kerr, Arnold D.: Elastic and Viscoelastic Foundation Models, *Transactions of the ASME Journal of Applied Mechanics*, September 1964, pp 491-498.
- /50/ Knutson, R. M.; Thompson, M. R.; Mullin, T. and Tayabji, S. D.: *Materials Evaluation Study - Ballast and Foundation Research Program*, FRA-OR&D-77-02, Federal Railroad Administration, U.S. Department of Transportation, Washington D.C., 1977.
- /51/ Kolisoja, P.: *Resilient Deformation Characteristics of Granular Materials*, Dr. Techn. Thesis, Tampere University of Technology, Finland, 1997.
- /52/ Kolymbas, D. and Herle, I.: Hypoplasticity: A framework to model granular materials, *Behaviour of granular materials*, B. Cambou (ed.), CISM courses and lectures no. 385, Springer-Verlag Wien New York, pp 239-268.
- /53/ Krieg, R. D.: A practical two-surface plasticity theory, *Journal of Applied Mechanics, Transactions of the ASME*, E42, 1975, pp 641-646.
- /54/ Lekarp, F. and Isacsson, U.: Development of a large-scale triaxial apparatus for characterization of granular materials, *Road Materials and Pavement Design*, vol.1, no. 2/2000, HERMES Science Europe Ltd., UK, pp 165-196.
- /55/ Lekarp, F.; Isacsson, U. and Dawson, A.: State of the Art. I: Resilient Response of Unbound Aggregates, *ASCE Journal of Transportation Engineering*, vol. 126, no. 1, 2000, pp 66-75.
- /56/ Lekarp, F.: *Permanent deformation behaviour of unbound granular materials*, licentiate thesis, Dept. of Infrastructure and Planning, Royal Institute of Technology, Stockholm, 1997.

- 
- /57/ Marquis, B. P.; Weinstock, H. and Carr, G.: The effect of load sequence on GRMS measurements, *Proceedings of the 1997 IEEE/ASME Joint Railroad Conference*, Boston, pp 237-246.
- /58/ Mayhew, H. C.: Resilient properties of unbound roadbase under repeated triaxial loading, Report No. LR 1088, Transport Research Laboratory, Great Britain, 1983.
- /59/ Mendelson, A.: *Plasticity: Theory and Application*, The MacMillan Company, New York, 1968.
- /60/ Mróz, Z.: Elastoplastic and viscoplastic constitutive models for granular materials, *Behaviour of granular materials*, B. Cambou (ed.), CISM courses and lectures no. 385, Springer-Verlag Wien New York, 1998, pp 269-337.
- /61/ Mróz, Z. and Zienkiewicz, O. C.: Uniform Formulation of Constitutive Equations for Clays and Sands, *Mechanics of Engineering Materials*, D. S. Desai and R. H. Gallagher (eds.), John Wiley & Sons Ltd., New York, 1984, pp 415-449.
- /62/ Mróz, Z.: On the description of anisotropic workhardening, *Journal of the Mechanics and Physics of Solids*, vol. 15, 1967, pp 163-175.
- /63/ Myrvang, A.: *Kompendium i bergmekanikk*, Department of Geology and Mineral Resources Engineering, The Norwegian University of Science and Technology, Trondheim, Norway, 1996 (in Norwegian).
- /64/ Nordal, S.: *Soil Modelling*, class notes from EEU course/dr.ing. course 33584, Dept. of Geotechnical Engineering, The Norwegian Institute of Technology, Trondheim, 1994.
- /65/ Nordal, S. and Grande, L.: *Forelesningsnotater i Geoteknikk 2*, Dept. of Geotechnical Engineering, The Norwegian Institute of Technology, Trondheim, 1989 (in Norwegian).
- /66/ Norwegian National Rail Administration, Hovedkontoret: *Teknisk regelverk, JD 530 Overbygning - Prosjektering*, Rev. 0, Oslo, 1998 (in Norwegian).
- /67/ Pappin, J. W. and Brown, S. F.: Resilient stress-strain behaviour of a crushed rock, *Proceedings of the international symposium on soils under cyclic and transient loading*, G. N. Pande and O. C. Zienkiewicz (eds.), Swansea, 7-11 Jan. 1980, pp169-177.
- /68/ Puzrin, A. M. and Houlsby, G. T.: Fundamentals of kinematic hardening hyperplasticity, *International Journal of Solids and Structures*, vol. 38, 2001, pp 3771-3794.
- /69/ Riessberger, K.: Track - Part of the System 'Railway', lecture notes for *Nordisk Baneteknisk Ingeniørutdanning*, part 3 of seminar arranged by NSB, Norway, 1994-95.
- /70/ Saada, A. S.: Hollow Cylinder Torsional Devices: Their Advantages and Limitations, *Advanced Triaxial Testing of Soil and Rock*, STP 977, Donaghe, R. T.; Chaney, R. C. and Silver M. L. (eds.), ASTM, Philadelphia, 1988, pp 766-795.
- /71/ Scott, R.: *Foundation Analysis*, Prentice-Hall, Inc., Englewood Cliffs, New Jersey, USA, 1981.
- /72/ Selig, E. and Waters, J. M.: *Track Geotechnology and Substructure Management*, Thomas Telford Publications, London, 1994 (reprint 1995).

- /73/ Selig, E.T. and Li, D.: Track Modulus: Its Meaning and Factors Influencing It, *Transportation Research Record 1470*, Transportation Research Board, Washington D. C., 1994, pp 47-54.
- /74/ Skoglund, K. A.: Dimensionless sensitivity diagrams in mechanistic railway design, paper accepted for publication in the *Proceedings of the Sixth International Conference on the Bearing Capacity of Roads, Railways and Airfields*, Lisbon, Portugal, June 24-26, 2002.
- /75/ Skoglund, K. A.; Hoseth, S. and Værnes, E.: Development of a large triaxial cell apparatus with variable deviatoric and confining stresses, *Proceedings of the fifth international symposium on unbound aggregates in roads* (UNBAR 5), Nottingham, UK, 21-23 June 2000, A. R. Dawson (ed.), A. A. Balkema, pp 145-152.
- /76/ Statens vegvesen: *Håndbok 014 Laboratorieundersøkelser*, Vegdirektoratet, Oslo, 1997 (in Norwegian).
- /77/ Strategic Highway Research Program (SHRP): *SHRP Protocol P46, for SHRP Test Designation UG07, SS07; Resilient modulus of unbound granular base/subbase materials and subgrade soils*, Strategic Highway Research Program, 1993.
- /78/ Timoshenko, S. P.: *Strength of Materials. Part II: Advanced Theory and Problems*, 3. ed., D. van Nostrand Company Inc., New York, 1956.
- /79/ Tsai, N.-C. and Westmann, R. A.: Beam on tensionless foundation, *Journal of the Engineering Mechanics Division*, ASCE, Oct. 1967, pp 1-12.
- /80/ Uzan, J.: Characterization of Granular Material, *Transportation Research Record 1022*, Transportation Research Board, Washington D.C., 1985, pp 52-59.
- /81/ Valanis, K. C.: Endochronic Plasticity: Physical Basis and Applications, *Mechanics of Engineering Materials*, D. S. Desai and R. H. Gallagher (eds.), John Wiley & Sons Ltd., New York, 1984, pp 591-609.
- /82/ Valanis, K. C.: A theory of viscoplasticity without a yield surface, Part I: General theory; Part II: Application to mechanical behaviour of metals, *Archives of Mechanics*, vol. 23, 1971, pp 517-551.
- /83/ van Niekerk, A. A.; van Scheers, J.; Muraya, P. and Kisimbi, A.: The effect of compaction on the mechanical behaviour of mix granulate base course materials and on pavement performance, *Proceedings of the fifth international symposium on unbound aggregates in roads* (UNBAR 5), Nottingham, UK, 21-23 June 2000, A. R. Dawson (ed.), A. A. Balkema, pp 125-136.
- /84/ Veverka, V.: Raming Van de Spoordiepte Bij Wgen met een Bitumineuze Verharding, *De Wegentechniek*, vol. XXIV, no. 3, 1979, pp 25-45 (in Dutch).
- /85/ Vik, A. (ed.): *Temarapport 1997: Ballast*, Nordisk Bro og Geoteknisk samarbeid, Oslo, 1997 (in Norwegian).
- /86/ Vik, G.: Sykliske vakuumbreaksialforsøk på pukk og grus. Sammenligning av resultater fra forsøk på 6 forskjellige grus og steinmaterialer, NGI-report no. 531001-4, Oslo, 1996 (in Norwegian).

- 
- /87/ Wood, D. M.: *Soil Behaviour and Critical State Soil Mechanics*, Cambridge University Press, Great Britain, 1990 (reprint 1996).
- /88/ Zarembski, A. M. and Choros, J.: On the Measurement and Calculation of Vertical Track Modulus, *Proceedings of AREA, Bulletin 675*, Vol. 81, 1980, pp 156-173.
- /89/ Ziegler, H.: *An introduction to thermomechanics*, North-Holland Publishing Company, Amsterdam, 1983.
- /90/ Zienkiewicz, O. C.; Chan, A. H. C.; Pastor, M.; Schrefler, B. A. and Shiomi, T.: *Computational Geomechanics with Special reference to Earthquake Engineering*, John Wiley & Sons Ltd., Great Britain, 1999.
- /91/ Zienkiewicz, O. C. and Taylor, R. L.: *The finite element method*, fourth ed., McGraw-Hill Book Company (UK) Limited, London, 1991.
- /92/ Zienkiewicz, O. C. and Mróz, Z.: Generalized Plasticity Formulation and Application to Geomechanics, *Mechanics of Engineering Materials*, D. S. Desai and R. H. Gallagher (eds.), John Wiley & Sons Ltd., New York, 1984, pp 655-679.
- /93/ Zienkiewicz, O. C.; Leung, K. H.; Hinton, E. and Chang, C. T.: Liquefaction and Permanent Deformation under Dynamic Conditions - Numerical Solution and Constitutive Relations, chapter 5 in G. N. Pande and O. C. Zienkiewicz (eds.): *Soil Mechanics - Transient and Cyclic Loads*, John Wiley & Sons, 1982, pp 71-103.



---

## References

---

- /1/ Adin, M. A.; Yankelevsky, D. Z. and Eisenberger, M: Analysis of beams on bi-moduli elastic foundation, *Computer Methods in Applied Mechanics and Engineering*, Elsevier Science Publishers B.V., vol. 49, 1985, pp 319-330.
- /2/ American Railway Engineering Association: *Manual for Railway Engineering*, Washington D. C., 1996.
- /3/ Bathe, K.-J.: *Finite element procedures*, Prentice-Hall, Inc., New Jersey, USA, 1996.
- /4/ Bishop, A. W. and Green, G. E.: The influence of end restraint on the compression strength of a cohesionless soil, *Géotechnique*, vol. 15, pp 243-266.
- /5/ Boyce, H. R.: A non-linear model for the elastic behaviour of granular materials under repeated loading, *Proceedings of the international symposium on soils under cyclic and transient loading*, Swansea, 7-11 Jan. 1980, G. N. Pande and O. C. Zienkiewicz (eds.), Balkema, pp 285-294.
- /6/ Brandl, H.: *Geotechnics of rail structures, Geotechnics for Roads, Rail Tracks and Earth Structures*, A. Gomes Correia and H. Brandl (eds.), Balkema, Lisse, The Netherlands, 2001, pp 271-288.
- /7/ Cai, Z.; Raymond, P. and Bathurst, R. J.: Estimate of Static Track Modulus Using Elastic Foundation Models, *Transportation Research Record 1470*, Transportation Research Board, Washington D. C., 1994, pp 65-72.
- /8/ CEN: Aggregates for railway ballast, Draft, *prEN 13450*, Brussels, 1999.
- /9/ CEN: Unbound and hydraulic bound mixtures for roads - Test methods - Cyclic load tri-axial test, *prEN 00227413*, Brussels, 1997.
- /10/ Chakrabarty, J.: *Theory of Plasticity*, McGraw-Hill Book Company, Singapore, 1987 (2nd printing 1988).
- /11/ Clough, R. W. and Penzien, J.: *Dynamics of Structures*, McGraw-Hill, USA, 1975.
- /12/ Cook, R. D., Malkus, D. S. and Plesha, M. E.: *Concepts and applications of finite element analysis*, third ed., John Wiley & Sons, Inc., New York, 1989.
- /13/ Dafalias, Y. F. and Popov, E. P.: A model of non-linearly hardening materials for complex loadings, *Acta Mechanica*, vol. 21, 1975, pp 173-192.



- 
- /14/ Dahlberg, T.: Some railroad settlement models - a critical review, paper submitted to *IMEchE Journal of Rail and Rapid Transit*, accepted for publication September 2000, revised October 16, 2000.
- /15/ Desai, C. S. and Siriwardane, H. J.: *Constitutive laws for engineering materials. With emphasis on geologic materials*, Prentice-Hall Inc., Englewood Cliffs, New Jersey, USA, 1984.
- /16/ Donaghe, R. T.; Chaney, R. C. and Silver M. L. (eds.): *Advanced Triaxial Testing of Soil and Rock*, STP 977, ASTM, Philadelphia, 1988.
- /17/ Duncan, J. M. and Dunlop, P.: The significance of cap and base restraint, *ASCE Journal of the Soil Mechanics and Foundation Division*, vol. 94, no. SM1, 1968, pp 271-290.
- /18/ Eisenmann, J.: Die Schiene als Träger und Fahrbahn - theoretische Grundlagen und praktische Beispiele, in Fastenrath, F. (ed.) *Die Eisenbahnschiene*, Verlag von Wilhlem Ernst & Sohn, Germany, 1977, pp 9-78 (in German).
- /19/ Elhannani, M.: *Modélisation et Simulation Numérique des Chaussées Souples*, Ph.D. thesis, University of Nantes, France, 1991 (in French).
- /20/ El-Sibaie, M.: On the component of track damping resistance and related damping measurements, *Applied Mechanics Rail Transportation Symposium 1988, Winter Annual Meeting of ASME*, pp 59-68.
- /21/ El-Sibaie, M.: A beam on elastic foundation track model for use in a multi-body system simulation, *Transportation Systems 1990, Winter Annual Meeting of ASME*, pp 149-156.
- /22/ Esveld, C.: *Modern Railway Track*, MRT-Productions, Duisburg, Germany, 1989.
- /23/ European Rail Research Institute (ERRI): *Unified assessment criteria for ballast quality and methods for assessing the ballast condition in the track. Determining the criteria for ballast durability using triaxial tests*, Report No. D 182/RP 3, European Rail Research Institute, Utrecht, The Netherlands, 1994.
- /24/ Finansdepartementet (Ministry of Finance): *Storingsproposisjon nr. 1 (2001-2002). For budsjetterminen 2002. Den kongelige proposisjon om statsbudsjettet medregnet folketrygden for budsjetterminen 1. januar - 31. desember 2002. Samferdselsdepartementets fagproposisjon*, Finansdepartementet, Oslo, 2001 (in Norwegian).
- /25/ Frýba, L: *Vibration of Solids and Structures under Moving Loads*, 3rd edition, Thomas Telford, London, 1999.
- /26/ Gaaljord, P. J.; Paute, J. L.; Dawson, A. R. and Gillett, S. D.: Comparison and performance of repeated load triaxial test equipment for unbound granular materials, *Proceedings Euroflex 93 Symposium*, LNEC, Lisbon, 1993, pp 1/1-1/26.
- /27/ Ghaboussi, J., Pecknold, D. A. W. and Wu, X.: *Nonlinear analysis in structural mechanics*, class notes from a graduate course at the Dept. of Civil Engineering, Univ. of Illinois at Urbana-Champaign, USA, 1996.
- /28/ Gåsemyr, H.: *Dimensjonering av overbygningen*, Baneteknikkurs, Jernbaneskolen, Oslo, 1995 (in Norwegian).

- 
- /29/ Hay, W. W.: *Railroad Engineering*, John Wiley, New York, 1982.
- /30/ Hetényi, M.: *Beams on elastic foundation. Theory with applications in the fields of civil and mechanical engineering*, The University of Michigan Press, Ann Arbor, 1946 (sixth printing 1961).
- /31/ Hicks, R.G. and Monismith, C.L.: Factors influencing the resilient response of granular materials, *Highway Research Record No. 345*, Highway Research Board, Washington D. C., 1971, pp 15-31.
- /32/ Hjelmstad, K. D. and Taciroglu, E.: A Coupled Hyperelastic Constitutive Model for Resilient Response of Granular Materials, *Proceedings: Aircraft/Pavement Technology in the Midst of Change*, Seattle, Washington, August 17-20, 1997, pp 178-189.
- /33/ Hoff, Inge and Nordal, R. S.: *Permanente deformasjoner i granulære lag i dekkekonstruksjoner*, report no. STF22 A00451, SINTEF, Trondheim, Norway, 2000.
- /34/ Hoff, I.: *Material Properties of Unbound Aggregates for Pavement Structures*, doctoral thesis, Department of Road and Railway Engineering, The Norwegian University of Science and Technology, Trondheim, Norway, 1999.
- /35/ Hoff, I., Nordal, S. and Nordal, R.: New hyperelastic model for granular materials in pavement structures, *Proceedings of the Fifth International Conference on the Bearing Capacity of Roads and Airfields*, Trondheim, Norway, July 6-8, 1998, pp 1315-1324.
- /36/ Hornych, P. and Gerard, A.: A pneumatic repeatd load triaxial apparatus for unbound granular materials and subgrade soils, *Workshop on Modelling and Advanced Testing for Unbound Granular Materials 21-22 January 1999*, organised by IST, Lisbon, Portugal (preprint).
- /37/ Hornych, P.; Kazai, A. and Piau, J.-M.: Study of the resilient behaviour of unbound granular materials, *Proceedings of the Fifth International Conference on the Bearing Capacity of Roads and Airfields*, Trondheim, Norway, July 6-8, 1998, pp1277-1287.
- /38/ Hunt, G. A.: Track Loading and Damage, paper 2 in *Vehicle/Track Interaction*, lecture to Nordic Seminar on Permanent Way Technology, Report No. LR TSM 003, British Rail Research, Derby, 1994.
- /39/ Iwan, W. D.: On a class of models for the yielding behaviour of continous and composite systems, *ASME Journal of Applied Mechanics*, vol. 34, 1967, pp 612-617.
- /40/ Iwnicki, S. D. (ed.): The Manchester Benchmarks for Rail Vehicle Simulation, contributions from 'International Workshop on Computer Simulation of Rail Vehicle Dynamics', Manchester June 23-24 1997, printed as a supplement to *Vehicle system dynamics*, vol. 31,1999.
- /41/ Jacobsson, L.: *A Plasticity Model for Cohesionless Material with Emphasis on Railway Ballast*, licentiate thesis, Department of Solid Mechanics, Chalmers University of Technology, Göteborg, 1999.
- /42/ Jefferies, M.: Plastic work and isotropic softening in unloading, Technical Note, *Géotechnique*, vol. 47, no. 5, 1997, pp 1037-1042.

- 
- /43/ Jernbaneverket (Norwegian National Rail Administration): JD 530 Overbygning, Regler for prosjektering, *Teknisk regelverk*, submitted by Hovedkontoret, Jernbaneverket, Oslo, 1998 (in Norwegian).
- /44/ Jernbaneverket (Norwegian National Rail Administration): *Teknisk spesifikasjon. Krav til ballastpukk*, m/vedlegg, versjon 2.0, Hovedkontoret, Teknisk avdeling, Oslo, 1998 (in Norwegian).
- /45/ Jernbaneverket (Norwegian National Rail Administration): *Jernbaneverkets rutiner for testing av ballastpukk*, JBV Ingeniørtjenesten, Oslo, 1997 (in Norwegian).
- /46/ Jernbaneverket (Norwegian National Rail Administration): A/S Franzefoss Bruk, Vassfjellet pukkverk. Vurdering av pukkprøve, *saksref. 97/537 JI 722*, Ingeniørtjenesten, Oslo, 1997 (in Norwegian).
- /47/ Khan, A. S. and Huang, S.: *Continuum theory of plasticity*, John Wiley & Sons Inc., New York, 1995.
- /48/ Kerr, Arnold D.: *On the stress analysis of rails and ties*, Report no. FRA-OR&D-76-284, Federal Railroad Administration, U.S. Department of Transportation, Washington D.C., 1976.
- /49/ Kerr, Arnold D.: Elastic and Viscoelastic Foundation Models, *Transactions of the ASME Journal of Applied Mechanics*, September 1964, pp 491-498.
- /50/ Knutson, R. M.; Thompson, M. R.; Mullin, T. and Tayabji, S. D.: *Materials Evaluation Study - Ballast and Foundation Research Program*, FRA-OR&D-77-02, Federal Railroad Administration, U.S. Department of Transportation, Washington D.C., 1977.
- /51/ Kolisoja, P.: *Resilient Deformation Characteristics of Granular Materials*, Dr. Techn. Thesis, Tampere University of Technology, Finland, 1997.
- /52/ Kolymbas, D. and Herle, I.: Hypoplasticity: A framework to model granular materials, *Behaviour of granular materials*, B. Cambou (ed.), CISM courses and lectures no. 385, Springer-Verlag Wien New York, pp 239-268.
- /53/ Krieg, R. D.: A practical two-surface plasticity theory, *Journal of Applied Mechanics, Transactions of the ASME*, E42, 1975, pp 641-646.
- /54/ Lekarp, F. and Isacsson, U.: Development of a large-scale triaxial apparatus for characterization of granular materials, *Road Materials and Pavement Design*, vol.1, no. 2/2000, HERMES Science Europe Ltd., UK, pp 165-196.
- /55/ Lekarp, F.; Isacsson, U. and Dawson, A.: State of the Art. I: Resilient Response of Unbound Aggregates, *ASCE Journal of Transportation Engineering*, vol. 126, no. 1, 2000, pp 66-75.
- /56/ Lekarp, F.: *Permanent deformation behaviour of unbound granular materials*, licentiate thesis, Dept. of Infrastructure and Planning, Royal Institute of Technology, Stockholm, 1997.

- 
- /57/ Marquis, B. P.; Weinstock, H. and Carr, G.: The effect of load sequence on GRMS measurements, *Proceedings of the 1997 IEEE/ASME Joint Railroad Conference*, Boston, pp 237-246.
- /58/ Mayhew, H. C.: Resilient properties of unbound roadbase under repeated triaxial loading, Report No. LR 1088, Transport Research Laboratory, Great Britain, 1983.
- /59/ Mendelson, A.: *Plasticity: Theory and Application*, The MacMillan Company, New York, 1968.
- /60/ Mróz, Z.: Elastoplastic and viscoplastic constitutive models for granular materials, *Behaviour of granular materials*, B. Cambou (ed.), CISM courses and lectures no. 385, Springer-Verlag Wien New York, 1998, pp 269-337.
- /61/ Mróz, Z. and Zienkiewicz, O. C.: Uniform Formulation of Constitutive Equations for Clays and Sands, *Mechanics of Engineering Materials*, D. S. Desai and R. H. Gallagher (eds.), John Wiley & Sons Ltd., New York, 1984, pp 415-449.
- /62/ Mróz, Z.: On the description of anisotropic workhardening, *Journal of the Mechanics and Physics of Solids*, vol. 15, 1967, pp 163-175.
- /63/ Myrvang, A.: *Kompendium i bergmekanikk*, Department of Geology and Mineral Resources Engineering, The Norwegian University of Science and Technology, Trondheim, Norway, 1996 (in Norwegian).
- /64/ Nordal, S.: *Soil Modelling*, class notes from EEU course/dr.ing. course 33584, Dept. of Geotechnical Engineering, The Norwegian Institute of Technology, Trondheim, 1994.
- /65/ Nordal, S. and Grande, L.: *Forelesningsnotater i Geoteknikk 2*, Dept. of Geotechnical Engineering, The Norwegian Institute of Technology, Trondheim, 1989 (in Norwegian).
- /66/ Norwegian National Rail Administration, Hovedkontoret: *Teknisk regelverk, JD 530 Overbygning - Prosjektering*, Rev. 0, Oslo, 1998 (in Norwegian).
- /67/ Pappin, J. W. and Brown, S. F.: Resilient stress-strain behaviour of a crushed rock, *Proceedings of the international symposium on soils under cyclic and transient loading*, G. N. Pande and O. C. Zienkiewicz (eds.), Swansea, 7-11 Jan. 1980, pp169-177.
- /68/ Puzrin, A. M. and Houlsby, G. T.: Fundamentals of kinematic hardening hyperplasticity, *International Journal of Solids and Structures*, vol. 38, 2001, pp 3771-3794.
- /69/ Riessberger, K.: Track - Part of the System 'Railway', lecture notes for *Nordisk Baneteknisk Ingeniørutdanning*, part 3 of seminar arranged by NSB, Norway, 1994-95.
- /70/ Saada, A. S.: Hollow Cylinder Torsional Devices: Their Advantages and Limitations, *Advanced Triaxial Testing of Soil and Rock*, STP 977, Donaghe, R. T.; Chaney, R. C. and Silver M. L. (eds.), ASTM, Philadelphia, 1988, pp 766-795.
- /71/ Scott, R.: *Foundation Analysis*, Prentice-Hall, Inc., Englewood Cliffs, New Jersey, USA, 1981.
- /72/ Selig, E. and Waters, J. M.: *Track Geotechnology and Substructure Management*, Thomas Telford Publications, London, 1994 (reprint 1995).

- /73/ Selig, E.T. and Li, D.: Track Modulus: Its Meaning and Factors Influencing It, *Transportation Research Record 1470*, Transportation Research Board, Washington D. C., 1994, pp 47-54.
- /74/ Skoglund, K. A.: Dimensionless sensitivity diagrams in mechanistic railway design, paper accepted for publication in the *Proceedings of the Sixth International Conference on the Bearing Capacity of Roads, Railways and Airfields*, Lisbon, Portugal, June 24-26, 2002.
- /75/ Skoglund, K. A.; Hoseth, S. and Værnes, E.: Development of a large triaxial cell apparatus with variable deviatoric and confining stresses, *Proceedings of the fifth international symposium on unbound aggregates in roads* (UNBAR 5), Nottingham, UK, 21-23 June 2000, A. R. Dawson (ed.), A. A. Balkema, pp 145-152.
- /76/ Statens vegvesen: *Håndbok 014 Laboratorieundersøkelser*, Vegdirektoratet, Oslo, 1997 (in Norwegian).
- /77/ Strategic Highway Research Program (SHRP): *SHRP Protocol P46, for SHRP Test Designation UG07, SS07; Resilient modulus of unbound granular base/subbase materials and subgrade soils*, Strategic Highway Research Program, 1993.
- /78/ Timoshenko, S. P.: *Strength of Materials. Part II: Advanced Theory and Problems*, 3. ed., D. van Nostrand Company Inc., New York, 1956.
- /79/ Tsai, N.-C. and Westmann, R. A.: Beam on tensionless foundation, *Journal of the Engineering Mechanics Division*, ASCE, Oct. 1967, pp 1-12.
- /80/ Uzan, J.: Characterization of Granular Material, *Transportation Research Record 1022*, Transportation Research Board, Washington D.C., 1985, pp 52-59.
- /81/ Valanis, K. C.: Endochronic Plasticity: Physical Basis and Applications, *Mechanics of Engineering Materials*, D. S. Desai and R. H. Gallagher (eds.), John Wiley & Sons Ltd., New York, 1984, pp 591-609.
- /82/ Valanis, K. C.: A theory of viscoplasticity without a yield surface, Part I: General theory; Part II: Application to mechanical behaviour of metals, *Archives of Mechanics*, vol. 23, 1971, pp 517-551.
- /83/ van Niekerk, A. A.; van Scheers, J.; Muraya, P. and Kisimbi, A.: The effect of compaction on the mechanical behaviour of mix granulate base course materials and on pavement performance, *Proceedings of the fifth international symposium on unbound aggregates in roads* (UNBAR 5), Nottingham, UK, 21-23 June 2000, A. R. Dawson (ed.), A. A. Balkema, pp 125-136.
- /84/ Veverka, V.: Raming Van de Spoordiepte Bij Wgen met een Bitumineuze Verharding, *De Wegentechniek*, vol. XXIV, no. 3, 1979, pp 25-45 (in Dutch).
- /85/ Vik, A. (ed.): *Temarapport 1997: Ballast*, Nordisk Bro og Geoteknisk samarbeid, Oslo, 1997 (in Norwegian).
- /86/ Vik, G.: Sykliske vakuumbreaksialforsøk på pukk og grus. Sammenligning av resultater fra forsøk på 6 forskjellige grus og steinmaterialer, NGI-report no. 531001-4, Oslo, 1996 (in Norwegian).

- 
- /87/ Wood, D. M.: *Soil Behaviour and Critical State Soil Mechanics*, Cambridge University Press, Great Britain, 1990 (reprint 1996).
- /88/ Zarembski, A. M. and Choros, J.: On the Measurement and Calculation of Vertical Track Modulus, *Proceedings of AREA, Bulletin 675*, Vol. 81, 1980, pp 156-173.
- /89/ Ziegler, H.: *An introduction to thermomechanics*, North-Holland Publishing Company, Amsterdam, 1983.
- /90/ Zienkiewicz, O. C.; Chan, A. H. C.; Pastor, M.; Schrefler, B. A. and Shiomi, T.: *Computational Geomechanics with Special reference to Earthquake Engineering*, John Wiley & Sons Ltd., Great Britain, 1999.
- /91/ Zienkiewicz, O. C. and Taylor, R. L.: *The finite element method*, fourth ed., McGraw-Hill Book Company (UK) Limited, London, 1991.
- /92/ Zienkiewicz, O. C. and Mróz, Z.: Generalized Plasticity Formulation and Application to Geomechanics, *Mechanics of Engineering Materials*, D. S. Desai and R. H. Gallagher (eds.), John Wiley & Sons Ltd., New York, 1984, pp 655-679.
- /93/ Zienkiewicz, O. C.; Leung, K. H.; Hinton, E. and Chang, C. T.: Liquefaction and Permanent Deformation under Dynamic Conditions - Numerical Solution and Constitutive Relations, chapter 5 in G. N. Pande and O. C. Zienkiewicz (eds.): *Soil Mechanics - Transient and Cyclic Loads*, John Wiley & Sons, 1982, pp 71-103.



---

## References

---

- /1/ Adin, M. A.; Yankelevsky, D. Z. and Eisenberger, M: Analysis of beams on bi-moduli elastic foundation, *Computer Methods in Applied Mechanics and Engineering*, Elsevier Science Publishers B.V., vol. 49, 1985, pp 319-330.
- /2/ American Railway Engineering Association: *Manual for Railway Engineering*, Washington D. C., 1996.
- /3/ Bathe, K.-J.: *Finite element procedures*, Prentice-Hall, Inc., New Jersey, USA, 1996.
- /4/ Bishop, A. W. and Green, G. E.: The influence of end restraint on the compression strength of a cohesionless soil, *Géotechnique*, vol. 15, pp 243-266.
- /5/ Boyce, H. R.: A non-linear model for the elastic behaviour of granular materials under repeated loading, *Proceedings of the international symposium on soils under cyclic and transient loading*, Swansea, 7-11 Jan. 1980, G. N. Pande and O. C. Zienkiewicz (eds.), Balkema, pp 285-294.
- /6/ Brandl, H.: *Geotechnics of rail structures, Geotechnics for Roads, Rail Tracks and Earth Structures*, A. Gomes Correia and H. Brandl (eds.), Balkema, Lisse, The Netherlands, 2001, pp 271-288.
- /7/ Cai, Z.; Raymond, P. and Bathurst, R. J.: Estimate of Static Track Modulus Using Elastic Foundation Models, *Transportation Research Record 1470*, Transportation Research Board, Washington D. C., 1994, pp 65-72.
- /8/ CEN: Aggregates for railway ballast, Draft, *prEN 13450*, Brussels, 1999.
- /9/ CEN: Unbound and hydraulic bound mixtures for roads - Test methods - Cyclic load tri-axial test, *prEN 00227413*, Brussels, 1997.
- /10/ Chakrabarty, J.: *Theory of Plasticity*, McGraw-Hill Book Company, Singapore, 1987 (2nd printing 1988).
- /11/ Clough, R. W. and Penzien, J.: *Dynamics of Structures*, McGraw-Hill, USA, 1975.
- /12/ Cook, R. D., Malkus, D. S. and Plesha, M. E.: *Concepts and applications of finite element analysis*, third ed., John Wiley & Sons, Inc., New York, 1989.
- /13/ Dafalias, Y. F. and Popov, E. P.: A model of non-linearly hardening materials for complex loadings, *Acta Mechanica*, vol. 21, 1975, pp 173-192.



- 
- /14/ Dahlberg, T.: Some railroad settlement models - a critical review, paper submitted to *IMEchE Journal of Rail and Rapid Transit*, accepted for publication September 2000, revised October 16, 2000.
- /15/ Desai, C. S. and Siriwardane, H. J.: *Constitutive laws for engineering materials. With emphasis on geologic materials*, Prentice-Hall Inc., Englewood Cliffs, New Jersey, USA, 1984.
- /16/ Donaghe, R. T.; Chaney, R. C. and Silver M. L. (eds.): *Advanced Triaxial Testing of Soil and Rock*, STP 977, ASTM, Philadelphia, 1988.
- /17/ Duncan, J. M. and Dunlop, P.: The significance of cap and base restraint, *ASCE Journal of the Soil Mechanics and Foundation Division*, vol. 94, no. SM1, 1968, pp 271-290.
- /18/ Eisenmann, J.: Die Schiene als Träger und Fahrbahn - theoretische Grundlagen und praktische Beispiele, in Fastenrath, F. (ed.) *Die Eisenbahnschiene*, Verlag von Wilhlem Ernst & Sohn, Germany, 1977, pp 9-78 (in German).
- /19/ Elhannani, M.: *Modélisation et Simulation Numérique des Chaussées Souples*, Ph.D. thesis, University of Nantes, France, 1991 (in French).
- /20/ El-Sibaie, M.: On the component of track damping resistance and related damping measurements, *Applied Mechanics Rail Transportation Symposium 1988, Winter Annual Meeting of ASME*, pp 59-68.
- /21/ El-Sibaie, M.: A beam on elastic foundation track model for use in a multi-body system simulation, *Transportation Systems 1990, Winter Annual Meeting of ASME*, pp 149-156.
- /22/ Esveld, C.: *Modern Railway Track*, MRT-Productions, Duisburg, Germany, 1989.
- /23/ European Rail Research Institute (ERRI): *Unified assessment criteria for ballast quality and methods for assessing the ballast condition in the track. Determining the criteria for ballast durability using triaxial tests*, Report No. D 182/RP 3, European Rail Research Institute, Utrecht, The Netherlands, 1994.
- /24/ Finansdepartementet (Ministry of Finance): *Storingsproposisjon nr. 1 (2001-2002). For budsjetterminen 2002. Den kongelige proposisjon om statsbudsjettet medregnet folketrygden for budsjetterminen 1. januar - 31. desember 2002. Samferdselsdepartementets fagproposisjon*, Finansdepartementet, Oslo, 2001 (in Norwegian).
- /25/ Frýba, L: *Vibration of Solids and Structures under Moving Loads*, 3rd edition, Thomas Telford, London, 1999.
- /26/ Gaaljord, P. J.; Paute, J. L.; Dawson, A. R. and Gillett, S. D.: Comparison and performance of repeated load triaxial test equipment for unbound granular materials, *Proceedings Euroflex 93 Symposium*, LNEC, Lisbon, 1993, pp 1/1-1/26.
- /27/ Ghaboussi, J., Pecknold, D. A. W. and Wu, X.: *Nonlinear analysis in structural mechanics*, class notes from a graduate course at the Dept. of Civil Engineering, Univ. of Illinois at Urbana-Champaign, USA, 1996.
- /28/ Gåsemeyr, H.: *Dimensjonering av overbygningen*, Baneteknikkurs, Jernbaneskolen, Oslo, 1995 (in Norwegian).

- 
- /29/ Hay, W. W.: *Railroad Engineering*, John Wiley, New York, 1982.
- /30/ Hetényi, M.: *Beams on elastic foundation. Theory with applications in the fields of civil and mechanical engineering*, The University of Michigan Press, Ann Arbor, 1946 (sixth printing 1961).
- /31/ Hicks, R.G. and Monismith, C.L.: Factors influencing the resilient response of granular materials, *Highway Research Record No. 345*, Highway Research Board, Washington D. C., 1971, pp 15-31.
- /32/ Hjelmstad, K. D. and Taciroglu, E.: A Coupled Hyperelastic Constitutive Model for Resilient Response of Granular Materials, *Proceedings: Aircraft/Pavement Technology in the Midst of Change*, Seattle, Washington, August 17-20, 1997, pp 178-189.
- /33/ Hoff, Inge and Nordal, R. S.: *Permanente deformasjoner i granulære lag i dekkekonstruksjoner*, report no. STF22 A00451, SINTEF, Trondheim, Norway, 2000.
- /34/ Hoff, I.: *Material Properties of Unbound Aggregates for Pavement Structures*, doctoral thesis, Department of Road and Railway Engineering, The Norwegian University of Science and Technology, Trondheim, Norway, 1999.
- /35/ Hoff, I., Nordal, S. and Nordal, R.: New hyperelastic model for granular materials in pavement structures, *Proceedings of the Fifth International Conference on the Bearing Capacity of Roads and Airfields*, Trondheim, Norway, July 6-8, 1998, pp 1315-1324.
- /36/ Hornych, P. and Gerard, A.: A pneumatic repeatd load triaxial apparatus for unbound granular materials and subgrade soils, *Workshop on Modelling and Advanced Testing for Unbound Granular Materials 21-22 January 1999*, organised by IST, Lisbon, Portugal (preprint).
- /37/ Hornych, P.; Kazai, A. and Piau, J.-M.: Study of the resilient behaviour of unbound granular materials, *Proceedings of the Fifth International Conference on the Bearing Capacity of Roads and Airfields*, Trondheim, Norway, July 6-8, 1998, pp1277-1287.
- /38/ Hunt, G. A.: Track Loading and Damage, paper 2 in *Vehicle/Track Interaction*, lecture to Nordic Seminar on Permanent Way Technology, Report No. LR TSM 003, British Rail Research, Derby, 1994.
- /39/ Iwan, W. D.: On a class of models for the yielding behaviour of continous and composite systems, *ASME Journal of Applied Mechanics*, vol. 34, 1967, pp 612-617.
- /40/ Iwnicki, S. D. (ed.): The Manchester Benchmarks for Rail Vehicle Simulation, contributions from 'International Workshop on Computer Simulation of Rail Vehicle Dynamics', Manchester June 23-24 1997, printed as a supplement to *Vehicle system dynamics*, vol. 31,1999.
- /41/ Jacobsson, L.: *A Plasticity Model for Cohesionless Material with Emphasis on Railway Ballast*, licentiate thesis, Department of Solid Mechanics, Chalmers University of Technology, Göteborg, 1999.
- /42/ Jefferies, M.: Plastic work and isotropic softening in unloading, Technical Note, *Géotechnique*, vol. 47, no. 5, 1997, pp 1037-1042.

- 
- /43/ Jernbaneverket (Norwegian National Rail Administration): JD 530 Overbygning, Regler for prosjektering, *Teknisk regelverk*, submitted by Hovedkontoret, Jernbaneverket, Oslo, 1998 (in Norwegian).
- /44/ Jernbaneverket (Norwegian National Rail Administration): *Teknisk spesifikasjon. Krav til ballastpukk*, m/vedlegg, versjon 2.0, Hovedkontoret, Teknisk avdeling, Oslo, 1998 (in Norwegian).
- /45/ Jernbaneverket (Norwegian National Rail Administration): *Jernbaneverkets rutiner for testing av ballastpukk*, JBV Ingeniørtjenesten, Oslo, 1997 (in Norwegian).
- /46/ Jernbaneverket (Norwegian National Rail Administration): A/S Franzefoss Bruk, Vassfjellet pukkverk. Vurdering av pukkprøve, *saksref. 97/537 JI 722*, Ingeniørtjenesten, Oslo, 1997 (in Norwegian).
- /47/ Khan, A. S. and Huang, S.: *Continuum theory of plasticity*, John Wiley & Sons Inc., New York, 1995.
- /48/ Kerr, Arnold D.: *On the stress analysis of rails and ties*, Report no. FRA-OR&D-76-284, Federal Railroad Administration, U.S. Department of Transportation, Washington D.C., 1976.
- /49/ Kerr, Arnold D.: Elastic and Viscoelastic Foundation Models, *Transactions of the ASME Journal of Applied Mechanics*, September 1964, pp 491-498.
- /50/ Knutson, R. M.; Thompson, M. R.; Mullin, T. and Tayabji, S. D.: *Materials Evaluation Study - Ballast and Foundation Research Program*, FRA-OR&D-77-02, Federal Railroad Administration, U.S. Department of Transportation, Washington D.C., 1977.
- /51/ Kolisoja, P.: *Resilient Deformation Characteristics of Granular Materials*, Dr. Techn. Thesis, Tampere University of Technology, Finland, 1997.
- /52/ Kolymbas, D. and Herle, I.: Hypoplasticity: A framework to model granular materials, *Behaviour of granular materials*, B. Cambou (ed.), CISM courses and lectures no. 385, Springer-Verlag Wien New York, pp 239-268.
- /53/ Krieg, R. D.: A practical two-surface plasticity theory, *Journal of Applied Mechanics, Transactions of the ASME*, E42, 1975, pp 641-646.
- /54/ Lekarp, F. and Isacsson, U.: Development of a large-scale triaxial apparatus for characterization of granular materials, *Road Materials and Pavement Design*, vol.1, no. 2/2000, HERMES Science Europe Ltd., UK, pp 165-196.
- /55/ Lekarp, F.; Isacsson, U. and Dawson, A.: State of the Art. I: Resilient Response of Unbound Aggregates, *ASCE Journal of Transportation Engineering*, vol. 126, no. 1, 2000, pp 66-75.
- /56/ Lekarp, F.: *Permanent deformation behaviour of unbound granular materials*, licentiate thesis, Dept. of Infrastructure and Planning, Royal Institute of Technology, Stockholm, 1997.

- 
- /57/ Marquis, B. P.; Weinstock, H. and Carr, G.: The effect of load sequence on GRMS measurements, *Proceedings of the 1997 IEEE/ASME Joint Railroad Conference*, Boston, pp 237-246.
- /58/ Mayhew, H. C.: Resilient properties of unbound roadbase under repeated triaxial loading, Report No. LR 1088, Transport Research Laboratory, Great Britain, 1983.
- /59/ Mendelson, A.: *Plasticity: Theory and Application*, The MacMillan Company, New York, 1968.
- /60/ Mróz, Z.: Elastoplastic and viscoplastic constitutive models for granular materials, *Behaviour of granular materials*, B. Cambou (ed.), CISM courses and lectures no. 385, Springer-Verlag Wien New York, 1998, pp 269-337.
- /61/ Mróz, Z. and Zienkiewicz, O. C.: Uniform Formulation of Constitutive Equations for Clays and Sands, *Mechanics of Engineering Materials*, D. S. Desai and R. H. Gallagher (eds.), John Wiley & Sons Ltd., New York, 1984, pp 415-449.
- /62/ Mróz, Z.: On the description of anisotropic workhardening, *Journal of the Mechanics and Physics of Solids*, vol. 15, 1967, pp 163-175.
- /63/ Myrvang, A.: *Kompendium i bergmekanikk*, Department of Geology and Mineral Resources Engineering, The Norwegian University of Science and Technology, Trondheim, Norway, 1996 (in Norwegian).
- /64/ Nordal, S.: *Soil Modelling*, class notes from EEU course/dr.ing. course 33584, Dept. of Geotechnical Engineering, The Norwegian Institute of Technology, Trondheim, 1994.
- /65/ Nordal, S. and Grande, L.: *Forelesningsnotater i Geoteknikk 2*, Dept. of Geotechnical Engineering, The Norwegian Institute of Technology, Trondheim, 1989 (in Norwegian).
- /66/ Norwegian National Rail Administration, Hovedkontoret: *Teknisk regelverk, JD 530 Overbygning - Prosjektering*, Rev. 0, Oslo, 1998 (in Norwegian).
- /67/ Pappin, J. W. and Brown, S. F.: Resilient stress-strain behaviour of a crushed rock, *Proceedings of the international symposium on soils under cyclic and transient loading*, G. N. Pande and O. C. Zienkiewicz (eds.), Swansea, 7-11 Jan. 1980, pp169-177.
- /68/ Puzrin, A. M. and Houlsby, G. T.: Fundamentals of kinematic hardening hyperplasticity, *International Journal of Solids and Structures*, vol. 38, 2001, pp 3771-3794.
- /69/ Riessberger, K.: Track - Part of the System 'Railway', lecture notes for *Nordisk Baneteknisk Ingeniørutdanning*, part 3 of seminar arranged by NSB, Norway, 1994-95.
- /70/ Saada, A. S.: Hollow Cylinder Torsional Devices: Their Advantages and Limitations, *Advanced Triaxial Testing of Soil and Rock*, STP 977, Donaghe, R. T.; Chaney, R. C. and Silver M. L. (eds.), ASTM, Philadelphia, 1988, pp 766-795.
- /71/ Scott, R.: *Foundation Analysis*, Prentice-Hall, Inc., Englewood Cliffs, New Jersey, USA, 1981.
- /72/ Selig, E. and Waters, J. M.: *Track Geotechnology and Substructure Management*, Thomas Telford Publications, London, 1994 (reprint 1995).

- /73/ Selig, E.T. and Li, D.: Track Modulus: Its Meaning and Factors Influencing It, *Transportation Research Record 1470*, Transportation Research Board, Washington D. C., 1994, pp 47-54.
- /74/ Skoglund, K. A.: Dimensionless sensitivity diagrams in mechanistic railway design, paper accepted for publication in the *Proceedings of the Sixth International Conference on the Bearing Capacity of Roads, Railways and Airfields*, Lisbon, Portugal, June 24-26, 2002.
- /75/ Skoglund, K. A.; Hoseth, S. and Værnes, E.: Development of a large triaxial cell apparatus with variable deviatoric and confining stresses, *Proceedings of the fifth international symposium on unbound aggregates in roads* (UNBAR 5), Nottingham, UK, 21-23 June 2000, A. R. Dawson (ed.), A. A. Balkema, pp 145-152.
- /76/ Statens vegvesen: *Håndbok 014 Laboratorieundersøkelser*, Vegdirektoratet, Oslo, 1997 (in Norwegian).
- /77/ Strategic Highway Research Program (SHRP): *SHRP Protocol P46, for SHRP Test Designation UG07, SS07; Resilient modulus of unbound granular base/subbase materials and subgrade soils*, Strategic Highway Research Program, 1993.
- /78/ Timoshenko, S. P.: *Strength of Materials. Part II: Advanced Theory and Problems*, 3. ed., D. van Nostrand Company Inc., New York, 1956.
- /79/ Tsai, N.-C. and Westmann, R. A.: Beam on tensionless foundation, *Journal of the Engineering Mechanics Division*, ASCE, Oct. 1967, pp 1-12.
- /80/ Uzan, J.: Characterization of Granular Material, *Transportation Research Record 1022*, Transportation Research Board, Washington D.C., 1985, pp 52-59.
- /81/ Valanis, K. C.: Endochronic Plasticity: Physical Basis and Applications, *Mechanics of Engineering Materials*, D. S. Desai and R. H. Gallagher (eds.), John Wiley & Sons Ltd., New York, 1984, pp 591-609.
- /82/ Valanis, K. C.: A theory of viscoplasticity without a yield surface, Part I: General theory; Part II: Application to mechanical behaviour of metals, *Archives of Mechanics*, vol. 23, 1971, pp 517-551.
- /83/ van Niekerk, A. A.; van Scheers, J.; Muraya, P. and Kisimbi, A.: The effect of compaction on the mechanical behaviour of mix granulate base course materials and on pavement performance, *Proceedings of the fifth international symposium on unbound aggregates in roads* (UNBAR 5), Nottingham, UK, 21-23 June 2000, A. R. Dawson (ed.), A. A. Balkema, pp 125-136.
- /84/ Veverka, V.: Raming Van de Spoordiepte Bij Wgen met een Bitumineuze Verharding, *De Wegentechniek*, vol. XXIV, no. 3, 1979, pp 25-45 (in Dutch).
- /85/ Vik, A. (ed.): *Temarapport 1997: Ballast*, Nordisk Bro og Geoteknisk samarbeid, Oslo, 1997 (in Norwegian).
- /86/ Vik, G.: Sykliske vakuumbreaksialforsøk på pukk og grus. Sammenligning av resultater fra forsøk på 6 forskjellige grus og steinmaterialer, NGI-report no. 531001-4, Oslo, 1996 (in Norwegian).

- 
- /87/ Wood, D. M.: *Soil Behaviour and Critical State Soil Mechanics*, Cambridge University Press, Great Britain, 1990 (reprint 1996).
- /88/ Zarembski, A. M. and Choros, J.: On the Measurement and Calculation of Vertical Track Modulus, *Proceedings of AREA, Bulletin 675*, Vol. 81, 1980, pp 156-173.
- /89/ Ziegler, H.: *An introduction to thermomechanics*, North-Holland Publishing Company, Amsterdam, 1983.
- /90/ Zienkiewicz, O. C.; Chan, A. H. C.; Pastor, M.; Schrefler, B. A. and Shiomi, T.: *Computational Geomechanics with Special reference to Earthquake Engineering*, John Wiley & Sons Ltd., Great Britain, 1999.
- /91/ Zienkiewicz, O. C. and Taylor, R. L.: *The finite element method*, fourth ed., McGraw-Hill Book Company (UK) Limited, London, 1991.
- /92/ Zienkiewicz, O. C. and Mróz, Z.: Generalized Plasticity Formulation and Application to Geomechanics, *Mechanics of Engineering Materials*, D. S. Desai and R. H. Gallagher (eds.), John Wiley & Sons Ltd., New York, 1984, pp 655-679.
- /93/ Zienkiewicz, O. C.; Leung, K. H.; Hinton, E. and Chang, C. T.: Liquefaction and Permanent Deformation under Dynamic Conditions - Numerical Solution and Constitutive Relations, chapter 5 in G. N. Pande and O. C. Zienkiewicz (eds.): *Soil Mechanics - Transient and Cyclic Loads*, John Wiley & Sons, 1982, pp 71-103.



---

## References

---

- /1/ Adin, M. A.; Yankelevsky, D. Z. and Eisenberger, M: Analysis of beams on bi-moduli elastic foundation, *Computer Methods in Applied Mechanics and Engineering*, Elsevier Science Publishers B.V., vol. 49, 1985, pp 319-330.
- /2/ American Railway Engineering Association: *Manual for Railway Engineering*, Washington D. C., 1996.
- /3/ Bathe, K.-J.: *Finite element procedures*, Prentice-Hall, Inc., New Jersey, USA, 1996.
- /4/ Bishop, A. W. and Green, G. E.: The influence of end restraint on the compression strength of a cohesionless soil, *Géotechnique*, vol. 15, pp 243-266.
- /5/ Boyce, H. R.: A non-linear model for the elastic behaviour of granular materials under repeated loading, *Proceedings of the international symposium on soils under cyclic and transient loading*, Swansea, 7-11 Jan. 1980, G. N. Pande and O. C. Zienkiewicz (eds.), Balkema, pp 285-294.
- /6/ Brandl, H.: *Geotechnics of rail structures, Geotechnics for Roads, Rail Tracks and Earth Structures*, A. Gomes Correia and H. Brandl (eds.), Balkema, Lisse, The Netherlands, 2001, pp 271-288.
- /7/ Cai, Z.; Raymond, P. and Bathurst, R. J.: Estimate of Static Track Modulus Using Elastic Foundation Models, *Transportation Research Record 1470*, Transportation Research Board, Washington D. C., 1994, pp 65-72.
- /8/ CEN: Aggregates for railway ballast, Draft, *prEN 13450*, Brussels, 1999.
- /9/ CEN: Unbound and hydraulic bound mixtures for roads - Test methods - Cyclic load tri-axial test, *prEN 00227413*, Brussels, 1997.
- /10/ Chakrabarty, J.: *Theory of Plasticity*, McGraw-Hill Book Company, Singapore, 1987 (2nd printing 1988).
- /11/ Clough, R. W. and Penzien, J.: *Dynamics of Structures*, McGraw-Hill, USA, 1975.
- /12/ Cook, R. D., Malkus, D. S. and Plesha, M. E.: *Concepts and applications of finite element analysis*, third ed., John Wiley & Sons, Inc., New York, 1989.
- /13/ Dafalias, Y. F. and Popov, E. P.: A model of non-linearly hardening materials for complex loadings, *Acta Mechanica*, vol. 21, 1975, pp 173-192.



- 
- /14/ Dahlberg, T.: Some railroad settlement models - a critical review, paper submitted to *IMechE Journal of Rail and Rapid Transit*, accepted for publication September 2000, revised October 16, 2000.
- /15/ Desai, C. S. and Siriwardane, H. J.: *Constitutive laws for engineering materials. With emphasis on geologic materials*, Prentice-Hall Inc., Englewood Cliffs, New Jersey, USA, 1984.
- /16/ Donaghe, R. T.; Chaney, R. C. and Silver M. L. (eds.): *Advanced Triaxial Testing of Soil and Rock*, STP 977, ASTM, Philadelphia, 1988.
- /17/ Duncan, J. M. and Dunlop, P.: The significance of cap and base restraint, *ASCE Journal of the Soil Mechanics and Foundation Division*, vol. 94, no. SM1, 1968, pp 271-290.
- /18/ Eisenmann, J.: Die Schiene als Träger und Fahrbahn - theoretische Grundlagen und praktische Beispiele, in Fastenrath, F. (ed.) *Die Eisenbahnschiene*, Verlag von Wilhlem Ernst & Sohn, Germany, 1977, pp 9-78 (in German).
- /19/ Elhannani, M.: *Modélisation et Simulation Numérique des Chaussées Souples*, Ph.D. thesis, University of Nantes, France, 1991 (in French).
- /20/ El-Sibaie, M.: On the component of track damping resistance and related damping measurements, *Applied Mechanics Rail Transportation Symposium 1988, Winter Annual Meeting of ASME*, pp 59-68.
- /21/ El-Sibaie, M.: A beam on elastic foundation track model for use in a multi-body system simulation, *Transportation Systems 1990, Winter Annual Meeting of ASME*, pp 149-156.
- /22/ Esveld, C.: *Modern Railway Track*, MRT-Productions, Duisburg, Germany, 1989.
- /23/ European Rail Research Institute (ERRI): *Unified assessment criteria for ballast quality and methods for assessing the ballast condition in the track. Determining the criteria for ballast durability using triaxial tests*, Report No. D 182/RP 3, European Rail Research Institute, Utrecht, The Netherlands, 1994.
- /24/ Finansdepartementet (Ministry of Finance): *Storingsproposisjon nr. 1 (2001-2002). For budsjetterminen 2002. Den kongelige proposisjon om statsbudsjettet medregnet folketrygden for budsjetterminen 1. januar - 31. desember 2002. Samferdselsdepartementets fagproposisjon*, Finansdepartementet, Oslo, 2001 (in Norwegian).
- /25/ Frýba, L: *Vibration of Solids and Structures under Moving Loads*, 3rd edition, Thomas Telford, London, 1999.
- /26/ Gaaljord, P. J.; Paute, J. L.; Dawson, A. R. and Gillett, S. D.: Comparison and performance of repeated load triaxial test equipment for unbound granular materials, *Proceedings Euroflex 93 Symposium*, LNEC, Lisbon, 1993, pp 1/1-1/26.
- /27/ Ghaboussi, J., Pecknold, D. A. W. and Wu, X.: *Nonlinear analysis in structural mechanics*, class notes from a graduate course at the Dept. of Civil Engineering, Univ. of Illinois at Urbana-Champaign, USA, 1996.
- /28/ Gåsemyr, H.: *Dimensjonering av overbygningen*, Baneteknikkurs, Jernbaneskolen, Oslo, 1995 (in Norwegian).

- 
- /29/ Hay, W. W.: *Railroad Engineering*, John Wiley, New York, 1982.
- /30/ Hetényi, M.: *Beams on elastic foundation. Theory with applications in the fields of civil and mechanical engineering*, The University of Michigan Press, Ann Arbor, 1946 (sixth printing 1961).
- /31/ Hicks, R.G. and Monismith, C.L.: Factors influencing the resilient response of granular materials, *Highway Research Record No. 345*, Highway Research Board, Washington D. C., 1971, pp 15-31.
- /32/ Hjelmstad, K. D. and Taciroglu, E.: A Coupled Hyperelastic Constitutive Model for Resilient Response of Granular Materials, *Proceedings: Aircraft/Pavement Technology in the Midst of Change*, Seattle, Washington, August 17-20, 1997, pp 178-189.
- /33/ Hoff, Inge and Nordal, R. S.: *Permanente deformasjoner i granulære lag i dekkekonstruksjoner*, report no. STF22 A00451, SINTEF, Trondheim, Norway, 2000.
- /34/ Hoff, I.: *Material Properties of Unbound Aggregates for Pavement Structures*, doctoral thesis, Department of Road and Railway Engineering, The Norwegian University of Science and Technology, Trondheim, Norway, 1999.
- /35/ Hoff, I., Nordal, S. and Nordal, R.: New hyperelastic model for granular materials in pavement structures, *Proceedings of the Fifth International Conference on the Bearing Capacity of Roads and Airfields*, Trondheim, Norway, July 6-8, 1998, pp 1315-1324.
- /36/ Hornych, P. and Gerard, A.: A pneumatic repeatd load triaxial apparatus for unbound granular materials and subgrade soils, *Workshop on Modelling and Advanced Testing for Unbound Granular Materials 21-22 January 1999*, organised by IST, Lisbon, Portugal (preprint).
- /37/ Hornych, P.; Kazai, A. and Piau, J.-M.: Study of the resilient behaviour of unbound granular materials, *Proceedings of the Fifth International Conference on the Bearing Capacity of Roads and Airfields*, Trondheim, Norway, July 6-8, 1998, pp1277-1287.
- /38/ Hunt, G. A.: Track Loading and Damage, paper 2 in *Vehicle/Track Interaction*, lecture to Nordic Seminar on Permanent Way Technology, Report No. LR TSM 003, British Rail Research, Derby, 1994.
- /39/ Iwan, W. D.: On a class of models for the yielding behaviour of continous and composite systems, *ASME Journal of Applied Mechanics*, vol. 34, 1967, pp 612-617.
- /40/ Iwnicki, S. D. (ed.): The Manchester Benchmarks for Rail Vehicle Simulation, contributions from 'International Workshop on Computer Simulation of Rail Vehicle Dynamics', Manchester June 23-24 1997, printed as a supplement to *Vehicle system dynamics*, vol. 31,1999.
- /41/ Jacobsson, L.: *A Plasticity Model for Cohesionless Material with Emphasis on Railway Ballast*, licentiate thesis, Department of Solid Mechanics, Chalmers University of Technology, Göteborg, 1999.
- /42/ Jefferies, M.: Plastic work and isotropic softening in unloading, Technical Note, *Géotechnique*, vol. 47, no. 5, 1997, pp 1037-1042.

- 
- /43/ Jernbaneverket (Norwegian National Rail Administration): JD 530 Overbygning, Regler for prosjektering, *Teknisk regelverk*, submitted by Hovedkontoret, Jernbaneverket, Oslo, 1998 (in Norwegian).
- /44/ Jernbaneverket (Norwegian National Rail Administration): *Teknisk spesifikasjon. Krav til ballastpukk*, m/vedlegg, versjon 2.0, Hovedkontoret, Teknisk avdeling, Oslo, 1998 (in Norwegian).
- /45/ Jernbaneverket (Norwegian National Rail Administration): *Jernbaneverkets rutiner for testing av ballastpukk*, JBV Ingeniørtjenesten, Oslo, 1997 (in Norwegian).
- /46/ Jernbaneverket (Norwegian National Rail Administration): A/S Franzefoss Bruk, Vassfjellet pukkverk. Vurdering av pukkprøve, *saksref. 97/537 JI 722*, Ingeniørtjenesten, Oslo, 1997 (in Norwegian).
- /47/ Khan, A. S. and Huang, S.: *Continuum theory of plasticity*, John Wiley & Sons Inc., New York, 1995.
- /48/ Kerr, Arnold D.: *On the stress analysis of rails and ties*, Report no. FRA-OR&D-76-284, Federal Railroad Administration, U.S. Department of Transportation, Washington D.C., 1976.
- /49/ Kerr, Arnold D.: Elastic and Viscoelastic Foundation Models, *Transactions of the ASME Journal of Applied Mechanics*, September 1964, pp 491-498.
- /50/ Knutson, R. M.; Thompson, M. R.; Mullin, T. and Tayabji, S. D.: *Materials Evaluation Study - Ballast and Foundation Research Program*, FRA-OR&D-77-02, Federal Railroad Administration, U.S. Department of Transportation, Washington D.C., 1977.
- /51/ Kolisoja, P.: *Resilient Deformation Characteristics of Granular Materials*, Dr. Techn. Thesis, Tampere University of Technology, Finland, 1997.
- /52/ Kolymbas, D. and Herle, I.: Hypoplasticity: A framework to model granular materials, *Behaviour of granular materials*, B. Cambou (ed.), CISM courses and lectures no. 385, Springer-Verlag Wien New York, pp 239-268.
- /53/ Krieg, R. D.: A practical two-surface plasticity theory, *Journal of Applied Mechanics, Transactions of the ASME*, E42, 1975, pp 641-646.
- /54/ Lekarp, F. and Isacsson, U.: Development of a large-scale triaxial apparatus for characterization of granular materials, *Road Materials and Pavement Design*, vol.1, no. 2/2000, HERMES Science Europe Ltd., UK, pp 165-196.
- /55/ Lekarp, F.; Isacsson, U. and Dawson, A.: State of the Art. I: Resilient Response of Unbound Aggregates, *ASCE Journal of Transportation Engineering*, vol. 126, no. 1, 2000, pp 66-75.
- /56/ Lekarp, F.: *Permanent deformation behaviour of unbound granular materials*, licentiate thesis, Dept. of Infrastructure and Planning, Royal Institute of Technology, Stockholm, 1997.

- 
- /57/ Marquis, B. P.; Weinstock, H. and Carr, G.: The effect of load sequence on GRMS measurements, *Proceedings of the 1997 IEEE/ASME Joint Railroad Conference*, Boston, pp 237-246.
- /58/ Mayhew, H. C.: Resilient properties of unbound roadbase under repeated triaxial loading, Report No. LR 1088, Transport Research Laboratory, Great Britain, 1983.
- /59/ Mendelson, A.: *Plasticity: Theory and Application*, The MacMillan Company, New York, 1968.
- /60/ Mróz, Z.: Elastoplastic and viscoplastic constitutive models for granular materials, *Behaviour of granular materials*, B. Cambou (ed.), CISM courses and lectures no. 385, Springer-Verlag Wien New York, 1998, pp 269-337.
- /61/ Mróz, Z. and Zienkiewicz, O. C.: Uniform Formulation of Constitutive Equations for Clays and Sands, *Mechanics of Engineering Materials*, D. S. Desai and R. H. Gallagher (eds.), John Wiley & Sons Ltd., New York, 1984, pp 415-449.
- /62/ Mróz, Z.: On the description of anisotropic workhardening, *Journal of the Mechanics and Physics of Solids*, vol. 15, 1967, pp 163-175.
- /63/ Myrvang, A.: *Kompendium i bergmekanikk*, Department of Geology and Mineral Resources Engineering, The Norwegian University of Science and Technology, Trondheim, Norway, 1996 (in Norwegian).
- /64/ Nordal, S.: *Soil Modelling*, class notes from EEU course/dr.ing. course 33584, Dept. of Geotechnical Engineering, The Norwegian Institute of Technology, Trondheim, 1994.
- /65/ Nordal, S. and Grande, L.: *Forelesningsnotater i Geoteknikk 2*, Dept. of Geotechnical Engineering, The Norwegian Institute of Technology, Trondheim, 1989 (in Norwegian).
- /66/ Norwegian National Rail Administration, Hovedkontoret: *Teknisk regelverk, JD 530 Overbygning - Prosjektering*, Rev. 0, Oslo, 1998 (in Norwegian).
- /67/ Pappin, J. W. and Brown, S. F.: Resilient stress-strain behaviour of a crushed rock, *Proceedings of the international symposium on soils under cyclic and transient loading*, G. N. Pande and O. C. Zienkiewicz (eds.), Swansea, 7-11 Jan. 1980, pp169-177.
- /68/ Puzrin, A. M. and Houlsby, G. T.: Fundamentals of kinematic hardening hyperplasticity, *International Journal of Solids and Structures*, vol. 38, 2001, pp 3771-3794.
- /69/ Riessberger, K.: Track - Part of the System 'Railway', lecture notes for *Nordisk Baneteknisk Ingeniørutdanning*, part 3 of seminar arranged by NSB, Norway, 1994-95.
- /70/ Saada, A. S.: Hollow Cylinder Torsional Devices: Their Advantages and Limitations, *Advanced Triaxial Testing of Soil and Rock*, STP 977, Donaghe, R. T.; Chaney, R. C. and Silver M. L. (eds.), ASTM, Philadelphia, 1988, pp 766-795.
- /71/ Scott, R.: *Foundation Analysis*, Prentice-Hall, Inc., Englewood Cliffs, New Jersey, USA, 1981.
- /72/ Selig, E. and Waters, J. M.: *Track Geotechnology and Substructure Management*, Thomas Telford Publications, London, 1994 (reprint 1995).

- /73/ Selig, E.T. and Li, D.: Track Modulus: Its Meaning and Factors Influencing It, *Transportation Research Record 1470*, Transportation Research Board, Washington D. C., 1994, pp 47-54.
- /74/ Skoglund, K. A.: Dimensionless sensitivity diagrams in mechanistic railway design, paper accepted for publication in the *Proceedings of the Sixth International Conference on the Bearing Capacity of Roads, Railways and Airfields*, Lisbon, Portugal, June 24-26, 2002.
- /75/ Skoglund, K. A.; Hoseth, S. and Værnes, E.: Development of a large triaxial cell apparatus with variable deviatoric and confining stresses, *Proceedings of the fifth international symposium on unbound aggregates in roads* (UNBAR 5), Nottingham, UK, 21-23 June 2000, A. R. Dawson (ed.), A. A. Balkema, pp 145-152.
- /76/ Statens vegvesen: *Håndbok 014 Laboratorieundersøkelser*, Vegdirektoratet, Oslo, 1997 (in Norwegian).
- /77/ Strategic Highway Research Program (SHRP): *SHRP Protocol P46, for SHRP Test Designation UG07, SS07; Resilient modulus of unbound granular base/subbase materials and subgrade soils*, Strategic Highway Research Program, 1993.
- /78/ Timoshenko, S. P.: *Strength of Materials. Part II: Advanced Theory and Problems*, 3. ed., D. van Nostrand Company Inc., New York, 1956.
- /79/ Tsai, N.-C. and Westmann, R. A.: Beam on tensionless foundation, *Journal of the Engineering Mechanics Division*, ASCE, Oct. 1967, pp 1-12.
- /80/ Uzan, J.: Characterization of Granular Material, *Transportation Research Record 1022*, Transportation Research Board, Washington D.C., 1985, pp 52-59.
- /81/ Valanis, K. C.: Endochronic Plasticity: Physical Basis and Applications, *Mechanics of Engineering Materials*, D. S. Desai and R. H. Gallagher (eds.), John Wiley & Sons Ltd., New York, 1984, pp 591-609.
- /82/ Valanis, K. C.: A theory of viscoplasticity without a yield surface, Part I: General theory; Part II: Application to mechanical behaviour of metals, *Archives of Mechanics*, vol. 23, 1971, pp 517-551.
- /83/ van Niekerk, A. A.; van Scheers, J.; Muraya, P. and Kisimbi, A.: The effect of compaction on the mechanical behaviour of mix granulate base course materials and on pavement performance, *Proceedings of the fifth international symposium on unbound aggregates in roads* (UNBAR 5), Nottingham, UK, 21-23 June 2000, A. R. Dawson (ed.), A. A. Balkema, pp 125-136.
- /84/ Veverka, V.: Raming Van de Spoordiepte Bij Wgen met een Bitumineuze Verharding, *De Wegentechniek*, vol. XXIV, no. 3, 1979, pp 25-45 (in Dutch).
- /85/ Vik, A. (ed.): *Temarapport 1997: Ballast*, Nordisk Bro og Geoteknisk samarbeid, Oslo, 1997 (in Norwegian).
- /86/ Vik, G.: Sykliske vakuumbreaksialforsøk på pukk og grus. Sammenligning av resultater fra forsøk på 6 forskjellige grus og steinmaterialer, NGI-report no. 531001-4, Oslo, 1996 (in Norwegian).

- 
- /87/ Wood, D. M.: *Soil Behaviour and Critical State Soil Mechanics*, Cambridge University Press, Great Britain, 1990 (reprint 1996).
- /88/ Zarembski, A. M. and Choros, J.: On the Measurement and Calculation of Vertical Track Modulus, *Proceedings of AREA, Bulletin 675*, Vol. 81, 1980, pp 156-173.
- /89/ Ziegler, H.: *An introduction to thermomechanics*, North-Holland Publishing Company, Amsterdam, 1983.
- /90/ Zienkiewicz, O. C.; Chan, A. H. C.; Pastor, M.; Schrefler, B. A. and Shiomi, T.: *Computational Geomechanics with Special reference to Earthquake Engineering*, John Wiley & Sons Ltd., Great Britain, 1999.
- /91/ Zienkiewicz, O. C. and Taylor, R. L.: *The finite element method*, fourth ed., McGraw-Hill Book Company (UK) Limited, London, 1991.
- /92/ Zienkiewicz, O. C. and Mróz, Z.: Generalized Plasticity Formulation and Application to Geomechanics, *Mechanics of Engineering Materials*, D. S. Desai and R. H. Gallagher (eds.), John Wiley & Sons Ltd., New York, 1984, pp 655-679.
- /93/ Zienkiewicz, O. C.; Leung, K. H.; Hinton, E. and Chang, C. T.: Liquefaction and Permanent Deformation under Dynamic Conditions - Numerical Solution and Constitutive Relations, chapter 5 in G. N. Pande and O. C. Zienkiewicz (eds.): *Soil Mechanics - Transient and Cyclic Loads*, John Wiley & Sons, 1982, pp 71-103.



---

## References

---

- /1/ Adin, M. A.; Yankelevsky, D. Z. and Eisenberger, M: Analysis of beams on bi-moduli elastic foundation, *Computer Methods in Applied Mechanics and Engineering*, Elsevier Science Publishers B.V., vol. 49, 1985, pp 319-330.
- /2/ American Railway Engineering Association: *Manual for Railway Engineering*, Washington D. C., 1996.
- /3/ Bathe, K.-J.: *Finite element procedures*, Prentice-Hall, Inc., New Jersey, USA, 1996.
- /4/ Bishop, A. W. and Green, G. E.: The influence of end restraint on the compression strength of a cohesionless soil, *Géotechnique*, vol. 15, pp 243-266.
- /5/ Boyce, H. R.: A non-linear model for the elastic behaviour of granular materials under repeated loading, *Proceedings of the international symposium on soils under cyclic and transient loading*, Swansea, 7-11 Jan. 1980, G. N. Pande and O. C. Zienkiewicz (eds.), Balkema, pp 285-294.
- /6/ Brandl, H.: *Geotechnics of rail structures, Geotechnics for Roads, Rail Tracks and Earth Structures*, A. Gomes Correia and H. Brandl (eds.), Balkema, Lisse, The Netherlands, 2001, pp 271-288.
- /7/ Cai, Z.; Raymond, P. and Bathurst, R. J.: Estimate of Static Track Modulus Using Elastic Foundation Models, *Transportation Research Record 1470*, Transportation Research Board, Washington D. C., 1994, pp 65-72.
- /8/ CEN: Aggregates for railway ballast, Draft, *prEN 13450*, Brussels, 1999.
- /9/ CEN: Unbound and hydraulic bound mixtures for roads - Test methods - Cyclic load tri-axial test, *prEN 00227413*, Brussels, 1997.
- /10/ Chakrabarty, J.: *Theory of Plasticity*, McGraw-Hill Book Company, Singapore, 1987 (2nd printing 1988).
- /11/ Clough, R. W. and Penzien, J.: *Dynamics of Structures*, McGraw-Hill, USA, 1975.
- /12/ Cook, R. D., Malkus, D. S. and Plesha, M. E.: *Concepts and applications of finite element analysis*, third ed., John Wiley & Sons, Inc., New York, 1989.
- /13/ Dafalias, Y. F. and Popov, E. P.: A model of non-linearly hardening materials for complex loadings, *Acta Mechanica*, vol. 21, 1975, pp 173-192.



- 
- /14/ Dahlberg, T.: Some railroad settlement models - a critical review, paper submitted to *IMEchE Journal of Rail and Rapid Transit*, accepted for publication September 2000, revised October 16, 2000.
- /15/ Desai, C. S. and Siriwardane, H. J.: *Constitutive laws for engineering materials. With emphasis on geologic materials*, Prentice-Hall Inc., Englewood Cliffs, New Jersey, USA, 1984.
- /16/ Donaghe, R. T.; Chaney, R. C. and Silver M. L. (eds.): *Advanced Triaxial Testing of Soil and Rock*, STP 977, ASTM, Philadelphia, 1988.
- /17/ Duncan, J. M. and Dunlop, P.: The significance of cap and base restraint, *ASCE Journal of the Soil Mechanics and Foundation Division*, vol. 94, no. SM1, 1968, pp 271-290.
- /18/ Eisenmann, J.: Die Schiene als Träger und Fahrbahn - theoretische Grundlagen und praktische Beispiele, in Fastenrath, F. (ed.) *Die Eisenbahnschiene*, Verlag von Wilhlem Ernst & Sohn, Germany, 1977, pp 9-78 (in German).
- /19/ Elhannani, M.: *Modélisation et Simulation Numérique des Chaussées Souples*, Ph.D. thesis, University of Nantes, France, 1991 (in French).
- /20/ El-Sibaie, M.: On the component of track damping resistance and related damping measurements, *Applied Mechanics Rail Transportation Symposium 1988, Winter Annual Meeting of ASME*, pp 59-68.
- /21/ El-Sibaie, M.: A beam on elastic foundation track model for use in a multi-body system simulation, *Transportation Systems 1990, Winter Annual Meeting of ASME*, pp 149-156.
- /22/ Esveld, C.: *Modern Railway Track*, MRT-Productions, Duisburg, Germany, 1989.
- /23/ European Rail Research Institute (ERRI): *Unified assessment criteria for ballast quality and methods for assessing the ballast condition in the track. Determining the criteria for ballast durability using triaxial tests*, Report No. D 182/RP 3, European Rail Research Institute, Utrecht, The Netherlands, 1994.
- /24/ Finansdepartementet (Ministry of Finance): *Storingsproposisjon nr. 1 (2001-2002). For budsjetterminen 2002. Den kongelige proposisjon om statsbudsjettet medregnet folketrygden for budsjetterminen 1. januar - 31. desember 2002. Samferdselsdepartementets fagproposisjon*, Finansdepartementet, Oslo, 2001 (in Norwegian).
- /25/ Frýba, L: *Vibration of Solids and Structures under Moving Loads*, 3rd edition, Thomas Telford, London, 1999.
- /26/ Gaaljord, P. J.; Paute, J. L.; Dawson, A. R. and Gillett, S. D.: Comparison and performance of repeated load triaxial test equipment for unbound granular materials, *Proceedings Euroflex 93 Symposium*, LNEC, Lisbon, 1993, pp 1/1-1/26.
- /27/ Ghaboussi, J., Pecknold, D. A. W. and Wu, X.: *Nonlinear analysis in structural mechanics*, class notes from a graduate course at the Dept. of Civil Engineering, Univ. of Illinois at Urbana-Champaign, USA, 1996.
- /28/ Gåsemyr, H.: *Dimensjonering av overbygningen*, Baneteknikkurs, Jernbaneskolen, Oslo, 1995 (in Norwegian).

- 
- /29/ Hay, W. W.: *Railroad Engineering*, John Wiley, New York, 1982.
- /30/ Hetényi, M.: *Beams on elastic foundation. Theory with applications in the fields of civil and mechanical engineering*, The University of Michigan Press, Ann Arbor, 1946 (sixth printing 1961).
- /31/ Hicks, R.G. and Monismith, C.L.: Factors influencing the resilient response of granular materials, *Highway Research Record No. 345*, Highway Research Board, Washington D. C., 1971, pp 15-31.
- /32/ Hjelmstad, K. D. and Taciroglu, E.: A Coupled Hyperelastic Constitutive Model for Resilient Response of Granular Materials, *Proceedings: Aircraft/Pavement Technology in the Midst of Change*, Seattle, Washington, August 17-20, 1997, pp 178-189.
- /33/ Hoff, Inge and Nordal, R. S.: *Permanente deformasjoner i granulære lag i dekkekonstruksjoner*, report no. STF22 A00451, SINTEF, Trondheim, Norway, 2000.
- /34/ Hoff, I.: *Material Properties of Unbound Aggregates for Pavement Structures*, doctoral thesis, Department of Road and Railway Engineering, The Norwegian University of Science and Technology, Trondheim, Norway, 1999.
- /35/ Hoff, I., Nordal, S. and Nordal, R.: New hyperelastic model for granular materials in pavement structures, *Proceedings of the Fifth International Conference on the Bearing Capacity of Roads and Airfields*, Trondheim, Norway, July 6-8, 1998, pp 1315-1324.
- /36/ Hornych, P. and Gerard, A.: A pneumatic repeatd load triaxial apparatus for unbound granular materials and subgrade soils, *Workshop on Modelling and Advanced Testing for Unbound Granular Materials 21-22 January 1999*, organised by IST, Lisbon, Portugal (preprint).
- /37/ Hornych, P.; Kazai, A. and Piau, J.-M.: Study of the resilient behaviour of unbound granular materials, *Proceedings of the Fifth International Conference on the Bearing Capacity of Roads and Airfields*, Trondheim, Norway, July 6-8, 1998, pp1277-1287.
- /38/ Hunt, G. A.: Track Loading and Damage, paper 2 in *Vehicle/Track Interaction*, lecture to Nordic Seminar on Permanent Way Technology, Report No. LR TSM 003, British Rail Research, Derby, 1994.
- /39/ Iwan, W. D.: On a class of models for the yielding behaviour of continous and composite systems, *ASME Journal of Applied Mechanics*, vol. 34, 1967, pp 612-617.
- /40/ Iwnicki, S. D. (ed.): The Manchester Benchmarks for Rail Vehicle Simulation, contributions from 'International Workshop on Computer Simulation of Rail Vehicle Dynamics', Manchester June 23-24 1997, printed as a supplement to *Vehicle system dynamics*, vol. 31,1999.
- /41/ Jacobsson, L.: *A Plasticity Model for Cohesionless Material with Emphasis on Railway Ballast*, licentiate thesis, Department of Solid Mechanics, Chalmers University of Technology, Göteborg, 1999.
- /42/ Jefferies, M.: Plastic work and isotropic softening in unloading, Technical Note, *Géotechnique*, vol. 47, no. 5, 1997, pp 1037-1042.

- 
- /43/ Jernbaneverket (Norwegian National Rail Administration): JD 530 Overbygning, Regler for prosjektering, *Teknisk regelverk*, submitted by Hovedkontoret, Jernbaneverket, Oslo, 1998 (in Norwegian).
- /44/ Jernbaneverket (Norwegian National Rail Administration): *Teknisk spesifikasjon. Krav til ballastpukk*, m/vedlegg, versjon 2.0, Hovedkontoret, Teknisk avdeling, Oslo, 1998 (in Norwegian).
- /45/ Jernbaneverket (Norwegian National Rail Administration): *Jernbaneverkets rutiner for testing av ballastpukk*, JBV Ingeniørtjenesten, Oslo, 1997 (in Norwegian).
- /46/ Jernbaneverket (Norwegian National Rail Administration): A/S Franzefoss Bruk, Vassfjellet pukkverk. Vurdering av pukkprøve, *saksref. 97/537 JI 722*, Ingeniørtjenesten, Oslo, 1997 (in Norwegian).
- /47/ Khan, A. S. and Huang, S.: *Continuum theory of plasticity*, John Wiley & Sons Inc., New York, 1995.
- /48/ Kerr, Arnold D.: *On the stress analysis of rails and ties*, Report no. FRA-OR&D-76-284, Federal Railroad Administration, U.S. Department of Transportation, Washington D.C., 1976.
- /49/ Kerr, Arnold D.: Elastic and Viscoelastic Foundation Models, *Transactions of the ASME Journal of Applied Mechanics*, September 1964, pp 491-498.
- /50/ Knutson, R. M.; Thompson, M. R.; Mullin, T. and Tayabji, S. D.: *Materials Evaluation Study - Ballast and Foundation Research Program*, FRA-OR&D-77-02, Federal Railroad Administration, U.S. Department of Transportation, Washington D.C., 1977.
- /51/ Kolisoja, P.: *Resilient Deformation Characteristics of Granular Materials*, Dr. Techn. Thesis, Tampere University of Technology, Finland, 1997.
- /52/ Kolymbas, D. and Herle, I.: Hypoplasticity: A framework to model granular materials, *Behaviour of granular materials*, B. Cambou (ed.), CISM courses and lectures no. 385, Springer-Verlag Wien New York, pp 239-268.
- /53/ Krieg, R. D.: A practical two-surface plasticity theory, *Journal of Applied Mechanics, Transactions of the ASME*, E42, 1975, pp 641-646.
- /54/ Lekarp, F. and Isacsson, U.: Development of a large-scale triaxial apparatus for characterization of granular materials, *Road Materials and Pavement Design*, vol.1, no. 2/2000, HERMES Science Europe Ltd., UK, pp 165-196.
- /55/ Lekarp, F.; Isacsson, U. and Dawson, A.: State of the Art. I: Resilient Response of Unbound Aggregates, *ASCE Journal of Transportation Engineering*, vol. 126, no. 1, 2000, pp 66-75.
- /56/ Lekarp, F.: *Permanent deformation behaviour of unbound granular materials*, licentiate thesis, Dept. of Infrastructure and Planning, Royal Institute of Technology, Stockholm, 1997.

- 
- /57/ Marquis, B. P.; Weinstock, H. and Carr, G.: The effect of load sequence on GRMS measurements, *Proceedings of the 1997 IEEE/ASME Joint Railroad Conference*, Boston, pp 237-246.
- /58/ Mayhew, H. C.: Resilient properties of unbound roadbase under repeated triaxial loading, Report No. LR 1088, Transport Research Laboratory, Great Britain, 1983.
- /59/ Mendelson, A.: *Plasticity: Theory and Application*, The MacMillan Company, New York, 1968.
- /60/ Mróz, Z.: Elastoplastic and viscoplastic constitutive models for granular materials, *Behaviour of granular materials*, B. Cambou (ed.), CISM courses and lectures no. 385, Springer-Verlag Wien New York, 1998, pp 269-337.
- /61/ Mróz, Z. and Zienkiewicz, O. C.: Uniform Formulation of Constitutive Equations for Clays and Sands, *Mechanics of Engineering Materials*, D. S. Desai and R. H. Gallagher (eds.), John Wiley & Sons Ltd., New York, 1984, pp 415-449.
- /62/ Mróz, Z.: On the description of anisotropic workhardening, *Journal of the Mechanics and Physics of Solids*, vol. 15, 1967, pp 163-175.
- /63/ Myrvang, A.: *Kompendium i bergmekanikk*, Department of Geology and Mineral Resources Engineering, The Norwegian University of Science and Technology, Trondheim, Norway, 1996 (in Norwegian).
- /64/ Nordal, S.: *Soil Modelling*, class notes from EEU course/dr.ing. course 33584, Dept. of Geotechnical Engineering, The Norwegian Institute of Technology, Trondheim, 1994.
- /65/ Nordal, S. and Grande, L.: *Forelesningsnotater i Geoteknikk 2*, Dept. of Geotechnical Engineering, The Norwegian Institute of Technology, Trondheim, 1989 (in Norwegian).
- /66/ Norwegian National Rail Administration, Hovedkontoret: *Teknisk regelverk, JD 530 Overbygning - Prosjektering*, Rev. 0, Oslo, 1998 (in Norwegian).
- /67/ Pappin, J. W. and Brown, S. F.: Resilient stress-strain behaviour of a crushed rock, *Proceedings of the international symposium on soils under cyclic and transient loading*, G. N. Pande and O. C. Zienkiewicz (eds.), Swansea, 7-11 Jan. 1980, pp169-177.
- /68/ Puzrin, A. M. and Houlsby, G. T.: Fundamentals of kinematic hardening hyperplasticity, *International Journal of Solids and Structures*, vol. 38, 2001, pp 3771-3794.
- /69/ Riessberger, K.: Track - Part of the System 'Railway', lecture notes for *Nordisk Baneteknisk Ingeniørutdanning*, part 3 of seminar arranged by NSB, Norway, 1994-95.
- /70/ Saada, A. S.: Hollow Cylinder Torsional Devices: Their Advantages and Limitations, *Advanced Triaxial Testing of Soil and Rock*, STP 977, Donaghe, R. T.; Chaney, R. C. and Silver M. L. (eds.), ASTM, Philadelphia, 1988, pp 766-795.
- /71/ Scott, R.: *Foundation Analysis*, Prentice-Hall, Inc., Englewood Cliffs, New Jersey, USA, 1981.
- /72/ Selig, E. and Waters, J. M.: *Track Geotechnology and Substructure Management*, Thomas Telford Publications, London, 1994 (reprint 1995).

- /73/ Selig, E.T. and Li, D.: Track Modulus: Its Meaning and Factors Influencing It, *Transportation Research Record 1470*, Transportation Research Board, Washington D. C., 1994, pp 47-54.
- /74/ Skoglund, K. A.: Dimensionless sensitivity diagrams in mechanistic railway design, paper accepted for publication in the *Proceedings of the Sixth International Conference on the Bearing Capacity of Roads, Railways and Airfields*, Lisbon, Portugal, June 24-26, 2002.
- /75/ Skoglund, K. A.; Hoseth, S. and Værnes, E.: Development of a large triaxial cell apparatus with variable deviatoric and confining stresses, *Proceedings of the fifth international symposium on unbound aggregates in roads* (UNBAR 5), Nottingham, UK, 21-23 June 2000, A. R. Dawson (ed.), A. A. Balkema, pp 145-152.
- /76/ Statens vegvesen: *Håndbok 014 Laboratorieundersøkelser*, Vegdirektoratet, Oslo, 1997 (in Norwegian).
- /77/ Strategic Highway Research Program (SHRP): *SHRP Protocol P46, for SHRP Test Designation UG07, SS07; Resilient modulus of unbound granular base/subbase materials and subgrade soils*, Strategic Highway Research Program, 1993.
- /78/ Timoshenko, S. P.: *Strength of Materials. Part II: Advanced Theory and Problems*, 3. ed., D. van Nostrand Company Inc., New York, 1956.
- /79/ Tsai, N.-C. and Westmann, R. A.: Beam on tensionless foundation, *Journal of the Engineering Mechanics Division*, ASCE, Oct. 1967, pp 1-12.
- /80/ Uzan, J.: Characterization of Granular Material, *Transportation Research Record 1022*, Transportation Research Board, Washington D.C., 1985, pp 52-59.
- /81/ Valanis, K. C.: Endochronic Plasticity: Physical Basis and Applications, *Mechanics of Engineering Materials*, D. S. Desai and R. H. Gallagher (eds.), John Wiley & Sons Ltd., New York, 1984, pp 591-609.
- /82/ Valanis, K. C.: A theory of viscoplasticity without a yield surface, Part I: General theory; Part II: Application to mechanical behaviour of metals, *Archives of Mechanics*, vol. 23, 1971, pp 517-551.
- /83/ van Niekerk, A. A.; van Scheers, J.; Muraya, P. and Kisimbi, A.: The effect of compaction on the mechanical behaviour of mix granulate base course materials and on pavement performance, *Proceedings of the fifth international symposium on unbound aggregates in roads* (UNBAR 5), Nottingham, UK, 21-23 June 2000, A. R. Dawson (ed.), A. A. Balkema, pp 125-136.
- /84/ Veverka, V.: Raming Van de Spoordiepte Bij Wgen met een Bitumineuze Verharding, *De Wegentechniek*, vol. XXIV, no. 3, 1979, pp 25-45 (in Dutch).
- /85/ Vik, A. (ed.): *Temarapport 1997: Ballast*, Nordisk Bro og Geoteknisk samarbeid, Oslo, 1997 (in Norwegian).
- /86/ Vik, G.: Sykliske vakuumbreaksialforsøk på pukk og grus. Sammenligning av resultater fra forsøk på 6 forskjellige grus og steinmaterialer, NGI-report no. 531001-4, Oslo, 1996 (in Norwegian).

- 
- /87/ Wood, D. M.: *Soil Behaviour and Critical State Soil Mechanics*, Cambridge University Press, Great Britain, 1990 (reprint 1996).
- /88/ Zarembski, A. M. and Choros, J.: On the Measurement and Calculation of Vertical Track Modulus, *Proceedings of AREA, Bulletin 675*, Vol. 81, 1980, pp 156-173.
- /89/ Ziegler, H.: *An introduction to thermomechanics*, North-Holland Publishing Company, Amsterdam, 1983.
- /90/ Zienkiewicz, O. C.; Chan, A. H. C.; Pastor, M.; Schrefler, B. A. and Shiomi, T.: *Computational Geomechanics with Special reference to Earthquake Engineering*, John Wiley & Sons Ltd., Great Britain, 1999.
- /91/ Zienkiewicz, O. C. and Taylor, R. L.: *The finite element method*, fourth ed., McGraw-Hill Book Company (UK) Limited, London, 1991.
- /92/ Zienkiewicz, O. C. and Mróz, Z.: Generalized Plasticity Formulation and Application to Geomechanics, *Mechanics of Engineering Materials*, D. S. Desai and R. H. Gallagher (eds.), John Wiley & Sons Ltd., New York, 1984, pp 655-679.
- /93/ Zienkiewicz, O. C.; Leung, K. H.; Hinton, E. and Chang, C. T.: Liquefaction and Permanent Deformation under Dynamic Conditions - Numerical Solution and Constitutive Relations, chapter 5 in G. N. Pande and O. C. Zienkiewicz (eds.): *Soil Mechanics - Transient and Cyclic Loads*, John Wiley & Sons, 1982, pp 71-103.



---

## References

---

- /1/ Adin, M. A.; Yankelevsky, D. Z. and Eisenberger, M: Analysis of beams on bi-moduli elastic foundation, *Computer Methods in Applied Mechanics and Engineering*, Elsevier Science Publishers B.V., vol. 49, 1985, pp 319-330.
- /2/ American Railway Engineering Association: *Manual for Railway Engineering*, Washington D. C., 1996.
- /3/ Bathe, K.-J.: *Finite element procedures*, Prentice-Hall, Inc., New Jersey, USA, 1996.
- /4/ Bishop, A. W. and Green, G. E.: The influence of end restraint on the compression strength of a cohesionless soil, *Géotechnique*, vol. 15, pp 243-266.
- /5/ Boyce, H. R.: A non-linear model for the elastic behaviour of granular materials under repeated loading, *Proceedings of the international symposium on soils under cyclic and transient loading*, Swansea, 7-11 Jan. 1980, G. N. Pande and O. C. Zienkiewicz (eds.), Balkema, pp 285-294.
- /6/ Brandl, H.: *Geotechnics of rail structures, Geotechnics for Roads, Rail Tracks and Earth Structures*, A. Gomes Correia and H. Brandl (eds.), Balkema, Lisse, The Netherlands, 2001, pp 271-288.
- /7/ Cai, Z.; Raymond, P. and Bathurst, R. J.: Estimate of Static Track Modulus Using Elastic Foundation Models, *Transportation Research Record 1470*, Transportation Research Board, Washington D. C., 1994, pp 65-72.
- /8/ CEN: Aggregates for railway ballast, Draft, *prEN 13450*, Brussels, 1999.
- /9/ CEN: Unbound and hydraulic bound mixtures for roads - Test methods - Cyclic load tri-axial test, *prEN 00227413*, Brussels, 1997.
- /10/ Chakrabarty, J.: *Theory of Plasticity*, McGraw-Hill Book Company, Singapore, 1987 (2nd printing 1988).
- /11/ Clough, R. W. and Penzien, J.: *Dynamics of Structures*, McGraw-Hill, USA, 1975.
- /12/ Cook, R. D., Malkus, D. S. and Plesha, M. E.: *Concepts and applications of finite element analysis*, third ed., John Wiley & Sons, Inc., New York, 1989.
- /13/ Dafalias, Y. F. and Popov, E. P.: A model of non-linearly hardening materials for complex loadings, *Acta Mechanica*, vol. 21, 1975, pp 173-192.



- 
- /14/ Dahlberg, T.: Some railroad settlement models - a critical review, paper submitted to *IMEchE Journal of Rail and Rapid Transit*, accepted for publication September 2000, revised October 16, 2000.
- /15/ Desai, C. S. and Siriwardane, H. J.: *Constitutive laws for engineering materials. With emphasis on geologic materials*, Prentice-Hall Inc., Englewood Cliffs, New Jersey, USA, 1984.
- /16/ Donaghe, R. T.; Chaney, R. C. and Silver M. L. (eds.): *Advanced Triaxial Testing of Soil and Rock*, STP 977, ASTM, Philadelphia, 1988.
- /17/ Duncan, J. M. and Dunlop, P.: The significance of cap and base restraint, *ASCE Journal of the Soil Mechanics and Foundation Division*, vol. 94, no. SM1, 1968, pp 271-290.
- /18/ Eisenmann, J.: Die Schiene als Träger und Fahrbahn - theoretische Grundlagen und praktische Beispiele, in Fastenrath, F. (ed.) *Die Eisenbahnschiene*, Verlag von Wilhlem Ernst & Sohn, Germany, 1977, pp 9-78 (in German).
- /19/ Elhannani, M.: *Modélisation et Simulation Numérique des Chaussées Souples*, Ph.D. thesis, University of Nantes, France, 1991 (in French).
- /20/ El-Sibaie, M.: On the component of track damping resistance and related damping measurements, *Applied Mechanics Rail Transportation Symposium 1988, Winter Annual Meeting of ASME*, pp 59-68.
- /21/ El-Sibaie, M.: A beam on elastic foundation track model for use in a multi-body system simulation, *Transportation Systems 1990, Winter Annual Meeting of ASME*, pp 149-156.
- /22/ Esveld, C.: *Modern Railway Track*, MRT-Productions, Duisburg, Germany, 1989.
- /23/ European Rail Research Institute (ERRI): *Unified assessment criteria for ballast quality and methods for assessing the ballast condition in the track. Determining the criteria for ballast durability using triaxial tests*, Report No. D 182/RP 3, European Rail Research Institute, Utrecht, The Netherlands, 1994.
- /24/ Finansdepartementet (Ministry of Finance): *Storingsproposisjon nr. 1 (2001-2002). For budsjetterminen 2002. Den kongelige proposisjon om statsbudsjettet medregnet folketrygden for budsjetterminen 1. januar - 31. desember 2002. Samferdselsdepartementets fagproposisjon*, Finansdepartementet, Oslo, 2001 (in Norwegian).
- /25/ Frýba, L: *Vibration of Solids and Structures under Moving Loads*, 3rd edition, Thomas Telford, London, 1999.
- /26/ Gaaljord, P. J.; Paute, J. L.; Dawson, A. R. and Gillett, S. D.: Comparison and performance of repeated load triaxial test equipment for unbound granular materials, *Proceedings Euroflex 93 Symposium*, LNEC, Lisbon, 1993, pp 1/1-1/26.
- /27/ Ghaboussi, J., Pecknold, D. A. W. and Wu, X.: *Nonlinear analysis in structural mechanics*, class notes from a graduate course at the Dept. of Civil Engineering, Univ. of Illinois at Urbana-Champaign, USA, 1996.
- /28/ Gåsemeyr, H.: *Dimensjonering av overbygningen*, Baneteknikkurs, Jernbaneskolen, Oslo, 1995 (in Norwegian).

- 
- /29/ Hay, W. W.: *Railroad Engineering*, John Wiley, New York, 1982.
- /30/ Hetényi, M.: *Beams on elastic foundation. Theory with applications in the fields of civil and mechanical engineering*, The University of Michigan Press, Ann Arbor, 1946 (sixth printing 1961).
- /31/ Hicks, R.G. and Monismith, C.L.: Factors influencing the resilient response of granular materials, *Highway Research Record No. 345*, Highway Research Board, Washington D. C., 1971, pp 15-31.
- /32/ Hjelmstad, K. D. and Taciroglu, E.: A Coupled Hyperelastic Constitutive Model for Resilient Response of Granular Materials, Proceedings: *Aircraft/Pavement Technology in the Midst of Change*, Seattle, Washington, August 17-20, 1997, pp 178-189.
- /33/ Hoff, Inge and Nordal, R. S.: *Permanente deformasjoner i granulære lag i dekkekonstruksjoner*, report no. STF22 A00451, SINTEF, Trondheim, Norway, 2000.
- /34/ Hoff, I.: *Material Properties of Unbound Aggregates for Pavement Structures*, doctoral thesis, Department of Road and Railway Engineering, The Norwegian University of Science and Technology, Trondheim, Norway, 1999.
- /35/ Hoff, I., Nordal, S. and Nordal, R.: New hyperelastic model for granular materials in pavement structures, *Proceedings of the Fifth International Conference on the Bearing Capacity of Roads and Airfields*, Trondheim, Norway, July 6-8, 1998, pp 1315-1324.
- /36/ Hornych, P. and Gerard, A.: A pneumatic repeatd load triaxial apparatus for unbound granular materials and subgrade soils, *Workshop on Modelling and Advanced Testing for Unbound Granular Materials 21-22 January 1999*, organised by IST, Lisbon, Portugal (preprint).
- /37/ Hornych, P.; Kazai, A. and Piau, J.-M.: Study of the resilient behaviour of unbound granular materials, *Proceedings of the Fifth International Conference on the Bearing Capacity of Roads and Airfields*, Trondheim, Norway, July 6-8, 1998, pp1277-1287.
- /38/ Hunt, G. A.: Track Loading and Damage, paper 2 in *Vehicle/Track Interaction*, lecture to Nordic Seminar on Permanent Way Technology, Report No. LR TSM 003, British Rail Research, Derby, 1994.
- /39/ Iwan, W. D.: On a class of models for the yielding behaviour of continous and composite systems, *ASME Journal of Applied Mechanics*, vol. 34, 1967, pp 612-617.
- /40/ Iwnicki, S. D. (ed.): The Manchester Benchmarks for Rail Vehicle Simulation, contributions from 'International Workshop on Computer Simulation of Rail Vehicle Dynamics', Manchester June 23-24 1997, printed as a supplement to *Vehicle system dynamics*, vol. 31,1999.
- /41/ Jacobsson, L.: *A Plasticity Model for Cohesionless Material with Emphasis on Railway Ballast*, licentiate thesis, Department of Solid Mechanics, Chalmers University of Technology, Göteborg, 1999.
- /42/ Jefferies, M.: Plastic work and isotropic softening in unloading, Technical Note, *Géotechnique*, vol. 47, no. 5, 1997, pp 1037-1042.

- 
- /43/ Jernbaneverket (Norwegian National Rail Administration): JD 530 Overbygning, Regler for prosjektering, *Teknisk regelverk*, submitted by Hovedkontoret, Jernbaneverket, Oslo, 1998 (in Norwegian).
- /44/ Jernbaneverket (Norwegian National Rail Administration): *Teknisk spesifikasjon. Krav til ballastpukk*, m/vedlegg, versjon 2.0, Hovedkontoret, Teknisk avdeling, Oslo, 1998 (in Norwegian).
- /45/ Jernbaneverket (Norwegian National Rail Administration): *Jernbaneverkets rutiner for testing av ballastpukk*, JBV Ingeniørtjenesten, Oslo, 1997 (in Norwegian).
- /46/ Jernbaneverket (Norwegian National Rail Administration): A/S Franzefoss Bruk, Vassfjellet pukkverk. Vurdering av pukkprøve, *saksref. 97/537 JI 722*, Ingeniørtjenesten, Oslo, 1997 (in Norwegian).
- /47/ Khan, A. S. and Huang, S.: *Continuum theory of plasticity*, John Wiley & Sons Inc., New York, 1995.
- /48/ Kerr, Arnold D.: *On the stress analysis of rails and ties*, Report no. FRA-OR&D-76-284, Federal Railroad Administration, U.S. Department of Transportation, Washington D.C., 1976.
- /49/ Kerr, Arnold D.: Elastic and Viscoelastic Foundation Models, *Transactions of the ASME Journal of Applied Mechanics*, September 1964, pp 491-498.
- /50/ Knutson, R. M.; Thompson, M. R.; Mullin, T. and Tayabji, S. D.: *Materials Evaluation Study - Ballast and Foundation Research Program*, FRA-OR&D-77-02, Federal Railroad Administration, U.S. Department of Transportation, Washington D.C., 1977.
- /51/ Kolisoja, P.: *Resilient Deformation Characteristics of Granular Materials*, Dr. Techn. Thesis, Tampere University of Technology, Finland, 1997.
- /52/ Kolymbas, D. and Herle, I.: Hypoplasticity: A framework to model granular materials, *Behaviour of granular materials*, B. Cambou (ed.), CISM courses and lectures no. 385, Springer-Verlag Wien New York, pp 239-268.
- /53/ Krieg, R. D.: A practical two-surface plasticity theory, *Journal of Applied Mechanics, Transactions of the ASME*, E42, 1975, pp 641-646.
- /54/ Lekarp, F. and Isacsson, U.: Development of a large-scale triaxial apparatus for characterization of granular materials, *Road Materials and Pavement Design*, vol.1, no. 2/2000, HERMES Science Europe Ltd., UK, pp 165-196.
- /55/ Lekarp, F.; Isacsson, U. and Dawson, A.: State of the Art. I: Resilient Response of Unbound Aggregates, *ASCE Journal of Transportation Engineering*, vol. 126, no. 1, 2000, pp 66-75.
- /56/ Lekarp, F.: *Permanent deformation behaviour of unbound granular materials*, licentiate thesis, Dept. of Infrastructure and Planning, Royal Institute of Technology, Stockholm, 1997.

- 
- /57/ Marquis, B. P.; Weinstock, H. and Carr, G.: The effect of load sequence on GRMS measurements, *Proceedings of the 1997 IEEE/ASME Joint Railroad Conference*, Boston, pp 237-246.
- /58/ Mayhew, H. C.: Resilient properties of unbound roadbase under repeated triaxial loading, Report No. LR 1088, Transport Research Laboratory, Great Britain, 1983.
- /59/ Mendelson, A.: *Plasticity: Theory and Application*, The MacMillan Company, New York, 1968.
- /60/ Mróz, Z.: Elastoplastic and viscoplastic constitutive models for granular materials, *Behaviour of granular materials*, B. Cambou (ed.), CISM courses and lectures no. 385, Springer-Verlag Wien New York, 1998, pp 269-337.
- /61/ Mróz, Z. and Zienkiewicz, O. C.: Uniform Formulation of Constitutive Equations for Clays and Sands, *Mechanics of Engineering Materials*, D. S. Desai and R. H. Gallagher (eds.), John Wiley & Sons Ltd., New York, 1984, pp 415-449.
- /62/ Mróz, Z.: On the description of anisotropic workhardening, *Journal of the Mechanics and Physics of Solids*, vol. 15, 1967, pp 163-175.
- /63/ Myrvang, A.: *Kompendium i bergmekanikk*, Department of Geology and Mineral Resources Engineering, The Norwegian University of Science and Technology, Trondheim, Norway, 1996 (in Norwegian).
- /64/ Nordal, S.: *Soil Modelling*, class notes from EEU course/dr.ing. course 33584, Dept. of Geotechnical Engineering, The Norwegian Institute of Technology, Trondheim, 1994.
- /65/ Nordal, S. and Grande, L.: *Forelesningsnotater i Geoteknikk 2*, Dept. of Geotechnical Engineering, The Norwegian Institute of Technology, Trondheim, 1989 (in Norwegian).
- /66/ Norwegian National Rail Administration, Hovedkontoret: *Teknisk regelverk, JD 530 Overbygning - Prosjektering*, Rev. 0, Oslo, 1998 (in Norwegian).
- /67/ Pappin, J. W. and Brown, S. F.: Resilient stress-strain behaviour of a crushed rock, *Proceedings of the international symposium on soils under cyclic and transient loading*, G. N. Pande and O. C. Zienkiewicz (eds.), Swansea, 7-11 Jan. 1980, pp169-177.
- /68/ Puzrin, A. M. and Houlsby, G. T.: Fundamentals of kinematic hardening hyperplasticity, *International Journal of Solids and Structures*, vol. 38, 2001, pp 3771-3794.
- /69/ Riessberger, K.: Track - Part of the System 'Railway', lecture notes for *Nordisk Baneteknisk Ingeniørutdanning*, part 3 of seminar arranged by NSB, Norway, 1994-95.
- /70/ Saada, A. S.: Hollow Cylinder Torsional Devices: Their Advantages and Limitations, *Advanced Triaxial Testing of Soil and Rock*, STP 977, Donaghe, R. T.; Chaney, R. C. and Silver M. L. (eds.), ASTM, Philadelphia, 1988, pp 766-795.
- /71/ Scott, R.: *Foundation Analysis*, Prentice-Hall, Inc., Englewood Cliffs, New Jersey, USA, 1981.
- /72/ Selig, E. and Waters, J. M.: *Track Geotechnology and Substructure Management*, Thomas Telford Publications, London, 1994 (reprint 1995).

- /73/ Selig, E.T. and Li, D.: Track Modulus: Its Meaning and Factors Influencing It, *Transportation Research Record 1470*, Transportation Research Board, Washington D. C., 1994, pp 47-54.
- /74/ Skoglund, K. A.: Dimensionless sensitivity diagrams in mechanistic railway design, paper accepted for publication in the *Proceedings of the Sixth International Conference on the Bearing Capacity of Roads, Railways and Airfields*, Lisbon, Portugal, June 24-26, 2002.
- /75/ Skoglund, K. A.; Hoseth, S. and Værnes, E.: Development of a large triaxial cell apparatus with variable deviatoric and confining stresses, *Proceedings of the fifth international symposium on unbound aggregates in roads* (UNBAR 5), Nottingham, UK, 21-23 June 2000, A. R. Dawson (ed.), A. A. Balkema, pp 145-152.
- /76/ Statens vegvesen: *Håndbok 014 Laboratorieundersøkelser*, Vegdirektoratet, Oslo, 1997 (in Norwegian).
- /77/ Strategic Highway Research Program (SHRP): *SHRP Protocol P46, for SHRP Test Designation UG07, SS07; Resilient modulus of unbound granular base/subbase materials and subgrade soils*, Strategic Highway Research Program, 1993.
- /78/ Timoshenko, S. P.: *Strength of Materials. Part II: Advanced Theory and Problems*, 3. ed., D. van Nostrand Company Inc., New York, 1956.
- /79/ Tsai, N.-C. and Westmann, R. A.: Beam on tensionless foundation, *Journal of the Engineering Mechanics Division*, ASCE, Oct. 1967, pp 1-12.
- /80/ Uzan, J.: Characterization of Granular Material, *Transportation Research Record 1022*, Transportation Research Board, Washington D.C., 1985, pp 52-59.
- /81/ Valanis, K. C.: Endochronic Plasticity: Physical Basis and Applications, *Mechanics of Engineering Materials*, D. S. Desai and R. H. Gallagher (eds.), John Wiley & Sons Ltd., New York, 1984, pp 591-609.
- /82/ Valanis, K. C.: A theory of viscoplasticity without a yield surface, Part I: General theory; Part II: Application to mechanical behaviour of metals, *Archives of Mechanics*, vol. 23, 1971, pp 517-551.
- /83/ van Niekerk, A. A.; van Scheers, J.; Muraya, P. and Kisimbi, A.: The effect of compaction on the mechanical behaviour of mix granulate base course materials and on pavement performance, *Proceedings of the fifth international symposium on unbound aggregates in roads* (UNBAR 5), Nottingham, UK, 21-23 June 2000, A. R. Dawson (ed.), A. A. Balkema, pp 125-136.
- /84/ Veverka, V.: Raming Van de Spoordiepte Bij Wgen met een Bitumineuze Verharding, *De Wegentechniek*, vol. XXIV, no. 3, 1979, pp 25-45 (in Dutch).
- /85/ Vik, A. (ed.): *Temarapport 1997: Ballast*, Nordisk Bro og Geoteknisk samarbeid, Oslo, 1997 (in Norwegian).
- /86/ Vik, G.: Sykliske vakuumbreaksialforsøk på pukk og grus. Sammenligning av resultater fra forsøk på 6 forskjellige grus og steinmaterialer, NGI-report no. 531001-4, Oslo, 1996 (in Norwegian).

- 
- /87/ Wood, D. M.: *Soil Behaviour and Critical State Soil Mechanics*, Cambridge University Press, Great Britain, 1990 (reprint 1996).
- /88/ Zarembski, A. M. and Choros, J.: On the Measurement and Calculation of Vertical Track Modulus, *Proceedings of AREA, Bulletin 675*, Vol. 81, 1980, pp 156-173.
- /89/ Ziegler, H.: *An introduction to thermomechanics*, North-Holland Publishing Company, Amsterdam, 1983.
- /90/ Zienkiewicz, O. C.; Chan, A. H. C.; Pastor, M.; Schrefler, B. A. and Shiomi, T.: *Computational Geomechanics with Special reference to Earthquake Engineering*, John Wiley & Sons Ltd., Great Britain, 1999.
- /91/ Zienkiewicz, O. C. and Taylor, R. L.: *The finite element method*, fourth ed., McGraw-Hill Book Company (UK) Limited, London, 1991.
- /92/ Zienkiewicz, O. C. and Mróz, Z.: Generalized Plasticity Formulation and Application to Geomechanics, *Mechanics of Engineering Materials*, D. S. Desai and R. H. Gallagher (eds.), John Wiley & Sons Ltd., New York, 1984, pp 655-679.
- /93/ Zienkiewicz, O. C.; Leung, K. H.; Hinton, E. and Chang, C. T.: Liquefaction and Permanent Deformation under Dynamic Conditions - Numerical Solution and Constitutive Relations, chapter 5 in G. N. Pande and O. C. Zienkiewicz (eds.): *Soil Mechanics - Transient and Cyclic Loads*, John Wiley & Sons, 1982, pp 71-103.



---

## References

---

- /1/ Adin, M. A.; Yankelevsky, D. Z. and Eisenberger, M: Analysis of beams on bi-moduli elastic foundation, *Computer Methods in Applied Mechanics and Engineering*, Elsevier Science Publishers B.V., vol. 49, 1985, pp 319-330.
- /2/ American Railway Engineering Association: *Manual for Railway Engineering*, Washington D. C., 1996.
- /3/ Bathe, K.-J.: *Finite element procedures*, Prentice-Hall, Inc., New Jersey, USA, 1996.
- /4/ Bishop, A. W. and Green, G. E.: The influence of end restraint on the compression strength of a cohesionless soil, *Géotechnique*, vol. 15, pp 243-266.
- /5/ Boyce, H. R.: A non-linear model for the elastic behaviour of granular materials under repeated loading, *Proceedings of the international symposium on soils under cyclic and transient loading*, Swansea, 7-11 Jan. 1980, G. N. Pande and O. C. Zienkiewicz (eds.), Balkema, pp 285-294.
- /6/ Brandl, H.: *Geotechnics of rail structures, Geotechnics for Roads, Rail Tracks and Earth Structures*, A. Gomes Correia and H. Brandl (eds.), Balkema, Lisse, The Netherlands, 2001, pp 271-288.
- /7/ Cai, Z.; Raymond, P. and Bathurst, R. J.: Estimate of Static Track Modulus Using Elastic Foundation Models, *Transportation Research Record 1470*, Transportation Research Board, Washington D. C., 1994, pp 65-72.
- /8/ CEN: Aggregates for railway ballast, Draft, *prEN 13450*, Brussels, 1999.
- /9/ CEN: Unbound and hydraulic bound mixtures for roads - Test methods - Cyclic load tri-axial test, *prEN 00227413*, Brussels, 1997.
- /10/ Chakrabarty, J.: *Theory of Plasticity*, McGraw-Hill Book Company, Singapore, 1987 (2nd printing 1988).
- /11/ Clough, R. W. and Penzien, J.: *Dynamics of Structures*, McGraw-Hill, USA, 1975.
- /12/ Cook, R. D., Malkus, D. S. and Plesha, M. E.: *Concepts and applications of finite element analysis*, third ed., John Wiley & Sons, Inc., New York, 1989.
- /13/ Dafalias, Y. F. and Popov, E. P.: A model of non-linearly hardening materials for complex loadings, *Acta Mechanica*, vol. 21, 1975, pp 173-192.



- 
- /14/ Dahlberg, T.: Some railroad settlement models - a critical review, paper submitted to *IMEchE Journal of Rail and Rapid Transit*, accepted for publication September 2000, revised October 16, 2000.
- /15/ Desai, C. S. and Siriwardane, H. J.: *Constitutive laws for engineering materials. With emphasis on geologic materials*, Prentice-Hall Inc., Englewood Cliffs, New Jersey, USA, 1984.
- /16/ Donaghe, R. T.; Chaney, R. C. and Silver M. L. (eds.): *Advanced Triaxial Testing of Soil and Rock*, STP 977, ASTM, Philadelphia, 1988.
- /17/ Duncan, J. M. and Dunlop, P.: The significance of cap and base restraint, *ASCE Journal of the Soil Mechanics and Foundation Division*, vol. 94, no. SM1, 1968, pp 271-290.
- /18/ Eisenmann, J.: Die Schiene als Träger und Fahrbahn - theoretische Grundlagen und praktische Beispiele, in Fastenrath, F. (ed.) *Die Eisenbahnschiene*, Verlag von Wilhlem Ernst & Sohn, Germany, 1977, pp 9-78 (in German).
- /19/ Elhannani, M.: *Modélisation et Simulation Numérique des Chaussées Souples*, Ph.D. thesis, University of Nantes, France, 1991 (in French).
- /20/ El-Sibaie, M.: On the component of track damping resistance and related damping measurements, *Applied Mechanics Rail Transportation Symposium 1988, Winter Annual Meeting of ASME*, pp 59-68.
- /21/ El-Sibaie, M.: A beam on elastic foundation track model for use in a multi-body system simulation, *Transportation Systems 1990, Winter Annual Meeting of ASME*, pp 149-156.
- /22/ Esveld, C.: *Modern Railway Track*, MRT-Productions, Duisburg, Germany, 1989.
- /23/ European Rail Research Institute (ERRI): *Unified assessment criteria for ballast quality and methods for assessing the ballast condition in the track. Determining the criteria for ballast durability using triaxial tests*, Report No. D 182/RP 3, European Rail Research Institute, Utrecht, The Netherlands, 1994.
- /24/ Finansdepartementet (Ministry of Finance): *Storingsproposisjon nr. 1 (2001-2002). For budsjetterminen 2002. Den kongelige proposisjon om statsbudsjettet medregnet folketrygden for budsjetterminen 1. januar - 31. desember 2002. Samferdselsdepartementets fagproposisjon*, Finansdepartementet, Oslo, 2001 (in Norwegian).
- /25/ Frýba, L: *Vibration of Solids and Structures under Moving Loads*, 3rd edition, Thomas Telford, London, 1999.
- /26/ Gaaljord, P. J.; Paute, J. L.; Dawson, A. R. and Gillett, S. D.: Comparison and performance of repeated load triaxial test equipment for unbound granular materials, *Proceedings Euroflex 93 Symposium*, LNEC, Lisbon, 1993, pp 1/1-1/26.
- /27/ Ghaboussi, J., Pecknold, D. A. W. and Wu, X.: *Nonlinear analysis in structural mechanics*, class notes from a graduate course at the Dept. of Civil Engineering, Univ. of Illinois at Urbana-Champaign, USA, 1996.
- /28/ Gåsemyr, H.: *Dimensjonering av overbygningen*, Baneteknikkurs, Jernbaneskolen, Oslo, 1995 (in Norwegian).

- 
- /29/ Hay, W. W.: *Railroad Engineering*, John Wiley, New York, 1982.
- /30/ Hetényi, M.: *Beams on elastic foundation. Theory with applications in the fields of civil and mechanical engineering*, The University of Michigan Press, Ann Arbor, 1946 (sixth printing 1961).
- /31/ Hicks, R.G. and Monismith, C.L.: Factors influencing the resilient response of granular materials, *Highway Research Record No. 345*, Highway Research Board, Washington D. C., 1971, pp 15-31.
- /32/ Hjelmstad, K. D. and Taciroglu, E.: A Coupled Hyperelastic Constitutive Model for Resilient Response of Granular Materials, *Proceedings: Aircraft/Pavement Technology in the Midst of Change*, Seattle, Washington, August 17-20, 1997, pp 178-189.
- /33/ Hoff, Inge and Nordal, R. S.: *Permanente deformasjoner i granulære lag i dekkekonstruksjoner*, report no. STF22 A00451, SINTEF, Trondheim, Norway, 2000.
- /34/ Hoff, I.: *Material Properties of Unbound Aggregates for Pavement Structures*, doctoral thesis, Department of Road and Railway Engineering, The Norwegian University of Science and Technology, Trondheim, Norway, 1999.
- /35/ Hoff, I., Nordal, S. and Nordal, R.: New hyperelastic model for granular materials in pavement structures, *Proceedings of the Fifth International Conference on the Bearing Capacity of Roads and Airfields*, Trondheim, Norway, July 6-8, 1998, pp 1315-1324.
- /36/ Hornych, P. and Gerard, A.: A pneumatic repeatd load triaxial apparatus for unbound granular materials and subgrade soils, *Workshop on Modelling and Advanced Testing for Unbound Granular Materials 21-22 January 1999*, organised by IST, Lisbon, Portugal (preprint).
- /37/ Hornych, P.; Kazai, A. and Piau, J.-M.: Study of the resilient behaviour of unbound granular materials, *Proceedings of the Fifth International Conference on the Bearing Capacity of Roads and Airfields*, Trondheim, Norway, July 6-8, 1998, pp1277-1287.
- /38/ Hunt, G. A.: Track Loading and Damage, paper 2 in *Vehicle/Track Interaction*, lecture to Nordic Seminar on Permanent Way Technology, Report No. LR TSM 003, British Rail Research, Derby, 1994.
- /39/ Iwan, W. D.: On a class of models for the yielding behaviour of continous and composite systems, *ASME Journal of Applied Mechanics*, vol. 34, 1967, pp 612-617.
- /40/ Iwnicki, S. D. (ed.): The Manchester Benchmarks for Rail Vehicle Simulation, contributions from 'International Workshop on Computer Simulation of Rail Vehicle Dynamics', Manchester June 23-24 1997, printed as a supplement to *Vehicle system dynamics*, vol. 31,1999.
- /41/ Jacobsson, L.: *A Plasticity Model for Cohesionless Material with Emphasis on Railway Ballast*, licentiate thesis, Department of Solid Mechanics, Chalmers University of Technology, Göteborg, 1999.
- /42/ Jefferies, M.: Plastic work and isotropic softening in unloading, Technical Note, *Géotechnique*, vol. 47, no. 5, 1997, pp 1037-1042.

- 
- /43/ Jernbaneverket (Norwegian National Rail Administration): JD 530 Overbygning, Regler for prosjektering, *Teknisk regelverk*, submitted by Hovedkontoret, Jernbaneverket, Oslo, 1998 (in Norwegian).
- /44/ Jernbaneverket (Norwegian National Rail Administration): *Teknisk spesifikasjon. Krav til ballastpukk*, m/vedlegg, versjon 2.0, Hovedkontoret, Teknisk avdeling, Oslo, 1998 (in Norwegian).
- /45/ Jernbaneverket (Norwegian National Rail Administration): *Jernbaneverkets rutiner for testing av ballastpukk*, JBV Ingeniørtjenesten, Oslo, 1997 (in Norwegian).
- /46/ Jernbaneverket (Norwegian National Rail Administration): A/S Franzefoss Bruk, Vassfjellet pukkverk. Vurdering av pukkprøve, *saksref. 97/537 JI 722*, Ingeniørtjenesten, Oslo, 1997 (in Norwegian).
- /47/ Khan, A. S. and Huang, S.: *Continuum theory of plasticity*, John Wiley & Sons Inc., New York, 1995.
- /48/ Kerr, Arnold D.: *On the stress analysis of rails and ties*, Report no. FRA-OR&D-76-284, Federal Railroad Administration, U.S. Department of Transportation, Washington D.C., 1976.
- /49/ Kerr, Arnold D.: Elastic and Viscoelastic Foundation Models, *Transactions of the ASME Journal of Applied Mechanics*, September 1964, pp 491-498.
- /50/ Knutson, R. M.; Thompson, M. R.; Mullin, T. and Tayabji, S. D.: *Materials Evaluation Study - Ballast and Foundation Research Program*, FRA-OR&D-77-02, Federal Railroad Administration, U.S. Department of Transportation, Washington D.C., 1977.
- /51/ Kolisoja, P.: *Resilient Deformation Characteristics of Granular Materials*, Dr. Techn. Thesis, Tampere University of Technology, Finland, 1997.
- /52/ Kolymbas, D. and Herle, I.: Hypoplasticity: A framework to model granular materials, *Behaviour of granular materials*, B. Cambou (ed.), CISM courses and lectures no. 385, Springer-Verlag Wien New York, pp 239-268.
- /53/ Krieg, R. D.: A practical two-surface plasticity theory, *Journal of Applied Mechanics, Transactions of the ASME*, E42, 1975, pp 641-646.
- /54/ Lekarp, F. and Isacsson, U.: Development of a large-scale triaxial apparatus for characterization of granular materials, *Road Materials and Pavement Design*, vol.1, no. 2/2000, HERMES Science Europe Ltd., UK, pp 165-196.
- /55/ Lekarp, F.; Isacsson, U. and Dawson, A.: State of the Art. I: Resilient Response of Unbound Aggregates, *ASCE Journal of Transportation Engineering*, vol. 126, no. 1, 2000, pp 66-75.
- /56/ Lekarp, F.: *Permanent deformation behaviour of unbound granular materials*, licentiate thesis, Dept. of Infrastructure and Planning, Royal Institute of Technology, Stockholm, 1997.

- 
- /57/ Marquis, B. P.; Weinstock, H. and Carr, G.: The effect of load sequence on GRMS measurements, *Proceedings of the 1997 IEEE/ASME Joint Railroad Conference*, Boston, pp 237-246.
- /58/ Mayhew, H. C.: Resilient properties of unbound roadbase under repeated triaxial loading, Report No. LR 1088, Transport Research Laboratory, Great Britain, 1983.
- /59/ Mendelson, A.: *Plasticity: Theory and Application*, The MacMillan Company, New York, 1968.
- /60/ Mróz, Z.: Elastoplastic and viscoplastic constitutive models for granular materials, *Behaviour of granular materials*, B. Cambou (ed.), CISM courses and lectures no. 385, Springer-Verlag Wien New York, 1998, pp 269-337.
- /61/ Mróz, Z. and Zienkiewicz, O. C.: Uniform Formulation of Constitutive Equations for Clays and Sands, *Mechanics of Engineering Materials*, D. S. Desai and R. H. Gallagher (eds.), John Wiley & Sons Ltd., New York, 1984, pp 415-449.
- /62/ Mróz, Z.: On the description of anisotropic workhardening, *Journal of the Mechanics and Physics of Solids*, vol. 15, 1967, pp 163-175.
- /63/ Myrvang, A.: *Kompendium i bergmekanikk*, Department of Geology and Mineral Resources Engineering, The Norwegian University of Science and Technology, Trondheim, Norway, 1996 (in Norwegian).
- /64/ Nordal, S.: *Soil Modelling*, class notes from EEU course/dr.ing. course 33584, Dept. of Geotechnical Engineering, The Norwegian Institute of Technology, Trondheim, 1994.
- /65/ Nordal, S. and Grande, L.: *Forelesningsnotater i Geoteknikk 2*, Dept. of Geotechnical Engineering, The Norwegian Institute of Technology, Trondheim, 1989 (in Norwegian).
- /66/ Norwegian National Rail Administration, Hovedkontoret: *Teknisk regelverk, JD 530 Overbygning - Prosjektering*, Rev. 0, Oslo, 1998 (in Norwegian).
- /67/ Pappin, J. W. and Brown, S. F.: Resilient stress-strain behaviour of a crushed rock, *Proceedings of the international symposium on soils under cyclic and transient loading*, G. N. Pande and O. C. Zienkiewicz (eds.), Swansea, 7-11 Jan. 1980, pp169-177.
- /68/ Puzrin, A. M. and Houlsby, G. T.: Fundamentals of kinematic hardening hyperplasticity, *International Journal of Solids and Structures*, vol. 38, 2001, pp 3771-3794.
- /69/ Riessberger, K.: Track - Part of the System 'Railway', lecture notes for *Nordisk Baneteknisk Ingeniørutdanning*, part 3 of seminar arranged by NSB, Norway, 1994-95.
- /70/ Saada, A. S.: Hollow Cylinder Torsional Devices: Their Advantages and Limitations, *Advanced Triaxial Testing of Soil and Rock*, STP 977, Donaghe, R. T.; Chaney, R. C. and Silver M. L. (eds.), ASTM, Philadelphia, 1988, pp 766-795.
- /71/ Scott, R.: *Foundation Analysis*, Prentice-Hall, Inc., Englewood Cliffs, New Jersey, USA, 1981.
- /72/ Selig, E. and Waters, J. M.: *Track Geotechnology and Substructure Management*, Thomas Telford Publications, London, 1994 (reprint 1995).

- /73/ Selig, E.T. and Li, D.: Track Modulus: Its Meaning and Factors Influencing It, *Transportation Research Record 1470*, Transportation Research Board, Washington D. C., 1994, pp 47-54.
- /74/ Skoglund, K. A.: Dimensionless sensitivity diagrams in mechanistic railway design, paper accepted for publication in the *Proceedings of the Sixth International Conference on the Bearing Capacity of Roads, Railways and Airfields*, Lisbon, Portugal, June 24-26, 2002.
- /75/ Skoglund, K. A.; Hoseth, S. and Værnes, E.: Development of a large triaxial cell apparatus with variable deviatoric and confining stresses, *Proceedings of the fifth international symposium on unbound aggregates in roads* (UNBAR 5), Nottingham, UK, 21-23 June 2000, A. R. Dawson (ed.), A. A. Balkema, pp 145-152.
- /76/ Statens vegvesen: *Håndbok 014 Laboratorieundersøkelser*, Vegdirektoratet, Oslo, 1997 (in Norwegian).
- /77/ Strategic Highway Research Program (SHRP): *SHRP Protocol P46, for SHRP Test Designation UG07, SS07; Resilient modulus of unbound granular base/subbase materials and subgrade soils*, Strategic Highway Research Program, 1993.
- /78/ Timoshenko, S. P.: *Strength of Materials. Part II: Advanced Theory and Problems*, 3. ed., D. van Nostrand Company Inc., New York, 1956.
- /79/ Tsai, N.-C. and Westmann, R. A.: Beam on tensionless foundation, *Journal of the Engineering Mechanics Division*, ASCE, Oct. 1967, pp 1-12.
- /80/ Uzan, J.: Characterization of Granular Material, *Transportation Research Record 1022*, Transportation Research Board, Washington D.C., 1985, pp 52-59.
- /81/ Valanis, K. C.: Endochronic Plasticity: Physical Basis and Applications, *Mechanics of Engineering Materials*, D. S. Desai and R. H. Gallagher (eds.), John Wiley & Sons Ltd., New York, 1984, pp 591-609.
- /82/ Valanis, K. C.: A theory of viscoplasticity without a yield surface, Part I: General theory; Part II: Application to mechanical behaviour of metals, *Archives of Mechanics*, vol. 23, 1971, pp 517-551.
- /83/ van Niekerk, A. A.; van Scheers, J.; Muraya, P. and Kisimbi, A.: The effect of compaction on the mechanical behaviour of mix granulate base course materials and on pavement performance, *Proceedings of the fifth international symposium on unbound aggregates in roads* (UNBAR 5), Nottingham, UK, 21-23 June 2000, A. R. Dawson (ed.), A. A. Balkema, pp 125-136.
- /84/ Veverka, V.: Raming Van de Spoordiepte Bij Wgen met een Bitumineuze Verharding, *De Wegentechniek*, vol. XXIV, no. 3, 1979, pp 25-45 (in Dutch).
- /85/ Vik, A. (ed.): *Temarapport 1997: Ballast*, Nordisk Bro og Geoteknisk samarbeid, Oslo, 1997 (in Norwegian).
- /86/ Vik, G.: Sykliske vakuumbreaksialforsøk på pukk og grus. Sammenligning av resultater fra forsøk på 6 forskjellige grus og steinmaterialer, NGI-report no. 531001-4, Oslo, 1996 (in Norwegian).

- 
- /87/ Wood, D. M.: *Soil Behaviour and Critical State Soil Mechanics*, Cambridge University Press, Great Britain, 1990 (reprint 1996).
- /88/ Zarembski, A. M. and Choros, J.: On the Measurement and Calculation of Vertical Track Modulus, *Proceedings of AREA, Bulletin 675*, Vol. 81, 1980, pp 156-173.
- /89/ Ziegler, H.: *An introduction to thermomechanics*, North-Holland Publishing Company, Amsterdam, 1983.
- /90/ Zienkiewicz, O. C.; Chan, A. H. C.; Pastor, M.; Schrefler, B. A. and Shiomi, T.: *Computational Geomechanics with Special reference to Earthquake Engineering*, John Wiley & Sons Ltd., Great Britain, 1999.
- /91/ Zienkiewicz, O. C. and Taylor, R. L.: *The finite element method*, fourth ed., McGraw-Hill Book Company (UK) Limited, London, 1991.
- /92/ Zienkiewicz, O. C. and Mróz, Z.: Generalized Plasticity Formulation and Application to Geomechanics, *Mechanics of Engineering Materials*, D. S. Desai and R. H. Gallagher (eds.), John Wiley & Sons Ltd., New York, 1984, pp 655-679.
- /93/ Zienkiewicz, O. C.; Leung, K. H.; Hinton, E. and Chang, C. T.: Liquefaction and Permanent Deformation under Dynamic Conditions - Numerical Solution and Constitutive Relations, chapter 5 in G. N. Pande and O. C. Zienkiewicz (eds.): *Soil Mechanics - Transient and Cyclic Loads*, John Wiley & Sons, 1982, pp 71-103.



## APPENDIX A Dimensionless sensitivity diagrams

When using dimensionless sensitivity diagrams in a design process one may need larger diagrams in order to achieve better accuracy. Such diagrams are reproduced here, both for the ordinary BOEF model and for the conventional beam element model.

### A.1 Diagrams for the ordinary BOEF model

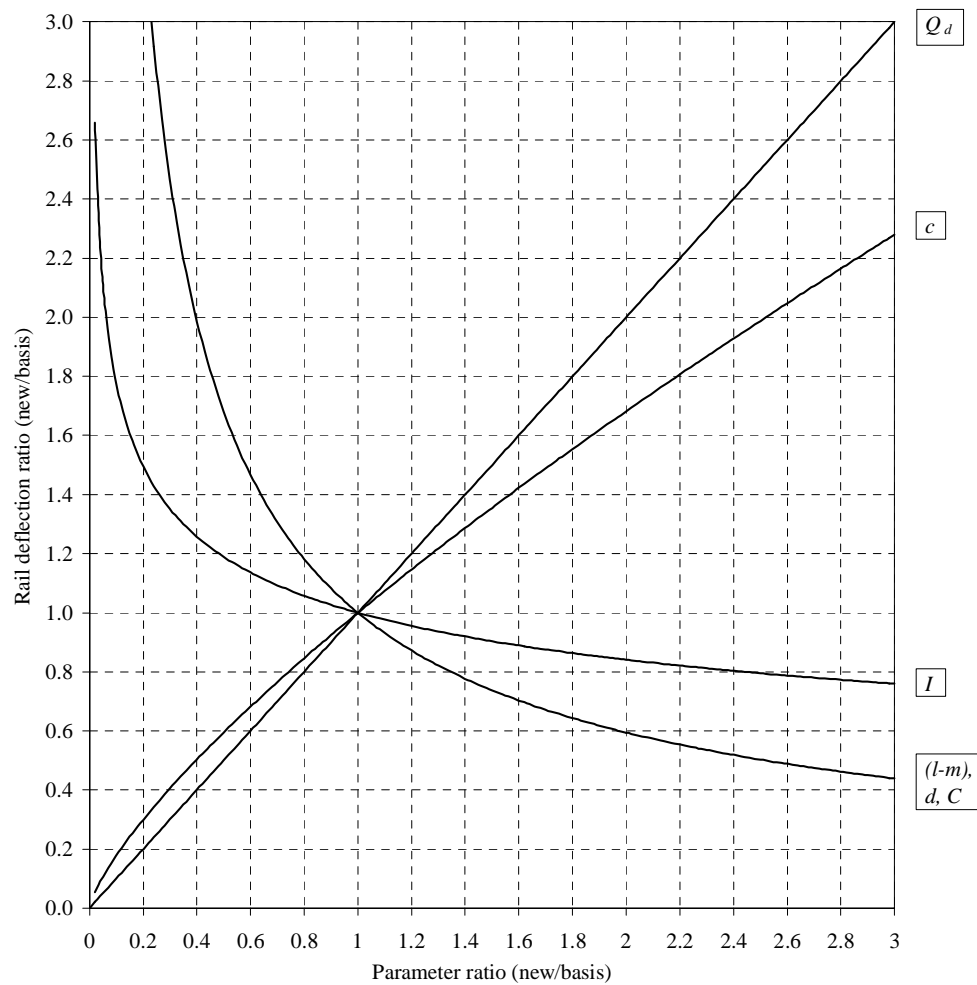


**Figure A.1:** Diagram for rail deflection.



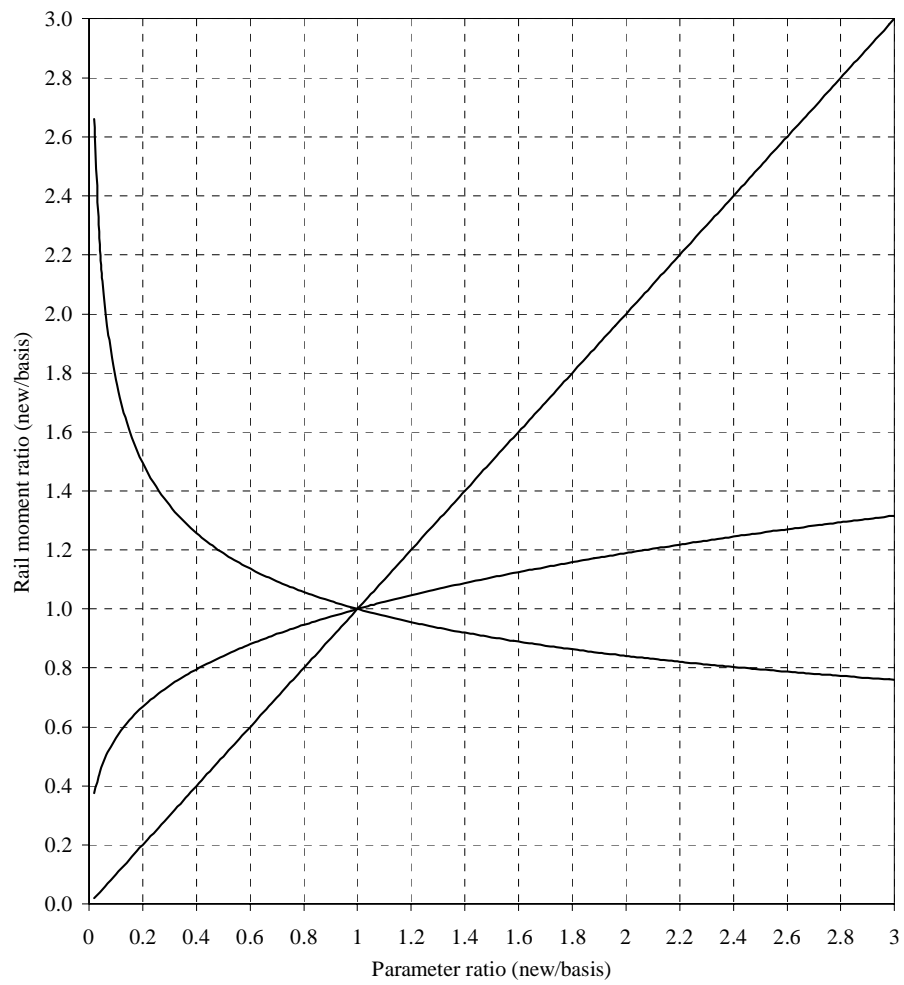


**Figure A.2:** *Diagram for rail moment.*

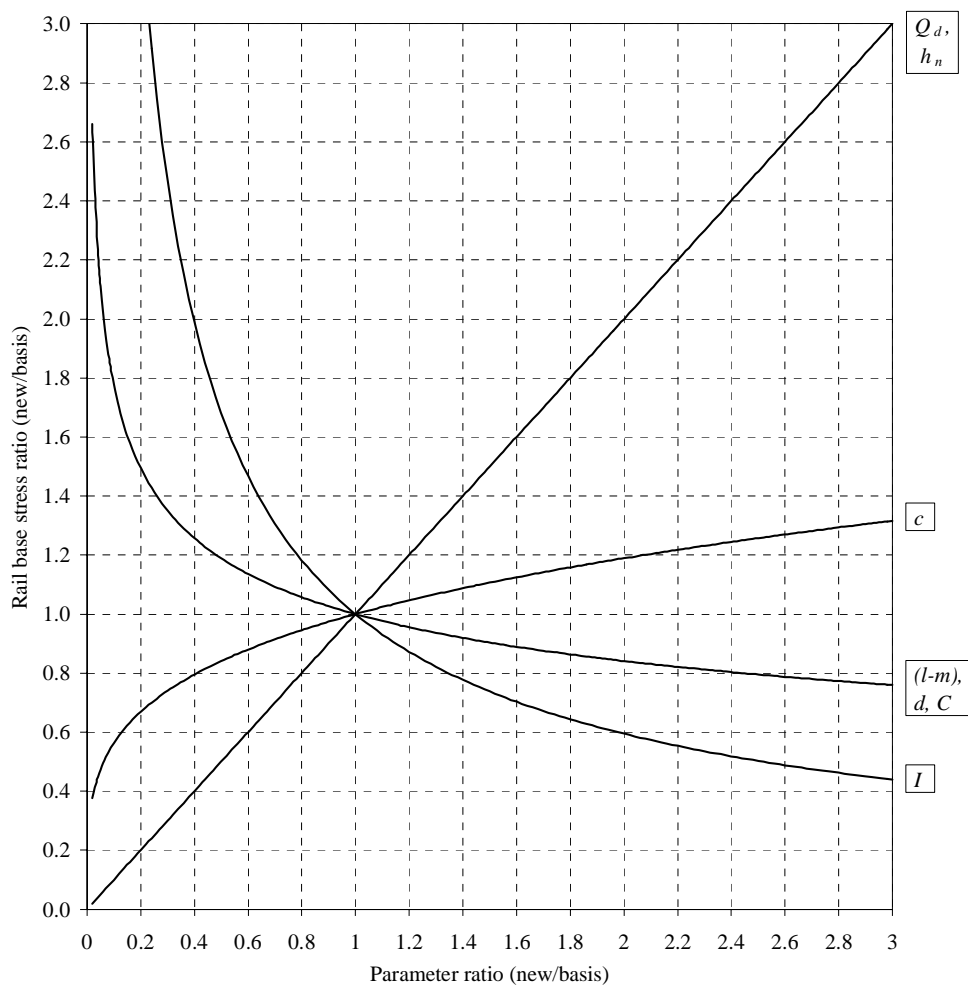
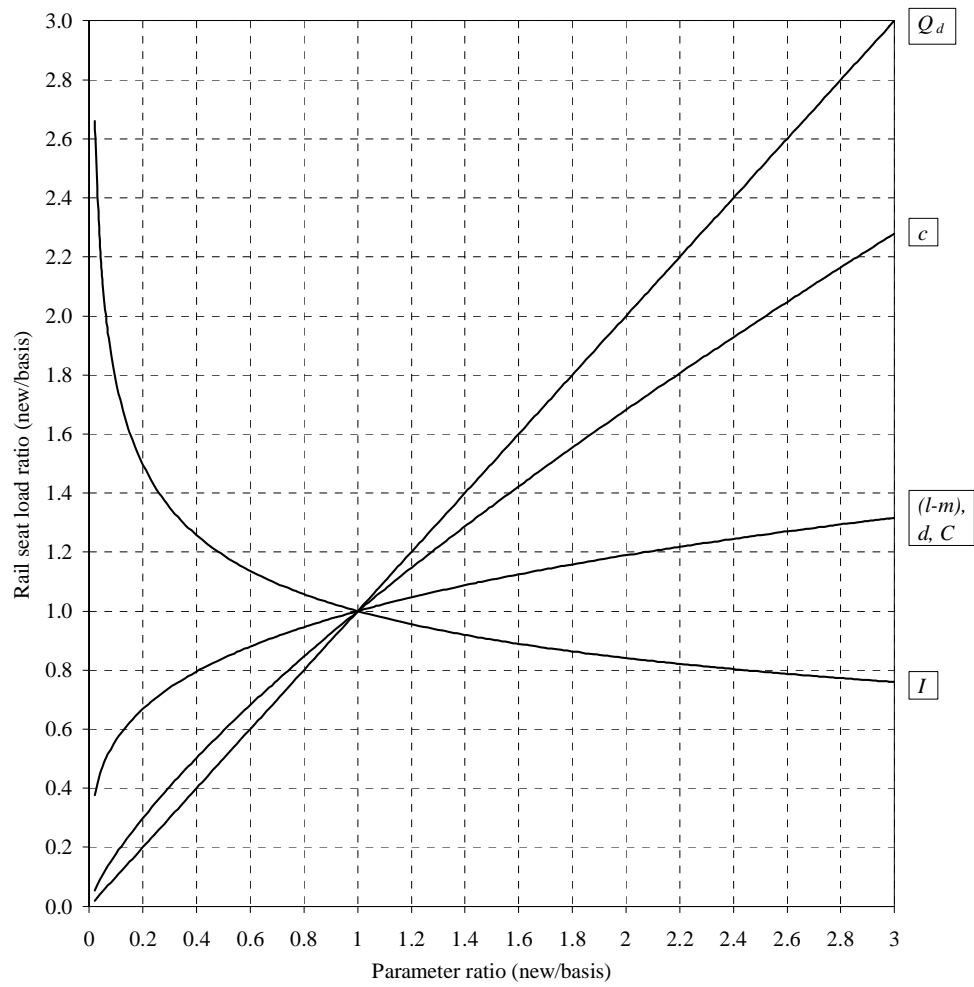
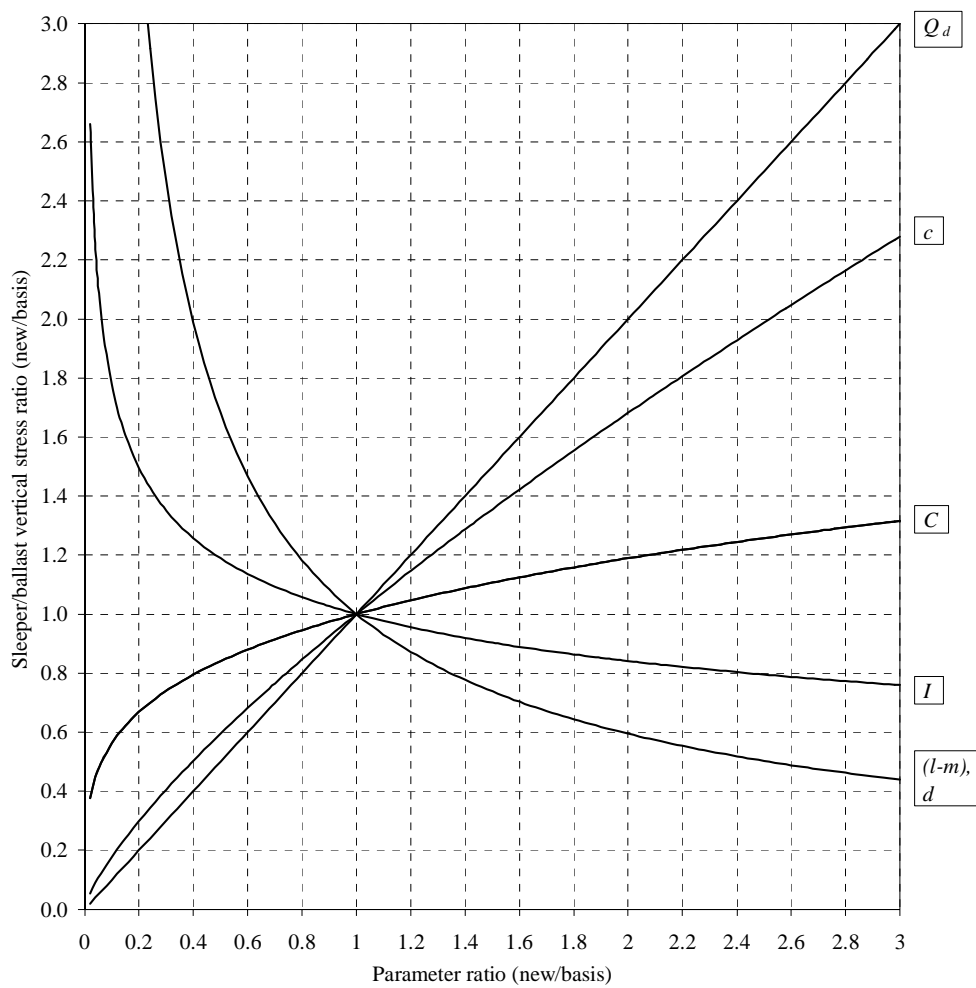


Figure A.3: Diagram for rail base stress.



**Figure A.4:** Diagram for rail seat load.



**Figure A.5:** Diagram for vertical stress between sleeper and ballast.

## A.2 Diagrams for a beam element model

Below three dimensionless diagrams for a beam element model are shown, i.e. for rail deflection, rail moment and for rail seat load. The data for the basis model are given in Table 2.8 on page 45. Regression curves are established and have also been extrapolated in order to cover the same range as in the ordinary BOEF model. Both BOEF curves and beam element model curves are shown, but in many cases the thicker curve of the beam element model hides the thinner one of the BOEF model.

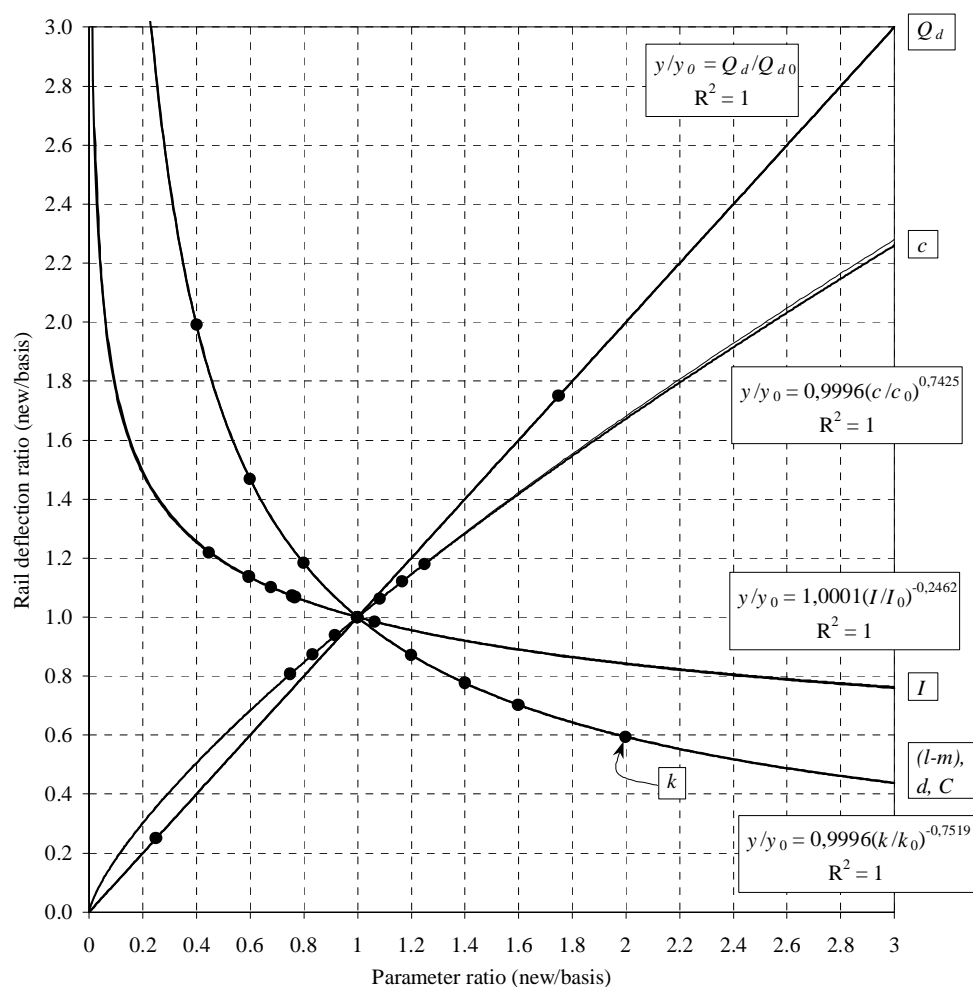


**Figure A.6:** Diagram for rail deflection. Markers represent actual calculated values, whereas the thick lines are regression curves. Regression curve formulas given in boxes along with the  $R^2$ -value. Thin lines represent the BOEF model. Note that the track modulus  $k$  has been used in the beam element model in stead of  $(l-m)$ ,  $d$  and  $C$  (as in the BOEF model).

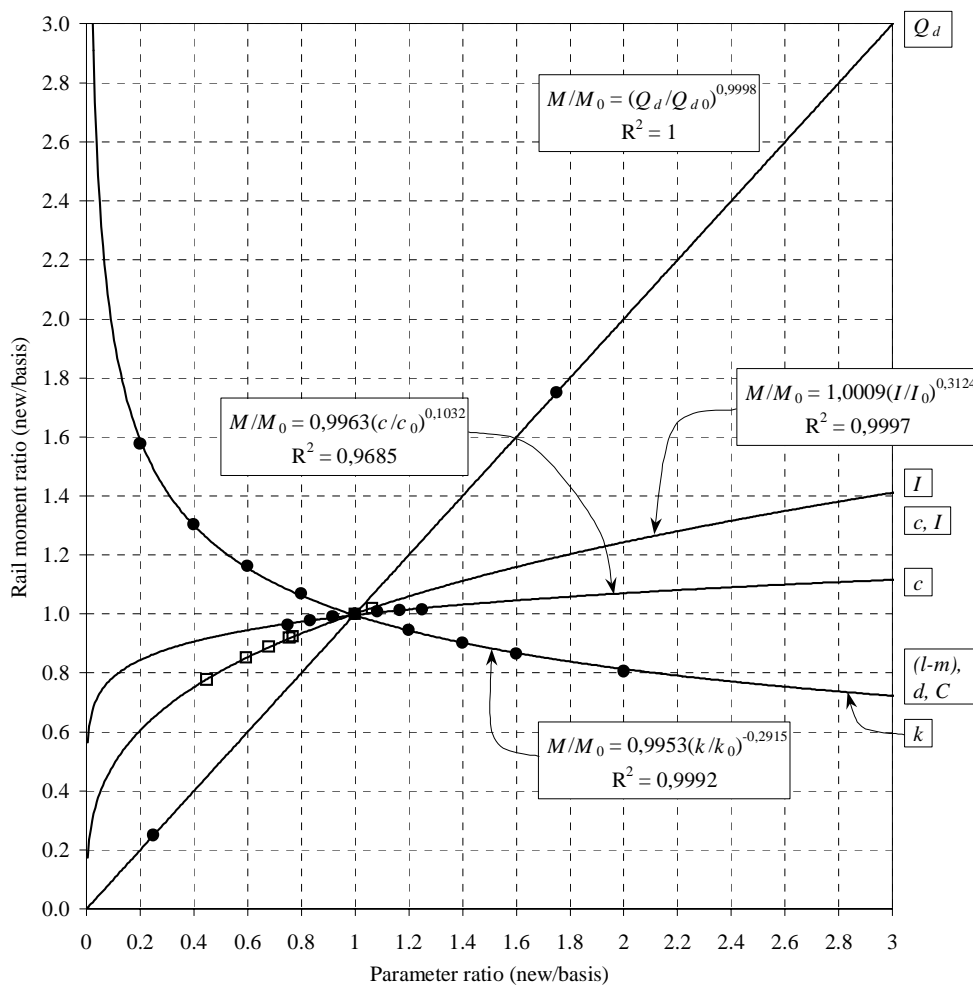


**Figure A.7:** Diagram for rail moment. Markers represent actual calculated values, whereas the thick lines are regression curves. Regression curve formulas given in boxes along with the  $R^2$ -value. Thin lines represent the BOEF model. Note that the track modulus  $k$  has been used in the beam element model in stead of  $(l-m)$ ,  $d$  and  $C$  (as in the BOEF model).

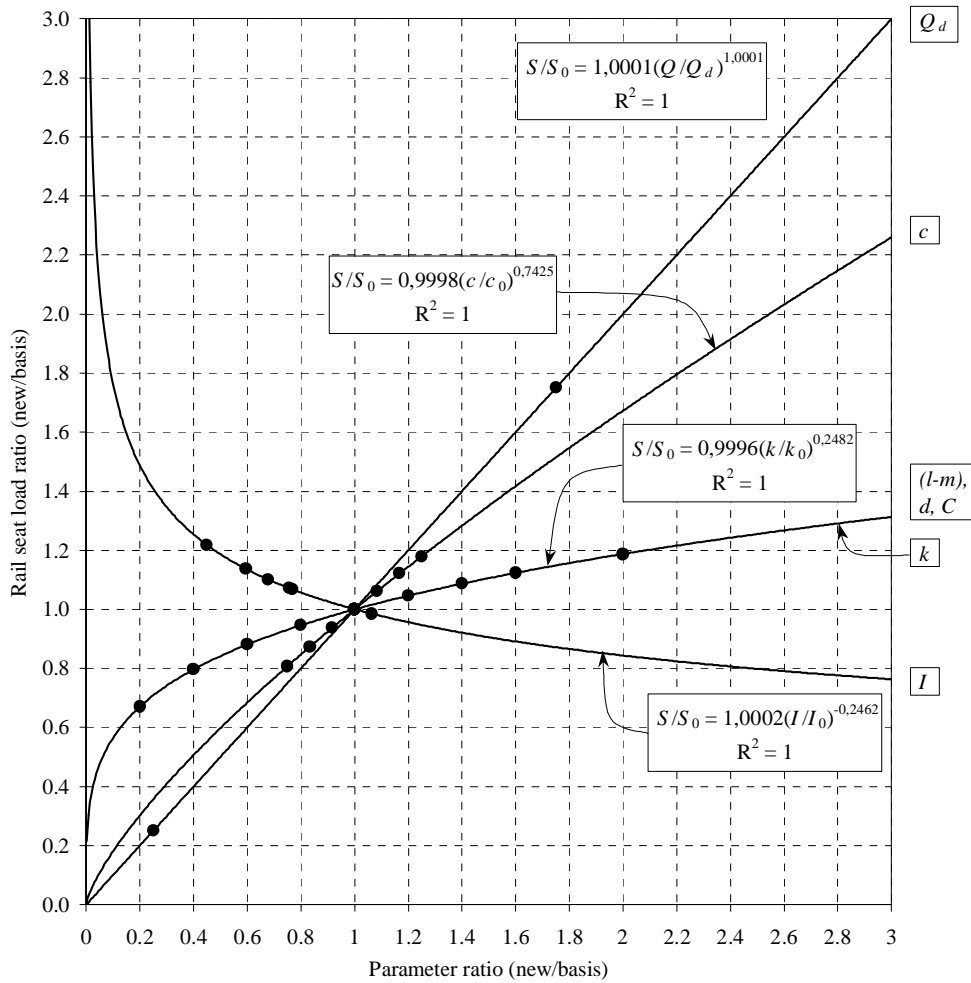


**Figure A.8:** Diagram for rail seat load. Markers represent actual calculated values, whereas the thick lines are regression curves. Regression curve formulas given in boxes along with the  $R^2$ -value. Thin lines represent the BOEF model. Note that the track modulus  $k$  has been used in the beam element model in stead of  $(l-m)$ ,  $d$  and  $C$  (as in the BOEF model).

## APPENDIX B Brief thermomechanical background

A brief introduction is given to thermomechanics, a branch of mechanics that emphasizes the mechanical properties of solids and fluids through thermodynamical principles. The description given here is adopted from Ziegler /89/<sup>1</sup>. The purpose of this exercise is to gain more and broader insight into dissipative systems including frictional ones. Especially, thermomechanics will bring about some more profound justification of the splitting of the stress into a conservative ('elastic') part and a dissipative part as in Eqn. (3.74).

Let a state of a system be described by a set of mutually independent *kinematical coordinates* or *parameters*  $a_k$  ( $k = 1, 2, \dots, n$ ) and by the *absolute temperature*  $T$ . In terms of the kinematical state, a particular useful case is when the strain components  $\varepsilon_{ij}$  play the roles of the  $a_k$ .

If the state of the system is infinitesimally altered, the elementary work done on the system is

$$dW = A_k da_k \quad (B.1)$$

where  $A_k$  are denoted the forces corresponding to  $a_k$ . In Eqn. (B.1) summation is implied over repeated indices (Einstein summation convention).

The *first fundamental law* of thermodynamics states the existence of a state function called the *internal energy*  $U(a_k, T)$  such that

$$dU = dW + dQ = A_k da_k + dQ \quad (B.2)$$

where  $dQ$  is the heat supply to the system. Eqn. (B.2) is often considered as an energy balance equation. When  $dQ = 0$  the process is *adiabatic*, and when  $dW = 0$  the process is referred to as *pure heating*.

The *second fundamental law* of thermodynamics states the existence of another state function called the *entropy*  $S(a_k, T)$  such that

$$T dS \geq dQ \quad (B.3)$$

where equality only holds for reversible processes as opposed to irreversible ones.

A useful decomposition of the entropy is the following:

$$dS = dS^r + dS^i \quad (B.4)$$

where

$$dS^r = \frac{dQ}{T} \quad (B.5)$$

is the reversible increment of  $S$ , also called the *entropy supply* from outside the system. Further,

$$dS^i \geq 0 \quad (B.6)$$

---

1. References are found in the Reference Section before Appendix A.



is the irreversible increment of  $S$  or the *entropy production* inside the system.

Using Eqn. (B.2), Eqn. (B.5) and Eqn. (B.4) the elementary work may be written

$$dW = dU - dQ = dU - T dS^r = dU - T dS + T dS^i \quad (B.7)$$

Recalling that  $U$  and  $S$  are state functions, Eqn. (B.7) is rewritten as follows

$$dW = A_k da_k = \left( \frac{\partial U}{\partial a_k} - T \frac{\partial S}{\partial a_k} \right) da_k + \left( \frac{\partial U}{\partial T} - T \frac{\partial S}{\partial T} \right) dT + T dS^i \quad (B.8)$$

It can be argued, e.g. by investigating Eqn. (B.2) and Eqn. (B.3) or by considering pure heating, that

$$\frac{\partial U}{\partial T} - T \frac{\partial S}{\partial T} = 0 \quad (B.9)$$

which simplifies Eqn. (B.8) to

$$dW = A_k da_k = \left( \frac{\partial U}{\partial a_k} - T \frac{\partial S}{\partial a_k} \right) da_k + T dS^i \quad (B.10)$$

Eqn. (B.10) suggests that the elementary work can be divided into two parts, namely, the *quasi-conservative elementary work*,  $dW^q$ , and the *dissipative elementary work*,  $dW^d$ :

$$dW^q = \left( \frac{\partial U}{\partial a_k} - T \frac{\partial S}{\partial a_k} \right) da_k = A_k^q da_k \quad (B.11)$$

$$dW^d = T dS^i = A_k^d da_k \quad (B.12)$$

Note that Eqn. (B.12) together with Eqn. (B.6) implies that

$$dW^d = A_k^d da_k \geq 0 \quad (B.13)$$

Hence, the dissipative elementary work is never negative.

From Eqn. (B.11) we see that the *quasi-conservative forces*  $A_k^q$  may be written

$$A_k^q = \frac{\partial U}{\partial a_k} - T \frac{\partial S}{\partial a_k} \quad (B.14)$$

Using Eqn. (B.10) and Eqn. (B.12) the *dissipative forces*  $A_k^d$  of the system will be

$$A_k^d = A_k - \frac{\partial U}{\partial a_k} + T \frac{\partial S}{\partial a_k} \quad (B.15)$$

Equations (B.10), (B.11), (B.12), (B.14), (B.15) make it possible to decompose the forces  $A_k$  corresponding to the  $a_k$  (e.g. the strains) as

$$A_k = A_k^q + A_k^d \quad (B.16)$$

Thus, in terms of thermodynamics, the mechanical stresses (interpreting what Ziegler /89/ denotes forces) of a system may be split into a quasiconservative part, as defined by Eqn. (B.14) and a dissipative part as defined by Eqn. (B.15). Also, the strains (interpreting the kinematic parameters) connected to these forces are the total ones. Hence, from a thermomechanical point of view there is no need to distinguish elastic strains from the plastic ones, it suffices that the dissipative work is possible to separate from the quasiconservative work. In this respect one may say that one has transferred from a total stress - divided strain setting in classic elasto-plasticity, to a divided stress - total strain setting with the help of thermomechanics.

Introducing a state function called the *free energy* of the system one may arrive at another expression for the quasiconservative forces. Defining the free energy as

$$\Psi = U - TS \quad (B.17)$$

the differential will be

$$d\Psi = dU - TdS - SdT \quad (B.18)$$

Writing out the terms of Eqn. (B.18) by the partial derivatives of  $\Psi$  with respect to  $T$  and  $a_k$ , and taking into account Eqn. (B.9), will produce the following two equations:

$$S = -\frac{\partial\Psi}{\partial T} \quad (B.19)$$

$$A_k^q = \frac{\partial\Psi}{\partial a_k^q} \quad (B.20)$$

In Eqn. (B.20) the result from Eqn. (B.14) has also been applied.

It is thus clear that the free energy plays the role of a potential as the partial derivatives with respect to temperature and kinematic parameters are the negative entropy and the quasiconservative forces, respectively. The adjective 'quasiconservative' may now be explained: The forces  $A_k^q$  are conservative in the sense that they can be derived from a potential (the free energy), but this potential is not dependent upon  $a_k$  alone but also upon temperature  $T$ . This justifies the prefix *quasi*.

The free energy we have been using here is also denoted the Helmholtz free energy /68/ or the strain energy. It is also possible to use Gibbs free energy, which is defined in terms of stresses in stead of strain as for the Helmholtz free energy. These two energy functions are related through the Legendre transformation /68/.

The plasticity theory based on thermomechanics is often denoted *hyperplasticity*. In this theory the constitutive behaviour of a material can be completely defined by two potential functions /89/: One that describes the free energy and another that describes the dissipation. As mentioned by /68/ the free energy function is either the Gibbs free energy or the Helmholtz free energy. Provided that Gibbs free energy is used, the second function needed is either a dissipation function or a yield function /68/.



## APPENDIX C Stresses applied to the specimens

Table C.1: Stresses applied to the specimens. Table continues until page C-4. Legend on page C-4.

Type of loading	q/p	$\sigma_{3,min}$ [kPa]	$\sigma_{3,max}$ [kPa]	$\sigma_{1,min}$ [kPa]	$\sigma_{1,max}$ [kPa]	$p_{min}$ [kPa]	$p_{max}$ [kPa]	$q_{min}$ [kPa]	$q_{max}$ [kPa]	Vassfjell specimen no.										
										A	B	C	D	D	E	F	G			
Repeated, isotropic	0.0	20.0	50.0	50.0	50.0	20.0	50.0	0.0	0.0	◇	◇	◇	◇	◇	◇	◇	◇			
			100.0 <sup>a</sup>	100.0	100.0		◇			◇	◇	◇	◇	◇	◇					
			150.0	150.0	150.0															
Repeated, proportional	0.3	20.0	50.0	66.7	66.7	26.7	55.6	16.7	16.7	◇	◇	◇	◇	◇	◇	◇	◇			
			110.0	146.7	146.7		122.2	6.7	6.7	◇	◇	◇	◇	◇	◇	◇	◇	◇		
			170.0	226.7	226.7		188.9			◇	◇	◇	◇	◇	◇	◇	◇	◇	◇	
Repeated, proportional	0.7	20.0	40.0	76.5	76.5	38.3	52.2	36.5	36.5	◇	◇	◇	◇	◇	◇	◇	◇			
			80.0	153.0	153.0		104.3	18.3	18.3	◇	◇	◇	◇	◇	◇	◇	◇	◇		
			120.0	229.6	229.6		156.5			◇	◇	◇	◇	◇	◇	◇	◇	◇	◇	
			160.0	306.1	306.1		208.7			◇	◇	◇	◇	◇	◇	◇	◇	◇	◇	
Repeated, proportional	1.2	20.0	30.0	90.0	90.0	60.0	50.0	60.0	60.0	◇	◇	◇	◇	◇	◇	◇	◇			
			60.0	180.0	180.0		100.0			◇	◇	◇	◇	◇	◇	◇	◇	◇		
			90.0	270.0	270.0		150.0	40.0	40.0	◇	◇	◇	◇	◇	◇	◇	◇	◇		
			120.0	360.0	360.0		200.0			◇	◇	◇	◇	◇	◇	◇	◇	◇	◇	
			150.0	450.0	450.0		250.0			◇	◇	◇	◇	◇	◇	◇	◇	◇	◇	
Repeated, proportional	1.5	20.0	30.0	120.0	120.0	80.0	60.0	90.0	90.0											
			50.0	200.0	200.0		100.0													
			70.0	280.0	280.0		140.0	60.0	60.0											
			90.0	360.0	360.0		180.0													
			110.0	440.0	440.0		220.0													
			130.0	520.0	520.0		260.0	390.0												

a. 85 kPa for specimen A and B

Type of loading	q/p	$\sigma_{3,min}$ [kPa]	$\sigma_{3,max}$ [kPa]	$\sigma_{1,min}$ [kPa]	$\sigma_{1,max}$ [kPa]	$p_{min}$ [kPa]	$p_{max}$ [kPa]	$q_{min}$ [kPa]	$q_{max}$ [kPa]	Vassfjell specimen no.								
										A	B	C	D	D	E	F	G	
Repeated, proportional	1.8	20.0	30.0	165.0	50.0	75.0	90.0	135.0	◇	◇	◇	◇	◇	◇	◇	◇	◇	◇
			40.0	220.0		180.0		◇	◇	◇	◇	◇	◇	◇	◇	◇		
			50.0	275.0		225.0		◇	◇	◇	◇	◇	◇	◇	◇	◇	◇	
			60.0	330.0		270.0		△	△	△	△	△	△	△	△	△	△	
			70.0	385.0		315.0												
			80.0	440.0		360.0												
			30.0	210.0		180.0												
			40.0	280.0		240.0												
Repeated, proportional	2.0	20.0	50.0	140.0	60.0	120.0	120.0	300.0										
			60.0	420.0		360.0												
			25.0	231.3		206.3		△	△	△	△	△	△	△	△	△		
			30.0	277.5		247.5												
Repeated, proportional	0.7	20.0	40.0	76.5	26.1	52.2	18.3	36.5	△	△	△	△	△	△	△	△	△	△
			80.0	153.0		73.0		◇	◇	◇	◇	◇	◇	◇	◇	◇		
			120.0	229.6		109.6		◇	◇	◇	◇	◇	◇	◇	◇	◇	◇	
			160.0	306.1		146.1		△	△	△	△	△	△	△	△	△	△	
Repeated, proportional	0.7	60.0	80.0	153.0	78.3	104.3	54.8	73.0	◇	◇	◇	◇	◇	◇	◇	◇	◇	◇
			120.0	229.6		109.6		◇	◇	◇	◇	◇	◇	◇	◇	◇		
			160.0	306.1		146.1		◇	◇	◇	◇	◇	◇	◇	◇	◇		
Repeated, proportional	1.2	60.0	70.0	210.0	100.0	116.7	120.0	140.0	◇	◇	◇	◇	◇	◇	◇	◇	◇	◇
			100.0	300.0		200.0		◇	◇	◇	◇	◇	◇	◇	◇	◇		
			130.0	390.0		260.0		△	△	△	△	△	△	△	△	△		



Type of loading	q/p	$\sigma_{3,min}$ [kPa]	$\sigma_{3,max}$ [kPa]	$\sigma_{1,min}$ [kPa]	$\sigma_{1,max}$ [kPa]	$p_{min}$ [kPa]	$p_{max}$ [kPa]	$q_{min}$ [kPa]	$q_{max}$ [kPa]	Vassfjell specimen no.														
										A	B	C	D	D	E	F	G							
Repeated, constant $\sigma_3$	3.0	60.0 <sup>a</sup>		62.0	180.0	60.7	100.0	2.0	120.0									◆						
					210.0																	◆		
					240.0																			◆
					270.0																			◆
Repeated, constant $\sigma_3$	3.0	150.0		152.0	250.0	150.7	183.3	2.0	100.0									◆						
					350.0																	◆		
					450.0																			◆
					550.0																			
Static, constant $\sigma_3$	3.0			150.0	20.0	20.0	86.7	0.0	200.0									◆						
					60.0																		◆	
					150.0																			

The static tests were load controlled and performed with a load rate of approx. 1.0 kPa/s.

a. For specimen D wet 100 kPa









◇ Dry specimen, completed test, △ Dry specimen, interrupted test

◆ Wet specimen completed test, ▲ Wet specimen interrupted test

## APPENDIX D Measured stresses and strains from the tests

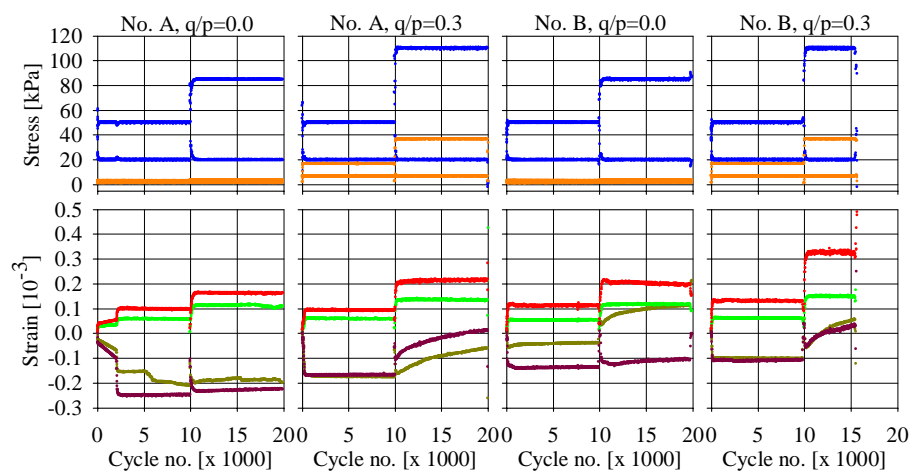
In the present Appendix the data from the tests are plotted. For the strains the data plotted are the average values for the vertical and horizontal LVDTs. Table D.1 contains a legend to the plots.

**Table D.1:** Legend for the figures for stress and strain from the triaxial tests.

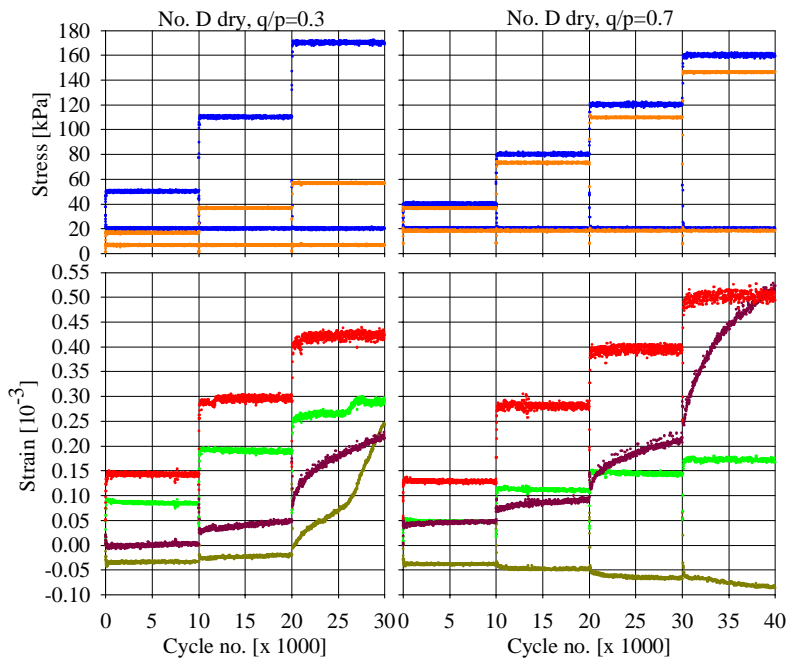
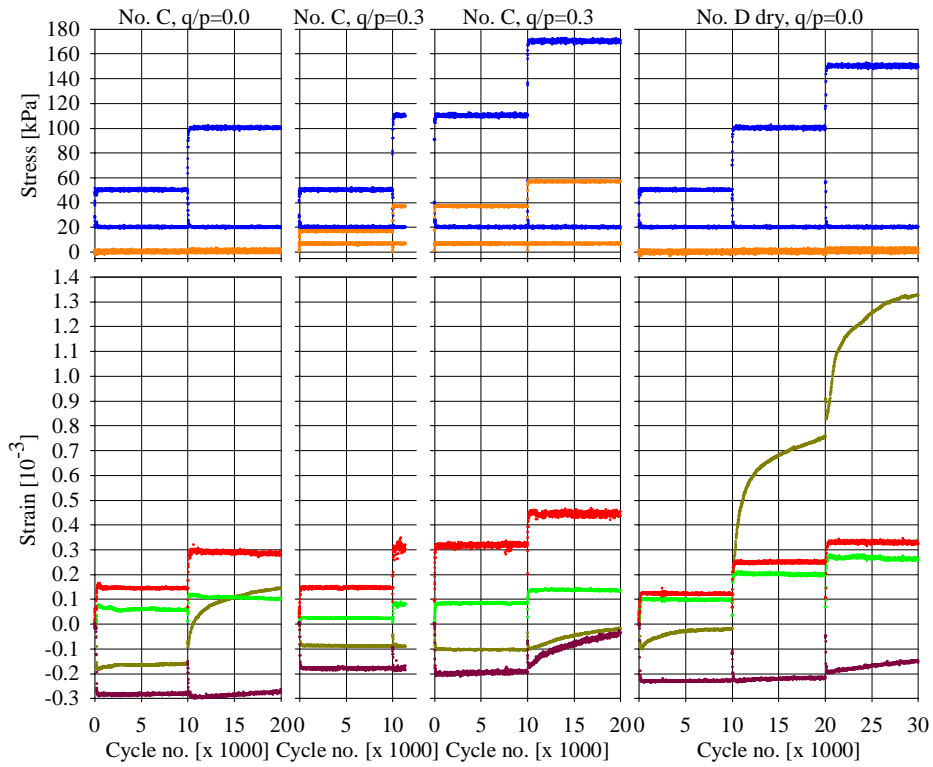
Stress		Strain	
Colour of curve	Type of stress	Colour of curve	Type of strain
	Cell, static, ( $\sigma_{3,min}$ )		Horizontal, cumulative and permanent, ( $\epsilon_3^p$ )
	Cell, static + repeated, ( $\sigma_{3,max}$ )		Horizontal, repeated, ( $\epsilon_3^e$ )
	Deviatoric, static, ( $q_{1,min}$ )		Vertical, cumulative and permanent, ( $\epsilon_1^p$ )
	Deviatoric, static + repeated, ( $q_{1,max}$ )		Vertical, repeated, ( $\epsilon_1^e$ )

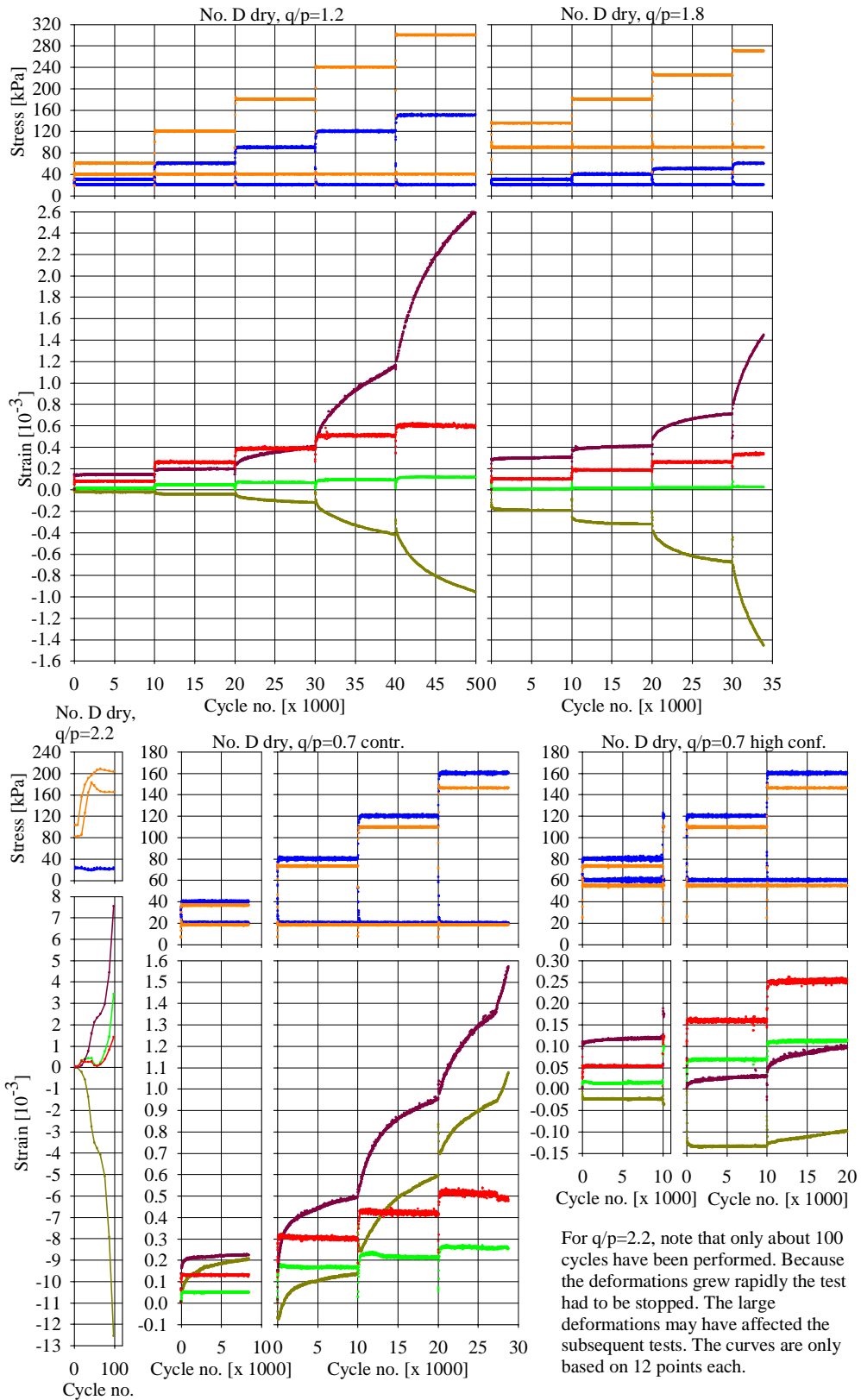
In the graphs the permanent strain is the minimum strain in the cycle relative to the beginning of the test, while the maximum strain is the permanent strain plus the resilient strain. The resilient strains are thus always positive, and one has to look into the individual cycles to determine whether the vertical and horizontal strains are in phase or 180 degrees out of phase.

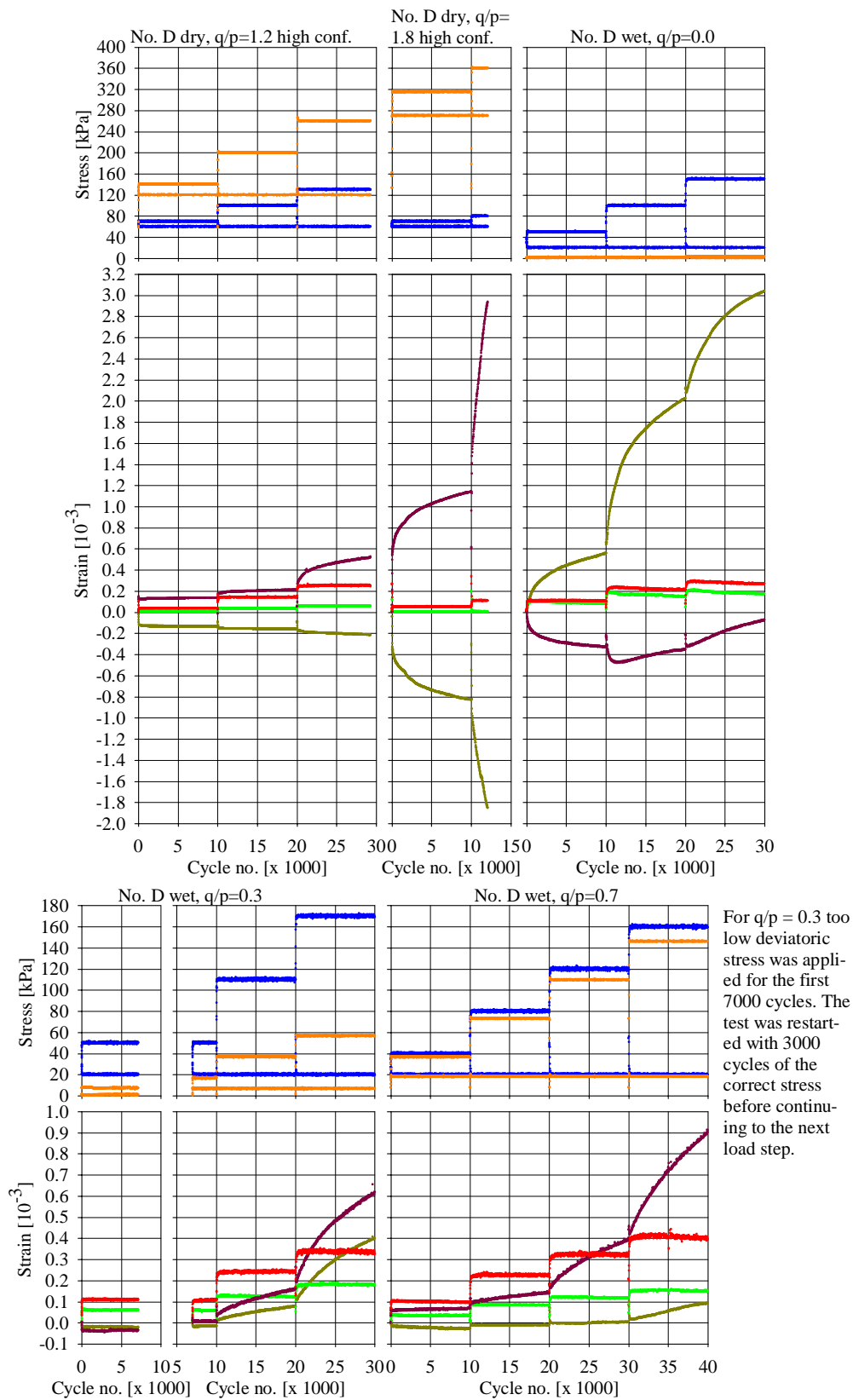
The graphs appear in the order the tests were performed; the order may differ a bit from that of Appendix C. The graphs are ordered in rows, i.e. for each test read horizontally first, then vertically. Also, results from some additional tests are shown, e.g. where specimens unintentionally have been run with partial internal vacuum, as these may give some additional information. Every graph is marked on top with specimen number and  $q/p$  ratio; figure captions as well as section headings are hence omitted. Note that the scale of the ordinate axes varies. Also refer to Appendix C for the intended stresses.

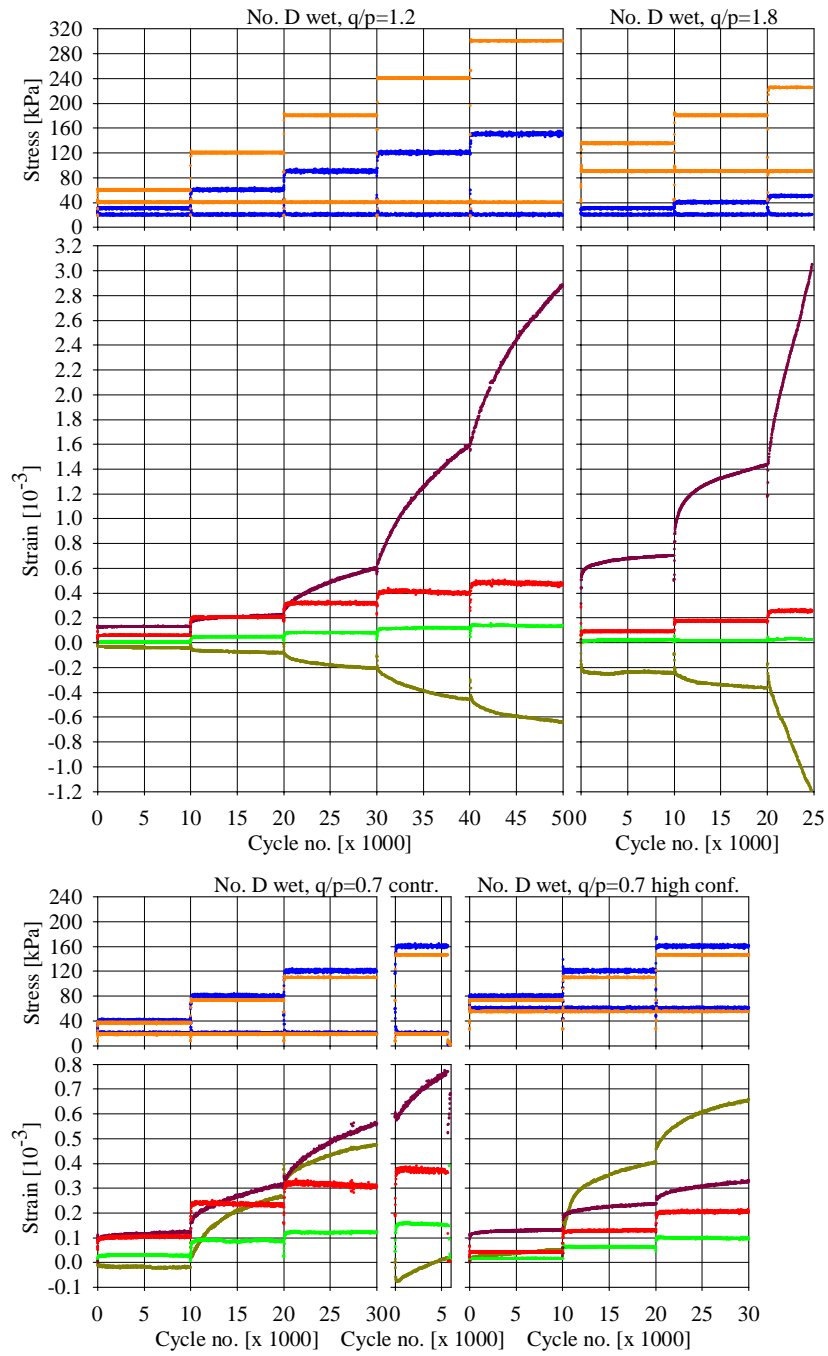


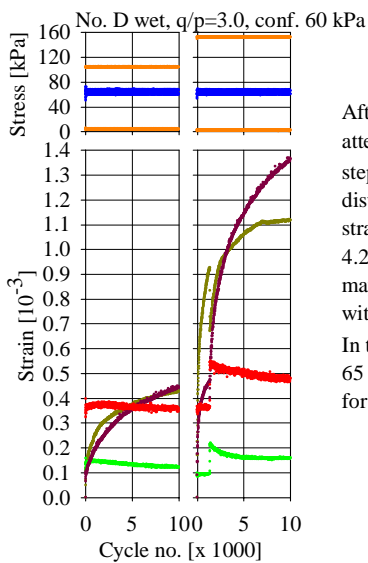
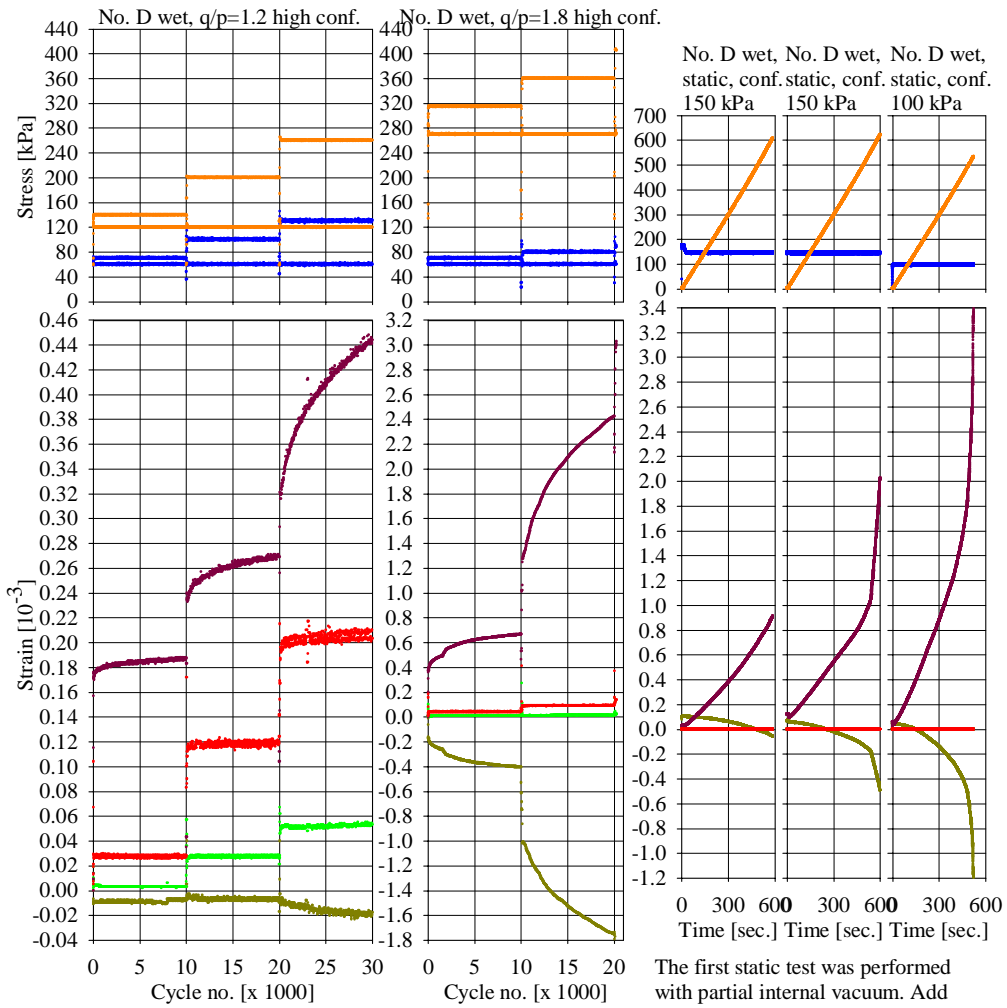




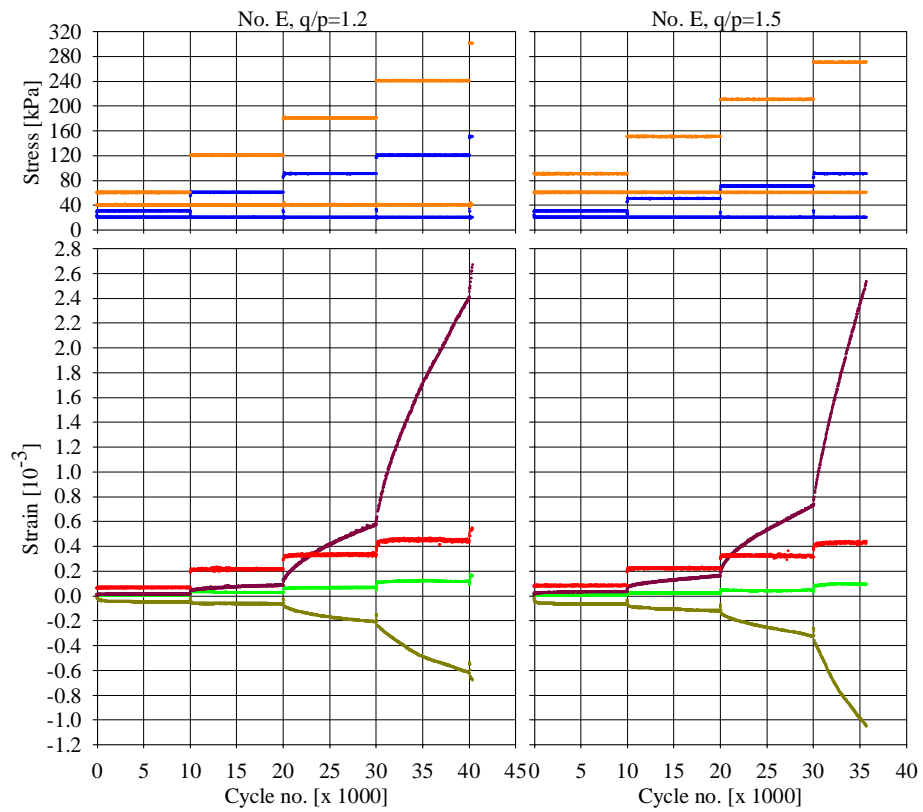
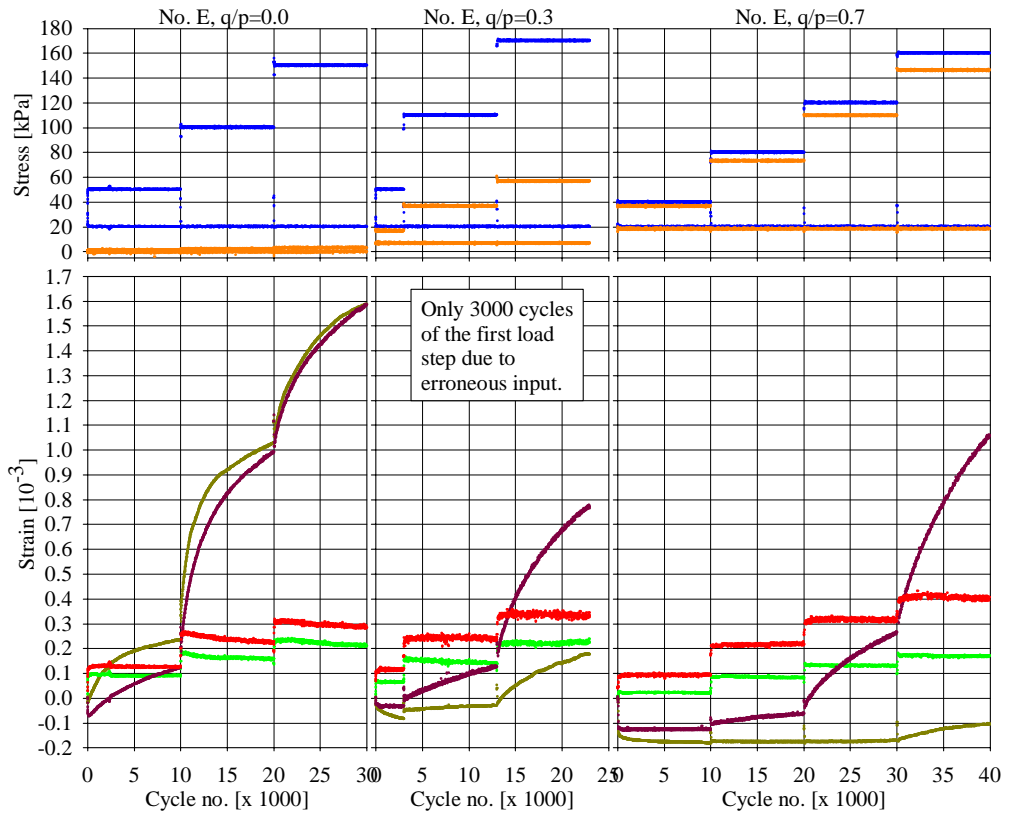


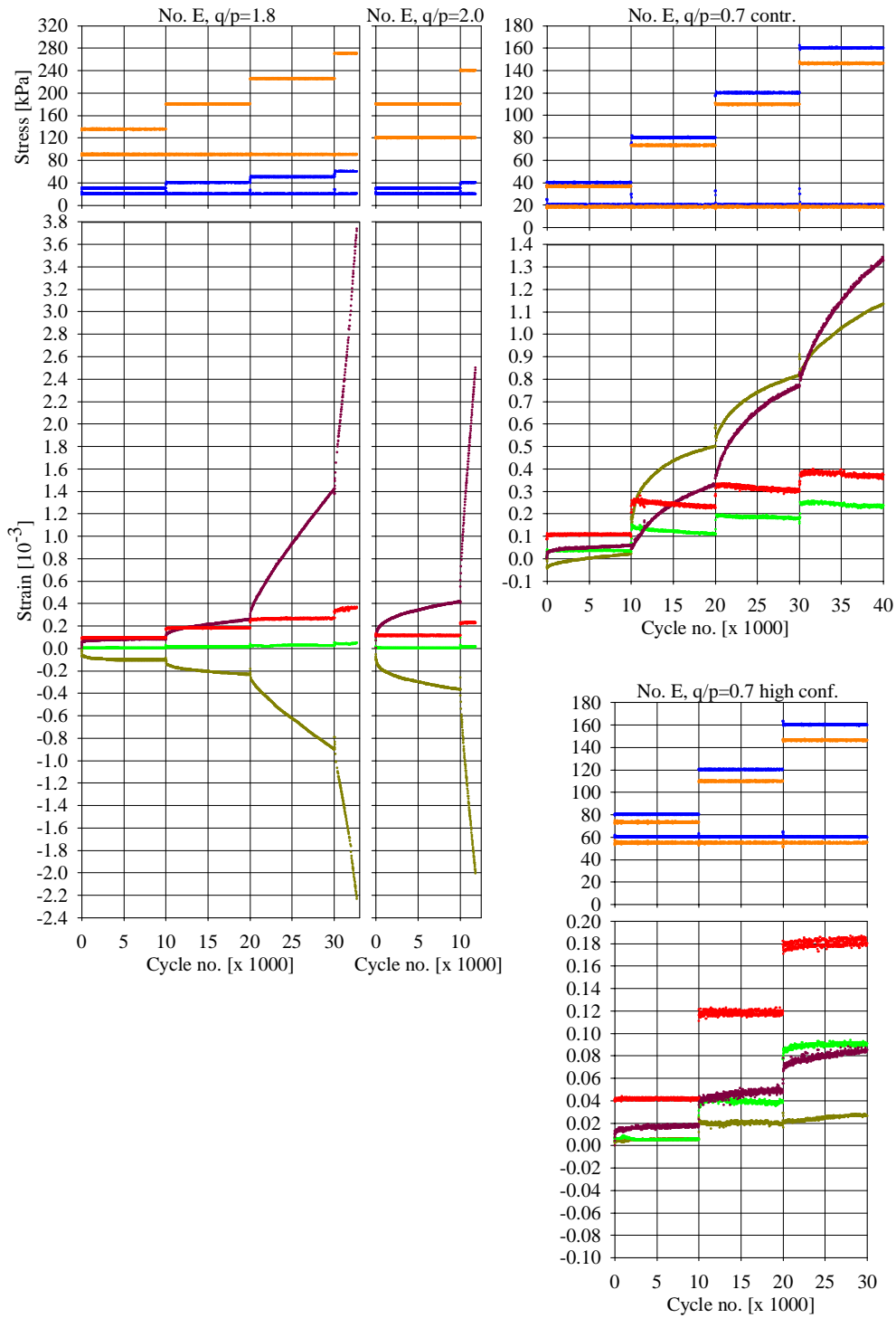


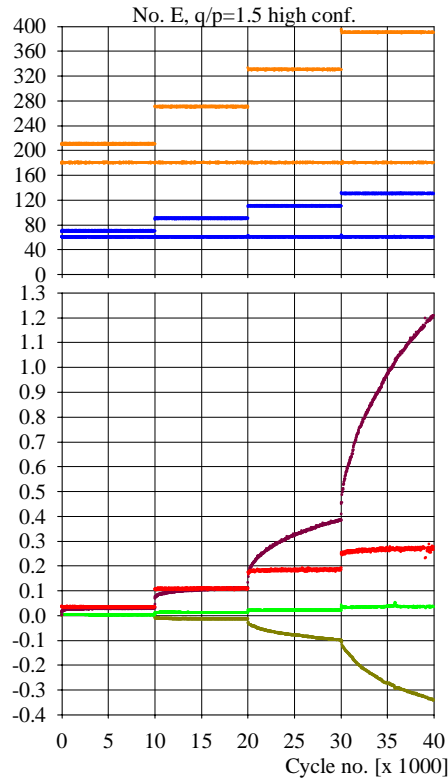
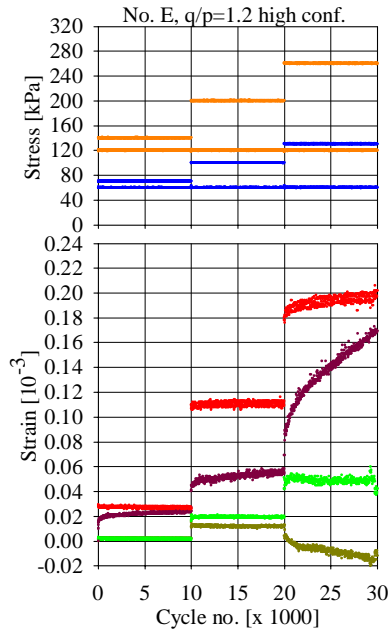




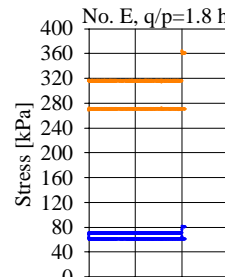
After the first load step a second load step was attempted with  $q_{max} = 200$  kPa. This second load step was applied for a few cycles only, but distorted the specimen a bit. Axial permanent strain of 3.7‰ and horizontal permanent strain of 4.2‰ accumulated during these few cycles. This may have affected the specimen. A new load step with  $q_{max} = 150$  kPa was then applied (as shown). In this new load step internal vacuum (approx. 65 kPa extra confinement) was erroneously applied for the first 1350 cycles.



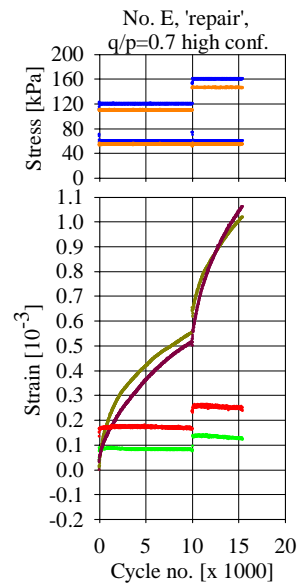
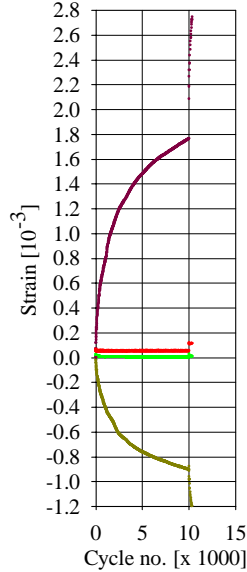
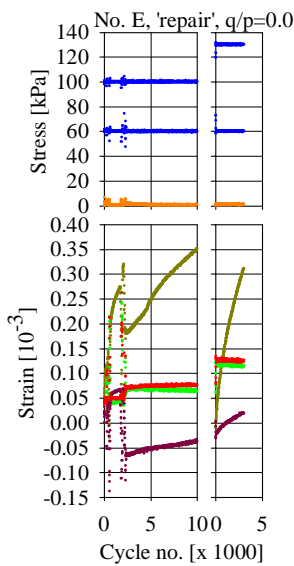




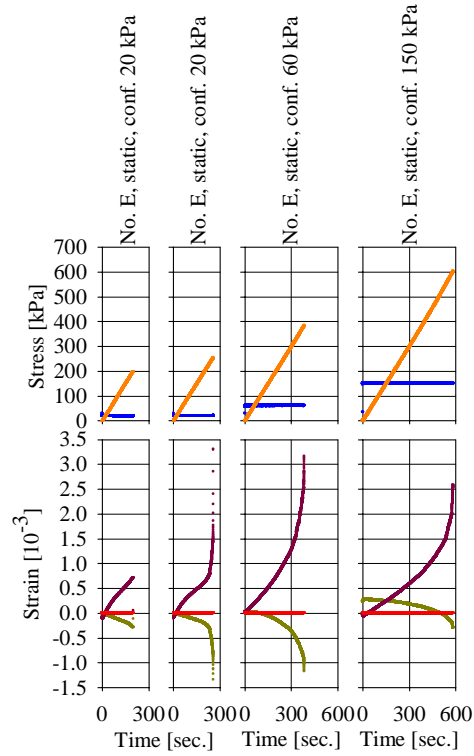
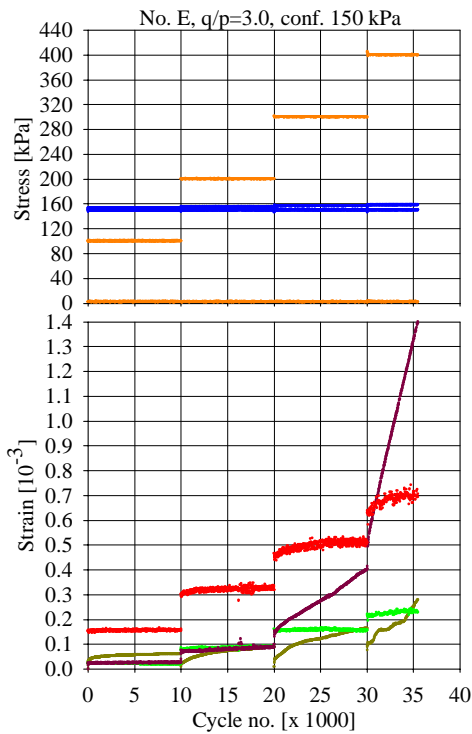
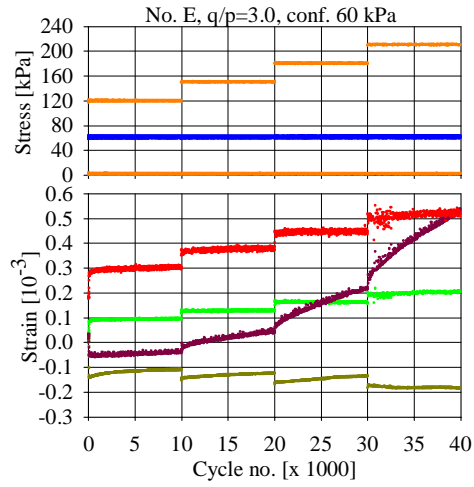
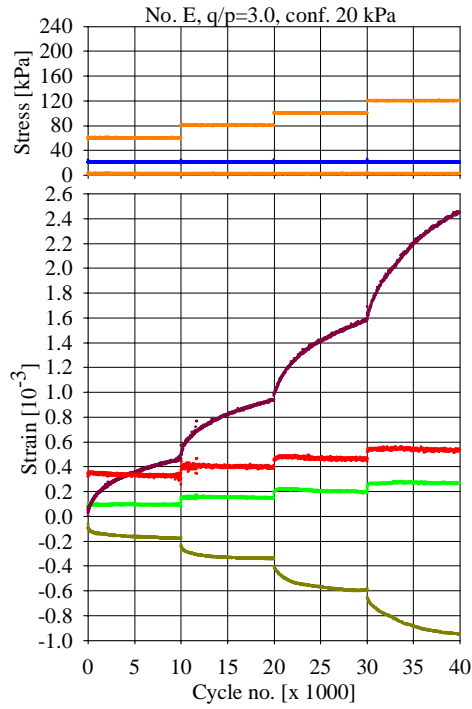
After completion of  $q/p=1.5$  with high confining stress, the specimen was unintentionally subjected to zero confining stress, which led to approx. 1.7‰ axial deformation and 25‰ horizontal deformation at the position of the uppermost instrumentation ring. It was decided to run some 'repair' load steps before further testing (shown directly below). The loss of confinement, despite the repair loads, may have affected the specimen so that subsequent results are not reliable.



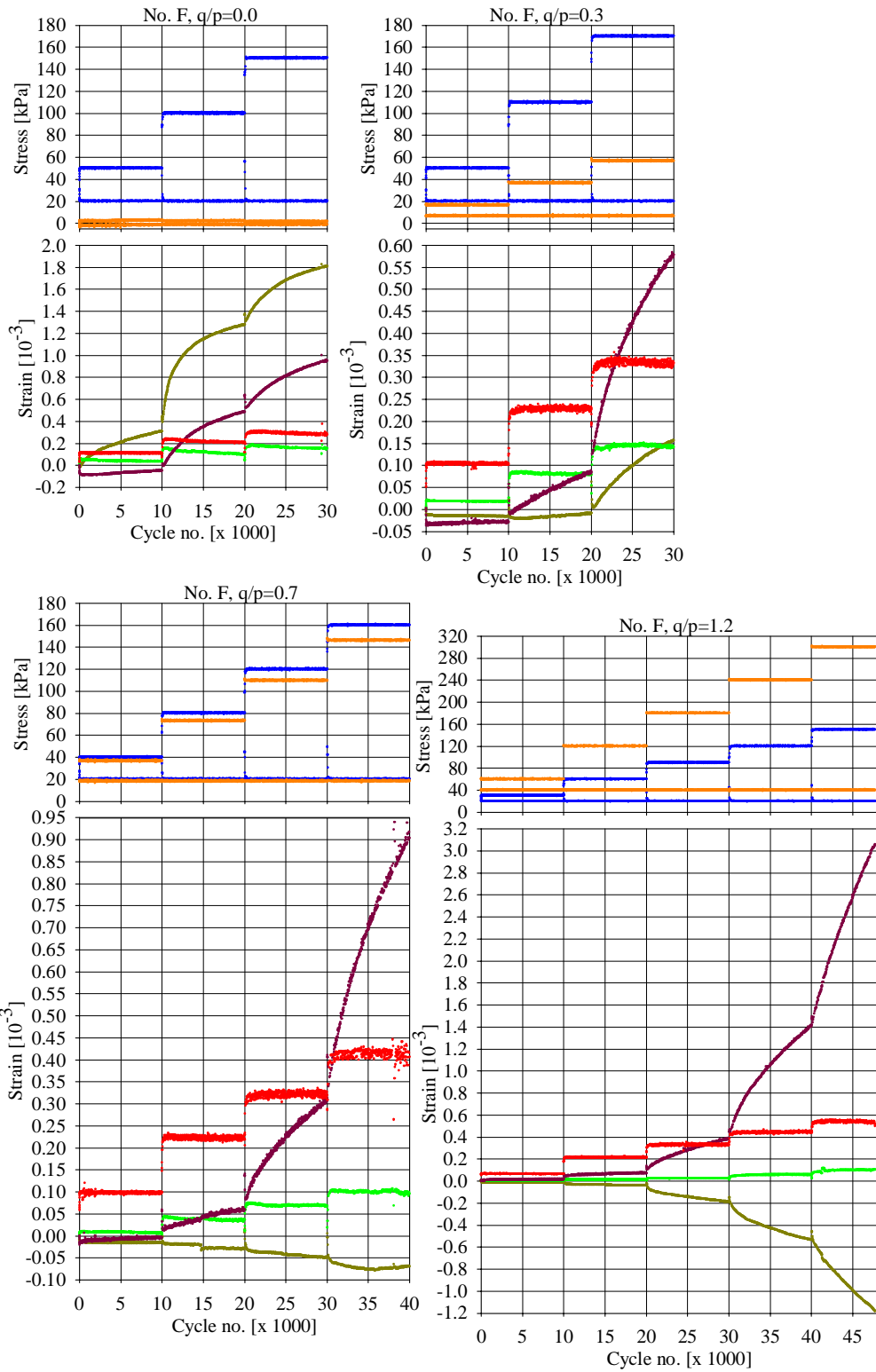
After  $q/p=1.8$  with high confining stress additional 'repair' loading was performed (see below) as it was felt that the previous 'repair' was not sufficient (permanent horizontal deformation at specimen top was still considerable).

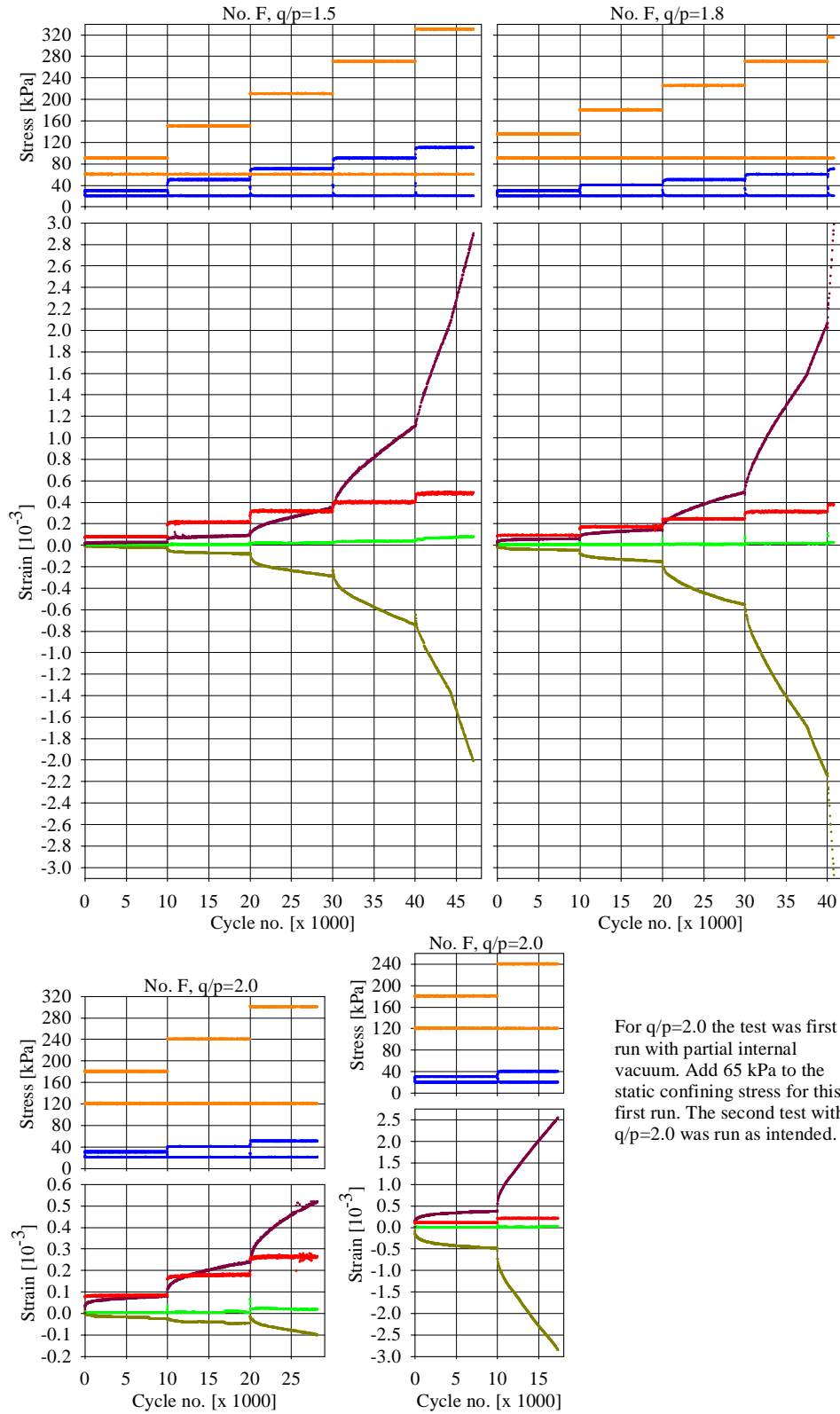




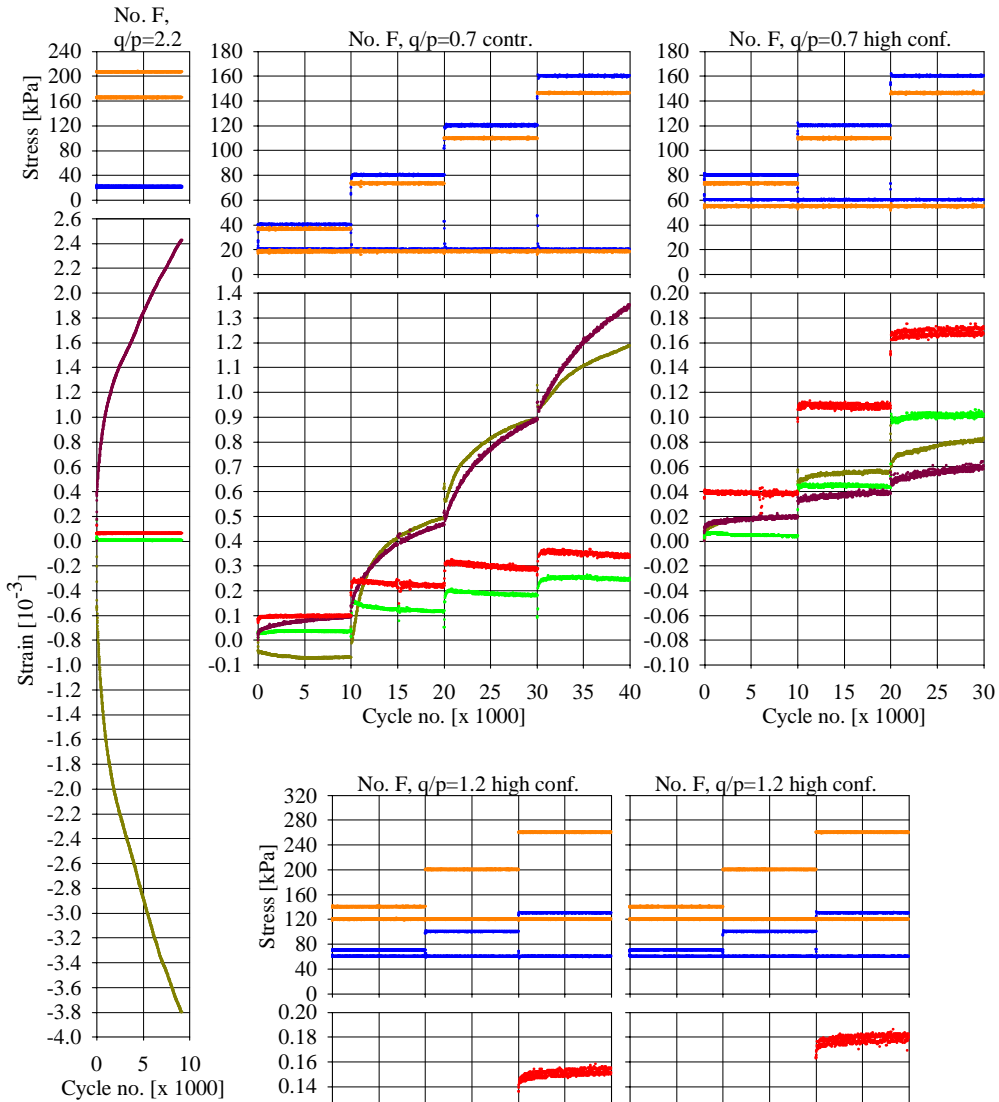


For the first static test the maximum load was not sufficient for failure. The test was therefore repeated with a higher maximum load.



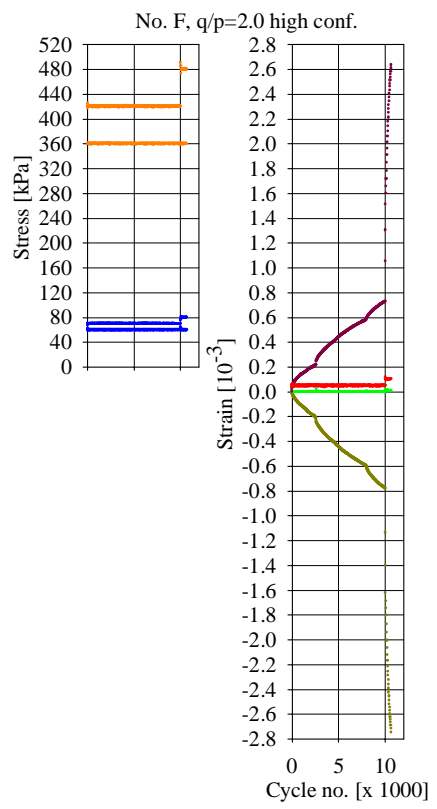
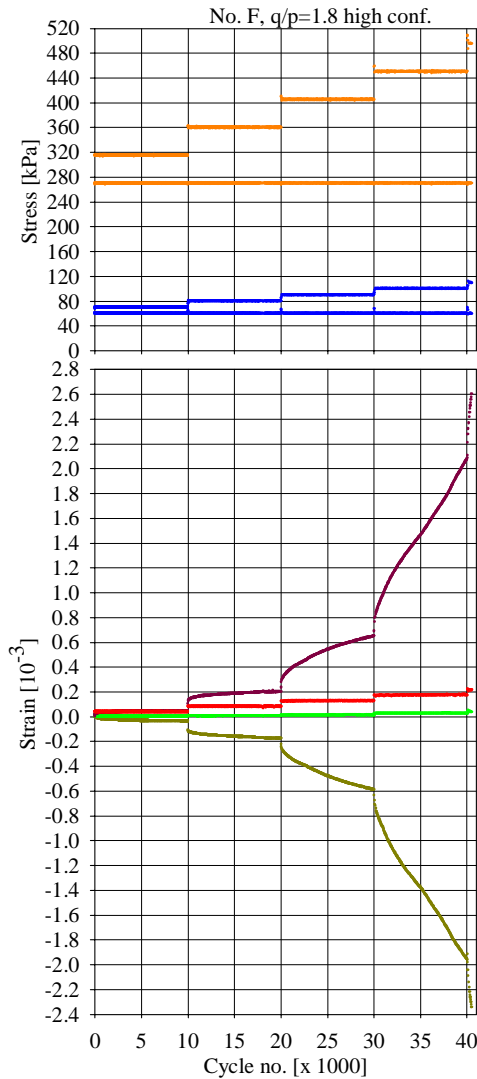
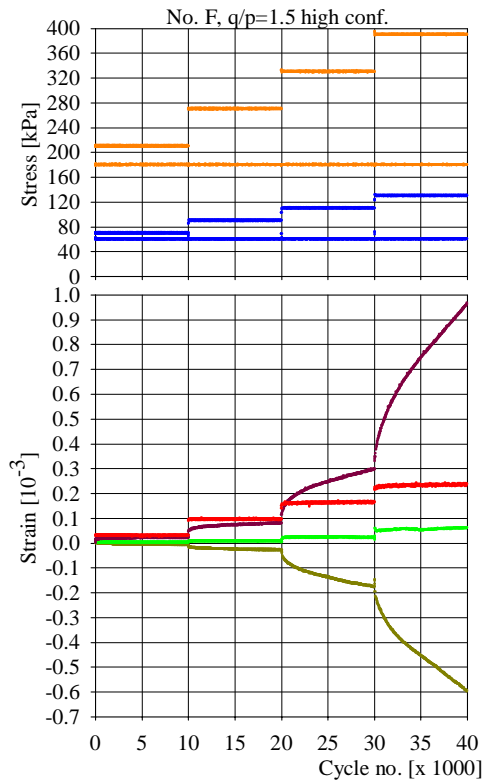


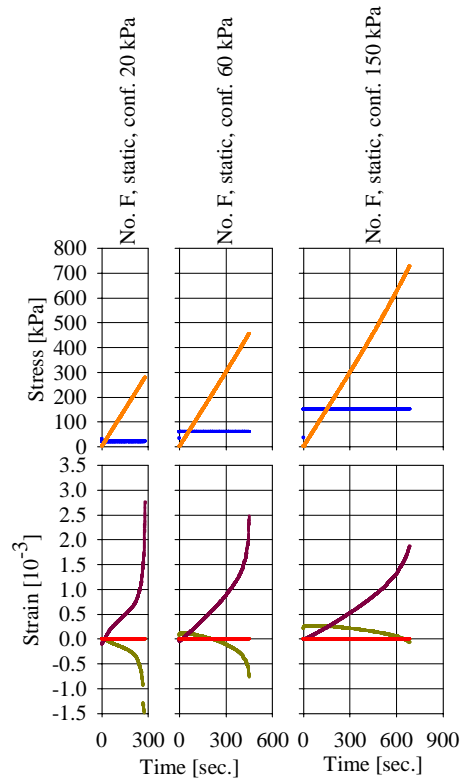
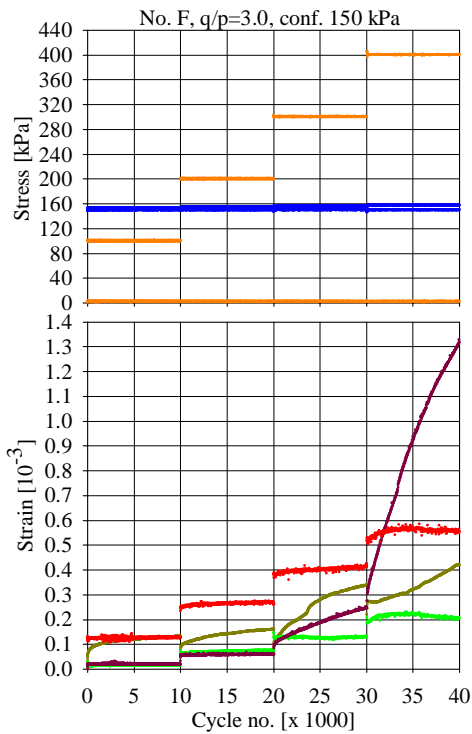
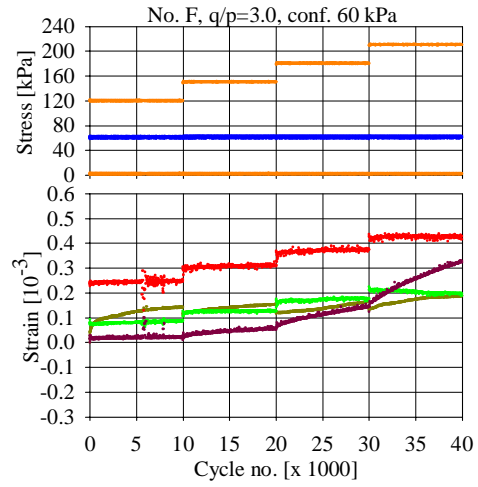
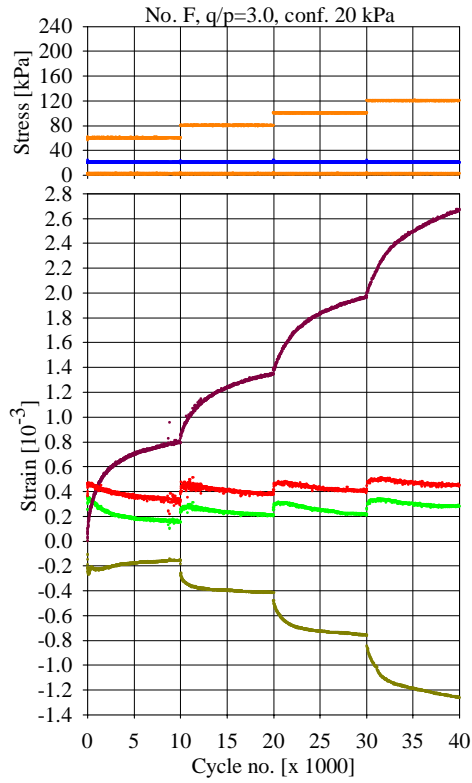
For  $q/p=2.0$  the test was first run with partial internal vacuum. Add 65 kPa to the static confining stress for this first run. The second test with  $q/p=2.0$  was run as intended.

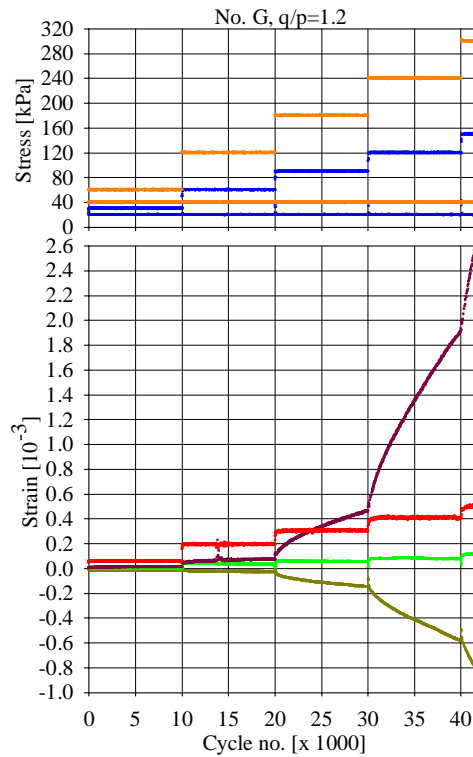
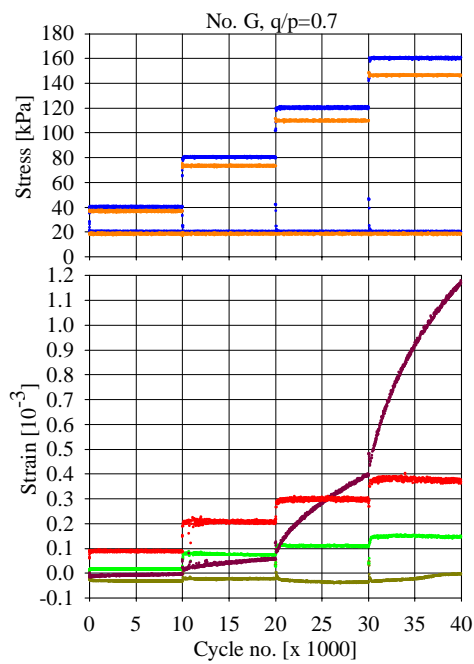
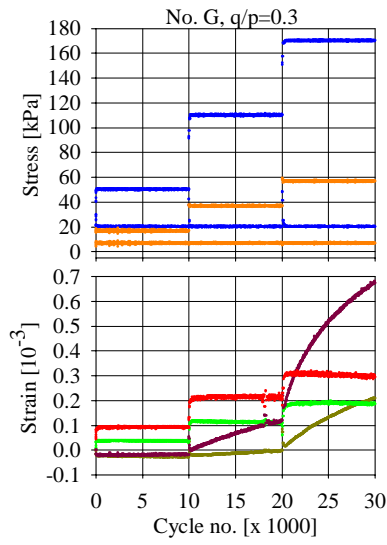
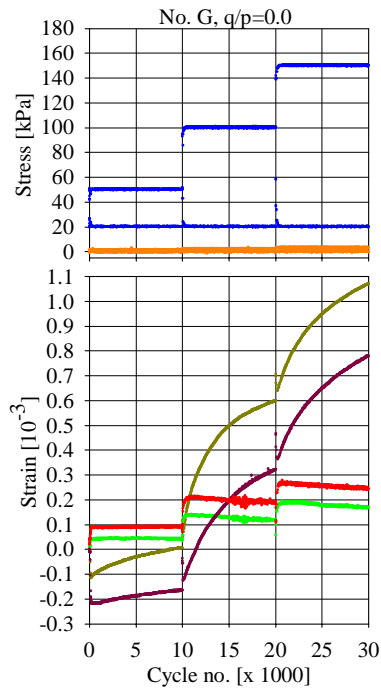


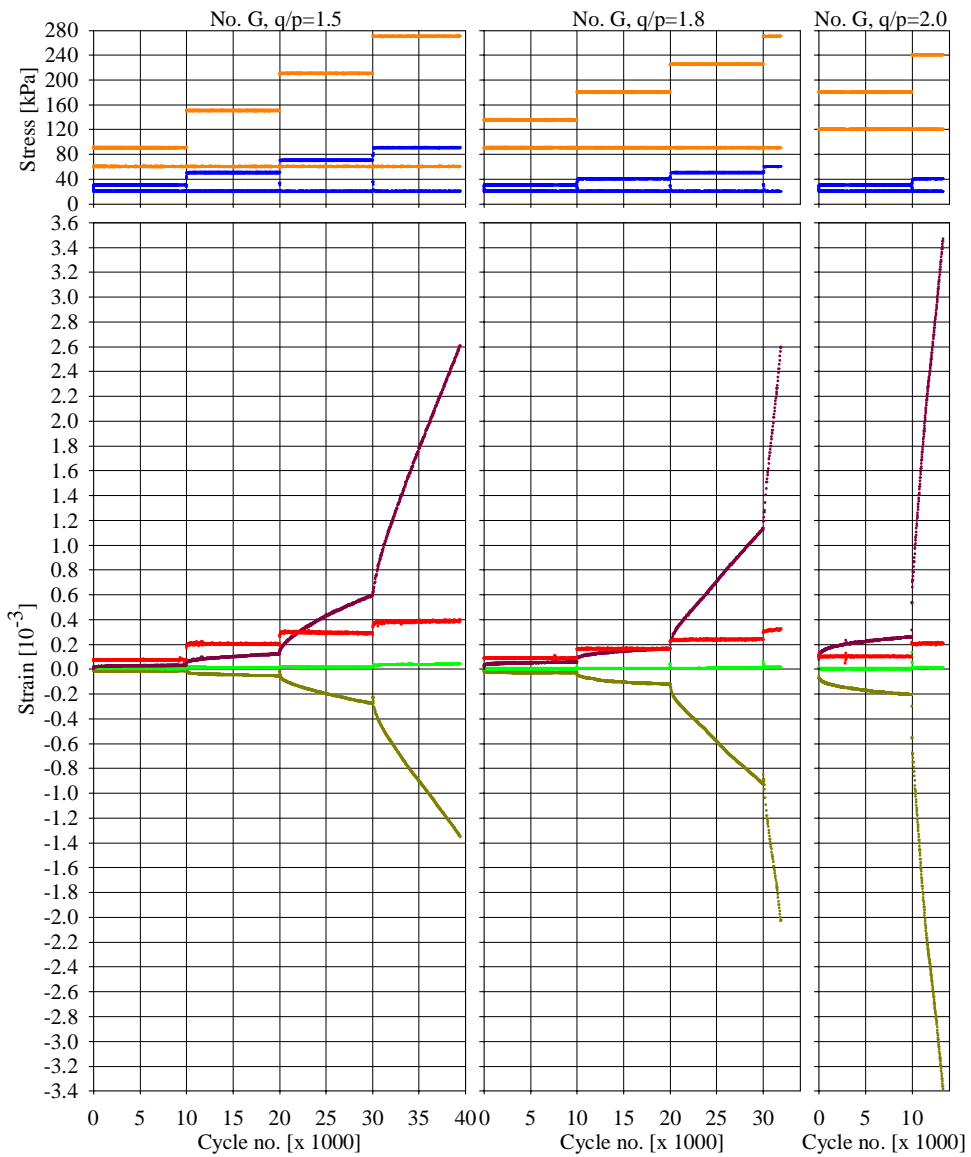
For  $q/p=2.2$  the applied repeated cell pressure is to low, only 1-1.5 kPa, while the intended repeated cell pressure is 5 kPa. The  $q/p$ -ratio is then raised to about 2.25 at maximum stress.

For  $q/p=1.2$  (with high confining pressure) the test was first run with partial internal vacuum. Add 65 kPa to the static confining stress for this first run. The second test with  $q/p=1.2$  was run as intended.

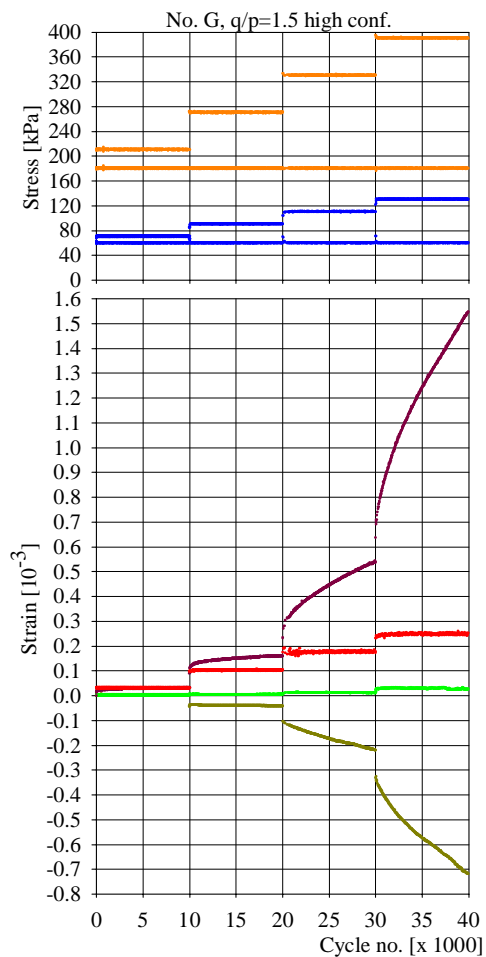
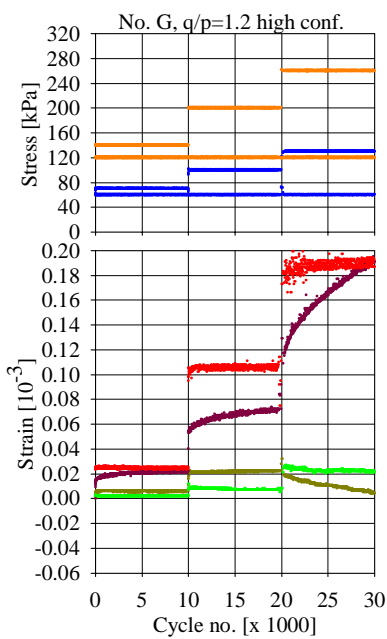
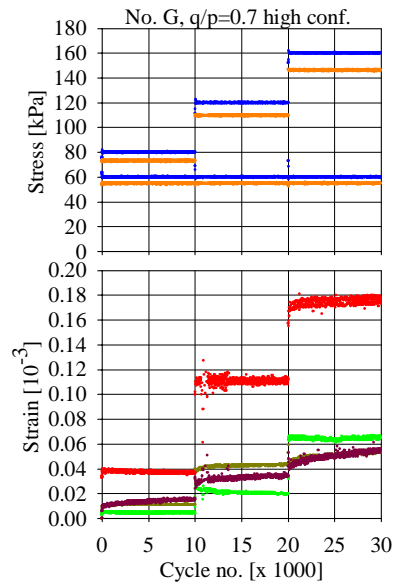
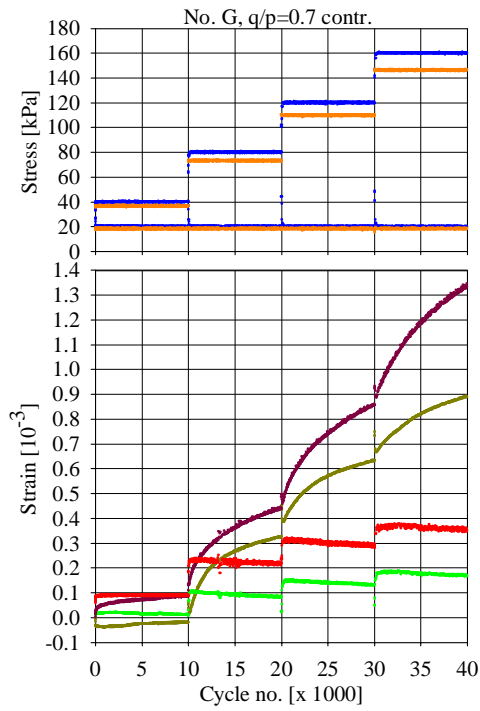


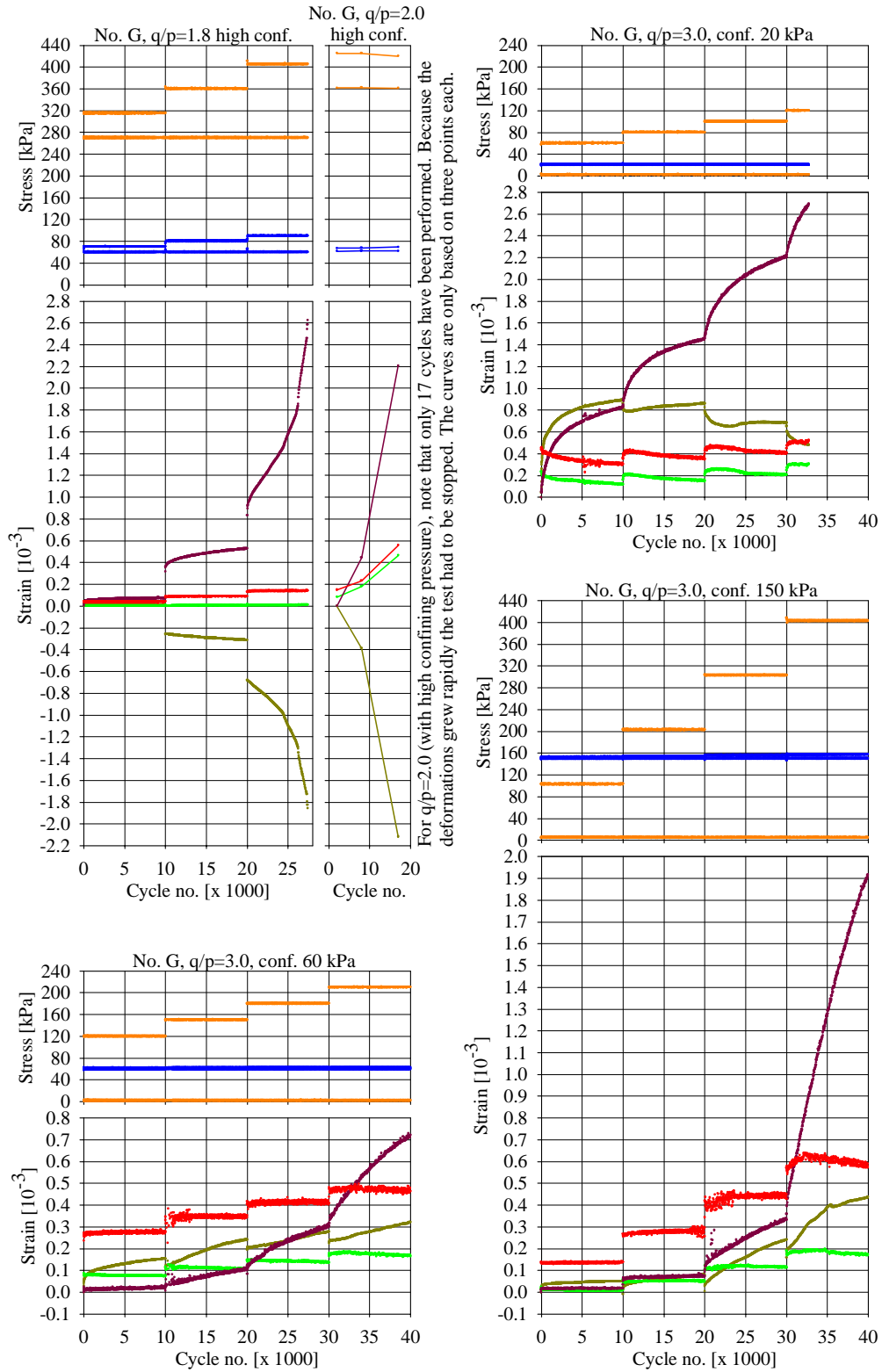


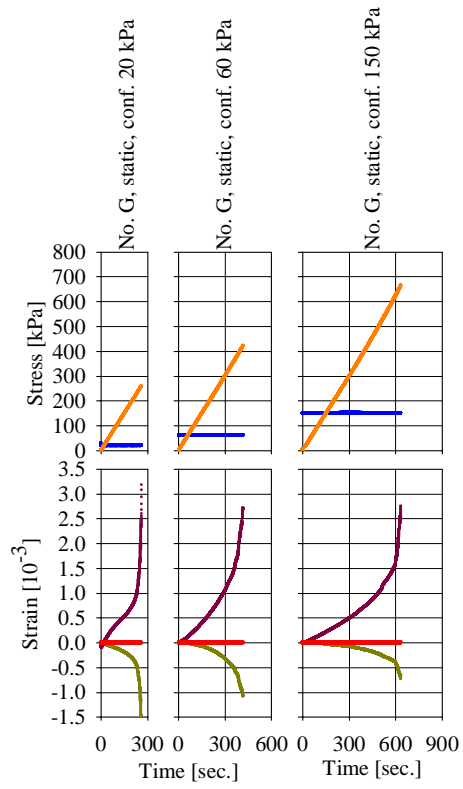












# Reports submitted by Department of Road and Railway Engineering

<i>Report no.</i>	<i>Author</i>	<i>Title</i>	<i>Year</i>
1	Kummeneje, Ottar	Rutebilstasjoner	1949
2	Riise, T.B.	Terrengets innflytelse på vindens retning og hastighet – styrke	1950
3	Lærum og Ødegård	Grunnlag for vurdering av den økonomiske verdi av vegforbedringer	1957
4	Ødegård, Erik	Vegen som forretning	1959
5	Ording, Jørgen	Undersøkelser av asfaltdekker i Trondheim	1961
6	Riise og Heim	Undersøkelse av torvmatters innflytelse på faste dekker	1962
7	Gustavsen, Øyvind	En analyse av trafikkutviklingen ved overgang fra ferje- til bruforbinding	1964
8	Sagen, Ragnvald	Traffic Simulation	1967
9	Riise, T.B.	Blandingsjordarters telefarlighet	1968
10	Kvåle, Kjell	Studiereise på veganlegg i Alpeland	1972
11	Norem, Harald	Utforming av veger i drivsnømråder	1974
12	Svennar, Odd	Nærtrafikk-baner	1975
13	Arnevik, Asbjørn	Overflatebehandling	1976
14	Noss, Per Magne	Poresug i jordarter	1978
15	Slyngstad, Tore	Filler i bituminøse vegdekker	1977
16	Melby, Karl	Repeterte belastninger på leire	1977
17	Tøndel, Ingvar	Sikring av veger mot snøskred	1977
18	Angen, Eigil	Fuktransport i jordarter	1978
19	Berger, Asle Ketil	Massedisponering. Beregning av kostnadsminimale transportmønstre for planering av fjell- og jordmasser ved bygging av veier	1978
20	Horvli, Ivar	Dynamisk prøving av leire for dimensjonering av veger	1979
21	Engstrøm, Jan Erik	Analyse av noen faktorer som påvirker anleggskostnader for veger	1979
22	Hovd, Asbjørn	En undersøkelse omkring trafikkulykker og avkjørsler	1979
23	Myre, Jostein	Utmatting av asfaltdekker	1988
24	Mork, Helge	Analyse av lastresponsar for vegkonstruksjonar	1990
25	Berntsen, Geir	Reduksjon av bæreevnen under teleløsningen	1993
26	Amundsen, Ingerlise	Vegutforming og landskapstilpassing	
		Visuelle forhold i norsk vegbygging fra 1930 til i dag	1995
27	Sund, Even K.	Life-Cycle Cost Analysis of Road Pavements	1996
28	Hoff, Inge	Material Properties of Unbound Granular Materials for Pavement Structures	1999
29	Lerfald, Bjørn Ove	A Study of Ageing and Degradation of Asphalt Pavements on Low Volume Roads	2000
30	Løhren, Alf Helge	Økt sidestabilitet i kurver med små radier	2001
31	Hjelle, Hallgeir	Geometrisk modellering av veger i 3D	2002
32	Skoglund, Kjell Arne	A Study of Some Factors in Mechanistic Railway Track Design	2002